

**Individual Differences in Excitation
and Inhibition in Visual Cortex**

Siân Ellen Robson

PhD Psychology

2012

Summary

The formation of a visual percept in the human brain involves multiple processes, the extent of which may be related to each other within individuals but may show variability between participants. The aim of this thesis was to investigate the relationships between individual variability in various measures of visual processing. The non-invasive neuroimaging methods of magnetic resonance imaging (MRI), magnetic resonance spectroscopy (MRS), magnetoencephalography (MEG) and functional MRI (fMRI) were employed to measure brain structure, neurotransmitter concentration, neuronal oscillations and haemodynamic activity, respectively. Reductions in haemodynamic activity in non-stimulated areas of visual cortex (negative blood oxygen level-dependent responses) were shown to hold useful information about the stimulus, in addition to the responses in stimulated cortex. In general, there were no strong relationships between increased or decreased functional responses in visual cortex and measures of brain structure or of neurotransmitter concentration. Age was the major determinant of individual variability in the frequency of neuronal oscillations. These findings do not replicate results from previous studies that have shown links between individual differences in these measures. This discrepancy was not due to poor repeatability of MRS measures, since methods for optimisation of MRS were identified in this thesis. Simulations were also conducted to determine the sample sizes required in correlational studies involving neuroimaging measures with associated measurement noise. The lack of replication of relationships between neuroimaging measures of individual differences in visual processing is likely to be influenced by low statistical power, due to the small sample sizes and weak relationships tested. Such studies should therefore be conducted and interpreted cautiously, bearing in mind issues of power, demographic mediators of relationships and the likely strength of relationships inferred from the physiological mechanisms linking the variables tested.

Acknowledgments

I would like to thank my supervisors, Prof Krish Singh and Dr Petroc Sumner for their advice and support throughout my three years in Cardiff. The expertise of these two men has been invaluable and I could not have hoped for better mentors to guide me through all I have learnt during this PhD.

Thanks also to the many colleagues and friends in Cardiff University Brain Research Imaging Centre who have helped to make working in the centre so enjoyable; in particular, to Dr C. John Evans for sharing his knowledge, patience and enthusiasm with me; to Dr Khalid Hamandi for his assistance with my ethics application; and to the other PhD students in the Analysis Room for the banter.

I am grateful to the School of Psychology for the studentship that funded me through this PhD and for the opportunity to gain experience in teaching. Credit must also be given to the staff and students who contributed additional data to this PhD and who are acknowledged in full in the relevant places in this thesis. Thanks also to my participants, who kindly spent hours looking at gratings and chequerboards for me.

To my parents, brother and other family members, including the new in-laws, I feel very lucky have such a caring, supportive family around me. I am also fortunate to have found an incredible group of fun-loving, happy friends in Cardiff and I especially thank the capoeiristas for so many good times.

Most importantly, I thank my wonderful husband, Kris for always being by my side, giving me strength when I need it and telling me I'm being silly when I need that. I have had some of the happiest times of my life in the last three years, with our engagement and marriage. Your support and sacrifices have brought me to this point, so this is for you.

Contents

Summary	ii
Statements and Declarations	iii
Acknowledgments	iv
Contents	v
Chapter 1	1
General Introduction	1
1.1 Rationale	1
1.2 Visual anatomy	3
1.3 Measures of neuronal structure and function	4
1.3.1 Methods	4
1.3.2 Measures of cortical excitation or activation	5
1.3.3 Measures of cortical inhibition or inactivity	6
1.3.4 Measures of cortical structure	10
1.4 Relationships between measures: Group level	11
1.5 Relationships between variables: Individual differences	14
1.6 Studying individual differences	17
1.7 Objectives	18
Chapter 2	20
Methods	20
2.1 Magnetic Resonance Imaging	20
2.1.1 Signal generation	20
2.1.2 Functional magnetic resonance imaging (fMRI).....	24
2.2 Magnetic Resonance Spectroscopy	25
2.2.1 Signal generation	25
2.2.2 GABA-edited spectroscopy.....	28
2.3 Magnetoencephalography	29
2.3.1 Signal generation	29
2.3.2 Analysis of signals	32
Chapter 3	36
Negative BOLD Responses Vary with Stimulus Contrast, Spatial Frequency and Position	36
3.1 Abstract	36
3.2 Background	37
3.3 Experiment 1: Spatial frequency and contrast tuning to a central stimulus	39
3.3.1 Rationale	39
3.3.2 Methods	39
3.3.2.1 Participants and procedure	39
3.3.2.2 MRI parameters	40
3.3.2.3 Pre-processing	40
3.3.2.4 Retinotopic mapping	40
3.3.2.5 Functional localiser and ROI definition	41
3.3.2.6 Contrast and spatial frequency task stimuli.....	41
3.3.3 Results and discussion	42
3.3.3.1 Testing for the presence of positive and negative BOLD responses.....	42
3.3.3.2 Contrast tuning results.....	43
3.3.3.3 Spatial frequency tuning results	44
3.3.3.4 Discussion of stimulus tuning in response to a centrally-presented stimulus	46

3.4 Experiment 2: Spatial frequency tuning to a surround stimulus.....	47
3.4.1 Rationale.....	47
3.4.2 Methods	48
3.4.3 Results and discussion	49
3.5 Experiment 3: Attentional influences on central negative BOLD.....	50
3.5.1 Rationale.....	50
3.5.2 Methods	51
3.5.3 Results and discussion	51
3.6 Experiment 4: Central negative BOLD from a small parafoveal stimulus.....	52
3.6.1 Rationale.....	52
3.6.2 Methods	52
3.6.3 Results and discussion	54
3.6.3.1 Testing for the presence of positive and negative BOLD responses.....	54
3.6.3.2 Central stimulus results	54
3.6.3.3 Parafoveal stimulus results.....	55
3.6.3.4 Discussion of the effect of stimulus position	56
3.7 General discussion	57
3.8 Conclusions.....	59
Chapter 4.....	61
GABA+ Concentration is Not Correlated With Positive or Negative BOLD in	
Visual Cortex	61
4.1 Abstract	61
4.2 Experiment 1: GABA+, positive BOLD and negative BOLD in visual cortex:	
Responses to a unilateral stimulus	61
4.2.1 Background	61
4.2.2 Methods	64
4.2.2.1 Participants and procedure	64
4.2.2.2 Visual task stimuli.....	64
4.2.2.3 Retinotopic mapping stimuli	65
4.2.2.4 fMRI acquisition and analysis.....	65
4.2.2.5 MRS acquisition and analysis	67
4.2.3 Results.....	67
4.2.3.1 Visual fMRI.....	67
4.2.3.2 MRS results	71
4.2.3.3 Relationship between BOLD and GABA+	71
4.2.4 Discussion	72
4.3 Experiment 2: GABA+, positive BOLD and negative BOLD in visual cortex:	
Responses to a centrally-presented stimulus.....	75
4.3.1 Rationale.....	75
4.3.2 Methods	76
4.3.2.1 Participants and stimulus.....	76
4.3.2.2 fMRI and MRS acquisition and analysis.....	77
4.3.3 Results.....	77
4.3.4 Discussion	79
4.4 General Discussion.....	80
4.5 Conclusion	82
Chapter 5.....	83
Inactivity and Inhibition in Visual Cortex: Negative BOLD, Alpha and GABA.	83
5.1 Abstract	83
5.2 Background	84
5.3 Methods	86
5.3.1 Participants	86

5.3.2 Visual grating task stimuli.....	86
5.3.3 Eyes Open/Eyes Closed (EO/EC) task stimuli.....	87
5.3.4 Retinotopic mapping stimuli and analysis.....	87
5.3.5 MRI acquisition and pre-processing.....	88
5.3.6 MRS acquisition and pre-processing.....	88
5.3.7 MEG acquisition and pre-processing.....	89
5.4 Results.....	91
5.4.1 MRS data.....	91
5.4.2 MEG data.....	91
5.4.3 BOLD data.....	92
5.4.4 Relationships between variables.....	93
5.5 Discussion.....	96
5.6 Conclusion.....	98
Chapter 6.....	99
Methodological Sources of Variability in GABA-Edited Magnetic Resonance Spectroscopy.....	99
6.1 Abstract.....	99
6.2 Background.....	100
6.3 Methods.....	106
6.3.1 Participants and procedure.....	106
6.3.2 MRS acquisition and analysis.....	107
6.4 Results.....	108
6.5 Discussion.....	112
6.6 Conclusion.....	115
Chapter 7.....	116
Simulating the Influence of Measurement Noise on the Relationship Between GABA and BOLD in Visual Cortex.....	116
7.1 Abstract.....	116
7.2 Background and Rationale.....	117
7.3 Methods.....	120
7.3.1 Participants and stimuli.....	120
7.3.2 MRI acquisition and analysis.....	121
7.3.3 MRS acquisition and analysis.....	122
7.3.4 Values used in the simulations.....	122
7.3.5 Simulation parameters and procedure.....	123
7.4 Results.....	124
7.4.1 Confirmation of expected outcomes.....	124
7.4.2 Quantitative implications for studies of GABA+ and BOLD.....	128
7.5 Discussion.....	129
7.6 Conclusions.....	132
Chapter 8.....	133
Structural and Neurochemical Parameters Driving Individual Variability in Gamma Frequency.....	133
8.1 Abstract.....	133
8.2 Background.....	133
8.3 Methods.....	136
8.3.1 Participants.....	136
8.3.2 MEG acquisition and analysis.....	136
8.3.3 MRS acquisition and analysis.....	138

8.3.4 V1 structure acquisition and analysis	139
8.3.5 Regression analysis	140
8.4 Results	140
8.5 Discussion	145
8.6 Conclusion	149
Chapter 9.....	150
General Discussion	150
9.1 Summary of findings	150
9.2 Interpretation of findings, context and future directions	150
9.2.1 Negative BOLD.....	150
9.2.2 Multiple measures of inhibition	153
9.2.3 Relationships between measures of excitation.....	157
9.2.4 MRS methods and repeatability	159
9.3 Summary of the impact of the current research.....	160
References	162
Appendices	178
Appendix 1.....	178
Correlations between variables measured in Chapter 5	178
Appendix 2.....	179
Correlations between variables measured in Chapter 8.	179

Chapter 1

General Introduction

1.1 Rationale

Of all of the physical senses, vision is the most important for the majority of people, enabling us to navigate and interact with the environment. The ability to open our eyes and instantaneously perceive the scene that presents itself is easily taken for granted; however, the processes involved in generation of a visual percept are in fact complex. This thesis employs neuroimaging techniques to measure different stages of visual processing in the brain. In particular, it focuses on differences between individuals in these measures, and on the brain's response to non-stimulated areas of the visual field.

The development of neuroimaging methods in recent decades has permitted detailed non-invasive investigation of the structure and function of the human brain. Consistencies are often found in the responses to a stimulus using different techniques, suggesting that different measures evaluate similar or related functions. For example, the optimal functional response in the brain to features of a visual stimulus such as its contrast, spatial frequency (the width of bars of opposing colour or contrast) and position is consistent when measured with functional magnetic resonance imaging (fMRI) and magnetoencephalography (MEG) (Muthukumaraswamy & Singh, 2008). These functional responses also correspond with neuronal preferences for the same stimulus features (Belliveau, Kennedy, McKinstry, Buchbinder, Weisskoff, Cohen et al., 1991; Boynton, Demb, Glover & Heeger, 1999); and match the optimal behavioural response, representing the individual's perceptual performance (Boynton et al., 1999; Singh, Smith & Greenlee, 2000; Mannion, McDonald & Clifford, 2010). These correspondences between neurophysiology, neuroimaging and behaviour indicate that the values obtained using neuroimaging provide a valid measure of stimulus processing and perception.

Differences between individual participants can be detected in functional, neurophysiological and anatomical variables measured using neuroimaging

techniques, yet few studies investigate this individual variability. Individual differences within a measure are generally considered to be noise that should be minimised, so are disregarded by taking measures of central tendency (Thompson-Schill, Braver & Jonides, 2002). However, it is important to investigate this variability, because it can provide useful information as to the cause of differences in individuals' perceptual performance. Studying the relationships between individual variability in multiple measures may also give information about how various structures and functions in the brain interact in order to create a percept.

The main context for this thesis was a study reporting a relationship between individual differences in inhibitory neurotransmitter concentration, neuronal activity and haemodynamic activity, measured with magnetic resonance spectroscopy (MRS), MEG and fMRI, respectively (Muthukumaraswamy, Edden, Jones, Swettenham & Singh, 2009). This study indicated that neuroimaging could be used to measure individual differences at various stages of the visual processing pathway and to identify links between these stages. This study and most other functional neuroimaging studies describe the brain's response to stimulation or to an experimental manipulation. In visual cortex, the responses in *non-stimulated* regions of cortex when a stimulus is present elsewhere are often disregarded, but may have an important role in visual processing, because suppression or inhibition of these areas may improve the perception of the stimulus in adjacent areas.

This thesis investigated these important but understudied factors of individual variability and inhibition in visual cortex. Specifically, the aims were to determine whether the response in non-stimulated areas differed with features of the stimulus; whether individual differences in functional measures of excitation and inhibition were related to each other or to measures of neurotransmission and cortical structure; whether measurement noise had a substantial effect on the strength of correlations; and how measurement noise could be minimised in order to give the best estimate of participant-related variance.

1.2 Visual anatomy

Visual processing is one of the most studied topics in neuroscience; therefore much of the anatomy of vision is already well understood. The main geniculostriate visual pathway (Figure 1.1) takes information from the eyes along the optic nerve, across the optic chiasm, through the optic tracts to the lateral geniculate nucleus (LGN), then along the optic radiations to the primary visual cortex in the occipital lobe of the brain, also known as the striate cortex or V1. The primary visual cortex in each hemisphere is divided by the calcarine sulcus, which extends from the posterior edge of the occipital lobes anteriorly along the interhemispheric fissure.

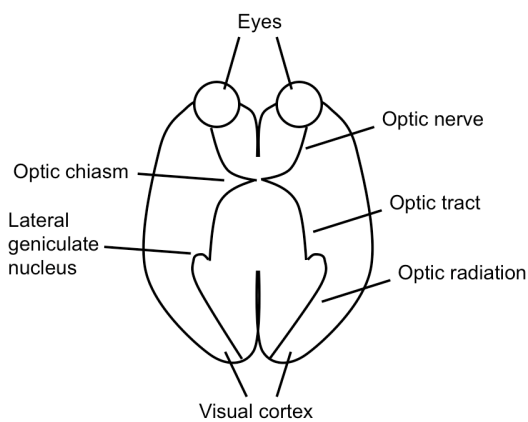


Figure 1.1. Representation of the geniculostriate visual pathway in the human brain.

Individual neurons in V1 respond to a particular region of the visual field (their receptive field) and the size of these receptive fields increases with distance from fixation (Hubel & Wiesel, 1974; Smith, Singh, Williams & Greenlee, 2001). V1 contains a topographic representation of the visual scene, whereby areas adjacent to each other in the visual field are represented on adjacent areas of the cortex (Hubel, 1995). The visual image is flipped horizontally and vertically so that, for example, the upper left visual field is projected onto the right striate cortex below the calcarine sulcus. The visual field is also topographically represented in the LGN and in some 'higher' visual areas in the extrastriate cortex (Figure 1.2). These different areas are specialised for processing certain stimulus features: V1 and V2 process basic form and structure, V3 is involved in the perception of retinal disparity, V4 is specialised for colour and V5 primarily processes motion (Grill-Spector & Malach, 2004). In addition to these regional specialisations, neurons within regions are also often specialised for particular stimulus features and may form clusters with similar

preferences. For instance, there are columns of neurons specialised for processing particular orientations and spatial frequencies in cat (Hubel & Wiesel, 1963; Tootell, Silverman & De Valois, 1981) and monkey (Tootell, Silverman, Hamilton, Switkes & De Valois, 1988; Silverman, Grosf, De Valois & Elfar, 1989) visual cortex.

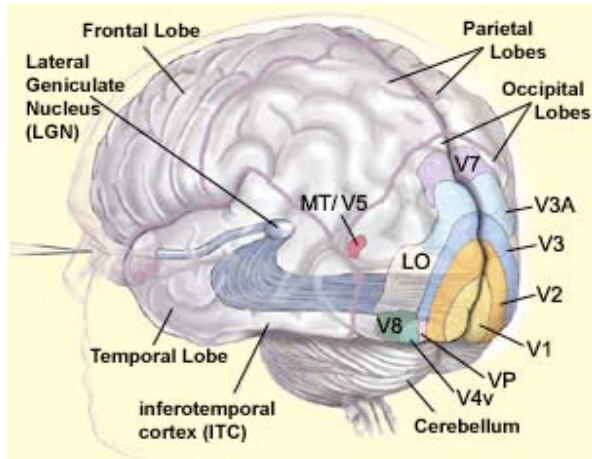


Figure 1.2. Anatomy of the visual areas in the human brain, reproduced from <http://thebrain.mcgill.ca/>.

1.3 Measures of neuronal structure and function

1.3.1 Methods

There are many methods through which the activity and anatomy of the brain can be investigated, from measurement of action potentials and neurotransmitter receptor densities in individual neurons, to measures of neuronal network activity and cortical volume across the whole brain. In this thesis, changes in haemodynamic activity in localised regions of the brain were represented in the blood oxygen level-dependent (BOLD) response (Ogawa, Lee, Kay & Tank, 1990), measured using fMRI. Neuronal activity was recorded using MEG (Cohen, 1968), which measures magnetic fields generated by electric currents in active neurons. MEG can be used to detect evoked responses that are time-locked to the stimulus, as well as induced oscillatory responses that are time but not phase-locked to the stimulus (Singh, 2006). Oscillatory activity in the alpha (8-12Hz) and gamma (30-100Hz) frequency bands was recorded in this thesis. Another variable of interest was the concentration of the principle inhibitory neurotransmitter in the brain, gamma-aminobutyric acid (GABA). The concentration of metabolites including neurotransmitters within a relatively large

voxel can be measured using MRS (Gujar, Maheshwari, Bjorkman-Burtscher & Sundgren, 2005; Bertholdo, Watcharakorn & Castillo, 2011). Finally, the area and thickness of primary visual cortex were measured using anatomical MRI, which provides high-resolution 3-D images of the brain and can be used to identify different tissue types, structures and regions in the cortex (Magnotta & Andreasen, 1999). The mechanisms behind generation and recording of signals from fMRI, MEG, MRS and anatomical MRI are described in Chapter 2. Each of the measures obtained from these methods reflect distinct functions in visual processing, but correlations between them may be present if they describe different stages of the same processing pathway.

1.3.2 Measures of cortical excitation or activation

In active or stimulated areas of cortex, positive BOLD and gamma frequency oscillations can be measured. Positive BOLD reflects increases in blood flow, blood volume and the rate of oxygen consumption in areas in which active neurons require oxygen to support glucose metabolism (Kwong, Belliveau, Chesler, Goldberg, Weisskoff, Poncelet et al., 1992; Ogawa, Tank, Menon, Ellermann, Kim, Merkle et al., 1992; Vazquez, Masamoto, Fukuda & Kim, 2010). Although fMRI does not directly measure neuronal activity, it can be said to reflect neurovascular coupling, as the BOLD signal correlates with invasive neurophysiological measures of evoked neuronal activity in the same region in monkey and human visual cortex (Logothetis, Pauls, Augath, Trinath & Oeltermann, 2001; Logothetis, 2002; Niessing, Ebisch & Schmidt, 2005), as well as with neuroimaging measures of neuronal activity such as magnetoencephalography and electroencephalography (EEG) (Goldman, Stern, Engel & Cohen, 2002; Muthukumaraswamy & Singh, 2008; Brookes, Hale, Zumer & Stevenson, 2011). Positive BOLD has been reported during many functions, from basic sensory processing (Engel, Glover & Wandell, 1997) and movement (Meier, Aflalo, Kastner & Graziano, 2008) to cognitive activity such as attention (Kastner, De Weerd, Desimone & Ungerleider, 1998) and memory (Henson, 2005). In visual cortex, similar to behavioural preferences for particular stimulus features (Campbell & Robson, 1968; Kulikowski, Abadi & King-Smith, 1973), positive BOLD varies with stimulus contrast (Boynton, Engel, Glover & Heeger, 1996), spatio-temporal frequency (Henriksson, Nurminen, Hyvarinen & Vanni, 2008) and orientation (Mannion et al., 2010).

Gamma frequency oscillations are produced by GABA-ergic inhibitory interneurons influencing activity in excitatory pyramidal cells and resulting in synchronous activity in the gamma frequency (Wang & Buzsáki, 1996). The amplitude of gamma oscillations measured using MEG has also been associated with several functions including basic sensory processing (Friedman-Hill, Maldonado & Gray, 2000; Donner & Siegel, 2011), movement generation (Cheyne, Bells, Ferrari, Gaetz & Bostan, 2008), orientation discrimination (Edden, Muthukumaraswamy, Freeman & Singh, 2009), visual attention (Fries, Reynolds, Rorie & Desimone, 2001), short-term memory (Lisman & Idiart, 1995) and temporal coordination of activity in spatially distinct areas of the cortex (Gray & Singer, 1989; Maldonado, Friedman-Hill & Gray, 2000). It was previously thought that the main role of gamma oscillations was in the binding of information from different areas of the brain (Buzsaki, Kaila & Raichle, 2007); however, this theory has since been refuted (Ray & Maunsell, 2010). It is now thought that gamma activity may be primarily involved in local control of sensory processing, while lower frequency alpha and beta oscillations reflect longer-distance interactions integrating information from different brain areas (Donner & Siegel, 2011).

1.3.3 Measures of cortical inhibition or inactivity

In this thesis, neuroimaging measures that could potentially represent inhibition of inactive areas of the brain were investigated in addition to measures of stimulated areas. Although most fMRI studies seek to quantify increases in BOLD in response to experimental manipulations, a reduction in BOLD below baseline levels can also be observed in non-stimulated areas adjacent to stimulated cortex (Huang, Plyka, Li, Einstein, Volkow & Springer, 1996; Tootell, Mendola, Hadjikhani, Liu & Dale, 1998; Smith, Singh & Greenlee, 2000; Shmuel, Yacoub, Pfeuffer, Van De Moortele, Adriany, Hu et al., 2002; Boorman, Kennerley, Johnston, Jones, Zheng, Redgrave et al., 2010). These decreases in BOLD are known as negative BOLD responses (Figure 1.3). The haemodynamic mechanisms by which negative BOLD is induced are the opposite to those producing positive BOLD: in human visual and motor cortices, combined BOLD and perfusion measurements have shown decreased cerebral blood flow (CBF) in areas of negative BOLD, which were also associated with decreases in the cerebral metabolic rate of oxygen consumption (Shmuel et al., 2002; Stefanovic, Warnking & Pike, 2004). Similarly, in rat somatosensory cortex, 2D optical imaging

spectroscopy revealed decreases in blood flow and increases in deoxyhaemoglobin in areas of negative BOLD, again reflecting the opposite mechanisms to those involved in production of a positive BOLD response (Boorman et al., 2010). Negative BOLD is a lower amplitude response than positive BOLD, but the timecourses and response profiles to stimulus features are similar, supporting the theory that positive and negative BOLD share similar vascular mechanisms (Harel, Lee, Nagaoka, Kim & Kim, 2002; Shmuel et al., 2002).

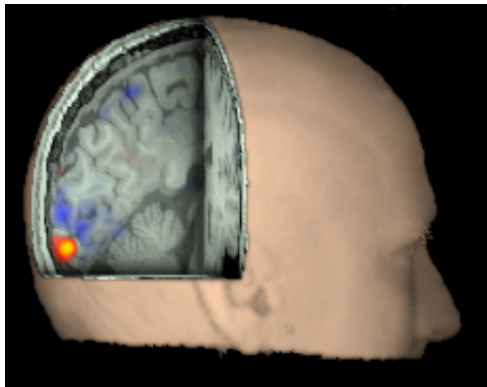


Figure 1.3. The response to a small, centrally-presented visual grating stimulus in one participant, measured using fMRI. A positive BOLD response (red) and surrounding weaker and more diffuse negative BOLD response (blue) are clearly visible.

The neurophysiological basis of the negative BOLD response has been the subject of some debate. One theory as to the source of negative BOLD is that it is due to ‘blood steal’ whereby active areas of the cortex require more oxygenated blood, so there is less available in neighbouring areas. This factor may contribute to the response, but cannot be the full explanation, since negative BOLD has been observed in the contralateral hemisphere to stimulation in visual (Smith, Williams & Singh, 2004), somatosensory (Kastrup, Baudewig, Schnaudigel, Huonker, Becker, Sohns et al., 2008) and motor (Allison, Meador, Loring, Figueroa & Wright, 2000; Stefanovic et al., 2004) cortices; and given that the two cerebral hemispheres have separate blood supplies, one cannot ‘steal’ blood from the other.

Several studies have now provided evidence that negative BOLD is primarily a result of decreases in neuronal activity and may in fact reflect active suppression of neuronal activity (Pasley, Inglis & Freeman, 2007). In areas of negative BOLD in rat

barrel cortex, there are decreases in multiunit spiking (Boorman et al., 2010) and neuronal hyperpolarisation (Devor, Tian, Nishimura, Teng, Hillman, Narayanan et al., 2007), both of which may be the result of increased inhibition. In macaque visual cortex, simultaneous fMRI and electrical recording has shown that negative BOLD is associated with decreases in local field potentials and multi-unit activity (Shmuel, Augath, Oeltermann & Logothetis, 2006). On the other hand, one study has reported the presence of negative BOLD and decreased CBF in higher-order visual areas in which increased neuronal spiking was expected, but this study did not directly measure neuronal activity in the region containing negative BOLD (Harel et al., 2002). The majority of evidence therefore suggests that non-stimulated cortex is actively inhibited and negative BOLD is consequently induced in these areas.

Negative BOLD responses have been recognised in fMRI data for many years, but are rarely reported. The precise role of decreased BOLD during stimulus processing is not yet known, but it has been suggested to improve the spatial resolution of stimulus perception (Bressler, Spotswood & Whitney, 2007) and to be involved in both attentional suppression and bottom-up processing of distractor stimuli (Heinemann, Kleinschmidt & Müller, 2009). One study has shown a link between negative BOLD and behaviour: negative BOLD was induced in areas of somatosensory cortex ipsilateral to medial nerve stimulation, and tactile discrimination thresholds to a contralateral stimulus consequently increased, suggesting that the negative BOLD reflected disruption of normal processing in that area (Kastrup et al., 2008). Of particular interest in this thesis was the relationship between negative BOLD and neuronal activity measured using MEG, and inhibitory neurotransmitter concentration measured using MRS, since it was hypothesised that the extent of the negative BOLD response could be under the control of one or both of these variables.

Alpha frequency oscillations are one possible neuronal correlate of negative BOLD. These oscillations are present in inactive areas of cortex (Berger, 1929) and have been said to reflect cortical 'idling' (Kelly, Lalor, Reilly & Foxe, 2006) or more recently, to be involved in suppression of non-stimulated regions (Jensen & Mazaheri, 2010). Alpha oscillatory power is reduced during cognitive activity and is enhanced when processing demands decrease. This effect is commonly reported in widespread areas of the brain on closing the eyes (Cohen, 1972; Lopes da Silva, 1991; Klimesch,

1996), but can also be localised in specific brain regions and can differ in amplitude depending on the task demands (Pfurtscheller, Stancák & Neuper, 1996; Neuper & Pfurtscheller, 2001). Alpha band activity is also strongly influenced by attention: it increases in response to non-attended regions or features of a visual scene (Vanni, Revonsuo & Hari, 1997; Worden, Foxe, Wang & Simpson, 2000; Kelly et al., 2006; Snyder & Foxe, 2010) and decreases in stimulated or attended regions of cortex (Thut, Nietzel, Brandt & Pascual-Leone, 2006; Sabate, Llanos, Enriquez, Gonzalez & Rodriguez, 2011). The role of increases in the power of alpha rhythms in non-stimulated or unattended cortex is said to be in actively suppressing these regions, allowing enhanced processing of the attended region (Kelly et al., 2006). Similarly, alpha oscillations prior to stimulus onset (Foxe, Simpson & Ahlfors, 1998; Fu, Foxe, Murray, Higgins, Javitt & Schroeder, 2001) may modulate the amount of information transferred to higher levels of processing, permitting selective stimulus processing (Foxe et al., 1998; Tuladhar, Ter Huurne, Schoffelen, Maris, Oostenveld & Jensen, 2007; Van Dijk, Schoffelen, Oostenveld & Jensen, 2008; Sabate et al., 2011). These ‘gating’ theories suggest that there is some level of active control of oscillatory activity, which could potentially be mediated by GABA-ergic inhibitory interneurons.

Baseline levels of the concentration of the inhibitory neurotransmitter, GABA can be investigated using MRS. The MRS measure includes both intra- and extra-cellular GABA molecules, which have different roles in inhibitory processing. Intra-cellular GABA acts in a phasic manner when it is released at the synapse and binds to post-synaptic receptors, allowing positively charged ions to enter the post-synaptic cell and cause hyperpolarisation, decreasing the likelihood of the neuron firing and creating an inhibitory post-synaptic potential (Gonzalez-Burgos & Lewis, 2008). GABA molecules in the extracellular space have a tonic inhibitory effect on receptors in non-synaptic regions of neurons (Buzsaki et al., 2007). In addition to intra- and extracellular GABA involved in neurotransmission, there is another form of GABA in the brain that is involved in energy metabolism (Martin & Rimvall, 1993). A disadvantage of MRS is that the GABA value reported does not discriminate between these different forms of GABA and it also potentially contains some signal from macromolecules that have peaks at a similar location on the spectrum, because the signals cannot easily be separated (Behar & Rothman, 1994). It is therefore not clear how much of the value obtained represents GABA that is actively involved in

neuronal inhibition. However, the values do appear to correlate with behavioural and imaging data hypothesised to be under inhibitory control (Edden et al., 2009; Muthukumaraswamy et al., 2009; Donahue, Near, Blicher & Jezzard, 2010; Sumner, Edden, Bompas, Evans & Singh, 2010; Boy, Evans, Edden, Lawrence, Singh, Husain et al., 2011; Stagg, Bachtiar & Johansen-Berg, 2011a), suggesting that GABA values obtained using MRS represent a useful measure of the concentration of the neurotransmitter within a region of the brain. Negative BOLD, alpha oscillations and GABA may therefore all be involved in inhibition in the brain, but at different stages of processing.

1.3.4 Measures of cortical structure

The amplitude and extent of functional responses and the concentration of neurotransmitters within a region may depend on anatomical features of the cortex. High-resolution anatomical MRI images can be used to quantify the area, thickness and volume of grey and white matter in certain regions of the brain. V1 can be identified structurally from masks on a template brain reconstructed from V1 defined cytoarchitectonically on postmortem brains (Figure 1.4A) (Amunts, Malikovic, Mohlberg, Schormann & Zilles, 2000), or on the basis of the curvature of the gyri around the calcarine sulcus in individuals' cortex (Figure 1.4B) (Hinds, Rajendran, Polimeni, Augustinack, Wiggins, Wald et al., 2008). Visual cortices can also be identified functionally using retinotopic mapping, whereby BOLD responses showing the topographical representation of visual areas on the cortex allow the boundaries of visual areas to be identified and mapped (Sereno, Dale, Reppas, Kwong, Belliveau, Brady et al., 1995; DeYoe, Carman, Bandettini, Glickman, Wieser, Cox et al., 1996; Engel et al., 1997). These techniques allow quantification of functional activity from within accurately-defined areas of specific interest.

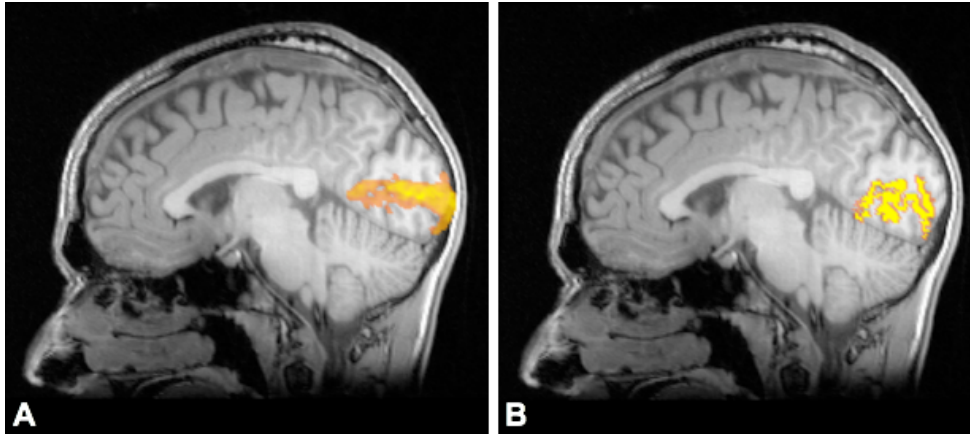


Figure 1.4. A) V1 region of interest (ROI) delineated from a cytoarchitectonically-defined template, showing voxels with a 50% probability of being in V1. B) V1 ROI identified on the basis of curvature of the gyri around the calcarine sulcus in the same participant.

1.4 Relationships between measures: Group level

A potential complication with using neuroimaging techniques to measure visual processing is that many responses can be obtained from the same region of cortex and the role of each these responses in stimulus processing is not always clear (Singh, 2012). When investigating these measures, it is therefore important to understand the processes that each represents and how they relate to each other. Previous studies have described relationships between many of the variables described above.

At the level of synaptic inhibition, GABA may have a role in modulation of neuronal and subsequently haemodynamic activity. As described above, GABA is involved in inducing gamma oscillations in networks of interneurons and pyramidal neurons (Wang & Buzsáki, 1996). GABA may also play a role in generating beta (Yamawaki, Stanford, Hall & Woodhall, 2008) and very low frequency (≤ 1 Hz) oscillations (Zhang, Perez Velazquez, Tian, Wu, Skinner, Carlen et al., 1998). However, a study has reported that movement-related gamma synchrony was not affected by a GABA_A receptor agonist, though movement-related beta desynchrony was increased (Hall, Stanford, Yamawaki, McAllister, Rönnqvist, Woodhall et al., 2011), therefore gamma oscillations may not be entirely under GABA-ergic control. Pharmacological studies have shown a link between GABA and BOLD: visual BOLD is reduced by

administration of the GABA agonist, zolpidem (Licata, Lowen, Trksak, Maclean & Lukas, 2011); and sensorimotor BOLD is reduced in rats given vigabatrin, a drug that blocks gabatransaminase, which breaks down GABA (Chen, Silva, Yang & Shen, 2005). GABA concentration in the anterior cingulate cortex measured using MRS also shows a positive correlation with negative BOLD in the anterior cingulate cortex during an emotion processing task (Northoff, Walter, Schulte, Beck, Dydak, Henning et al., 2007). These studies show potentially causal relationships of GABA with BOLD and neuronal activity that may be measurable using neuroimaging techniques.

As mentioned above, BOLD has also been reported to be related to neuronal activity: a positive correlation has been shown between positive BOLD and neuronal activity (Logothetis et al., 2001; Logothetis, 2002; Mukamel, Gelbard, Arieli, Hasson, Fried & Malach, 2005), while negative BOLD is associated with decreases in neuronal activity (Shmuel et al., 2006; Boorman et al., 2010). The relationship between BOLD and neuronal activity is not always simple (Singh, 2012), as BOLD has been shown to relate to local field potentials (LFPs) but not to neuronal firing rates (Logothetis et al., 2001; Niessing et al., 2005), suggesting that it may reflect changes in oscillatory activity. Consistent with this theory, good spatial correspondence between induced MEG signals and fMRI has been reported in visual (Singh, Barnes, Hillebrand, Forde & Williams, 2002; Brookes, Gibson, Hall, Furlong, Barnes, Hillebrand et al., 2005; Winterer, Carver, Musso, Mattay, Weinberger & Coppola, 2007) and sensorimotor (Stevenson, Wang, Brookes, Zumer, Francis & Morris, 2012) cortices, as well as in widespread functional connectivity signals measured at rest (Brookes & Woolrich, 2011). The positive BOLD response also relates to different frequencies of oscillatory activity in different ways, indicating diverse responses to the same stimulus: there is an inverse relationship between BOLD and lower frequency (5-15Hz) oscillations and a positive relationship with high frequency (40-130Hz) oscillatory activity in invasive (Mukamel et al., 2005; Zumer, Brookes, Stevenson & Francis, 2010) and MEG (Zumer et al., 2010) studies. Both low frequency alpha oscillations and higher frequency gamma oscillations were investigated in this thesis in relation to BOLD, GABA and V1 structure.

Supporting the theory that alpha represents inactive or suppressed cortex, alpha oscillations (8-12Hz) in inactive areas of cortex have previously been linked to

reductions in positive BOLD in the same regions (Goldman et al., 2002; Laufs, Kleinschmidt, Beyerle, Eger, Salek-Haddadi, Preibisch et al., 2003; Wu, Eichele & Calhoun, 2010) and conversely, decreases in alpha in stimulated cortex correlate with increased positive BOLD (Ritter, Moosmann & Villringer, 2009). The inverse relationship between positive BOLD and alpha suppression is not present in all participants, indicating that the way in which these variables interact differs across participants (Gonçalves, de Munck, Pouwels, Schoonhoven, Kuijer, Maurits et al., 2006). Alpha in the thalamus and insula is related to *increased* positive BOLD (Goldman et al., 2002), suggesting that these areas are involved in generation of the alpha oscillations. There may also be a relationship between alpha and negative BOLD, since in areas adjacent to stimulated cortex where negative BOLD would be expected to occur, increases in alpha have been recorded using electrocorticography (Harvey, Vansteensel, Ferrier, Petridou, Zuiderbaan, Aarnoutse et al., 2012). These findings provide a basis for the hypothesised relationships between individual differences in negative BOLD and alpha investigated in this thesis.

The link between gamma oscillations and BOLD is not as clear. Stimuli inducing strong gamma oscillations using EEG have been shown to produce a strong positive BOLD response (Zaehle, Fründ & Schadow, 2009). However, BOLD and gamma oscillations are not always equivalent: they show different spatio-temporal frequency tuning profiles in visual cortex (Muthukumaraswamy & Singh, 2008, 2009); and isoluminant red-green stimuli do not induce gamma oscillations (Adjamian & Hadjipapas, 2008) but do produce positive BOLD (Mullen & Dumoulin, 2007). It has also been reported that the amplitude of gamma band activity does not correlate with positive BOLD, but gamma frequency does (Muthukumaraswamy et al., 2009; Gaetz, Edgar, Wang & Roberts, 2011). The different relationships of alpha and gamma oscillations with positive BOLD indicate that the two frequencies may have different roles in processing of similar aspects of the stimulus to positive BOLD.

To summarise the relationships that have been reported between the measures of interest in this thesis: GABA-ergic inhibition may modulate gamma oscillations, suppress positive BOLD and enhance negative BOLD; alpha and gamma oscillations show good spatial correspondence with positive BOLD; and increases in BOLD are inversely related to the amplitude of alpha oscillations and positively related to

gamma amplitude. GABA concentration, neuronal oscillations and haemodynamic activity have also been related to behavioural perception. There is currently a lack of information about relationships between neuronal oscillations and negative BOLD. Figure 1.5 shows the variables of interest in this thesis and the hypothesised direction of causality along the visual processing pathway.

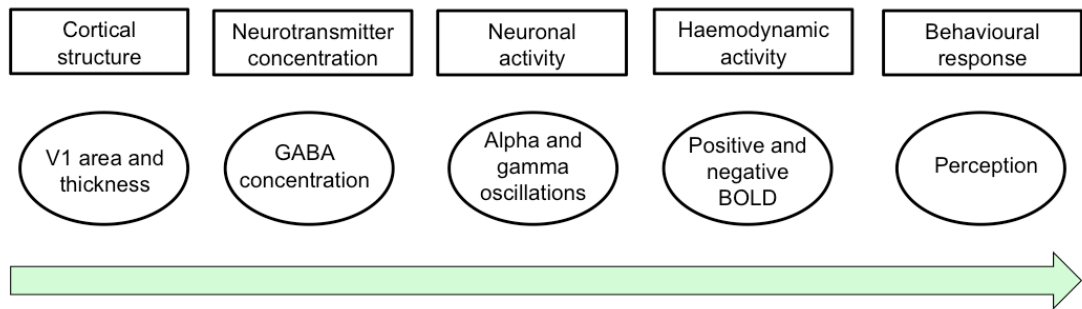


Figure 1.5. Factors potentially involved in visual processing (rectangles) and corresponding variables measured in this thesis (ellipses). Green arrow represents proposed direction of causality.

1.5 Relationships between variables: Individual differences

As described above, individual differences have previously been reported in all of the variables of interest in this study. However, these findings describe spatio-temporal relationships between variables, or relationships between experimental conditions, whereas this thesis was concerned with relationships between individual variability in these measures. The size of V1 is highly variable between participants, both when measured anatomically from the stripe of Gennari separating V1 and V2 (Stensaas, Eddington & Dobbelle, 1974; Andrews, Halpern & Purves, 1997) and when measured functionally based on the fMRI response during retinotopic mapping (Miki, Liu, Englander, Raz, van Erp, Modestino et al., 2001). GABA concentration measured using MRS also varies between participants (Bogner, Gruber, Doelken, Stadlbauer, Ganslandt, Boettcher et al., 2010; Evans, McGonigle & Edden, 2010). In terms of functional activity, there is individual variability in the area and amplitude of positive BOLD in visual (Rombouts, Barkhof, Hoogenraad, Sprenger, Valk & Scheltens, 1997; Miki, Raz, van Erp, Liu, Haselgrove & Liu, 2000), somatosensory (Desmond & Glover, 2002), sensorimotor (Aguirre, Zarahn & D'esposito, 1998) and frontal

(Handwerker, Ollinger & Esposito, 2004) areas of the brain, as well as in the profile of haemodynamic response functions (Aguirre et al., 1998). Similarly, individual differences are present in the amplitude and peak frequency of alpha oscillations in the resting brain (Klimesch, 1996; Doppelmayr, Klimesch, Pachinger & Ripper, 1998; Thut et al., 2006) and in the amplitude of visual gamma oscillations (Zaehle et al., 2009). These studies indicate that variability exists in neuroimaging measures of visual processing, neurophysiology and anatomy; however, the source of individual differences in these variables is not always clear. Differences in cognitive strategies, brain morphology and abnormalities in the modulation of neurotransmitter levels may contribute to variability in functional activation (Macdonald, Nyberg & Backman, 2006; Van Horn, Grafton & Miller, 2008). This thesis investigated whether structural (cortical area and thickness) and neurophysiological (GABA concentration) measures contribute to individual variability in functional (MEG and fMRI) responses.

A study that inspired some of the experiments conducted in this thesis investigated individual differences in GABA concentration, oscillatory neuronal activity and positive BOLD (Muthukumaraswamy et al., 2009). In this study, participants were presented with the same visual task in MEG and fMRI experiments. It was found that individuals' peak gamma frequency (but not power) was inversely correlated with their positive BOLD amplitude in corresponding areas of visual cortex, while their GABA concentration in occipital cortex measured using MRS was positively correlated with peak gamma frequency and inversely correlated with positive BOLD. The relationship between GABA and gamma frequency was explained based on a neurophysiological model in which the frequency of gamma oscillations is dependent on the cell types present: in participants with more excitatory pyramidal cells, the time required for the cycle of neuronal firing, inhibition and reactivation is extended, leading to slower gamma oscillations. A higher excitation/inhibition ratio therefore results in lower frequency oscillations (Banks, White & Pearce, 2000; Brunel & Wang, 2003). The relationship between GABA and BOLD was attributed to increased levels of inhibition in participants with more GABA causing a reduced haemodynamic response to the stimulus, either through direct modulation of vasoconstriction by GABA-ergic interneurons or through reduced evoked glutamatergic excitatory activity. Therefore, although the activity of the neuronal

population was increased in response to visual stimulation, the increase was smaller in individuals with more GABA.

A similar relationship between GABA and gamma was reported in motor cortex, whereby individual variability in the frequency but not the power of gamma oscillations was positively correlated with GABA concentration (Gaetz et al., 2011). Conversely, beta power but not frequency was positively associated with GABA (Gaetz et al., 2011). The relationship between individual differences in GABA concentration and positive BOLD has also been replicated (Donahue et al., 2010; Gu, Chen & Yang, 2012; Muthukumaraswamy, Evans, Edden, Wise & Singh, 2012). Individual differences in MRS measures of neurotransmitter concentration and BOLD have not been investigated in relation to alpha oscillations to date. Measurement of this neuronal activity may give some information relating to a stage of stimulus processing that may come between GABA and BOLD.

Cortical activity may also be related to individual differences in brain structure. Alpha power is reported to correlate with grey and white matter volume (Smit, Boomsma, Schnack, Hulshoff Pol & de Geus, 2012). Gamma frequency has been related to the surface area of V1 and through the association described above between gamma frequency and GABA, GABA concentration has also been proposed to be related to the size of V1 (Schwarzkopf, Robertson, Song, Barnes & Rees, 2012). V1 contains a high density of GABA receptors in comparison to other areas of the cortex (Zilles & Amunts, 2009) and GABA is said to vary more through the layers than across them (Albus & Whale, 1994), with a high density of GABA receptors (Zilles, Palomero-Gallagher & Schleicher, 2004) and a high number of GABA-ergic neurons (Hendry & Huntsman, 1994) in cortical layers II-III, IVA, IVCbeta and VI. The thickness as well as the area of V1 may therefore also be related to GABA concentration.

These studies show that individual differences can be measured at different stages of the visual processing pathway and that links between these measures can be identified. Importantly, these differences also relate to behaviour, indicating that neuroimaging measures describe processes that ultimately have a measurable effect on perception. Individual differences in GABA concentration have been shown to

predict impulsivity (Boy et al., 2011), orientation discrimination (Edden et al., 2009), tactile discrimination (Puts, Edden, Evans, McGlone & McGonigle, 2011), motor learning (Stagg et al., 2011a) and eye movements (Sumner et al., 2010). Orientation discrimination also correlates with gamma frequency (Edden et al., 2009) and individuals with low alpha at rest have good perceptual performance but poor memory performance (Hanslmayr, Klimesch, Sauseng, Gruber, Doppelmayr, Freunberger et al., 2005).

Based on the relationships described in this section and on an understanding of the neurophysiology at different stages of the visual processing pathway, predictions were made as to relationships between the variables tested in this thesis: measures of haemodynamic activity in visual cortex were expected to show a dependency on individual differences in neuronal activity, which themselves would be predicted by neurotransmission, and neurotransmitter concentration may be affected by the structure of visual cortex (Figure 1.5). Correlations between individual differences in these variables were investigated in Chapters 4 and 5, and the ability to predict one variable from another was investigated in Chapter 8.

1.6 Studying individual differences

There are generic issues that apply to all studies of individual differences, regardless of the experimental modality: such studies tend to be correlative, therefore it is important to ensure that both variables measured are sufficiently reliable, since a correlation between two noisy variables will be weakened or may give a spuriously high result if the measures do not give repeatable estimates of the variable. Poor repeatability can arise from genuine within-subjects variability or from measurement noise. The within-subjects variability in a measure must be lower than the between-subjects variability in order for investigations of individual differences to have sufficient power; otherwise differences between individuals cannot be distinguished from experimental noise.

Greater within subjects and sessions reliability than between subjects and sessions reliability has been reported for positive BOLD (Aguirre et al., 1998) as well as for GABA (Evans et al., 2010). Negative BOLD is repeatable when tested within the

same session (Shmuel et al., 2002), gamma oscillations are repeatable within subjects over several weeks (Muthukumaraswamy, Singh, Swettenham & Jones, 2010), alpha is repeatable over several days (Nikulin & Brismar, 2004) and V1 structure would not be expected to vary across weeks (Magnotta & Andreasen, 1999). The measures of interest in this thesis are therefore generally stable over time, but are not entirely free from within-subject variability or measurement noise. Methods and analytical parameters influencing the extent of measurement noise in MRS are investigated in Chapter 6.

When conducting correlations, even when both measures are sufficiently reliable to give a repeatable correlation on retest, the probability of detecting the true effect is dependent on the power of the experiment. Statistical power is the probability of rejecting the null hypothesis when it is false (not making a type II error) and is dependent on the size of the effect, the level of significance required and the sample size (Faul, Erdfelder, Lang & Buchner, 2007). Since neuroimaging studies are often of limited sample size due to the costs associated with the technology, the power in such studies is not always optimal, preventing accurate estimation of the genuine intrinsic relationship between the variables. The power of fMRI studies to detect differences between experimental and control conditions has been investigated using simulations (Desmond & Glover, 2002) and a sample size of 25 was recommended when multiple comparisons must be controlled for. A similar investigation has not yet been conducted into the power to detect correlations between two different neuroimaging variables, each of which may contain measurement noise. The issues of the required sample size and the effect of measurement noise on correlations between neuroimaging variables were addressed in Chapter 7 of this thesis. It is important to take into account these data when interpreting findings of correlations between individual differences in neuroimaging measures.

1.7 Objectives

Investigations of the interactions between neuronal activity, haemodynamic activity, neurotransmitters and brain structure can be used to build a more holistic understanding of how these factors contribute to the complex perceptions and behaviours that humans are capable of. In this thesis, individual differences in

different neuroimaging measures involved in visual processing are investigated and relationships between these measures are considered. Negative BOLD is an understudied response in fMRI that could play an important role in stimulus processing. The first experimental chapter of this thesis seeks to characterise the optimal stimulus parameters for inducing a negative BOLD response in visual cortex. The following two chapters investigate whether negative BOLD is related to alpha oscillations and GABA concentration, since all three variables may be involved in similar processes of inhibition of non-stimulated areas. Issues relating to the repeatability of GABA measurement are investigated in Chapter 6, followed by simulations of the relationship between GABA and BOLD given the repeatability of both measures in Chapter 7. The final experimental chapter investigates whether structural or functional variables account for a significant proportion of individual variability in neuronal activity.

Chapter 2

Methods

In this thesis, the neuroimaging methods of magnetic resonance imaging, magnetic resonance spectroscopy and magnetoencephalography were employed in order to tackle the research questions. This chapter describes the generation and analysis of signals from these techniques.

2.1 Magnetic Resonance Imaging

2.1.1 Signal generation

The discovery of nuclear magnetic resonance (NMR) in 1946 by two independent groups (Bloch, Hansen & Packard, 1946; Purcell & Torrey, 1946) paved the way for the development of magnetic resonance imaging (MRI). Signals obtained using these techniques were later used to create images of solid materials (Lauterbur, 1973; Mansfield, 1973) and soon after, MRI began to be used *in vivo* to visualise structures within the body. The discovery that changes in blood oxygenation could be mapped on the basis of signals affected by the oxy- to deoxy-haemoglobin ratio (Bandettini, Wong, Hinks, Tikofsky & Hyde, 1992; Kwong et al., 1992; Ogawa et al., 1992) resulted in the advent of functional MRI (fMRI). MRI has since become a major tool in non-invasive *in vivo* investigations of the structure and function of brain through the development of several techniques applied to the basic mechanistic principles.

The main components of an MRI scanner are the magnet used to induce the principle static magnetic field (B_0); radiofrequency (RF) transmit and receive coils; and gradient coils, which are used to perturb B_0 in specific directions. The magnetic fields required for MRI are thousands of times stronger than the earth's magnetic field, so to obtain such strong fields, superconducting magnets made of alloys that lose electrical resistance at very low temperatures are used. A current applied to these magnets is maintained at a constant strength and the resolution of a scanner is mostly determined by the strength of the magnetic field produced by this current. This static magnetic field is oriented in the direction of the bore in which the participant lies.

The basis of NMR is that since protons have a small positive charge and they spin on an axis, they produce a small electric current and consequently a magnetic field perpendicular to that current. The spinning protons (spins) in the body are typically randomly orientated. However, when subject to an external magnetic field such as the static field in an MRI scanner, spins align at a particular angle from that field and precess around it (www.mrinotes.com/; www.simplyphysics.com/). Spins of different nuclei have unique gyromagnetic ratios: the ratio of the spin's magnetic moment (its field strength) and angular momentum (its tendency to continue to spin). The rate at which a spin precesses (the Larmor frequency (ω)) is dependent on the gyromagnetic ratio (g) and is linearly related to the strength of the magnetic field (B_0):

$$\omega = gB_0$$

Protons aligned with a magnetic field can be in either a low-energy parallel state, precessing around the direction of the magnetic field, or a high-energy antiparallel state, precessing around the direction opposite to the magnetic field. There is a slight excess of atoms in the lower energy state, so the longitudinal component of magnetisation is in the direction of the applied field. The transverse component of the magnetisation (perpendicular to the applied field) is zero since spins are out of phase and cancel each other out.

When nuclei in magnetic fields are subjected to RF pulses, they are forced into the higher energy state; then as they relax to the lower energy state, they emit RF energy (Bloch et al., 1946; Purcell & Torrey, 1946). The switch to the high-energy state reduces the longitudinal component of the magnetic field, increases the transverse component and forces the spins to precess in phase. After an RF pulse, longitudinal magnetisation increases as the protons return to their original low energy state. The time taken to reach 63% of the original magnetisation is the T1 relaxation time, which is shorter for more dense tissues. The transverse component decays rapidly as spins are dephased by inhomogeneities in the local magnetic field caused by the charge of neighbouring atoms (T2 or spin-spin relaxation). Spin-spin interactions are affected by thermal motion, with faster dephasing in more solid materials. T2 is the time at which the transverse component has lost 63% of its original value. Inhomogeneities in the static magnetic field caused by imperfections in the magnet, tissue boundaries, the presence of metal and the de-oxygenation of haemoglobin also result in different

spins being subjected to slightly different field strengths. As a consequence, they spin at different frequencies, causing further dephasing and further shortening of the transverse magnetisation relaxation time, to what is known as T_2^* relaxation time. The signal measured in MRI is the transverse magnetic field (B_1) created by the RF pulse, which is measured by an RF receiver. The profile of the amplitude of B_1 as it decays over time with T_2^* relaxation is known as Free Induction Decay (FID; Figure 2.1).

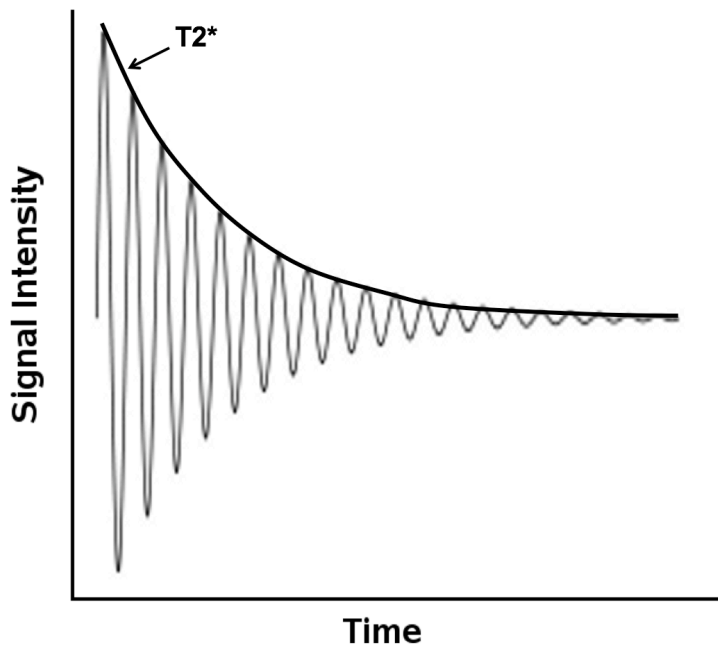


Figure 2.1. Free induction decay fMRI signal, reflecting the decrease in transverse magnetisation after application of an RF pulse.

To generate MRI images, a combination of pulses from gradient and RF coils are used. The largest possible transverse signal is generated by a 90° RF pulse. In a typical spin-echo sequence, a 90° pulse is applied and an FID signal is obtained as spins dephase and longitudinal magnetisation increases while transverse magnetisation decreases. A 180° pulse then flips the spins so that they begin to rephase, increasing the transverse component to a peak at twice the time between the 90° and 180° pulses (the echo time, TE). Several of these sequences are used and the repetition time (TR) is the time between successive 90° pulses. Echo amplitude varies across tissues due to differences in their T1 and T2 relaxation properties, and their proton density (the number of protons per unit volume). The signal also depends

on the TR and TE chosen: if TE is increased, more T2* relaxation will have occurred by the time of measurement so the echo signal will be smaller and there will be a greater difference between the echoes of different tissues. If TR is reduced, the longitudinal component will not have fully recovered by the next 90° pulse, so differences between T1 relaxations of tissues are measurable. The transverse component and consequently the T2* relaxation curve and echo signal will also be reduced. TE and TR are therefore selected depending on whether T1 or T2-weighted images are desired.

In order to localise the signals obtained, magnetic field gradients are used to manipulate the static magnetic field strength in all three dimensions, changing the Larmor frequency to different extents along the gradients. Since RF pulses only rotate the longitudinal component of the magnetic field when applied at the same frequency as the rotation of spins, RF pulses applied to a band of frequencies in the desired position along the gradient allow selective stimulation of slices. Slice thickness can be changed by altering the bandwidth or the gradient strength. Gradients can also be used to localise the source of signals measured with the RF receiver, allowing creation of images. A gradient applied in the 'phase encoding' direction creates a phase difference between spins in this plane and a gradient in the orthogonal direction alters the frequency of spins in the 'frequency encoding' plane. Each voxel therefore has distinct frequency and phase characteristics depending on its position. Applying a Fourier transform converts the data acquired to the spatial frequency domain. A k-space map is produced in which each position in k-space corresponds to a time point and contains a 2D sinusoid with a particular amplitude and spatial frequency representing the signal at that point in time. The application of magnetic field gradients allows all locations in k-space to be sampled, with the phase encode gradient sampling a new row every TR and the frequency encode gradient sampling across the row in k-space every TR. The k-space image is Fourier transformed to give an image, with low frequency components of k-space (the inner rows) containing information about contrast in the image and high spatial frequency components (the outer rows) containing information about the detail of structures in the image (Moratal, Vallés-Luch, Martí-Bonmatí & Brummer, 2008).

2.1.2 Functional magnetic resonance imaging (fMRI)

fMRI measures changes in blood flow, blood volume and oxygen consumption in the brain (Fox & Raichle, 1986; Vazquez et al., 2010), which are together represented in the blood oxygen level-dependent (BOLD) response (Ogawa et al., 1990). To obtain a BOLD signal, fMRI makes use of the fact that deoxyhaemoglobin is paramagnetic (slightly attracted to a magnetic field) as it has unpaired electrons, while oxyhaemoglobin is diamagnetic (slightly repelled by a magnetic field). Deoxyhaemoglobin creates inhomogeneities in the magnetic field, resulting in more rapid dephasing of spins which can be detected in T2 and T2*-weighted MRI sequences (www.fmrib.ox.ac.uk/education/fmri/introduction-to-fmri/).

In response to stimulation, the BOLD response produces a typical signal profile known as the haemodynamic response function (HRF; Figure 2.2). Initially, blood oxygenation decreases as active neurons use oxygen for glucose metabolism, creating an ‘initial dip’ in the HRF, although this is not a universally accepted phenomenon. Blood flow to the active area then increases to a peak about six seconds after stimulus onset. Blood oxygenation rises and exceeds demand, so deoxyhaemoglobin concentration is reduced and the T2* signal is increased. Blood flow then decreases and oxygenation falls below the initial baseline (‘post-stimulus undershoot’) at about 10 seconds, before returning to baseline by around 20 seconds after the stimulus. The level of haemodynamic activity in an MRI voxel is defined by how closely the observed signal matches this typical profile.

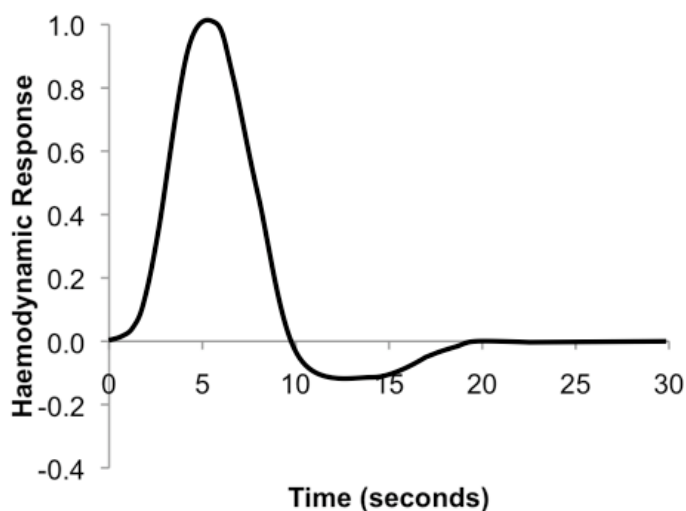


Figure 2.2. Typical fMRI haemodynamic response function (HRF) in arbitrary units.

The main advantage of fMRI is its excellent spatial resolution, which allows measurement of voxels of a few millimetres isotropic dimensions at typical (3 tesla) MRI field strengths, or as low as 1mm isotropic at high (7 tesla) field strengths (Olman & Yacoub, 2011). A disadvantage of fMRI is that it measures the haemodynamic response in the brain, rather than neuronal activity, and it also has poor temporal resolution, as this response takes a few seconds to propagate (Buxton, Wong & Frank, 2005).

2.2 Magnetic Resonance Spectroscopy

2.2.1 Signal generation

Magnetic resonance spectroscopy (MRS) employs similar hardware and principles as magnetic resonance imaging (MRI), but rather than producing images, it gives information about the relative concentrations of different molecules present in the volume of interest, derived from differences in absorption and emission of electromagnetic radiation from these molecules (De Graaf, 2007). In addition to the influence of the magnetic field strength and the gyromagnetic ratio, the resonance frequency of nuclei depends on their chemical environment. Electrons in nuclei rotate along the principle static magnetic field (B_0), perpendicular to proton precession, and slightly shield the nucleus from the magnetic field. The more electrons in a molecule, the more shielding occurs and the more the spin's precession frequency is reduced. This effect is known as chemical shift. It is quantified as the ratio of the frequency of the molecule of interest to a reference molecule, multiplied by a constant that accounts for variables specific to the scanner and the acquisition. Chemical shift is therefore reported in the field independent units of parts per million (ppm), so regardless of field strength, metabolites are always at the same known positions on the chemical shift axis. However, the frequency of the reference can differ between scanners so the concentration ratios are reported in institutional units. The molecule used as a reference is generally a chemically inert compound of which the concentration within the voxel is known or can be accurately estimated, such as water, creatine or the methyl component of N-acetyl aspartate (NAA). Methods of quantification may involve 'external referencing' to quantities of solutions in phantoms, or 'internal referencing' to a voxel within the participant. Internal

referencing is beneficial as the reference is acquired from the same session as the metabolite of interest, so issues with voxel position and instability in the system over time are minimised. However, internal referencing is not ideal when comparing patient and control populations, as the two groups may show different concentrations of the reference molecule (Bogner et al., 2010).

In MRS spectra, signal amplitude is plotted along the chemical shift axis with the area under peaks representing the concentration of the metabolite with that particular chemical shift value (Figure 2.3). Molecules with more electrons and therefore more shielding such as lipids appear lower on the spectrum (on the right hand side of the x axis, which is plotted from high to low frequency). The quality of a spectrum depends on the line width, which determines the resolution of peaks; and on the signal to noise ratio, which determines the height of metabolite peaks in comparison to noise. The signal to noise ratio (SNR) in a spectrum can be increased by using longer acquisitions from which more spectra can be averaged, or by increasing the voxel size to obtain more signal. Spectral quality is reduced by small variations in the magnetic field induced by magnet imperfections or proximity to regions of high magnetic susceptibility such as bone, water, cerebro-spinal fluid (CSF) or haemorrhages (Gujar et al., 2005).

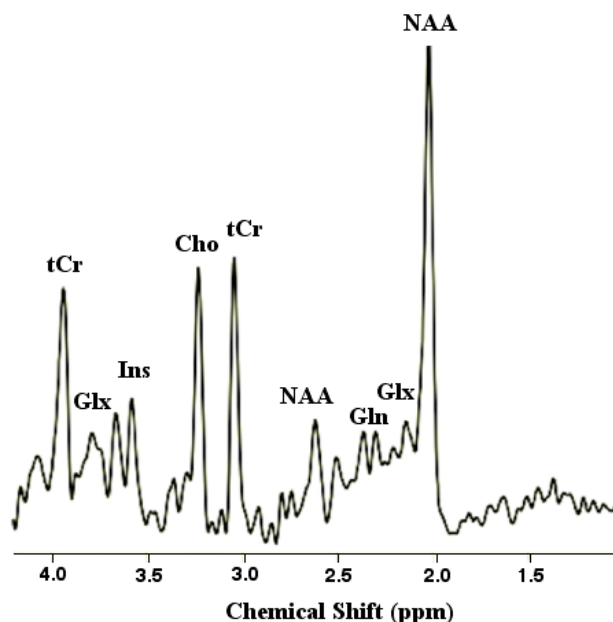


Figure 2.3. Example of an MRS spectrum. The area under the peaks represents the concentration of molecules with that chemical shift (adapted from limpeter-mriblog.blogspot.co.uk/2009_08_01_archive.html).

MRS is typically based on the signal from hydrogen protons because they have the highest gyromagnetic ratio, they are abundant so give a higher signal-to-noise ratio, and they form functional groups with specific resonances, allowing separation of signals from within metabolites (Barker & Lin, 2006). Coupling between hydrogen and larger atoms influences the position of molecules on the chemical shift axis, with a greater effect the fewer the number of bonds separating the larger atom and the hydrogen. Subpeaks can be identified from a single molecule with more than one hydrogen atom, as hydrogen spins can be in one of two orientations (up or down). In molecules with two hydrogen atoms, if both of these spins are up, the spectral peak will be at a higher ppm than the molecule's normal spin frequency; if both are down, the peak will be at a lower ppm. With more than two hydrogen spins, multiple subpeaks are produced, with different amplitudes depending on the proportion of spins in each potential combination of orientations.

In MRS, once the cortical region(s) and molecules for which the signal is to be obtained are decided, the sequence and processing parameters are customised accordingly. Signal can be acquired from a single voxel or from multiple voxels simultaneously using a hybrid MRS and imaging (MRSI) or chemical shift imaging (CSI) experiment. In single voxel MRS, there are two main techniques for localisation of signals based on the area of intersection of three RF pulses applied in orthogonal directions. Stimulated echo acquisition mode (STEAM) uses three 90° pulses, while point resolved spectroscopy sequence (PRESS) uses one 90° pulse and two 180° refocusing pulses. The first pulse creates transverse magnetisation. Spin-echoes are obtained from the following pulses, which are applied in different orientations, and only signals that are intersected by the three planes remain. Signals from non-desired regions are eliminated by 'crusher' gradients, which dephase the spins (De Graaf, 2007). The signal from water must also be suppressed, as it is several orders of magnitude larger than the signal from the metabolites of interest. MEGA water suppression involves applying an even number of 180° refocusing pulses at the water frequency, dephasing its signal (Mescher, Merkle, Kirsch, Garwood & Gruetter, 1998; Barker & Lin, 2006). The experiments described in this thesis use a PRESS pulse sequence with MEGA water suppression.

Since neurotransmitters are generally present in low concentrations in the brain, their peaks on the chemical shift axis can be hidden by molecules with higher concentrations. There are three potential ways of reducing signal overlap in a spectrum: spectral editing, in which sequences are designed to enhance the signal at certain positions on the chemical shift spectrum; separating signals out on another frequency dimension (two-dimensional MRS); and using higher field strengths (Puts & Edden, 2012). Spectral editing was used in this project to isolate the signal from the neurotransmitter of interest, gamma-aminobutyric acid (GABA).

2.2.2 GABA-edited spectroscopy

Methods capable of quantifying the principle inhibitory neurotransmitter in the brain, GABA have only recently been developed. The molecule has three methylene (CH₂) groups (Figure 2.4) with signatures at 1.9, 2.3 and 3.0ppm. The signals at 3.0ppm and 1.9ppm are coupled. In a GABA-edited MRS pulse sequence, a 180° frequency selective pulse at 1.9ppm therefore affects the 3.0ppm GABA signal but has no effect on non-GABA signals at 3.0ppm (De Graaf, 2007). There will be signals at 1.9ppm caused by the direct effect of the pulse and at 3.0ppm caused by coupled signals (Puts & Edden, 2012). The signal obtained with this editing pulse (the “on” spectrum) is subtracted from the signal of an acquisition with the pulse on the opposite side of the water peak (the “off” spectrum), so that the resulting difference spectrum only contains signals affected by the pulse (Barker & Lin, 2006). This procedure is known as J-difference editing. The on and off spectra are acquired in interleaved acquisitions in order to minimise potential subtraction artefacts from instrumental factors or participant movement.

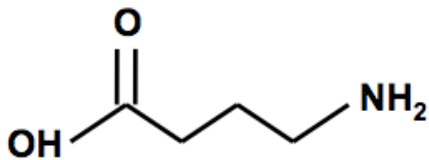


Figure 2.4. Gamma aminobutyric acid (GABA) molecule.

GABA is produced from glutamate by glutamic acid decarboxylase (GAD) and is metabolised to succinic acid semialdehyde by GABA transaminase (GABA-T) (Gupta, Jansen, Senephansiri, Jakobs, Snead, Grompe et al., 2004). Phasic

GABAergic inhibition occurs when action potentials in interneurons trigger the release of GABA from presynaptic vesicles. GABA diffuses across the synaptic cleft and binds to receptors on several postsynaptic pyramidal cells, opening chloride and bicarbonate channels (Gonzalez-Burgos & Lewis, 2008). Negatively-charged ions enter the cell and cause hyperpolarisation, inhibiting cell firing (Kuffler & Edwards, 1958). This change in charge is known as an inhibitory postsynaptic potential (IPSP). After the IPSP, there is a higher likelihood of synchronous firing (Farrant & Nusser, 2005; Gonzalez-Burgos & Lewis, 2008). Phasic inhibition is relatively temporally and spatially specific and is dependent on action potentials, whereas tonic GABAergic inhibition is indirect and independent of action potentials. It is brought about by low concentrations of GABA in the extracellular space, which act on GABA-A receptors on non-synaptic regions of neurons (Buzsaki et al., 2007). There are two main subtypes of GABA receptor on post-synaptic cells that mediate the synaptic effects of GABA. GABA-A receptors are ligand-gated chloride channels, while GABA-B receptors are GTP binding proteins that conduct calcium and potassium (Young & Chu, 1990). GABA transporters remove excess GABA from the synaptic cleft (Bernstein & Quick, 1999). There are also extrasynaptic GABA receptors, which pick up GABA released but not taken up at the synapse (Farrant & Nusser, 2005).

Although 15-20% of the brain's neurons are GABAergic (Rothman, Petroff, Behar & Mattson, 1993; Bogner et al., 2010), the concentration of GABA is only around 1 micromol/cm³ (Bogner et al., 2010). The size of a GABA-edited MRS voxel at 3 Tesla must therefore be 2-3cm in all three dimensions in order to achieve sufficient signal to noise, therefore the spatial resolution of MRS is very low.

2.3 Magnetoencephalography

2.3.1 Signal generation

Magnetoencephalography (MEG) records magnetic fields generated by active neurons and allows estimation of their probable source within the brain. It was first used to show magnetic fields outside the scalp generated by alpha band oscillations (Cohen, 1968). It is a non-invasive, silent technique and unlike MRI, MEG does not require the use of strong magnetic fields. MEG also directly measures neuronal activity and has extremely high temporal resolution, whereas MRI measures haemodynamic

changes that take a few seconds to occur. MEG does not have the spatial resolution of MRI, but can still discriminate peaks in activity a few centimetres apart. The spatial resolution of MEG is better than that of electroencephalography (EEG), which measures the electrical currents generated by neuronal activity. This is because electrical currents are conducted differently by different tissues and the conductivity profile of the head is not known; however, for MEG this is not important as magnetic fields are unaffected by tissues.

MEG signals are produced by post-synaptic potentials (PSPs) in the dendritic processes of pyramidal neurons (Singh, 2006). Action potentials cause a change in the permeability of the post-synaptic membrane to ions, inducing an electrical current. These currents are known as inhibitory or excitatory PSPs, depending on whether the result is hyperpolarisation or depolarisation of the neurons. A magnetic field is produced in the perpendicular orientation to the electric current. These magnetic fields are very weak, so in order for them to be measurable, there must be synchronous activity of thousands of similarly oriented neurons, otherwise the current would be distributed in all directions and the signal would sum to nothing. MEG signals do not reflect action potentials, as these are too fast to allow summation of their signals. However, in the regularly aligned dendritic processes of pyramidal neurons, PSPs can be summed and detected using MEG (Baillet, Mosher & Leahy, 2001).

The current circling in the dendritic processes of neurons is known as the primary current. A secondary extracellular signal known as the volume current is also produced as a result of the electric field on extracellular charge carriers (Baillet et al., 2001). MEG primarily measures the primary current because magnetic fields from volume currents in a spherically symmetric conductor cancel out. EEG only measures the secondary volume currents because the sensors are in contact with the medium (Hämäläinen & Hari, 2002). Since magnetic fields circle perpendicularly to the current source, signals cannot be measured optimally from all areas of the cortex: if we consider the head to be perfectly spherical (a common model), magnetic fields in the bottom of sulci and the crests of gyri (both radial sources) are cancelled by fields from the secondary volume currents. However, there are few truly radial sources in the brain (Hillebrand & Barnes, 2002); most sources project anteriorly-posteriorly or

left-right (tangential sources), so are measurable. MEG is not as sensitive to sources deep in the brain, since magnetic fields fall off rapidly with distance; however, it is possible to measure from deep structures if the signal to noise is high (Tesche & Karhu, 2000; Cornwell, Johnson, Holroyd, Carver & Grillon, 2008).

Magnetic fields produced by the brain are in the order of 50-500fT (Hämäläinen, Hari, Ilmoniemi, Knuutila & Lounasmaa, 1993), which is thousands of times weaker than the earth's magnetic field and that of other sources of magnetic fields such as muscle movement, metal and electrical equipment. The MEG scanner therefore must be contained within a magnetically shielded room (MSR) to exclude any interference from outside the room and superconducting devices must be used to measure the signals (Cohen, 1972). In an MEG system, sensors detect the magnetic fields and pick-up coils transfer these signals to superconducting quantum interference devices (SQUIDS). SQUIDS are coils with breaks in them across which current flows and is modulated by the magnetic field. They convert the magnetic fields to electric signals and amplify them. The SQUIDS must be kept at very low temperatures (4K or -269°C) to maintain their superconducting properties. The signal acquired is digitised, ensuring the sampling rate and bit depth are high enough to accurately portray the genuine signal. It is filtered to remove noise and manually checked for artefacts.

The pick up coils that transfer signals to the SQUIDS and help to remove external magnetic noise can be gradiometers or magnetometers. Axial magnetometers have one coil, so measure the field at one location and are sensitive to noise from outside the area of interest. First-order axial gradiometers have two coils, one above the other, wound in opposing directions. Since magnetic fields decay with distance from the source, the difference in the measurement from the two coils can be used to exclude signals from distant sources, as these show little difference between the two sensors. Second order gradiometers have another coil on top of this so are even more sensitive to signal decay, but are difficult to manufacture. Magnetometers can be used to synthetically create third order gradiometers during post-processing. First order planar gradiometers have two coils wound in a figure of eight. The topographic maps of activity generated by axial and planar gradiometers look very different: axial gradiometers record peaks of opposite polarities entering and leaving the head on

opposite sides of the source current dipole; whereas planar gradiometers measure a single peak above the dipole.

2.3.2 Analysis of signals

MEG signals are measured in sensor space (in relation to the position of the sensors) and then ideally are converted to source space (in relation to an individual's brain anatomy). Using source space allows virtual sensors to be placed, restricting analyses to a limited number of locations and reducing multiple comparisons issues. Localisation of sources involves identifying the likely source in the brain of the acquired signals by comparing the signals obtained with simulated signals that would be predicted from the solution to the forward model (Hämäläinen & Hari, 2002). The forward problem in MEG involves identifying the magnetic fields that would be generated from a source of known location, magnitude and orientation – this is known as the lead-field for that location. There is a unique solution to this problem as there is only one possible distribution of external magnetic fields that can be generated by a specific current distribution. Conversely, the inverse problem involves identifying the location and power of the source, given the external magnetic field. There are an infinite number of possible combinations of sources that could generate the measured fields (non-uniqueness), so it is impossible to find the solution to the problem from the acquired data alone. Additional information about the spatial or temporal nature of the currents is required (Hämäläinen et al., 1993). The forward model can be solved with spherical models, assuming the head is a set of concentric spheres representing the brain, skull and scalp; or by using MRI scans to extract more accurate surface boundaries for these tissues (Baillet et al., 2001). There are several different approaches to solving the inverse problem to localise sources and different techniques are more effective for different types of data (Singh, 2006).

Dipole fitting involves estimating the source location, simulating the magnetic field that would be given by a dipole at this location then varying the position, orientation and field strength to achieve the best fit between the data and the simulation. If the fit does not reach a statistical threshold, another dipole is added to the simulation until the fit improves. This method works well for simple sources, but with more complex sources, the correct pairings of dipoles are difficult to identify. Current density modelling assumes the sources are distributed and uses information about the brain to

estimate the most likely distribution of current in the brain that could generate the acquired signal. For example, a minimum-norm estimate (MNE) aims to explain the obtained data with the solution that has the minimum overall power while still minimising the difference between measured and estimated fields. However, the result obtained may not be physiologically valid as it often gives widespread activity when more localised peaks are expected (Somersalo, 2007). Minimum-current estimates (MCE) aim to explain the data with the minimum possible number of sources. These models are biased towards superficial sources as the current required to explain the data is smaller with sources closer to the sensors. This bias can be corrected using a-priori information such as weighting the solution so that deeper sources will be more likely, or the use of other spatial information, such as fMRI, as a prior. Statistical parametric maps (SPMs) can be used to reflect the confidence in the estimated sources by presenting spatial maps of test statistics (Hämäläinen & Hari, 2002). Minimum-norm models are generally used to localise evoked responses, while beamformers are used for induced responses.

Beamformers estimate the contribution of a single location in the brain to the measured field (Vrba & Robinson, 2001; Hillebrand, Singh, Holliday, Furlong & Barnes, 2005). Weights are created for each point in source space from the lead field and the covariance of the channels contributing to the signal at that location. A signal in a particular location is therefore represented by a linear combination of weighted sensors and signals from elsewhere are attenuated. Beamforming aims to minimise the variance and maximise the projected power at a particular location. Synthetic aperture magnetometry (SAM) is a beamformer algorithm that assumes the data are generated by discrete dipolar sources and that the sources are not temporally correlated with each other. Simultaneous events therefore cannot be localised. With beamforming, there is no need to specify the number, position or orientation of dipoles a priori or to average the data in the time domain. After generation of the weights, a statistical parametric map is computed to show changes in the signal in the voxels across the task duration (Barnes, Hillebrand, Fawcett & Singh, 2004). Virtual sensors can be calculated for any point of interest within the source space. These allow estimation of activity at that location as if a sensor had physically been placed at that point.

MEG can be used to record activity which is phase-locked to the onset of stimuli by averaging in the time-domain across many trials, cancelling out noise and leaving only the typical response to that stimulus. These signals are known as evoked fields. Steady-state evoked fields can be generated through several brief presentations at a fixed frequency, which drives oscillations at the stimulation frequency or its harmonics. In addition, MEG can also be used to measure induced oscillatory responses, which are time- but not phase-locked to stimuli. As these responses are out of phase, averaging them in the time domain would leave little or no signal. However, averaging in the Fourier domain shows changes in activity in particular frequency bands of neuronal oscillations in response to the stimulus (Hämäläinen et al., 1993).

Oscillations in different frequency bands are believed to represent different states of activity or different functions. As a brief summary, delta (0-3Hz) band oscillations are present during deep sleep (Crunelli & Hughes, 2009); theta (4-7Hz) oscillations may be involved in working memory (Tesche & Karhu, 2000); alpha (8-12Hz) oscillations occur in resting cortex (Pfurtscheller et al., 1996); beta (13-30Hz) waves are associated with active thought and muscle contraction (Murthy & Fetz, 1992); while gamma (30-100Hz) activity may reflect basic processing of sensory stimuli (Singh, 2012). Sub-bands within the gamma range have also been described (Buzsaki & Wang, 2012). MEG can localise evoked and induced signals with a degree of spatial accuracy that is not as good as fMRI, but which is better than electroencephalography (EEG).

Oscillatory signals from a particular sensor or virtual sensor can be plotted on a time frequency analysis spectrogram; in which the change in amplitude at different frequencies is plotted throughout the period of measurement. Values during an active period are contrasted with a baseline phase, to give the percentage change from the mean of the baseline period, averaged over all the trials. The terms event-related synchronisation (ERS) and desynchronisation (ERD) are often used to describe increases or decreases in the amplitude of oscillatory signals, though the responses could either represent a change in the synchronicity of neuronal firing or a change in the overall power detected. The amplitude of oscillatory signals is the peak-to-peak height of the waveform, power is the amplitude squared, while phase is angle of the

sine wave at a particular sampling point. Phase locking factors show how consistent phase is across trials on a scale of 1 (completely synchronised) to 0 (completely desynchronised).

The methods described above all give non-invasive measures of the structure or function of the human brain, allowing the investigation of various aspects of visual processing.

Chapter 3

Negative BOLD Responses Vary with Stimulus Contrast, Spatial Frequency and Position

3.1 Abstract

Functional magnetic resonance imaging (fMRI) can be used to measure decreases in the blood oxygen level-dependent (BOLD) response in non-stimulated areas of cortex, in addition to the more commonly reported increases in BOLD in stimulated regions. These ‘negative BOLD’ responses have been shown to vary with stimulus contrast (Shmuel et al., 2002) and position (Wade & Rowland, 2010), but their spatial frequency tuning profile has not previously been described in humans. This series of experiments investigated the influence of stimulus spatial frequency, contrast and position on both positive and negative BOLD in primary visual cortex. In response to a centrally-presented stimulus, negative BOLD in the cortical representation of the surround and positive BOLD in the centre both increased with stimulus contrast. On the other hand, spatial frequency tuning of negative BOLD in the surround was lowpass, whereas central positive BOLD showed a bandpass profile. With increasing eccentricity, there are more visual cortical neurons sensitive to lower spatial frequencies (De Valois, Albrecht & Thorell, 1982), therefore the negative BOLD response profile may reflect underlying neuronal stimulus preferences. The difference between the profiles of positive and negative BOLD to spatial frequency also suggests that negative BOLD is not dependent on the amplitude of the positive BOLD response. Negative BOLD was not induced at the fovea by a surrounding annulus or a small parafoveal stimulus, regardless of the location or timing of an attentional task, suggesting that the presence even of a small fixation cross prevents generation of negative BOLD at the fovea. Future studies could investigate whether negative BOLD contributes additional information regarding stimulus processing to that provided by positive BOLD; how stimulus-specific information is transferred to non-stimulated cortex; and what the role of negative BOLD may be in stimulus perception.

3.2 Background

Functional magnetic resonance imaging (fMRI) studies typically describe increases in the blood oxygen level-dependent (BOLD) response (Ogawa et al., 1990) as a result of manipulations imposed. In addition to stimulus-related increases in BOLD, a reduction below baseline levels can also be observed in non-stimulated cortex when a stimulus is presented elsewhere (Tootell, Mendola et al., 1998; Smith et al., 2000; Shmuel et al., 2002), although the role of this response in stimulus processing is not yet entirely clear. If this negative BOLD can be shown to vary with stimulus features, particularly in a manner independent of the positive BOLD response, it could be inferred that non-stimulated regions have an active role in processing of these features.

Positive BOLD in visual cortex has been reported to differ with various stimulus features: it increases with stimulus contrast (Boynton et al., 1999), shows bandpass spatial and temporal frequency tuning (Singh et al., 2000) and is enhanced for oblique as opposed to cardinal stimulus orientations (Mannion et al., 2010). These responses correlate with neuronal activity (Logothetis, 2002) and behavioural performance (Boynton et al., 1999; Singh et al., 2000; Mannion et al., 2010), indicating that positive BOLD is a meaningful marker of stimulus processing.

Negative BOLD tends to be weaker and more diffuse than positive BOLD (Harel et al., 2002; Shmuel et al., 2002; Boorman et al., 2010), but has also been reported to show stimulus specificity. In human primary visual cortex (V1), negative BOLD increases with stimulus contrast (Shmuel et al., 2002); shows weaker responses for red-green as opposed to blue-yellow stimuli (Wade & Rowland, 2010); increases with distance from the stimulus, before decreasing again (Heinemann et al., 2009); and even allows prediction of stimulus eccentricity when analysed with pattern matching techniques (Bressler et al., 2007). In cat visual cortex, negative BOLD has been reported to show bandpass spatial frequency tuning, in a profile that was proportional to that of positive BOLD (Harel et al., 2002). These findings of differential negative BOLD responses depending on stimulus features suggest that negative BOLD is not simply a constant response to any stimulation. It may even influence behaviour: medial nerve stimulation decreases BOLD in ipsilateral somatosensory cortex and subsequently increases detection thresholds for vibrotactile stimulation of the

contralateral finger (Kastrup et al., 2008). Assessments of the contribution of stimulated and non-stimulated cortex to measures of behavioural performance, neuronal activity and haemodynamic activity may therefore provide a more complete understanding of stimulus processing than analysis of stimulated areas alone.

Processing of particular stimulus parameters often depends on the underlying neurophysiology of the cortex, since some neurons are specialised for detection of specific features. For instance, in spatial frequency selective columns of neurons in visual cortex, the preferred frequency decreases with eccentricity (Movshon, Thompson & Tolhurst, 1978; Tootell et al., 1981; De Valois et al., 1982; Xu, Anderson & Casagrande, 2007). In humans, this selectivity is reflected in behavioural and neuroimaging measures of responses to stimuli of different spatial frequencies in different areas of visual cortex: in central vision, spatial frequency tuning is bandpass with a peak around 3 cycles per degree (cpd) for behavioural detection (De Valois, Morgan & Snodderly, 1974) and between 1 and 4cpd for positive BOLD (Singh et al., 2000; Henriksson et al., 2008). However, in the periphery, perceptual (Wright & Johnston, 1983) and BOLD (Henriksson et al., 2008) responses peak at lower frequencies. On the other hand, as stimulus contrast increases, positive BOLD increases in all areas of visual cortex, in correspondence with increases in neuronal firing rate (Heeger, Huk, Geisler & Albrecht, 2000), local field potentials (Logothetis et al., 2001) and psychophysical detection. With changes in stimulus contrast, the same neuronal populations are recruited but show an altered level of response, whereas variations in spatial frequency optimally stimulate only those neurons preferentially tuned for each spatial frequency.

Both positive and negative BOLD are strongly influenced by attention: when cued to attend to a particular area, increases in BOLD can be detected in the location of visual cortex corresponding to stimulation and decreases in BOLD are present in unattended areas (Somers, Dale, Seiffert & Tootell, 1999; Smith et al., 2000; Slotnick, Schwarzbach & Yantis, 2003; Sestieri, Sylvester, Jack, D'Avossa, Shulman & Corbetta, 2008). Even in the absence of visual stimulation, direction of attention to an area of the visual field increases BOLD in the corresponding visual cortex, perhaps due to top-down processes whereby anticipation of a stimulus increases neuronal activity and consequently the BOLD response (Kastner et al., 1998; Munneke,

Heslenfeld & Theeuwes, 2008; Sestieri et al., 2008). Negative BOLD responses have been proposed to reflect both top-down attentional suppression and bottom-up processing of distractor stimuli (Heinemann et al., 2009)

This series of experiments aimed to investigate positive and negative BOLD responses to stimulus contrast and spatial frequency; and to determine how these responses are affected by attention and stimulus position.

3.3 Experiment 1: Spatial frequency and contrast tuning to a central stimulus

3.3.1 Rationale

This experiment aimed to determine whether negative BOLD varies with stimulus spatial frequency in human visual cortex. If positive and negative BOLD responses are generated by the same mechanisms, or if negative BOLD is simply a by-product of the positive BOLD response, negative BOLD would be expected to show similar but lower amplitude tuning profiles to stimulus features as the positive BOLD response, as previously described in cat visual cortex (Harel et al., 2002). If on the other hand, positive and negative BOLD reflect independent neuronal processes of activation and suppression, negative BOLD might be expected to show a different profile in the surround region in which it was measured in this study, since neuronal preferences in the periphery are for lower frequency stimuli (De Valois et al., 1982). Contrast tuning in positive and negative BOLD was also measured, with the expectation that both would increase with contrast, with negative BOLD reaching lower amplitudes, as previously reported (Shmuel et al., 2002).

3.3.2 Methods

3.3.2.1 Participants and procedure

Participants (N=15, mean age 28.3 years, SD 3.8 years) were tested in two sessions: the first involved retinotopic mapping, an anatomical MRI scan and either the contrast or spatial frequency fMRI task; the second included a repeat of the retinotopic mapping, a functional localiser and the fMRI task not yet completed. The order of the contrast and spatial frequency tasks was randomised across participants.

3.3.2.2 MRI parameters

Data were acquired on a 3.0T GE HDx system (GE Healthcare, Chalfont St Giles, UK) using a body coil for transmission and an eight-channel receive-only head coil. T1-weighted anatomical images for coregistration were acquired with a 3D Fast Spoiled Gradient-Echo (FSPGR) sequence (TR/TE/inversion time = 7.8/3.0/450ms; flip angle = 20°; 1mm isotropic resolution). For the localiser, contrast and spatial frequency tasks, a gradient-echo echoplanar imaging (EPI) sequence, centered over the occipital cortex took twenty-two slices in 3mm isotropic voxels using a 64x64 matrix. The TR was 3.0s, TE 35ms and flip angle 90°. Retinotopic mapping parameters were similar, but with 37 slices at 2mm isotropic resolution and a 128x128 matrix.

3.3.2.3 Pre-processing

The fMRI data were analysed using the FMRIB software library (FSL; www.fmrib.ox.ac.uk/fsl). Preprocessing parameters were as follows: motion correction using MCFLIRT (Jenkinson, Bannister, Brady & Smith, 2002); non-brain removal with BET (Smith, 2002); spatial smoothing using a Gaussian kernel of full-width-half-maximum (FWHM) 0.5mm for the retinotopic mapping, 5mm for the contrast and spatial frequency tasks and no smoothing for the localiser; high-pass temporal filtering and gamma convolution of the haemodynamic response function. The fMRI data were initially registered to a whole-brain EPI with equivalent field of view and slice thickness to the fMRI sequence, then to the individual's FSPGR.

3.3.2.4 Retinotopic mapping

Since vision is represented topographically in the brain, functional MRI can be used to map the visual cortex (Belliveau et al., 1991). To obtain these retinotopic maps, the response to stimuli at different visual angles and stimulus eccentricities is plotted on flattened images of the visual cortex and the boundaries between visual areas (defined by the midpoint of the representation of the vertical meridian) are identified (Serenio et al., 1995; DeYoe et al., 1996; Engel et al., 1997).

Using in-house software, phase angle estimates (Φ) were calculated and automatically corrected for the haemodynamic lag by taking the average phase angle from clockwise and anticlockwise runs in each voxel after reflecting the data from one

direction around a phase angle of zero. An estimate of the strength of retinotopy (r) was given by the correlation between the phase angle of the predicted and measured timeseries at a frequency of 1rpm. A measure of the similarity of the phase angle represented in each voxel between the two sessions of retinotopic mapping was then obtained using the formula

$$sim = (1 - (|\Phi_1 - \Phi_2| / \pi)) * r_1 * r_2$$

Voxels with a high phase angle correlation coefficient and a similar phase angle in both sessions therefore have a high *sim* value. The session-averaged phase angles were visualised as a colour overlay on participants' flattened occipital cortices in mri3dX (<https://cubic.psych.cf.ac.uk/Documentation/mri3dX/>), with the intensity of the coloured representation dependent on the similarity metric, *sim*. V1 regions of interest (ROIs) were defined from these data as the area between the calcarine sulcus and the midpoint of the first representation of the vertical meridian, both dorsal and ventral to the calcarine.

3.3.2.5 Functional localiser and ROI definition

Central and surround regions of the visual field were stimulated with a maximum contrast chequerboard, reversing at 7.5Hz. The central stimulus consisted of a ring around fixation of 0.5-2° radius, while the surround annulus was 2-11° radius (Figure 3.1A). The background and a 0.5° radius circle behind the fixation-cross were of mean luminance. The red fixation-cross at the centre of the screen subtended 0.6°. Surround, central and fixation-only stimuli were presented sequentially for 15 seconds each and this cycle was repeated eight times. Participants maintained fixation throughout this six-minute block. On FSPGR anatomical scans, individuals' occipital lobes were cut, opened along the calcarine sulcus (Figure 3.1B), then flattened using Freesurfer (Fischl, Sereno & Dale, 1999). Localiser data from central and surround chequerboard phases contrasted with the fixation-only baseline phase were used to define ROIs in the left and right hemisphere centre and surround (the sum of dorsal and ventral areas; Figure 3.1D). Retinotopic mapping data were used to ensure these ROIs were limited to V1.

3.3.2.6 Contrast and spatial frequency task stimuli

A circular sinusoidal grating patch reversing at 7.5Hz was presented in a 15s on/off boxcar. The stimulus subtended a 2° radius around fixation (Figure 3.1C). The two

tasks included four six-minute blocks, each containing three of the following stimuli: 0.5, 1, 3 and 6 cycles per degree (cpd) at maximum contrast in the spatial frequency task; and 0.1, 0.2, 0.4 and 1.0 Michelson contrast at 1cpd in the contrast task. This protocol resulted in a total of 12 presentations of each stimulus. Participants pressed a button when the fixation-cross turned from red to green (once per on/off period). The general linear model (GLM) was used to model a 15s on/15s off on boxcar for the task blocks and a fixed effects model obtained the mean BOLD response across the four blocks for each contrast and spatial frequency for each participant.

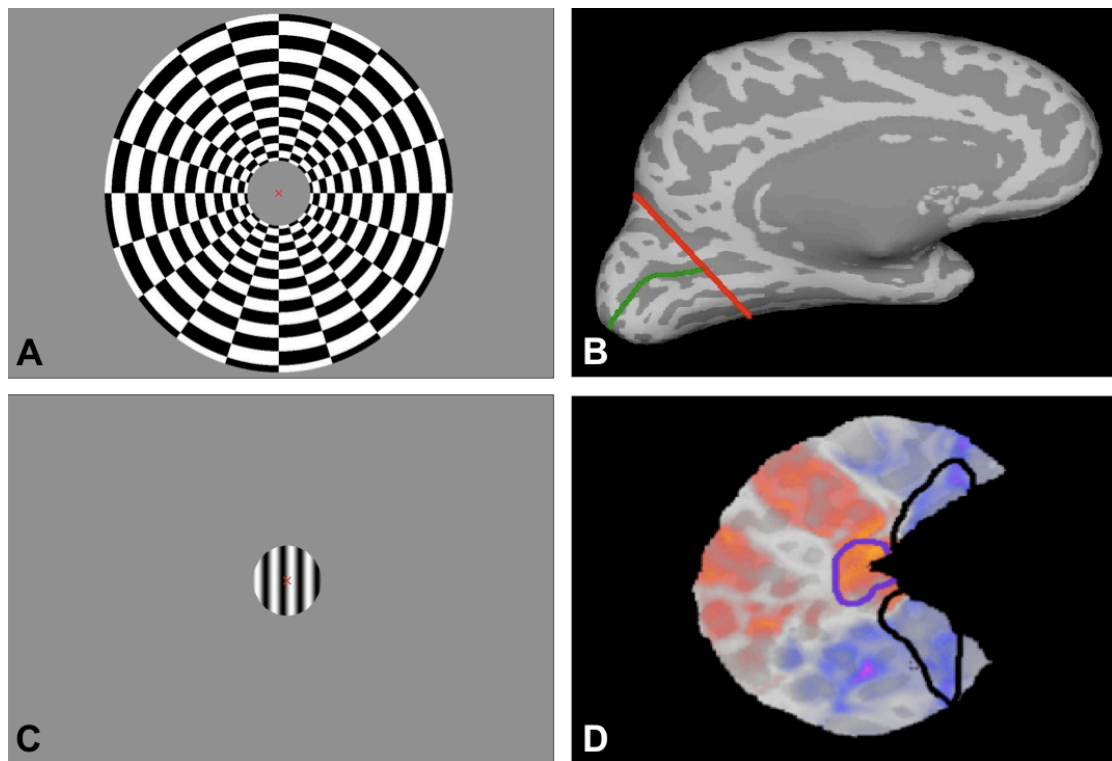


Figure 3.1. A) Localiser stimulus for the surround ROI. B) Left hemisphere mesh with occipital lobe (red) and calcarine sulcus (green) cuts. C) 1cpd, maximum contrast grating task stimulus. D) Left occipital flat map for a representative participant with central (purple) and surround (black) ROIs and the response to 1cpd, maximum contrast stimulus.

3.3.3 Results and discussion

3.3.3.1 Testing for the presence of positive and negative BOLD responses

BOLD responses were measured in arbitrary contrast of parameter estimate (COPE) values. Responses from left and right hemisphere ROIs were averaged to give overall mean positive and negative BOLD values for the central and surround regions. In

order to confirm that the stimulated central area of visual cortex contained a mostly positive BOLD response and that the non-stimulated peripheral surround area was mostly negative, the group mean percentages of positive and negative voxels within the ROIs were investigated using one-sample t-tests. There were significantly more than 50% positive voxels in the central ROI and more than 50% negative voxels in the surround ROI at all contrasts and spatial frequencies (all $t(14) > 3.51$; $p < .05$, Bonferroni corrected for eight t-tests per experiment). The group mean BOLD amplitude in the central ROI was also significantly greater than zero for all contrasts and spatial frequencies ($t(14) > 8.2$; $p < .05$, Bonferroni corrected). In the surround ROI, the response was smaller than zero ($t(14) > 2.32$; $p < .05$) for all contrasts other than 0.1 and for all spatial frequencies other than 3.0, although these differences did not survive correction for multiple comparisons. These results indicate that significant positive and negative responses occur in the anticipated regions, but that the negative response is weaker.

In order to determine the consistency of the positive and negative BOLD responses over the four blocks of each experiment, individuals' data were averaged across the four spatial frequencies and across the four contrasts. Two-way random model intraclass correlation coefficients with absolute agreement demonstrated that individuals' mean positive and negative BOLD were repeatable across the four blocks for both contrast and spatial frequency (all ICC $> .30$; $F(14,42) > 2.80$; $p < .001$). Similarly, the number of positive voxels in the central ROI and negative voxels in the surround ROI was consistent (ICCs $> .50$; $F(14,42) > 5.00$; $p < .001$).

For subsequent analyses, the dependent variable was the unthresholded mean BOLD amplitude from the positive voxels in the central ROI and from the negative voxels in the surround ROI. These BOLD amplitudes were normalised for each participant to a maximum of 1 for the greatest absolute response from the central and surround ROIs.

3.3.3.2 Contrast tuning results

The mean positive BOLD response in the central ROI increased with contrast ($F(3,42) = 81.26$; $p < .001$; Figure 3.2A), with significant differences at all levels apart from between 0.2 and 0.4 (all pairwise comparisons $p < .05$, Bonferroni corrected). Negative BOLD in the surround also increased with contrast ($F(1.6,22.7) = 13.86$;

$p < .001$, Greenhouse-Geisser) and pairwise comparisons indicated that the maximum contrast stimulus induced a greater response than the lower three contrasts (Bonferroni corrected $p < .05$). The percentage of positive voxels in the central ROI did not differ significantly with stimulus contrast ($F(2.1, 29.7) = 1.68$; $p = \text{ns}$, Greenhouse Geisser), though this may be due to a ceiling effect (Figure 3.2B). In the surround, there was a main effect of the percentage of negative voxels ($F(3, 42) = 2.98$; $p < .05$), but none of the pairwise comparisons reached significance. These results suggest that the greater BOLD amplitudes observed with increasing contrast can be attributed to an increased response within a similar proportion of active voxels within the ROIs.

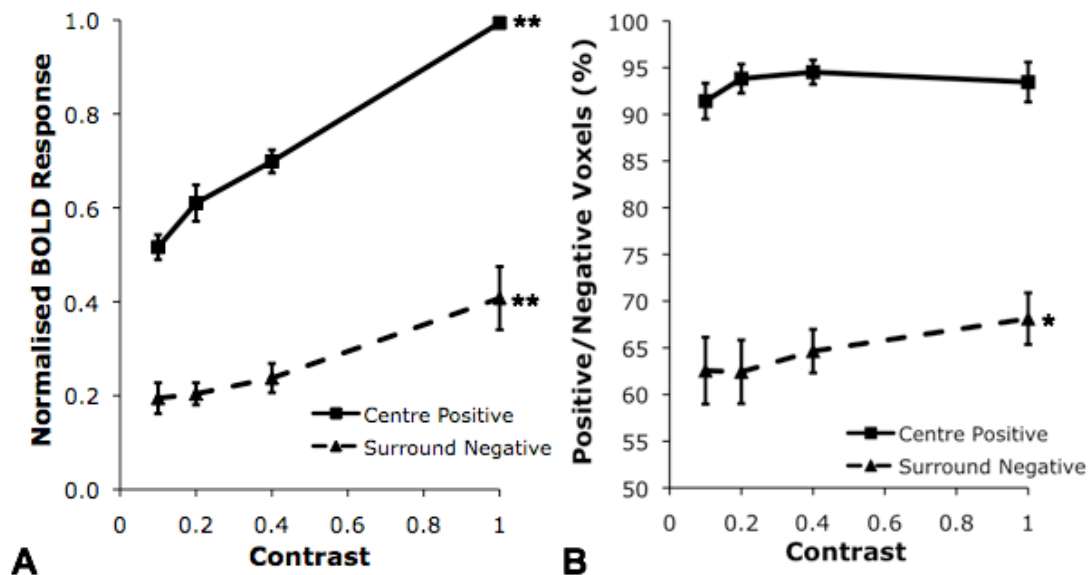


Figure 3.2A) The effect of stimulus contrast on mean BOLD amplitude (negative BOLD sign reversed for comparison with positive BOLD profile). B) The percentage of positive voxels in the centre and negative voxels in the periphery with different contrasts. Error bars show standard error of the mean, * = $p < .05$, ** = $p < .001$.

3.3.3.3 Spatial frequency tuning results

Mean positive BOLD amplitude showed the expected bandpass profile with a peak at 1cpd (Figure 3.3A). The main effect of spatial frequency on the positive BOLD response ($F(1.8, 25.6) = 18.05$; $p < .001$, Greenhouse Geisser) was attributable to a lower BOLD response to 6cpd gratings than to all other spatial frequencies (all pairwise comparisons $p < .05$, Bonferroni corrected), and to 0.5cpd gratings inducing a smaller

response than 1cpd gratings ($p < .05$). In the negative surround area, there was a main effect of spatial frequency on the mean BOLD amplitude ($F(3,42)=5.02$; $p < .05$), attributable to a greater response at 0.5cpd than at 3 and 6cpd (pairwise comparisons $p < .05$, Bonferroni corrected). The percentage of positive voxels in the central ROI varied with spatial frequency ($F(3,42)=5.09$; $p < .05$; Figure 3.3B) due to there being fewer positive voxels when the stimulus was 0.5cpd than 1cpd ($p < .05$). In the non-stimulated surround region, there was no significant effect of spatial frequency on the percentage of negative voxels ($F(3,42)=.29$; $p = ns$). These results again indicate a reasonably stable proportion of voxels responding positively or negatively to stimuli of different spatial frequencies.

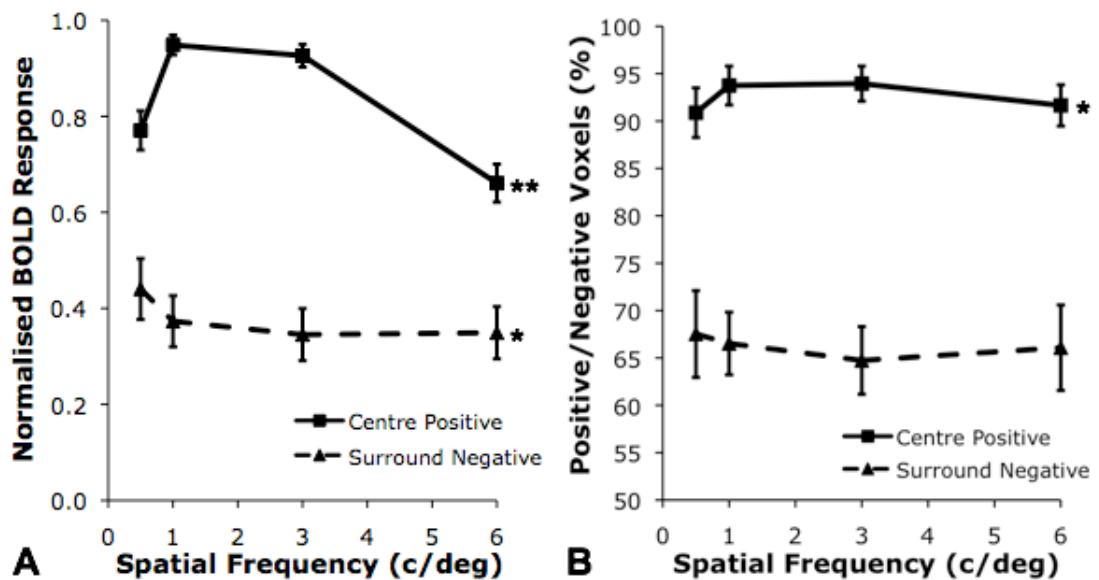


Figure 3.3A) The effect of spatial frequency on mean BOLD amplitude (negative BOLD sign reversed for comparison with positive BOLD profile). B) The percentage of positive voxels in the centre and negative voxels in the periphery with different spatial frequencies.

There were no correlations between the amplitude of individuals' positive and negative BOLD responses to any stimuli (Figure 3.4A&B; all $R^2 < .24$; $p = ns$), so BOLD increases and decreases in different parts of the cortex in response to the same stimulus appear to be unrelated to each other.

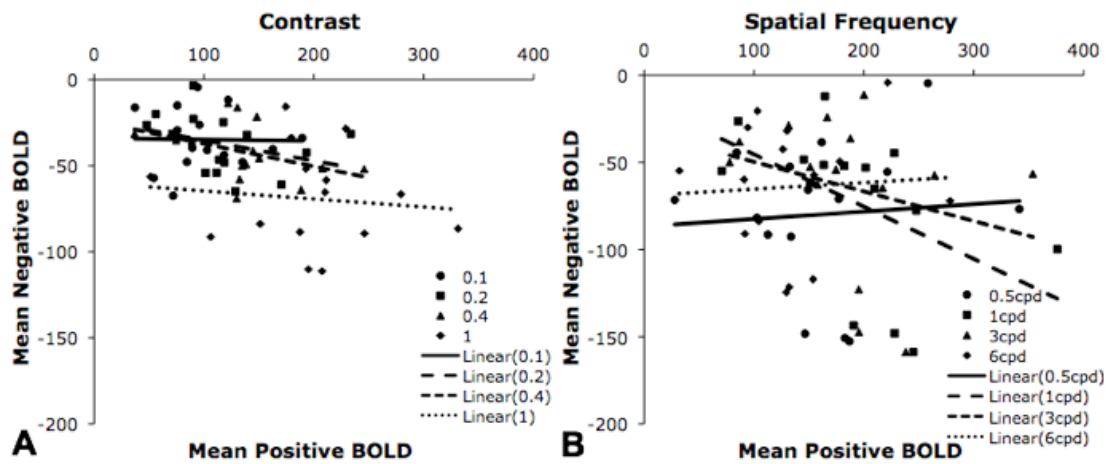


Figure 3.4. Correlation between positive and negative BOLD across participants (N=15) for each of the four contrasts (A) and spatial frequencies (B).

3.3.3.4 Discussion of stimulus tuning in response to a centrally-presented stimulus

The important finding from this experiment is that positive and negative BOLD amplitude tuning profiles were similar for stimulus contrast but different for spatial frequency. Since negative BOLD did not always change in proportion with positive BOLD, it is unlikely to be a “by-product” of positive BOLD or to represent blood steal. It is more likely that non-stimulated regions of cortex are actively involved in stimulus processing in addition to stimulated regions. Information about stimulus properties must therefore be transmitted to these areas from stimulated cortex.

Both positive and negative BOLD increased with stimulus contrast, replicating the findings of Shmuel et al. (2002). Negative BOLD tended to be about a third the amplitude of positive BOLD, similar to proportions previously reported (Harel et al., 2002; Boorman et al., 2010; Liu, Shen, Zhou & Hu, 2011). In the spatial frequency experiment, there was evidence that the BOLD response reflects underlying neurophysiological preferences: in peripheral areas where there are more neurons specialised for low spatial frequencies (De Valois et al., 1982; Jamar, Kwakman & Koenderink, 1984), the negative BOLD response was greatest for the lowest frequency presented; while in the centre, the largest positive BOLD response was observed at 1cpd. This negative BOLD profile contradicts previous findings that positive and negative BOLD were similarly tuned to spatial frequency (Harel et al., 2002); however, in the study by Harel and colleagues, positive BOLD was measured in V1 and negative BOLD in the extrastriate cortex. Negative BOLD may be based

on neuronal preferences in V1, but on the positive BOLD amplitude in higher visual areas.

The peak positive response at 1cpd is similar to previous findings (Singh et al., 2000; Henriksson et al., 2008) but is slightly lower than the optimal frequency for behavioural detection of 3cpd (De Valois et al., 1974). This discrepancy might be due to the stimulus dimensions: in the imaging studies, an annulus was left around the fixation-cross. Since the foveal region is sensitive to higher spatial frequencies, if it is not stimulated, the apparent peak response will be at a lower frequency. In the current experiment, the whole central region was stimulated, but the mean BOLD response was measured from a 4° diameter area around fixation, which is likely to encompass many neurons specialised for low spatial frequencies. There was no significant difference between the responses at 1 and 3cpd, so the optimal spatial frequency for positive BOLD may be between these values.

The percentage of positive voxels in the stimulated ROI did not differ with stimulus contrast, but did show slight variability with spatial frequency, resembling the amplitude of the positive BOLD response. This finding supports the fact that the same neurons are recruited when processing stimulus contrast, while different neurons are recruited to process different spatial frequencies. The percentage of negative voxels in the surround ROI showed a trend towards contrast tuning, which may suggest that since negative BOLD is such a weak response, a stronger (higher contrast) stimulus is required to result in the suppression of voxels in the surrounding area. There was no main effect of spatial frequency on the percentage of negative voxels, but there was a hint of an increase at lower frequencies, which may suggest that again, the response is too weak to show clear spatial frequency tuning but the tendency may be for the effect expected: more negative voxels at lower frequencies.

3.4 Experiment 2: Spatial frequency tuning to a surround stimulus

3.4.1 Rationale

In order to further investigate the neurophysiological source of the negative BOLD response, this experiment aimed to measure negative BOLD in the cortical representation of central vision induced by a surround stimulus: the opposite stimulus

layout to Experiment 1. If negative BOLD depends on neuronal specificity in the area in which it is measured, the optimal surround stimulus would be between 1 and 3cpd, since this is the preferred range for foveal neurons based on the results of Experiment 1 and on previous literature (De Valois et al., 1974; Singh et al., 2000). Alternatively, if negative BOLD depends on the neuronal response in the stimulated area, the greatest negative BOLD response in the centre may be induced by a low spatial frequency, high contrast surround stimulus, which would give optimal neuronal and positive BOLD responses in the periphery (De Valois et al., 1982; Henriksson et al., 2008). It has previously been reported that negative BOLD is not generated in the cortical representation of the central visual field by a peripheral stimulus (Wade & Rowland, 2010). The current study investigated whether the spatial frequency of a stimulus has an impact on the ability to generate a negative BOLD response at the fovea.

3.4.2 Methods

Stimuli were rings of maximum contrast sinusoidal gratings of the same spatial frequencies as the previous experiment (0.5, 1, 3 and 6cpd), extending from 3-11° with an area of mean luminance in the centre (Figure 3.5). Central and surround regions of interest were defined using the localiser data from Experiment 1, in which a chequerboard was presented in the central 2° and a ring from 2-11°. The inner radius of the stimulus in the current experiment therefore left a gap of 0.5° before the edge of the central ROI in order to minimise a perceptual effect of leakage of luminance from the gratings into the central grey area. A subset of the participants from Experiment 1 (N=4) was tested. Participants pressed a button whenever the fixation-cross changed colour (once per on/off phase). Four blocks containing three of each spatial frequency in a 15s on/off boxcar were presented. A second run of the localiser task was also conducted and the two runs were combined using a fixed effects model, allowing better definition of the regions of interest. Data were processed and analysed in the same way as in Experiment 1.

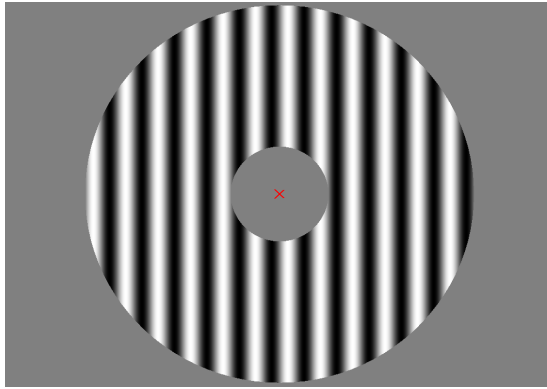


Figure 3.5. Surround stimulus for Experiment 2.

3.4.3 Results and discussion

The mean BOLD response across participants from positive voxels in the surround and from negative voxels in the centre is plotted in Figure 3.6. One-sample t-tests indicated that in the surround, the mean BOLD response was significantly greater than zero and the percentage of positive voxels was greater than 50% at all spatial frequencies (all $t(3) > 7.06$; $p < .05$, Bonferroni corrected). As expected, positive BOLD decreased with spatial frequency ($F(3,9) = 55.43$; $p < .001$), and paired t-tests indicated a significantly greater mean positive BOLD response to 0.5 and 1cpd gratings than to 6cpd gratings ($p < .05$, Bonferroni corrected). The percentage of voxels in the central ROI that were negative was less than 50% and the BOLD amplitude was in fact positive for all spatial frequencies, so it was not relevant to analyse the central negative BOLD response profile further. Negative BOLD was therefore not induced in the cortical representation of the central visual field by a large surround stimulus.

Experiments 1 and 2 have shown that in the cortical representation of the periphery, both positive and negative BOLD are greatest for lower spatial frequencies. Peripheral spatial frequency selective neurons can therefore be recruited both when the area is stimulated in order to increase the BOLD response, and when a different region is stimulated in order to decrease the BOLD response. However, the profiles are not exactly equivalent. Figure 3.6 shows the peripheral positive and negative BOLD responses both scaled to a maximum value of 1. For negative BOLD, the only significant pairwise comparison was between 0.5 and 1cpd, whereas positive BOLD shows differences between the lower and higher frequencies. The negative BOLD tuning profile in the surround was much shallower at high spatial frequencies, giving

a greater negative BOLD response than would be expected from the neuronal preferences in this area. This finding may suggest that negative BOLD amplitude is not entirely based on cell preferences in the region in which it is measured. Perhaps negative BOLD is enhanced only for spatial frequencies for which there are few neurons selective in the centre and more neurons selective in the surround i.e. low spatial frequencies. Information about stimulus properties may be passed from the stimulated central area to the surround; therefore it is not unfeasible that neuronal preferences in both areas influence the negative BOLD signal in the surround.

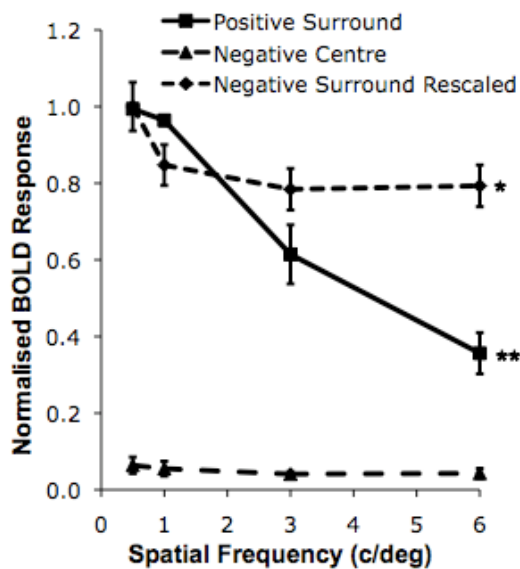


Figure 3.6. The effect of stimulus spatial frequency on mean positive BOLD in the stimulated surround and on negative BOLD (sign reversed) in the centre. Also shown is negative BOLD in the surround during stimulation of the centre (Experiment 1; sign reversed and scaled to a maximum of 1 for comparison with Experiment 2). Error bars show standard error of the mean.

3.5 Experiment 3: Attentional influences on central negative BOLD

3.5.1 Rationale

The absence of negative BOLD at the fovea in response to a surround stimulus in Experiment 2 replicates findings from Wade and Rowland (2010). One factor potentially influencing the results of Experiment 2 and known to affect the negative BOLD response is attention. Negative BOLD can be produced by an attentional task without a large area of visual stimulation (Smith et al., 2000); it may be present in

stimulated areas when attention is directed elsewhere (Tootell, Hadjikhani, Hall, Marrett, Vanduffel, Vaughan et al., 1998; Heinemann et al., 2009); and it is greatest in the periphery when stimulus presentation and attentional focus are at the centre of the visual field (Heinemann et al., 2009). The timing of the attentional task is also relevant: the greatest negative BOLD response is induced when there is a task during the stimulus period but not during the baseline (Smith et al., 2000).

In Experiment 2, the task at fixation may have increased the BOLD response at the fovea and therefore prevented observation of a negative response in that location. The experiment was therefore repeated with the colour change detection task in a ring around the surround stimulus. Two versions of this experiment were conducted, one with the colour change during the stimulus ‘On’ phase only, the other with the task during stimulus and baseline phases. Experiment 3 therefore aimed to determine whether a negative BOLD response could be observed under what should be optimal stimulus conditions: conducting the attentional task in the periphery rather than at the centre and presenting the task only during the stimulus phase, rather than during stimulation and baseline phases.

3.5.2 Methods

The stimuli were the same as in Experiment 2: rings of gratings extending from 3-11° around fixation. Only spatial frequencies of 0.5 and 1cpd were used as they were expected to generate the greatest negative BOLD response. Again, a central ROI (2° radius circle) and peripheral ROI (2-11° ring) were identified from two blocks of the chequerboard localiser task. The task stimulus was a thin red ring around the edge of the stimulus (11° radius). This ring could turn green for 0.5 seconds once during each stimulus phase or once during each stimulus and baseline phase. Participants (N=2) pressed a button when the stimulus ring changed colour.

3.5.3 Results and discussion

Negative BOLD was not generated in the central ROI either with the task present during the stimulus and baseline periods or only during stimulation: the mean response in the central ROI was positive rather than negative and there were less than 50% negative voxels for both spatial frequencies and both attentional task timings (Table 3.1). These findings again replicate those of Wade and Rowland (2010),

showing that negative BOLD is not generated in the fovea in response to a peripheral annulus, even when the stimuli and attentional conditions should be optimal for negative BOLD generation. This result may indicate that negative BOLD is never generated in the centre. Alternatively, it is possible that the strong positive BOLD signal generated in V1 by the annulus stimulus obscured any negative response in the small central region.

Table 3.1. Mean BOLD responses and the percentage of negative voxels in the central ROI during presentation of a surround stimulus with an attentional task in the surround.

Task presentation period	Spatial frequency	Mean BOLD (COPE)	Negative voxels (%)
Stimulus only	0.5	19.85	47.38
	1	25.06	40.05
Stimulus and baseline	0.5	16.31	40.23
	1	29.45	37.58

3.6 Experiment 4: Central negative BOLD from a small parafoveal stimulus

3.6.1 Rationale

The presentation of a large stimulus around fixation in Experiments 2 and 3 induced a very strong positive BOLD response, which may have contaminated the central area and prevented the generation of negative BOLD in the centre. Experiment 4 therefore used a small stimulus in one quadrant of the visual field to investigate whether a reduction in BOLD was seen in the opposite, non-stimulated cortical representation of the fovea. The spatial frequency tuning in response to this parafoveal stimulus was examined and a central stimulus was also presented in order to replicate the results of Experiment 1.

3.6.2 Methods

Stimuli were 2° radius circular sinusoidal gratings, presented in a 15 second on/off boxcar paradigm. Four spatial frequencies were presented (0.5, 1, 3 and 6cpd) in a random order, three times each per block. There were four blocks in which the stimulus was centred at fixation and four blocks in which it was centred 2.5° below

and to the right of fixation. Participants (N=12, all different to those in the previous experiments) of mean age 26 years 8 months (SD 2 years 11 months) pressed a button whenever the fixation-cross turned from red to green for 0.5 seconds. This colour change could happen three, four or five times per stimulus or baseline phase, which ensured better attention was paid to the task than with one colour change per phase.

The chequerboard localiser task in this experiment consisted of 15-second presentations of a surround annulus (2-11°), a central circle (2° radius), a parafoveal circle (2° radius centred 2.5° below and to the right of fixation) and fixation only. Participants maintained fixation throughout two six-minute blocks of this task. Data from these two blocks were combined. Rather than using retinotopic mapping, structural definitions of V1 were created using an automated surface-based approach (Hinds et al., 2008) to ensure that the ROIs defined from the localiser task were restricted to V1.

Data from the four blocks of the task in each location were combined and the mean responses were normalised so that the maximum response from the two ROIs and the four spatial frequencies was equal to one. For the central stimulation experiment, mean normalised positive BOLD in the central ROI and negative BOLD in the surround ROI were recorded; while for the parafoveal stimulus, positive BOLD in the parafoveal ROI and negative BOLD in the central ROI in the opposite hemisphere to the stimulus (Figure 3.7) were measured.

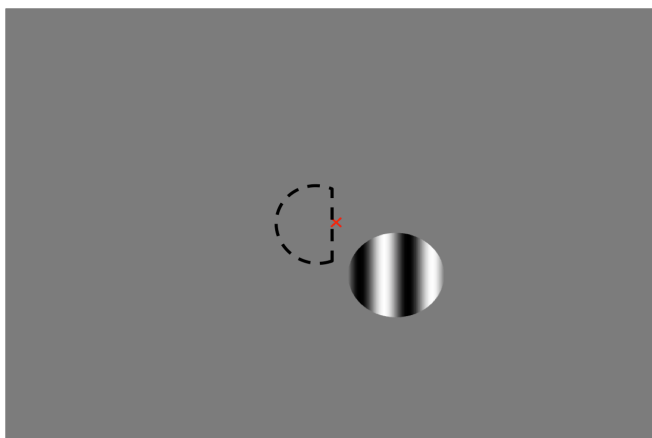


Figure 3.7. Example of the parafoveal stimulus (0.5cpd). Dotted lines represent the area in which the negative BOLD response was measured.

3.6.3 Results and discussion

3.6.3.1 Testing for the presence of positive and negative BOLD responses

The mean BOLD responses in the central ROI to a central stimulus and in the parafoveal ROI to a parafoveal stimulus were significantly greater than zero for all spatial frequencies (all $t(11) > 10.84$; $p < .001$, Bonferroni corrected). The percentage of positive voxels in these stimulated areas was also significantly greater than 50% (all $t(11) > 22.57$; $p < .001$, Bonferroni corrected), indicating the stimulated regions showed a clear increase in BOLD. There were significantly more than 50% negative voxels in the surround when the stimulus was presented in the centre for all spatial frequencies (all $t(11) > 5.41$; $p < .001$, Bonferroni corrected) and the mean response in the surround to a central stimulus was less than zero for all spatial frequencies other than 3cpd (all $t(11) > 3.08$; $p < .05$), though these differences did not survive Bonferroni correction. On the other hand, the response in the centre to a parafoveal stimulus was not different to zero for any spatial frequency ($t(11) < 1.85$; $p = \text{ns}$) and only at 3cpd was the percentage of negative voxels significantly greater than 50% ($t(11) = 2.44$; $p < .05$, uncorrected), all other frequencies did not differ significantly from 50% ($t(11) < 2.07$; $p = \text{ns}$). These results again indicate that negative BOLD was present in the surround in response to a central stimulus, but was not induced in the centre in response to a parafoveal stimulus.

The mean positive BOLD responses in the stimulated regions and the negative responses in the non-stimulated ROIs were consistent across the four blocks (all single measures $\text{ICC} > .49$; $F(11,33) > 4.61$; $p < .001$). The percentage of positive and negative voxels was also consistent in the stimulated and non-stimulated ROIs, respectively ($\text{ICC} > .28$; $F(11,33) > 2.56$; $p < .05$) apart from in the central ROI when this area was stimulated ($\text{ICC} = .12$; $F(11,33) = 1.54$; $p = \text{ns}$). This finding is likely to be a ceiling effect: there was very high percentage of positive voxels in this location, so any variability was more apparent.

3.6.3.2 Central stimulus results

When the stimulus was presented in the centre, the mean normalised positive BOLD response showed a main effect of spatial frequency ($F(3,33) = 67.02$; $p < .001$). There was again a bandpass spatial frequency tuning profile, in this case peaking at 3cpd,

and paired sample t-tests indicated that the response was different between all pairs of spatial frequencies ($p < .05$, Bonferroni corrected) apart from between 0.5 and 6cpd (Figure 3.8A). In the surround region, when the stimulus was at the centre, the mean negative BOLD response did not show significant spatial frequency tuning ($F(3,33)=2.00$; $p=ns$), though there was most negative BOLD at the lower spatial frequencies. The percentage of positive voxels was not different across spatial frequencies for the stimulated central region ($F(3,33)=1.98$; $p=ns$), nor was the percentage of negative voxels in the surrounding non-stimulated region ($F(1.8,19.4)=1.77$; $p=ns$), so again, the same proportion of voxels within the ROI were recruited for processing the stimulus, regardless of its spatial frequency.

3.6.3.3 Parafoveal stimulus results

When the stimulus was positioned in the lower right visual field, the positive BOLD at this location showed spatial frequency tuning ($F(3,33)=65.54$; $p < .001$) with a peak at 1cpd (Figure 3.8B). There was a significant difference ($p < .05$, Bonferroni corrected paired samples t-tests) between all pairs of spatial frequencies other than between 0.5 and 1cpd and between 0.5 and 3cpd. There was no main effect of the percentage of negative voxels at the four spatial frequencies ($F(3,33)=1.98$; $p=ns$). The central region did not contain a significant amount of negative BOLD, so it was not relevant to investigate spatial frequency tuning further in this area.

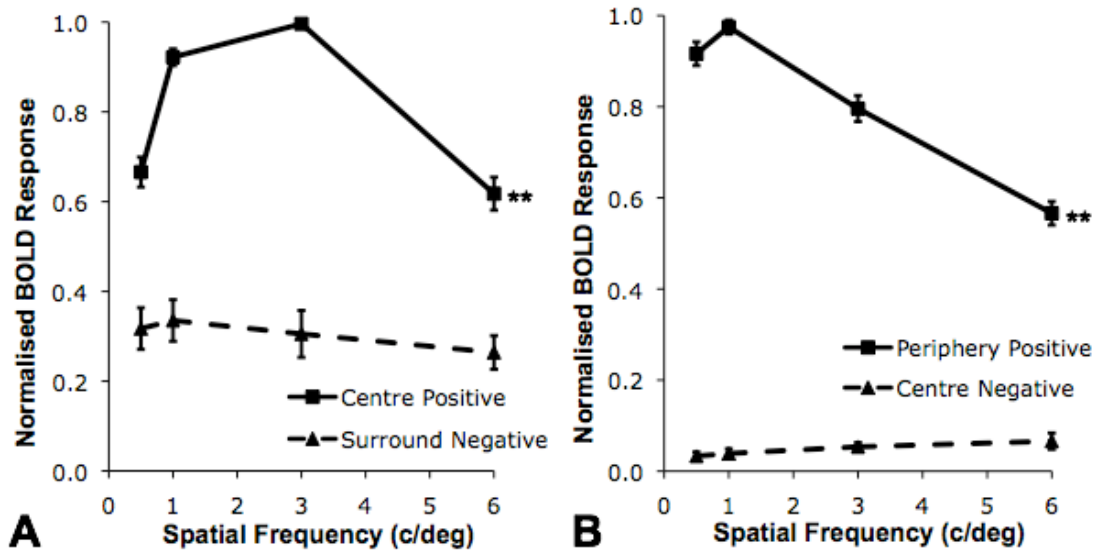


Figure 3.8A) Positive BOLD at the centre and negative BOLD (sign reversed) in the surround to a central stimulus. B) Positive BOLD in the parafoveal region and negative BOLD (sign reversed) at the centre to a parafoveal stimulus.

3.6.3.4 Discussion of the effect of stimulus position

Positive BOLD in the central ROI in response to a central stimulus peaked at a higher spatial frequency in this experiment than in Experiment 1. This result may be because the task at fixation was more involved, causing participants to focus their attention more on the foveal area of the stimulus. Attending more closely to the fovea would lead to stimulation of more neurons sensitive to medium spatial frequencies than a task in which the target appeared only briefly and therefore attention was not required to be fully focused on the centre for the entire duration of the stimulus and could be directed to areas specialised for lower spatial frequencies. Alternatively, the true peak positive BOLD response may be between 1 and 3cpd, as the difference between the two spatial frequencies was not significant in either experiment. In contrast to Experiment 1, negative BOLD in the surrounding ROI in response to a central stimulus did not show a main effect of spatial frequency, though it was greater at lower spatial frequencies. Negative BOLD is weaker than positive BOLD, therefore small variability in the responses may have a large effect on the results observed. A greater number of participants may be necessary to observe consistent negative BOLD effects.

Parafoveal positive BOLD peaked at 1cpd, which is to be expected for a stimulus slightly offset from fixation (Henriksson et al., 2008). Even with a small stimulus that should not induce positive BOLD in the central ROI, the negative response was negligible. This result gives additional support to previous findings that negative BOLD does not occur at the foveal representation in the cortex (Wade & Rowland, 2010). It may suggest that neuronal and haemodynamic activity are never suppressed at fixation by a stimulus presented elsewhere. Alternatively, negative BOLD may be present but as it is a weak response, the attentional influence of maintaining fixation and the visual stimulation due to the fixation point itself may be sufficient to mask the negative BOLD response.

3.7 General discussion

This series of experiments investigated contrast and spatial frequency tuning of the positive and negative BOLD responses in visual cortex. With a centrally-presented grating, positive BOLD in the central ROI and negative BOLD in the surround both increased with contrast; while spatial frequency tuning in the central area was bandpass for positive BOLD and in the peripheral area was lowpass for negative BOLD. Because negative BOLD was not always proportional to positive BOLD, but the relationship between the two differed depending on the stimulus feature manipulated, negative BOLD is unlikely to represent blood steal. Supporting this conclusion, there was also no significant correlation between individuals' positive and negative BOLD. Previous studies have shown relationships between positive and negative BOLD across stimulus features (Harel et al., 2002; Shmuel et al., 2002), but correlations have not previously been described in the context of individual differences. The current findings suggest that there are different processes involved in generation of the two responses.

The BOLD responses obtained generally reflected underlying neuronal preferences: neurons representing all areas of the visual field fire at greater rates to higher contrast stimuli, resulting in a greater positive BOLD response. The negative BOLD response obtained in this and a previous study (Shmuel et al., 2002) suggests that there is also greater suppression of non-stimulated regions with higher contrast. There are more neurons specialised for processing lower spatial frequencies in the periphery (De

Valois et al., 1982) and this physiological profile is reflected in increased positive and negative BOLD for low frequency stimuli in the surround region in this study. This effect was not significant for negative BOLD in Experiment 4, which may indicate that the negative BOLD response is more variable or that it is likely to be affected to a greater extent by outliers as it is a weaker response. The positive and negative BOLD responses in the surround region also did not show exactly equivalent profiles: negative BOLD only differed at the lowest spatial frequencies, whereas positive BOLD differed more at higher frequencies. Negative BOLD amplitude may therefore not only reflect underlying neuronal preferences in the non-stimulated areas, but may also be related to the strength of the signal in the stimulated area. It may be greatest when there are few neurons responding in the centre and a high number of neurons responsive to the relevant stimulus feature in the periphery. Within the surround ROI, there are neurons with optimal spatial frequencies between about 0.5 and 1.5cpd (Henriksson et al., 2008). The proportion of responsive voxels within this region did not change with stimulus features, but the amplitude of the response did. Different spatial frequencies may therefore recruit different neurons within the same ROIs. Localisation of the actual neurons responding may require the use of a series of smaller ROIs, which could be investigated using higher field MRI.

Negative BOLD correlates with decreases in neuronal activity (Shmuel et al., 2006; Devor et al., 2007; Boorman et al., 2010), therefore non-stimulated cortex must experience either decreased excitatory input or increased inhibitory input. The variation in negative BOLD with stimulus features also suggests that this suppression is somehow modulated by the transfer of stimulus-specific information to non-stimulated cortex; however, the mechanism by which this occurs is not known. GABA-ergic interneurons could carry signals between stimulated and non-stimulated areas of V1 (Shmuel et al., 2006) and GABA concentration has been shown to correlate with negative BOLD amplitude in the anterior cingulate cortex, implicating GABAergic inhibition in negative BOLD production (Northoff et al., 2007). However, increases in inhibitory interneuron activity would *increase* the local BOLD response, therefore it is possible that decreases in BOLD may be attributable to increased inhibition or reduced excitation from other areas of the brain. Negative BOLD is not likely to be induced solely by horizontal connections within the cortex since it can be caused by stimuli represented further in visual cortex than horizontal

connections reach (Shmuel et al., 2006) and it can be induced in the periphery without any significant foveal stimulation (Smith et al., 2000). It is therefore likely to be produced by inhibitory signals from more distant areas, either from earlier stages in the visual processing pathway such as the lateral geniculate nucleus or thalamus (Raichle, 1998); or from feedback connections from higher visual areas.

In these experiments, negative BOLD was not induced in the cortical representation of central vision by a large surround stimulus or a smaller parafoveal stimulus, regardless of the period of presentation of the attentional task. This may be because stimulus-specific information is not transferred from the periphery to the centre to cause a decrease in BOLD; or because attention to or the presence of the small fixation stimulus produces sufficient positive BOLD to mask the negative BOLD response. The presence of negative BOLD at the foveal representation in the cortex could be tested through a task similar to that used by Pasley and colleagues (2007): a negative baseline could be induced in the centre by a surround stimulus. If negative BOLD was induced by this surround stimulus, the increase in positive BOLD on subsequent presentation of a central stimulus should be greater from this negative baseline condition than from a fixation-only baseline.

3.8 Conclusions

Positive and negative BOLD responses were found to show different profiles to stimulus contrast and spatial frequency, suggesting that they are induced independently by increases or decreases in neuronal activity, and this activity may depend on stimulus preferences in the underlying neuronal architecture. Negative BOLD may therefore provide useful information about stimulus processing. It would be interesting to determine whether the combination of measures of positive and negative BOLD gives additional information about stimulus processing than a measure of positive BOLD alone. Future studies could develop behavioural measures in order to investigate the role of negative BOLD in visual cortex in stimulus processing. Negative BOLD was not generated at the fovea by a peripheral surround or a parafoveal stimulus, regardless of the location of attention. Additional studies are required to confirm whether negative BOLD is always absent at the fovea or whether it is masked by increased BOLD at fixation due to the fixation stimulus and task. It

would also be interesting to determine the neurophysiology through which the negative BOLD response is mediated.

Chapter 4

GABA+ Concentration Shows No Significant Correlation With Positive or Negative BOLD in Visual Cortex

4.1 Abstract

Individual differences in the concentration of the inhibitory neurotransmitter, gamma-aminobutyric acid (GABA+) in visual cortex have previously been shown to be inversely related to increases in the blood oxygen level-dependent (BOLD) response to a visual stimulus (Muthukumaraswamy et al., 2009; Donahue et al., 2010) in functional magnetic resonance imaging (fMRI). Decreases in BOLD can also be observed in non-stimulated regions of visual cortex, therefore it was hypothesised that individual differences in these negative BOLD responses would show a positive relationship with GABA+: the inverse relationship to positive BOLD. The correlation between GABA+ concentration, measured with magnetic resonance spectroscopy (MRS) and positive and negative BOLD from fMRI was investigated in two experiments. There was no clear relationship between GABA+ and BOLD, despite improvement of the methodology in the second experiment by selecting a more homogenous participant cohort and improving the stimulus to give a stronger BOLD signal. The negative BOLD signal was much weaker and less reliable within subjects than positive BOLD, therefore the potential for detection of individual differences in negative BOLD was limited. The lack of replication of the previously reported inverse correlation between GABA+ and positive BOLD may be due to an insufficient number of participants given the variability in measurement of both factors; to differences in voxel positioning by different operators; or to differences in data quality caused by varying amounts of head movement across participants.

4.2 Experiment 1: GABA+, positive BOLD and negative BOLD in visual cortex: Responses to a unilateral stimulus

4.2.1 Background

In order to maintain equilibrium and to execute functions in the brain, there is a constant interaction between excitation and inhibition. These opposing forces are mediated by the release and uptake of neurotransmitters, which influence neuronal

firing rates, oscillatory dynamics, haemodynamic activity and ultimately behaviour. All of these factors show differences between individuals and these differences may be correlated with each other, indicating generally enhanced or reduced excitability of the cortex in different participants.

In fMRI, the blood oxygen level-dependent (BOLD) response (Ogawa et al., 1990) represents a change in the ratio of oxy- to deoxy-haemoglobin, brought about by changes in blood volume, blood flow and the rate of oxygen consumption in a localised area of cortex (Belliveau et al., 1991; Kwong et al., 1992; Ogawa et al., 1992). Typically, *increases* in BOLD induced by experimental manipulations are reported; however, decreases in the BOLD response (negative BOLD) are also seen in non-stimulated regions of cortex when a stimulus is present elsewhere. This reduction in BOLD can be observed in primary visual (Shmuel et al., 2002; Shmuel et al., 2006; Heinemann et al., 2009), somatosensory (Kastrup et al., 2008; Boorman et al., 2010) and motor (Stefanovic et al., 2004) cortices in areas adjacent or contralateral to areas of increased (positive) BOLD.

The amplitude of positive and negative BOLD responses is dependent on stimulus parameters. For example, in visual cortex, positive BOLD increases with stimulus contrast (Boynton et al., 1999); and shows bandpass spatial and temporal frequency tuning profiles (Henriksson et al., 2008). Similarly, negative BOLD in visual cortex varies with stimulus eccentricity (Bressler et al., 2007), contrast (Shmuel et al., 2002) and spatial frequency (Chapter 3). In addition to these stimulus-driven changes in positive and negative BOLD, there are also differences between individuals in the BOLD responses induced by particular stimuli. The neurophysiological basis for these inter-individual differences is not known.

One potential source of variability in BOLD is the concentration of the principle inhibitory neurotransmitter in the human brain, gamma-aminobutyric acid (GABA) in relevant areas of individuals' cortex. GABA is released by GABA-ergic interneurons and affects neuronal activation by hyperpolarising postsynaptic neurons, making them less likely to generate action potentials (Kuffler & Edwards, 1958). This suppression of neuronal activity may therefore result in a negative BOLD response. GABA-ergic connections are generally involved in local interactions (Uhlhaas, Pipa & Lima,

2009); however, it has been speculated that negative BOLD in the ipsilateral sensorimotor cortex to stimulation is induced by inhibition by long-range cross-callosal GABA-ergic interneurons (Allison et al., 2000). GABA may therefore play a role in short- and long-range suppression of non-stimulated cortex.

The baseline concentration of GABA within a region of the brain can be recorded using edited magnetic resonance spectroscopy (MRS). This measure of GABA has been found to inversely correlate with behavioural measures of perception: the greater the GABA plus macromolecules (GABA+) concentration measured by MRS, the better individuals' tactile discrimination (Puts et al., 2011) and visual orientation discrimination (Edden et al., 2009). An inverse relationship has also been reported between GABA and positive BOLD whereby the more GABA+, the smaller the BOLD response in visual (Muthukumaraswamy et al., 2009; Donahue et al., 2010; Muthukumaraswamy, Evans et al., 2012), somatosensory (Puts et al., 2011) and motor (Stagg et al., 2011a) cortices. An opposing relationship might be expected of the negative BOLD response, in that individuals with higher occipital GABA+ concentration would show more negative BOLD. In the anterior cingulate cortex, GABA+ concentration does indeed positively correlate with negative BOLD during emotional processing tasks, suggesting there is a link between GABA+, negative BOLD and behaviour (Northoff et al., 2007).

The GABA+ concentration recorded with MRS is a crude measure of cortical inhibition, as it does not distinguish between intra- and extracellular GABA, or between GABA involved in metabolism and that involved in inhibitory neurotransmission (Stagg, Bachtiar & Johansen-Berg, 2011b). However, the studies described above suggest that the GABA+ concentration measured using MRS is functionally relevant. It may represent a general propensity for inhibition of neuronal activity, with reductions in GABA causing increased neuronal activity and therefore a greater positive BOLD response (Logothetis, 2002), and increases in GABA causing decreased neuronal activity, resulting in a greater negative BOLD response (Shmuel et al., 2006). This study therefore investigated whether individual differences in GABA+ in visual cortex relate to positive and negative BOLD responses to a visual stimulus. It was hypothesised that there would be a positive correlation between GABA+ and negative BOLD and that the inverse correlation between positive BOLD

and GABA+ would be replicated. The effect of stimulus spatial frequency on positive and negative BOLD was also investigated, with the expectation that previous findings of bandpass positive BOLD spatial frequency tuning peaking at 1-3cpd (Henriksson et al., 2008) would be replicated. This study was conducted prior to the experiments in Chapter 3, therefore spatial frequency tuning of the negative BOLD response was also anticipated.

4.2.2 Methods

4.2.2.1 Participants and procedure

Fifteen right-handed individuals (eight female) of mean age 26 years 11 months (SD 4 years 8 months) were recruited from staff, postgraduates and undergraduates at Cardiff University and gave informed written consent. One participant was excluded from analysis due to a lack of fixation during functional mapping of the visual field (retinotopic mapping), which meant that regions of interest (ROIs) could not be identified. Participants completed two experimental sessions, the first of which included retinotopic mapping and the fMRI task. The second session involved further retinotopic mapping and GABA edited spectroscopy.

4.2.2.2 Visual task stimuli

The stimuli consisted of maximum contrast square-wave gratings subtending $4 \times 4^\circ$, positioned with the top left corner 0.5° below and to the right of a white fixation cross, which subtended 0.6° . Stimuli were displayed on a mean luminance background. Spatial frequencies of 0.5, 1.0, 3.0 and 6.0 cycles per degree (cpd) were presented in a 15 second boxcar paradigm, with fixation only for 15 seconds followed by a grating for 15 seconds. Two gratings of each spatial frequency were presented in a random order in four-minute blocks and there were five blocks, giving 10 presentations of each spatial frequency. At a random time between one and thirteen seconds into the presentation of the grating, a thin red box appeared around the edge of the grating for one second (Figure 4.1A). Participants responded to the onset of this box with a button press.

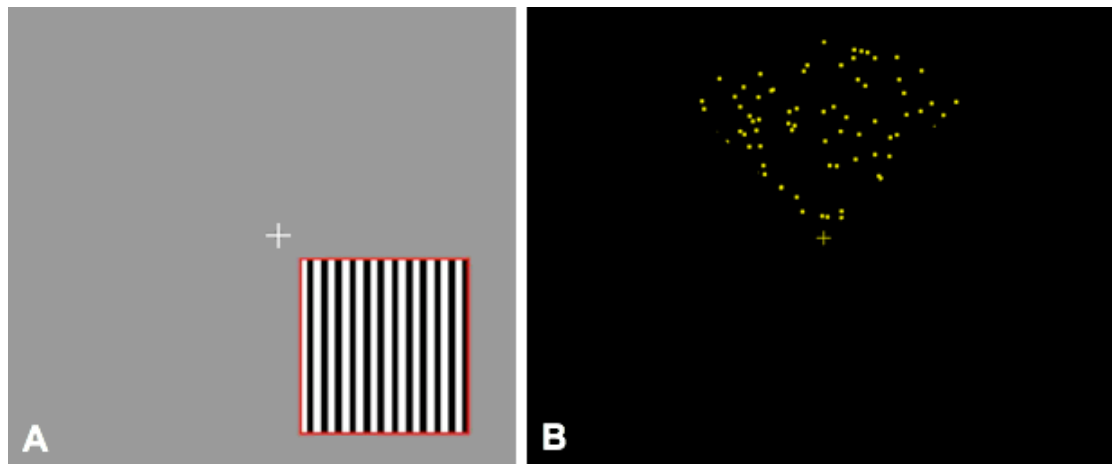


Figure 4.1. A) 3cpd stimulus and the red box for the detection task. B) Retinotopic mapping stimulus.

4.2.2.3 Retinotopic mapping stimuli

Primary visual cortex (V1) regions of interest (ROIs) were delineated using retinotopic mapping (Belliveau et al., 1991; Sereno et al., 1995; DeYoe et al., 1996), which involves stimulating the visual field and defining the cortical boundaries of visual areas based on the resulting fMRI response. The stimuli in this experiment consisted of small yellow dots, which moved and flickered on a black background. The dots were contained within a 70° wedge, which extended 11.5° into the periphery (Figure 4.1B) and which rotated around a yellow fixation cross once per minute. Five-minute blocks of clockwise and anti-clockwise rotation were presented in each of the two scan sessions, with the order of presentation of these conditions randomised across participants.

4.2.2.4 fMRI acquisition and analysis

All data were acquired on a 3.0T GE HDx system (GE Healthcare, Chalfont St Giles, UK) using a body coil for transmission and an eight-channel receive-only head coil. Functional MRI scans were gradient-echo echoplanar imaging (EPI) sequences, taking 22 slices through occipital cortex in $4 \times 4 \times 3$ mm voxels, using a 64×64 matrix. Echo time (TE) was 35ms, repetition time (TR) was 1.5s and the flip angle was 90° . Retinotopic mapping parameters were similar, but with 37 slices at 2mm isotropic resolution, a 128×128 matrix and a TR of 3.0s. Anatomical images were acquired with a 3D Fast Spoiled Gradient-Echo (FSPGR) sequence (TR/TE/inversion time = 7.8/3.0/450ms; flip angle = 20° ; 1mm isotropic resolution). Whole brain EPI images

with equivalent slice thickness and field of view to the fMRI sequences were also obtained for registering the retinotopic mapping and visual task data to the anatomical scans.

The fMRI data were analysed using FMRIB software library (FSL; www.fmrib.ox.ac.uk/fsl). Preprocessing parameters were: motion correction using MCFLIRT (Jenkinson et al., 2002); non-brain removal with BET (Smith, 2002); spatial smoothing using a Gaussian kernel of full-width-half-maximum (FWHM) 5mm for the grating task, 0.5mm for retinotopic mapping; high-pass temporal filtering and gamma convolution of the HRF. For the grating task, for each of the five blocks and for every participant, the GLM was used to model a 15 second off/on boxcar for the four spatial frequencies. These data were registered to the whole-brain EPI equivalent to the grating task fMRI sequence, then to the individual's FSPGR. Occipital regions were cut (Figure 4.2A), opened along the calcarine sulcus and flattened using Freesurfer (Fischl et al., 1999).

Retinotopic mapping data were analysed in the same manner as described in Chapter 3, with dorsal and ventral ROIs identified on the left and right hemisphere flattened occipital lobes (Figure 4.2B). Data from the fMRI task were then overlaid in mri3dX (<https://cubic.psych.cf.ac.uk/Documentation/mri3dX/>; Figure 4.2C) and the BOLD amplitude and the BOLD responses in the ROIs were calculated.

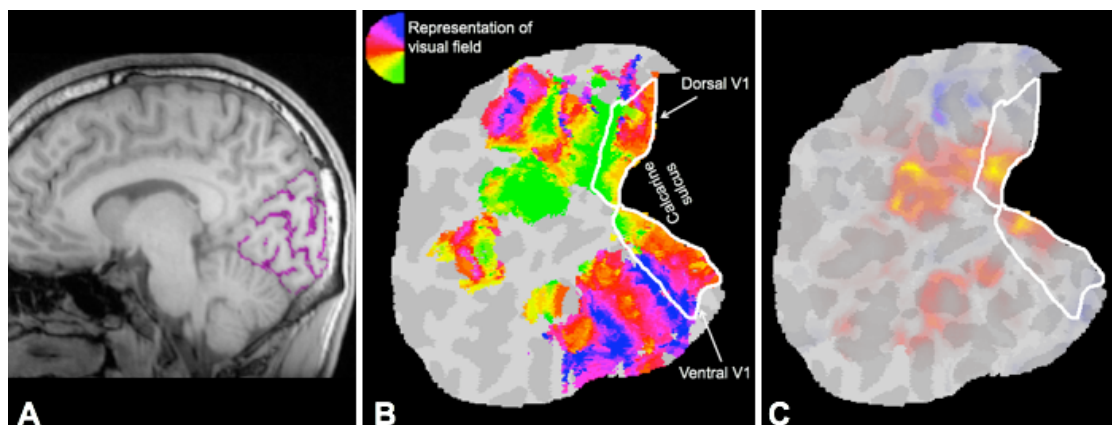


Figure 4.2A) Occipital region identified to be flattened for one participant. B) A representative participant's left hemisphere occipital flat map overlaid with retinotopic mapping data. V1 regions of interest are shown in white. C) BOLD response to 3cpd gratings in the lower right visual field in the same participant.

4.2.2.5 MRS acquisition and analysis

In the MRS sequence, a 3x3x3cm voxel was positioned with the lower plane aligned with the cerebellar tentorium, the leading edge roughly aligned with the parieto-occipital sulcus and the posterior edge avoiding the sagittal sinus while remaining as much inside the occipital lobe as possible. Two runs of this sequence were acquired with the following parameters: TE=68ms, TR=1.8s, 332 measurements per voxel and 16ms Gaussian editing pulses applied at 1.9ppm and 7.46ppm in alternate scans. Locally written software was used to apply a high-pass water filter and produce a MEGA-PRESS difference spectrum. The edited GABA+ signal at 3ppm and the unsuppressed PRESS water signal were integrated. A concentration measurement in institutional units was derived by accounting for the editing efficiency and the T1 and T2 relaxation times of water and GABA. Automatic phasing of the GABA peaks was conducted, with small manual adjustments made where necessary. Segmentation of the voxel into grey matter, white matter and CSF was conducted using FMRIB's Automated Segmentation Tool (FAST; (Zhang, Brady & Smith, 2001)), which also gives a measure of the tissue fraction. The obtained GABA+ values were corrected for the fraction of tissue in the voxel and the average value from the two runs was calculated for each participant.

4.2.3 Results

4.2.3.1 Visual fMRI

The four ROIs (left and right hemisphere dorsal and ventral) contained similar numbers of voxels ($F(3,42)=.319$; $p=ns$), therefore it was not necessary to control for the size of ROIs. In each ROI, the mean amplitude (in arbitrary contrast of parameter estimate (COPE) values) and the percentage of voxels with positive or negative signals were considered to represent the strength and area of the BOLD responses to gratings, respectively (Table 4.1). One sample t-tests on the mean BOLD responses indicated that only the responses in the stimulated left hemisphere (LH) dorsal quadrant to the four spatial frequencies were significantly greater than zero after Bonferroni correction for 16 comparisons ($4.95 < t(13) < 7.14$; $p < .05$); the non-stimulated quadrants did not show a significantly different response to baseline. Similarly, there were more than 50% positive voxels in the LH dorsal ROI and this difference was significant for all spatial frequencies other than 3cpd after Bonferroni

correction ($-3.46 < t(13) < -4.63$; $p < .05$); however, the percentage of negative voxels was not different to 50% in any of the other ROIs. These results indicate that in the LH dorsal V1, there was a significant increase in the amplitude and spatial extent of the positive BOLD response to a grating in the lower right visual field. In non-stimulated quadrants, the negative BOLD response was not significant. The LH ventral response was in fact slightly positive, indicating a spread of positive BOLD across the calcarine sulcus (also visible in Figure 4.1C).

Table 4.1. Mean BOLD amplitude and number of negative voxels in each ROI, averaged across all spatial frequencies.

ROI	LH Dorsal	LH Ventral	RH Dorsal	RH Ventral
Mean BOLD (COPE)	74.52	9.70	-8.52	-13.54
(SEM)	(13.05)	(11.19)	(7.06)	(8.29)
Negative Voxels (%)	35.13	52.80	61.69	62.83
(SEM)	(3.61)	(7.02)	(6.50)	(8.91)

Subsequent analyses were conducted on the mean BOLD response from the positive voxels only in the stimulated (LH dorsal) ROI and from the negative voxels only in the opposite (right hemisphere (RH) ventral) ROI. The repeatability of the BOLD responses across the five blocks was investigated in these two regions. Mean within-subjects coefficients of variance (CVs) were very high for the mean BOLD response in both the LH dorsal (19.61%) and RH ventral (51.16%) responses, suggesting poor repeatability. However, a different measure of repeatability, the intraclass correlation coefficient (ICC) with two-way random effects and absolute agreement, indicated that between subject variability accounted for 93% of the total variance in positive BOLD (average measures $ICC=.93$; $F(13,52)=14.79$; $p < .001$) and 57% in negative BOLD (average measures $ICC=.57$; $F(14,52)=2.35$; $p < .05$). The significant ICCs suggest good repeatability of BOLD between the runs. The discrepancy between the CVs and ICCs indicates that although individuals' BOLD responses were not significantly consistent across the five blocks, differences between individuals were even greater, allowing participants' data to be discriminated from each other on the basis of their BOLD responses. In the percentage of negative voxels, there was a large amount of within subject variation across the five blocks in LH dorsal V1 ($CV=25.65\%$) and in RH ventral V1 ($CV=28.75\%$); however, a greater proportion of the variance in the

stimulated quadrant was explained by differences between individuals (average measures ICC=.71; $F(13,52)=3.41$; $p<.05$). In the RH ventral, a non-significant 47% of the variance of the number of negative voxels was explained by the variance between subjects (average measures ICC=.47; $F(13,52)=1.88$; $p=ns$). The positive BOLD response and the amplitude but not the spatial extent of negative BOLD were therefore repeatable within individuals across blocks.

The mean BOLD responses were normalised in each participant so that the maximum absolute positive or negative response from all spatial frequencies in the stimulated and opposite ROI was equal to one (Figure 4.3A). Repeated measures ANOVAs indicated a significant main effect of spatial frequency in the stimulated LH dorsal ROI ($F(3,39)=34.43$; $p<.001$) but not in the non-stimulated RH ventral ROI ($F(3,39)=.80$; $p=ns$). The negative BOLD response was therefore not tuned to spatial frequency. Bonferroni corrected pairwise comparisons indicated that in the stimulated ROI, all pairs of spatial frequencies were significantly different apart from between 0.5 and 3cpd (all $p<.05$). These results are similar to Chapter 3, in which a parafoveal stimulus induced a positive BOLD response peaking at 1cpd but no spatial frequency tuning of the negative BOLD response. The percentage of positive voxels in the stimulated ROI and of negative voxels in the opposite ROI showed no main effect of ROI ($F(1,13)=.02$; $p=ns$) or spatial frequency ($F(3,39)=.66$; $p=ns$). There was therefore no spatial frequency tuning of the proportion of positive or negative BOLD voxels.

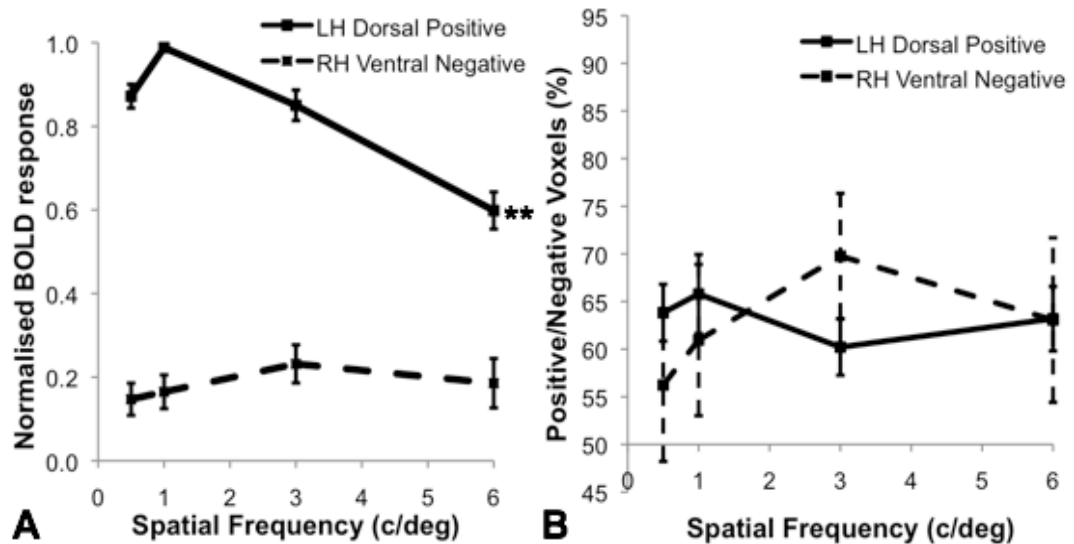


Figure 4.3A) Mean normalised BOLD response for positive and negative (sign reversed) voxels in the stimulated (LH dorsal) and opposite (RH ventral) ROIs. B) The percentage of positive voxels in LH dorsal V1 and negative voxels in RH ventral V1 for different spatial frequencies. Error bars show the standard error of the mean.

There were no significant correlations between the non-normalised amplitude of the positive and negative BOLD responses at any of the spatial frequencies (all $R < .24$; $p = ns$; Figure 4.4A). Correlations between the number of positive voxels in LH dorsal V1 and the number of negative voxels in RH ventral V1 were in an inverse direction, indicating that the more positive voxels in an individual's stimulated visual cortex, the fewer negative voxels in non-stimulated cortex. After multiple comparisons correction, this relationship was significant at 6.0cpd ($R = -.76$; $p < .05$); but not at any other spatial frequency (all $R > -.63$; $p = ns$). However, these correlations should be treated with caution, as there are many points with fewer than 50% negative voxels in the non-stimulated ROI, yet this area should contain mostly negative voxels. This result indicates that the stimulus did not produce a large area of negative BOLD in all participants. It also shows a large amount of variability in negative BOLD between participants. This result may suggest that the task is not optimal for generation of a negative BOLD response, or that negative BOLD is indeed a weaker, more variable response than positive BOLD.

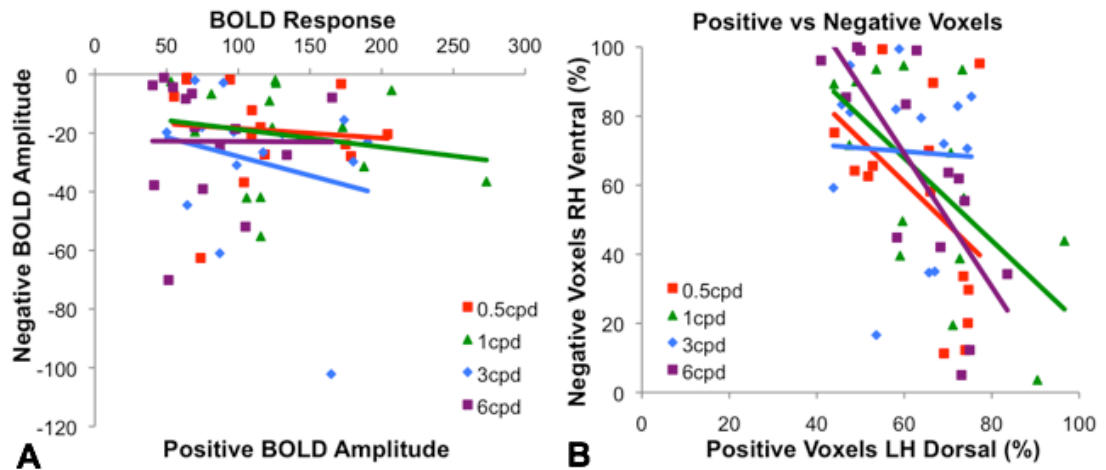


Figure 4.4. The relationship between mean BOLD amplitude (A) and the percentage of negative voxels (B) in stimulated and opposite quadrants of V1.

4.2.3.2 MRS results

The mean GABA+ value in institutional units (IU) was 1.45 (SD=.11) for the first acquisition and 1.39 (SD=.06) for the second acquisition, giving a mean of 1.42 (SD=.07) from the two runs. The coefficient of variance between the two runs was low (4.99%), indicating good within-subjects repeatability; however a two-way random effects ICC with absolute agreement was not significant (average measures ICC=.18; $F(13,13)=1.25$; $p=ns$). The ICC result indicates a low ratio of between- to within-subject variability. The between subjects CV was 6.40%, which also shows that variability between subjects was only slightly higher than within-subjects.

4.2.3.3 Relationship between BOLD and GABA+

The main analysis in this experiment was the comparison of GABA+ and BOLD. Correlations between GABA+ and mean BOLD amplitude (non-normalised) in the stimulated (LH dorsal) and opposite (RH ventral) ROIs were conducted for each spatial frequency. Contrary to the hypotheses of this study, all correlations between positive BOLD amplitude and GABA+ were in a positive direction (Figure 4.5A) with a significant effect at 0.5cpd ($R=.61$; $p<.05$), though this result did not survive correction for multiple comparisons for four spatial frequencies. Negative BOLD amplitude also generally increased with GABA+ concentration (Figure 4.5B) with a significant relationship at 3cpd ($R=-.58$; $p<.05$), but which also did not withstand multiple comparisons correction. Correlations with GABA+ were not significant at

any other spatial frequencies for positive (all $R < .51$; $p = ns$) or negative (all $R > -.38$; $p = ns$) BOLD. There were no significant correlations between GABA+ and the percentage of negative voxels at any frequency in either ROI (all $R < .36$; $p = ns$; Figure 4.5C&D).

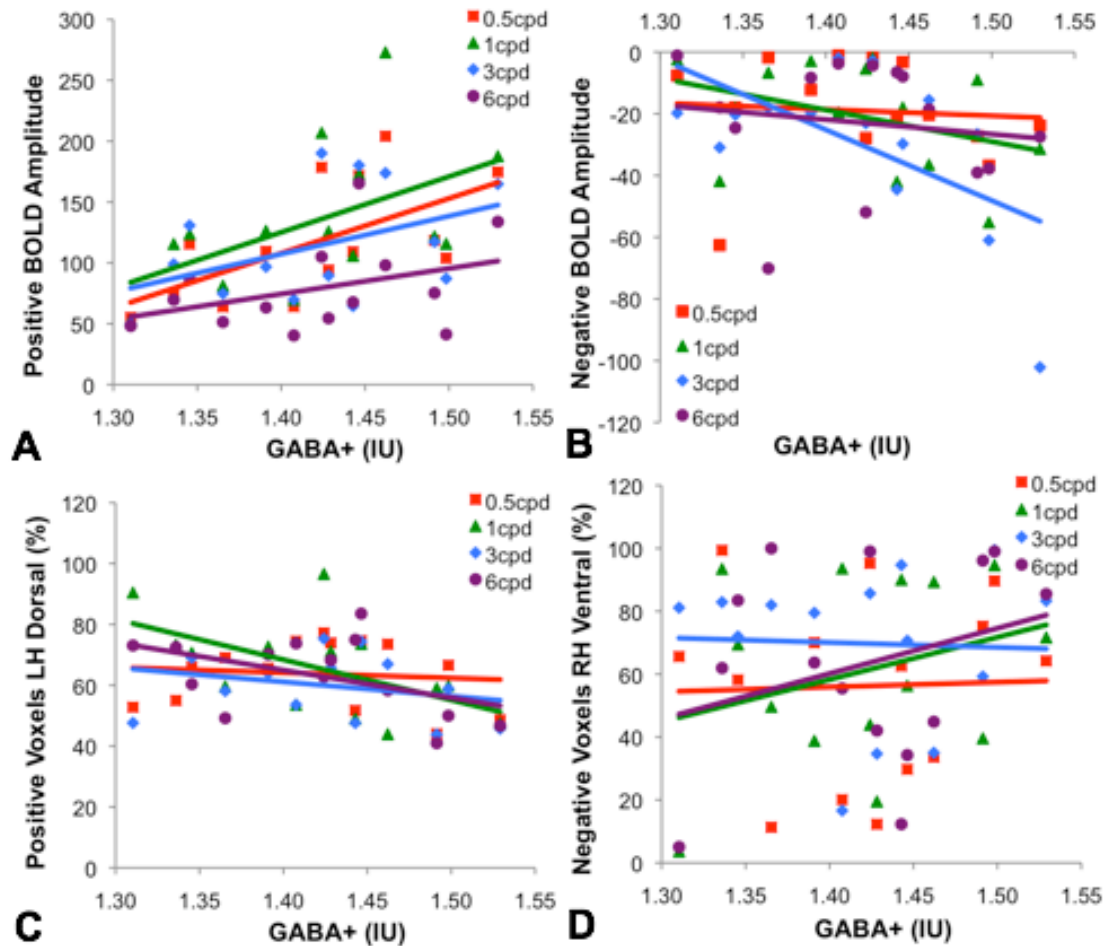


Figure 4.5. Correlations of GABA+ concentration with mean positive BOLD (A) and the percentage of positive voxels (C) in the stimulated ROI, and with mean negative BOLD (B) and the percentage of negative voxels (D) in the opposite ROI, at four spatial frequencies.

4.2.4 Discussion

This experiment showed no clear relationship between occipital GABA+ concentration and the BOLD response in V1 to a visual stimulus: previous findings of an inverse relationship between positive BOLD and GABA+ (Muthukumaraswamy et al., 2009; Donahue et al., 2010; Stagg et al., 2011a) were not replicated; and the

hypothesised positive correlation with negative BOLD was not found. There are various methodological reasons that might explain the lack of relationship between BOLD and GABA+ in this study.

The stimulus used in this study was clearly not optimal, as it did not induce a significant negative BOLD response either in terms of the decrease from baseline or in the area of negative voxels. Investigations of individual differences in negative BOLD and their relation to GABA+, and of the spatial frequency tuning profile of the negative BOLD signal are therefore of questionable validity. Measurement of negative BOLD in the diagonally opposite region of visual cortex to stimulation ensured that the negative BOLD response was not influenced by blood steal from more active areas, since the two hemispheres have separate blood supplies; however, investigating negative BOLD in an area so distant from positive BOLD can be expected to give a lower amplitude response than the area adjacent to stimulation (Heinemann et al., 2009). The positive BOLD response was more diffuse than expected, with leakage of signal across the calcarine sulcus, therefore it was not possible to assess negative BOLD in the same hemisphere as stimulation. This positive signal in the non-stimulated quadrant of the stimulated hemisphere may have resulted from excessive smoothing of the data or from poor maintenance of fixation by participants. Reanalysis of the data with no spatial smoothing gave similar results to those reported above, ruling out this issue. Fixation monitoring could give an indication as to whether eye movements induced positive BOLD in the non-stimulated cortex.

An additional issue with the task is that it may also have not been sufficiently demanding to induce a reliable BOLD response across trials: a response was only required once per 15-second stimulus or baseline phase and after making a response, participants could theoretically stop attending (whilst still maintaining fixation) until the next phase. Attention is known to influence positive and negative BOLD in visual cortex (Smith et al., 2000), therefore a task requiring more consistent maintenance of attention should give greater signals.

The repeatability of the MRS and fMRI measures is important when investigating the relationship between these variables, since if a measure itself is not consistent, the

strength of its correlation with another measure will be reduced. Although the BOLD responses showed poor repeatability across the five blocks acquired, there was a very wide range of individual differences in BOLD, which ensured participants' data could be distinguished from each other. Previous studies have shown GABA measurement to be repeatable within subjects, with coefficients of variation of 10-12% (Bogner et al., 2010), 6.5% (Evans et al., 2010) and 7% (O'Gorman, Michels, Edden, Murdoch & Martin, 2011). In this study, the CV was even lower (4.99%), indicating the good within subjects repeatability of the measurement (<http://www.westgard.com/lesson34.htm#6>). However, ICCs indicated that GABA+ was not consistent across runs, perhaps due to low between subjects variance. Methods of optimising spectroscopy acquisition and analysis parameters to ensure reliability are considered in detail in Chapter 6. Since both male and female participants were tested in this study, gender differences in MRS measures of GABA+ concentration (Ke, Cohen, Bang, Yang & Renshaw, 2000; O'Gorman et al., 2011) or differences throughout the female menstrual cycle (Smith, Keel, Greenberg, Adams, Schmidt, Rubinow et al., 1999; Epperson, Haga, Mason, Sellers, Gueorguieva, Zhang et al., 2002; Epperson, O'Malley, Czarkowski, Gueorguieva, Jatlow, Sanacora et al., 2005b; Harada, Kubo, Nose, Nishitani & Matsuda, 2011) may have introduced between-subjects variability in GABA+ concentration.

A final potential methodological issue may have been the area of cortex included within the regions of interest. The static fixation cross and surrounding annulus in the retinotopic mapping paradigm do not fully stimulate the fovea and since the area of cortex corresponding to an area of the visual field is greatest at the fovea (Sereno et al., 1995), this could result in the omission of a large proportion of the cortical representation of the fovea from the ROIs. Since the stimulus in the current task was presented close to the fovea, the entire positive BOLD response may not be represented in the ROIs. Also, since negative BOLD is likely to be greater in close proximity to positive BOLD (Heinemann et al., 2009), since the ROI in the non-stimulated quadrant also does not cover the foveal area (which would be closest to the response to the stimulus), the chances of detecting a negative BOLD response may have been reduced. Retinotopic mapping to define ROIs is also strongly dependent on the participant maintaining fixation. Alternative methods of identifying ROIs may give a better representation of the responses: for instance, using a localiser stimulus of

the same size as the task stimulus to functionally delineate ROIs, or using features of the cortical structure to identify the boundaries of V1 anatomically (Hinds et al., 2008).

Considering the BOLD response independently of GABA⁺ concentration, positive BOLD showed a bandpass profile with a peak at 1.0cpd, which was very similar to the profile reported in Chapter 3. These findings may reconcile differences between studies that have (Henriksson et al., 2008) or have not (Muthukumaraswamy & Singh, 2008) shown modulation of positive BOLD with spatial frequency. The latter study used 0.5 and 3.0cpd stimuli, which were not significantly different in the current experiment, as the response peaked between these frequencies. The negative BOLD data should be treated with caution since the mean BOLD response in non-stimulated ROIs was not significantly reduced from baseline, however, the lack of correlation between positive and negative BOLD amplitudes could suggest that different mechanisms are involved in producing these responses.

In summary, this experiment found that the positive BOLD response in human V1 showed spatial frequency tuning with a peak at 1cpd. There was no evidence for a correlation between positive BOLD and GABA⁺ concentration in occipital cortex, which may have been due to the low amount of between-subjects variability in GABA⁺. Non-stimulated areas did not show significant negative BOLD responses when compared with baseline and when negative voxels were selected, they did not show spatial frequency tuning or a significant relationship with GABA⁺ concentration. The task was therefore not optimal for inducing a negative BOLD response.

4.3 Experiment 2: GABA⁺, positive BOLD and negative BOLD in visual cortex: Responses to a centrally-presented stimulus

4.3.1 Rationale

This experiment aimed to address several methodological issues potentially contributing to the weak negative BOLD response and to the absence of a correlation between BOLD and GABA⁺ in Experiment 1: the position and form of the stimulus, the level of the attention, the method of identifying regions of interest and the gender

of the participant group. Gender differences in GABA+ concentration have been reported (Ke et al., 2000; O'Gorman et al., 2011), therefore to avoid including data from groups who differed in the variable of interest, only male participants were recruited for Experiment 2. There is evidence that the negative BOLD response is strongest with a centrally-presented stimulus (Chapter 2), therefore, the stimulus in Experiment 2 was presented at the fovea. Since both positive and negative BOLD responses increase with attentional load (Smith et al., 2000; Heinemann et al., 2009), the attentional task in Experiment 2 was more demanding, requiring detection of several fixation colour changes per stimulus and baseline phase, as opposed to a single colour change as in Experiment 1. A method for delineating V1 based on cortical folds in structural MRI scans (Hinds et al., 2008) was used, as this method avoids the issue with retinotopic mapping whereby the foveal region of V1 is not always included in ROIs. This technique was used to define V1 and to separate it into 10 regions of equal length along the calcarine sulcus. With these experimental parameters, it was expected that negative BOLD would be induced in the non-stimulated parafoveal regions and that positive BOLD would show an inverse correlation with GABA+, while negative BOLD would show a positive correlation with GABA+.

4.3.2 Methods

4.3.2.1 Participants and stimulus

Fourteen men of mean age 30 years 1 month (SD 5 years 8 months) took part in this experiment. This was an entirely separate sample from Experiment 1. The functional MRI task was a boxcar design in which the stimulus and fixation were present for 15 seconds, followed by a fixation-only baseline for 15 seconds. The stimulus was a circular chequerboard subtending 5° of visual angle on a grey background (Figure 4.6). The black and white checks were maximum contrast and increased in width from the centre to the periphery in line with the cortical magnification factor, which accounts for increases in the receptive field size with increasing distance from fixation (Daniel & Whitteridge, 1961; Sereno et al., 1995). The fixation point was a red circle in the centre of the screen, which subtended 0.4°. This circle turned green for 0.5 seconds either three, four or five times per stimulus and baseline phase. Participants pressed a button whenever they detected this colour change. There were 12 stimulus

on/off phases per block and two blocks were presented, each of which was six minutes long.

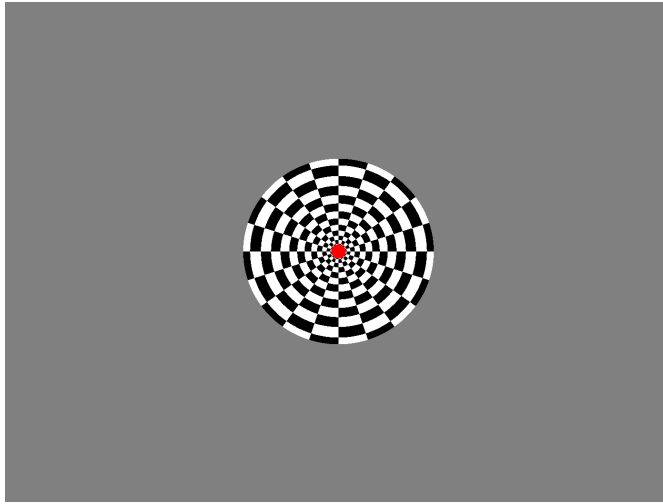


Figure 4.6. The chequerboard stimulus for the fMRI component of Experiment 2.

4.3.2.2 *fMRI and MRS acquisition and analysis*

The experiment took approximately one hour in total. The two blocks of fMRI data were acquired with a similar sequence to the grating task in Experiment 1, but in this experiment, the voxels were 3mm isotropic in a 64x64 matrix and the TR was 3.0. Pre-processing was also similar, except that less spatial smoothing was used for this task (1mm) in order to minimise the spatial spread of the fMRI response. An EPI of equivalent slice thickness and field of view to this task was obtained for coregistration with a high-resolution structural FSPGR scan. The MRS acquisition was similar to Experiment 1, again with two 10-minute runs each containing 332 measurements per voxel. The GABA+ values were corrected for the fraction of tissue within the voxel, obtained using FAST (Zhang et al., 2001). Left and right hemisphere V1 ROIs were identified based on cortical folds (Hinds et al., 2008) and these ROIs were then split into 10 equal-length sections along the striate cortex.

4.3.3 Results

For each participant, the 10 sections of V1 in each hemisphere were loaded in mri3dX (<https://cubic.psych.cf.ac.uk/Documentation/mri3dX/>) and the mean BOLD amplitudes (contrast of parameter estimates (COPE)) in each section were calculated and averaged across the two hemispheres. The BOLD response profile shown in

Figure 4.7A indicates that the highest amplitude response was observed in the second most posterior V1 region. The first region representing the very extremity of the striate cortex was in fact slightly lateral to this second region in both hemispheres. The BOLD response decreased but remained positive until the fifth region, then was negative from the sixth to the tenth regions, which extended most anteriorly along the calcarine sulcus. The response in the most positive and most negative regions (2 and 7, respectively) were subsequently investigated. One sample t-tests against a value of zero indicated that the BOLD response in the positive region was significantly greater than zero ($t(13)=19.85$; $p<.001$) and the negative response was significantly smaller than zero ($t(13)=-3.71$; $p<.05$). This task therefore gave stronger negative BOLD responses than Experiment 1. There was again no significant relationship between individuals' positive and negative BOLD responses in these areas ($R=-.08$; $p=ns$; Figure 4.7B).

The mean GABA+ concentrations across participants from the first acquisition was 1.46 (SD=0.09) and from the second acquisition was 1.45 (SD=0.12). The overall mean GABA+ concentration from both acquisitions was therefore 1.46 (SD=.10). These values are very slightly higher than the mean and SD from Experiment 1.

The repeatability of BOLD and GABA+ was investigated across the two acquisitions of each measure. The within subjects CV was very low for GABA+ (4.02%) and was acceptable for BOLD in V1 region 2 (12.14%) but was very poor in region 7 (92.80%). A single measures ICCs with two-way random effects and absolute agreement indicated that the GABA+ measure gave reliable results across the two blocks (average measures ICC=.59; $F(13,13)=3.73$; $p<.05$). Similarly, positive BOLD in region 2 was reliable (average measures ICC=.49; $F(13,13)=2.89$; $p<.001$). Negative BOLD also showed significant ICC (average measures ICC=.88; $F(13,13)=15.09$; $p<.05$), despite the extremely high CV, indicating that the variability between subjects is even larger than the variability within subjects.

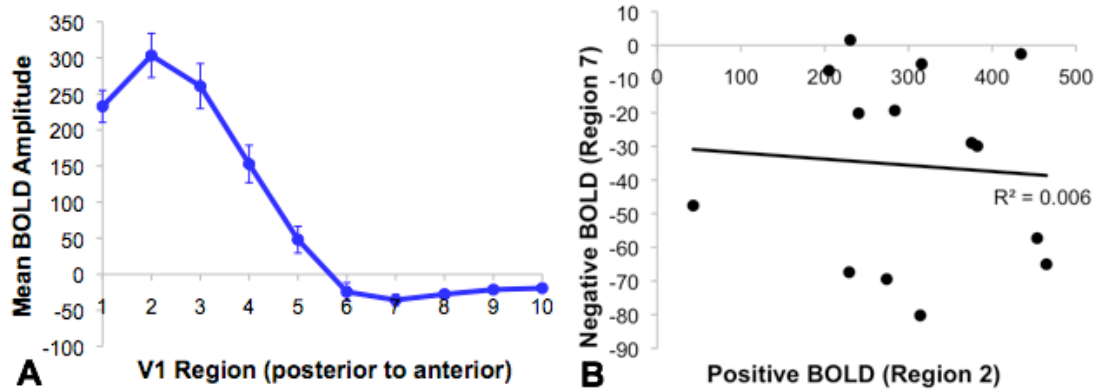


Figure 4.7A) Mean BOLD response to a 5° centrally-presented stimulus in 10 sections of V1. Error bars = SEM. B) Correlation between maximum positive and negative BOLD responses to a centrally-presented chequerboard stimulus.

The correlation coefficients between GABA+ and the BOLD response in the most positive and negative regions of V1 are plotted in Figure 4.8A&B. Again, contrary to the hypotheses of this study, there was no significant correlation between GABA+ and either positive BOLD ($R=.17$; $p=ns$) or negative BOLD ($R=.15$; $p=ns$).

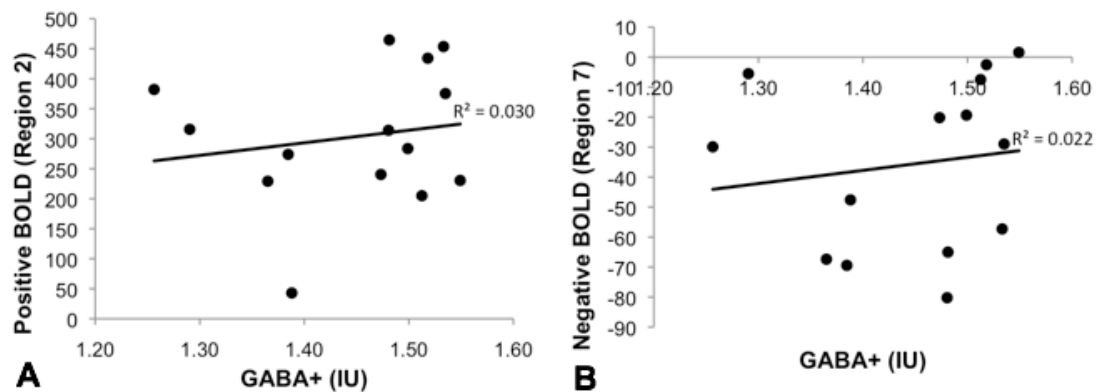


Figure 4.8. Correlation between GABA+ concentration and positive (A) and negative (B) BOLD responses to a centrally-presented chequerboard.

4.3.4 Discussion

This study again failed to replicate reports of an inverse relationship between GABA+ and positive BOLD (Muthukumaraswamy et al., 2009; Donahue et al., 2010; Stagg et al., 2011a) or between GABA+ and negative BOLD (Northoff et al., 2007). The absence of correlations was not due to a weak BOLD signal in this experiment, as the

BOLD response was significantly greater than baseline in central stimulated areas and significantly reduced from baseline in peripheral non-stimulated areas. The attentionally-demanding task at fixation also contributed to generation of a strong BOLD response; while the use of only male participants avoided potential variability in GABA+ between the genders (Ke et al., 2000; O'Gorman et al., 2011). The lack of correlation between GABA+ and BOLD is therefore unlikely to be attributable to the methodology and participant selection in Experiment 2.

The negative BOLD responses induced by the larger, central stimulus in this experiment were of greater amplitude than in Experiment 1, but they were not reliable. Since negative BOLD was recorded from the same hemisphere and therefore from areas of the brain with the same blood supply as positive BOLD in this experiment, there could have been an element of blood steal in negative BOLD regions, whereby blood is diverted to active cortex leaving less available for adjacent non-stimulated regions. The lack of correlation between positive and negative BOLD suggests that negative BOLD is unlikely to be entirely due to this effect, otherwise the responses would be proportional to each other. However, the poor repeatability of the negative BOLD response prevents strong conclusions being made about its correlation with other variables.

4.4 General Discussion

Neither of the experiments in this study showed the expected relationship between GABA+ and positive BOLD in visual cortex. It is possible that this relationship is not as strong as previously assumed, or that the numbers of participants generally recruited for these studies are not sufficient to demonstrate this correlation consistently, given that the measures can be variable and are sensitive to small alterations in the stimulus. With correlations based on individual differences, if within subject test-retest repeatability of either measure is poor, it is unlikely that a strong correlation will be found and there is a danger of reporting spurious significant correlations. Simulations to investigate the impact of sample size and experimental noise are conducted in Chapter 7.

Within-subjects variability in positive BOLD was better in this study (CVs=19.61% and 12.14%) than in other studies (e.g. CV=21-53% (Loubinoux, Carel, Alary, Boulanouar, Viillard, Manelfe et al., 2001)). Although this is still a large difference between acquisitions, the variability between participants was even greater and so individuals' data can be considered sufficiently repeatable in order to conduct correlations with other measures. The proportion of variability in GABA+ accounted for by between-subjects variability differed for the two experiments in this study (ICC=.18 and .59) and was lower than reported in a previous study (ICC=.87) using similar acquisition and analysis procedures. This finding suggests that repeatability of GABA+ may be greatly affected by small but systematic differences between experiments. For instance, MRS is sensitive to participant movement (Felblinger, Kreis & Boesch, 1998), so better spectra may be obtained from more MR-experienced participants. The use of mixed gender groups may also add variability to GABA+ measurement (Ke et al., 2000). Slightly different voxel positioning by different operators may also impact on the quality of the spectra and consequently on the repeatability of the data. Such differences between experiments may explain the lack of replication of the relationship between positive BOLD and GABA+.

Another explanation for the poor replicability of the correlation between positive BOLD and GABA+ may be that there is a factor mediating the relationship between these measures, so without a direct relationship, the effect is less likely to be replicated. Such mediating factors could include the number of GABAergic interneurons, the density of GABA receptors in the cortex, or the shift from passive to active state in the brain as opposed to a stimulus-specific functional response (Gu et al., 2012). Alternatively, individual differences in BOLD may not be driven by GABA, but by differences in vascular reactivity, or by cortical excitability through other neurotransmitters such as glutamine and glutamate. Future MRS studies could investigate the relationship between these other neurotransmitters and positive and negative BOLD. An issue with MRS is that the voxels are very large, therefore the BOLD and GABA+ values correlated with each other were not measured from equivalent areas of cortex. This discrepancy is not an issue if GABA+ concentration is consistent throughout the voxel, but variations in GABA+ concentration within MRS voxels are currently unknown. GABA receptor density has been reported to vary throughout cortical layers, but to be consistent horizontally (Hendry & Carder,

1992; Albus & Whale, 1994), suggesting that GABA⁺ concentration may be consistent across the cortex within the voxel. Higher field MRS would allow the measurement of metabolites within a smaller area.

The absence of a correlation between negative BOLD and GABA⁺ is not entirely surprising, since negative BOLD is weaker than positive BOLD (Shmuel et al., 2002; Boorman et al., 2010), so identification of individual differences is problematic. In addition, negative BOLD is likely to be caused by active suppression of neuronal activity (Shmuel et al., 2006; Boorman et al., 2010), which requires increased activity in inhibitory neurons. This activity would *increase* the BOLD response in the area inducing the inhibition; therefore the source of the negative BOLD response may be in a different region of the brain and so correlations with GABA⁺ in the same region may not be relevant. It has been suggested that negative BOLD is induced by long-range, cross-callosal inhibitory interneurons (Allison et al., 2000). However, GABA-ergic inhibitory connections tend to act more locally (Jinno, Klausberger, Marton, Dalezios, Roberts, Fuentealba et al., 2007). If positive BOLD were under more local GABA-ergic control, this could explain why previous studies have shown a relationship between GABA⁺ and positive BOLD in the same regions of cortex. The current study suggests that different mechanisms may be involved in generation of positive and negative BOLD responses, since their amplitudes are uncorrelated with each other.

4.5 Conclusion

There was no relationship between GABA⁺ concentration in occipital cortex and positive or negative BOLD responses to visual stimuli in V1, even after optimisation of the experimental design. The weak relationship could be due to noise in the measures or to an insufficient number of participants. Alternatively, the cause of individual variability in task-related visual BOLD responses may be other factors, such as the concentration of excitatory neurotransmitters, or individual differences in resting state levels of BOLD.

Chapter 5

Inactivity and Inhibition in Visual Cortex: Negative BOLD, Alpha and GABA

5.1 Abstract

In areas of the brain not currently required for stimulus processing, differences in synaptic, neuronal network and haemodynamic activity from more active states can be measured using neuroimaging techniques. Inhibition of activity in these non-stimulated areas can be brought about at the level of the synapse by neurotransmitters such as gamma-aminobutyric acid (GABA). Neuronal oscillations in the alpha frequency band are thought to represent suppression of irrelevant areas of cortex, while the negative blood oxygen level-dependent (BOLD) response reflects decreases in haemodynamic activity in non-stimulated regions. In this study, the hypothesis was that these three variables would be related: the higher an individual's occipital GABA concentration, the stronger their alpha suppression and negative BOLD responses in non-stimulated visual cortex. GABA plus macromolecules (GABA+) concentration was measured using magnetic resonance spectroscopy (MRS), while alpha and negative BOLD responses to a unilateral visual grating were measured using magnetoencephalography (MEG) and functional magnetic resonance imaging (fMRI), respectively. An Eyes Open/Eyes Closed paradigm was also used to measure alpha reactivity. The grating stimulus did not induce clear alpha increases in non-stimulated cortex and there were no significant correlations between GABA+, negative BOLD and alpha using this task. However, strong alpha was generated in the Eyes Open/Eyes Closed paradigm, and this signal showed a correlation with GABA+ concentration whereby individuals with more GABA+ showed less alpha suppression on opening the eyes: the opposite result to that hypothesised. This finding may suggest that individuals with more GABA+ have reduced reactivity in visual cortex, resulting in a smaller change in alpha between eyes-open and eyes-closed. Suggestions are made for tasks that could more optimally measure the relationships between GABA, alpha and negative BOLD within the same participants.

5.2 Background

Although the popularly-held belief that humans only make use 10% of our brains is a misconception, there are certainly situations in which some areas of the cortex are not required for stimulus processing, and their activity can be downregulated. Suppression of neuronal activity plays a vital role in the regulation of processing in the brain and can be brought about by different mechanisms, the effects of which can be measured using neuroimaging techniques. At the level of synapses between individual neurons, neurotransmitters influence the movement of ions, increasing or decreasing the likelihood of postsynaptic neuronal firing. Magnetic resonance spectroscopy (MRS) allows quantification of the concentration of molecules in a region of the brain, including that of neurotransmitters such as gamma-aminobutyric acid (GABA), which has an inhibitory role in the cortex. At the level of cortical networks, thousands of neurons act together, increasing or decreasing their level of activity depending on task demands. These changes in activity can be measured using electroencephalography (EEG) or magnetoencephalography (MEG), both of which show that increases in oscillatory activity in the alpha frequency band (8-12Hz) are a prominent feature in inactive regions of cortex (Berger, 1929), particularly when the eyes are closed (Cohen, 1972). Haemodynamic activity in the brain is also affected by processing demands and can be measured using functional magnetic resonance imaging (fMRI). Changes in blood volume, blood flow and the rate of oxygen consumption are represented in the blood oxygen level-dependent (BOLD) fMRI response (Ogawa et al., 1990) and a negative BOLD response is observed in non-stimulated cortex when haemodynamic activity falls below baseline levels. These variables of GABA, alpha and negative BOLD therefore all potentially reflect inhibition or suppression of activity in the brain. Investigation of the relationships between these factors within individuals may indicate whether they reflect different stages of the same inhibitory processes, or whether each fulfills a different role in stimulus processing.

As described in the introductory chapter, some relationships between these variables have previously been reported. Individual differences in GABA⁺ concentration measured using MRS are inversely correlated with positive BOLD amplitude in response to visual and motor stimuli (Muthukumaraswamy et al., 2009; Donahue et al., 2010; Stagg et al., 2011a; Muthukumaraswamy, Evans et al., 2012), and are

positively correlated with negative BOLD responses in the anterior cingulate cortex (Northoff et al., 2007). The relationship between GABA⁺ and haemodynamic activity may be mediated by an intervening step involving changes in neuronal activity. GABA-ergic inhibition has been shown to reduce neuronal firing and consequently to influence behaviour (orientation tuning) in the cat visual cortex (Eysel, Shevelev, Lazareva & Sharaev, 1998). Measurement of neuronal activity using MEG has also shown a positive correlation between individual differences in GABA⁺ and the frequency (but not the power) of gamma oscillations (Muthukumaraswamy et al., 2009; Gaetz et al., 2011), as well as with the power but not the frequency of beta oscillations (Gaetz et al., 2011). However, the relationship between GABA⁺ and alpha has not been investigated to date.

Simultaneous EEG and fMRI studies have shown a link between alpha and BOLD in resting cortex. The timecourses of alpha and positive BOLD in Eyes Open/Eyes Closed tasks are inversely correlated in parietal, frontal, occipital and cingulate cortices and are positively correlated in the thalamus (Goldman et al., 2002; Laufs et al., 2003; De Munck, Gonçalves, Huijboom, Kuijer, Pouwels, Heethaar et al., 2007), suggesting that increased alpha and reduced positive BOLD may represent similar processes of suppression of resting cortex, and that alpha oscillations may be generated in the thalamus. Since alpha and positive BOLD show this inverse correlation, negative BOLD in non-stimulated cortex might therefore be expected to increase in line with increased alpha band activity, making alpha a neuronal marker of the negative BOLD response. Negative BOLD is known to reflect a reduction in neuronal activity over a wide range of oscillatory frequencies (Shmuel et al., 2006; Boorman et al., 2010) and a recent study has inferred a link between negative BOLD and alpha, using electrocorticography to detect alpha oscillations in the region surrounding the stimulated area of primary visual cortex (V1): the same region in which negative BOLD would be expected (Harvey et al., 2012). These studies all report spatio-temporal links between alpha and BOLD; however, the relationship between individual differences in these measures is not known.

This study therefore investigated correlations between individual differences in GABA, alpha and negative BOLD in visual cortex, as they may all represent some form of inhibition of inactive areas of the brain. Based on an understanding of the

neurophysiology mediating these responses, identification of relationships between these variables may allow inferences to be made about the predictive roles of synaptic and neuronal activity in the generation of the BOLD response. Occipital GABA+ concentration was measured using MRS. The same paradigm was used in fMRI and MEG experiments to induce negative BOLD and alpha oscillations in non-stimulated cortex on presentation of a unilateral visual grating stimulus. An Eyes Open/Eyes Closed paradigm also gave an additional measure of alpha reactivity. It was hypothesised that participants would lie on a continuum of ‘generalised cortical inhibition’, in which participants with high levels of inhibition would show higher GABA+ concentration, greater alpha suppression and more negative BOLD than those with lower levels of inhibition. If the measures were uncorrelated, it would suggest that they describe different processes, or that different stages of inhibition are unrelated to each other.

5.3 Methods

5.3.1 Participants

Fourteen male participants (mean age=31.2 years, SD=4.8 years) were recruited from staff and postgraduates at Cardiff University and gave written informed consent. Only male participants were selected because differences in GABA concentration have been reported between the genders (Ke et al., 2000; O’Gorman et al., 2011) and across the female menstrual cycle (Smith et al., 1999; Epperson et al., 2002; Harada et al., 2011). This selection criterion prevented these group differences from influencing the investigation of individual differences in GABA+. The experiment was run in two separate sessions: the MRI/MRS session lasted approximately 90 minutes, while the MEG session was approximately 45 minutes long.

5.3.2 Visual grating task stimuli

The same functional task was used in the MEG and the fMRI in order to permit direct comparison of the resulting alpha and negative BOLD responses. The stimulus was a maximum contrast, 0.5 cycles per degree (cpd) sinusoidal grating, reversing at 7.5Hz, presented on a grey background (Figure 5.1A). The task was programmed in Pascal (Delphi 7, Borland Software Corporation) using the OpenGL software library for graphics hardware. In the MRI, the grating subtended 4° at a viewing distance of 57cm and was centred 2° below and to the right of a red fixation cross. In the MEG,

stimuli subtended 5.6° diameter and were centred 2.8° from fixation. The baseline phase consisted of a grey screen with a red fixation cross which was alternated with the stimulus phase in a 15 second on/off boxcar paradigm. Participants maintained fixation and pressed a button whenever the cross turned green for 0.5 seconds, which could happen three, four or five times per stimulus and baseline phase, at random time intervals. There were 12 stimulus and baseline phases per block, making each block 6 minutes long. Two blocks were presented.

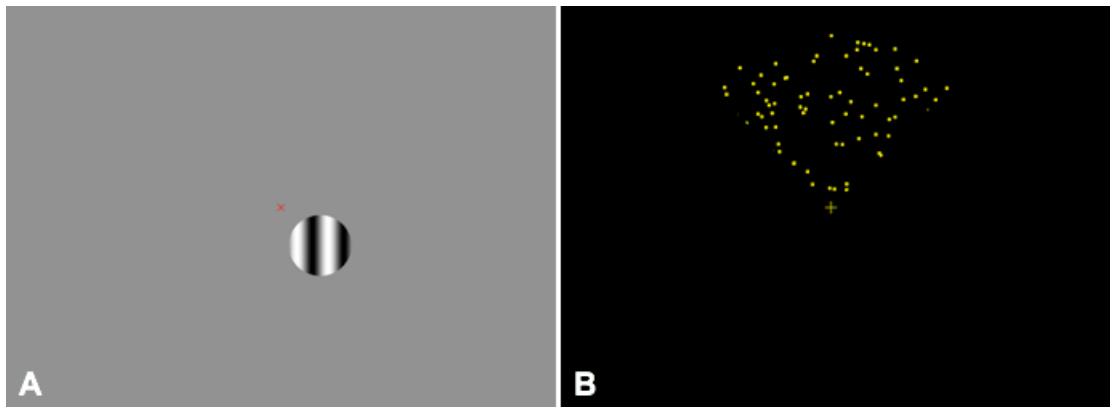


Figure 5.1. A) The visual grating task stimulus presented in the fMRI and MEG experiments. B) The retinotopic mapping stimulus used to delineate boundaries of visual areas in the brain.

5.3.3 Eyes Open/Eyes Closed (EO/EC) task stimuli

A basic test of alpha reactivity was also conducted in the MEG whereby participants were signaled to open and close their eyes in 15 second phases for six minutes by a verbal instruction of “Open” or “Closed” presented through an earphone in their left ear. In the EO phase, participants fixated on a small red square in the centre of a screen. This task was programmed in Matlab (The Mathworks, Inc.).

5.3.4 Retinotopic mapping stimuli and analysis

In order to define regions of interest (ROIs) in primary visual cortex (V1) for investigation of the BOLD response, retinotopic mapping (Belliveau et al., 1991) was conducted on all participants using fMRI. The stimulus (Figure 5.1B) and analysis procedures were identical to those described in Chapter 3.

5.3.5 MRI acquisition and pre-processing

All MRI data were acquired on a 3T General Electric HDx system (GE Healthcare, Waukesha, USA), using a body coil for transmission and an eight-channel receive-only head coil. For the grating fMRI task, a gradient-echo echoplanar imaging (EPI) sequence took 22 slices at an acute angle over occipital cortex in 3mm isotropic voxels using a 64x64 matrix. The TR was 3.0s, TE 35ms and flip angle 90°. Retinotopic mapping parameters were similar, but with 37 slices at 2mm isotropic resolution and a 128x128 matrix. Anatomical images required for coregistration were acquired with a 3D Fast Spoiled Gradient-Echo (FSPGR) sequence (TR/TE/inversion time = 7.8s/3.0s/450ms; flip angle = 20°; 1mm isotropic resolution).

fMRI data were analysed using the FMRIB software library (FSL; www.fmrib.ox.ac.uk/fsl). Preprocessing parameters were: motion correction using MCFLIRT (Jenkinson et al., 2002); non-brain removal with BET (Smith, 2002); spatial smoothing using a Gaussian kernel of full-width-half-maximum (FWHM) 0.5mm for the retinotopic mapping, 5mm for the visual grating task; high-pass temporal filtering and gamma convolution of the HRF. The fMRI data were initially registered to a whole-brain EPI with equivalent field of view and slice thickness to the fMRI sequence, then to the individual's FSPGR. Individuals' occipital lobes were cut, opened along the calcarine sulcus and flattened using Freesurfer (Fischl et al., 1999). Retinotopic mapping data were overlaid onto the flattened occipital cortex and regions of interest were defined. The BOLD response from the fMRI task in these regions was analysed in mri3dX (<https://cubic.psych.cf.ac.uk/Documentation/mri3dX/>).

5.3.6 MRS acquisition and pre-processing

The 3x3x3cm spectroscopy voxel was centred across the interhemispheric fissure, with the lower edge aligned with the cerebellar tentorium and the leading edge with the parieto-occipital sulcus. A compromise was made between this ideal position and the need to ensure that the voxel was predominantly in the occipital lobe, avoiding the sagittal sinus and CSF (Figure 5.2). In this sequence, 332 measurements were taken per voxel and a 16ms Gaussian editing pulse was applied at 1.9ppm (the 'on' acquisitions) and 7.46ppm (the 'off' acquisitions) in alternate scans. The TE was 68ms and TR 1.8s. Eight unsuppressed acquisitions were collected at the end of the

MEGA-PRESS scan to serve as an internal concentration (and phase) reference. Two blocks of MRS were obtained, each of which took approximately 10 minutes.

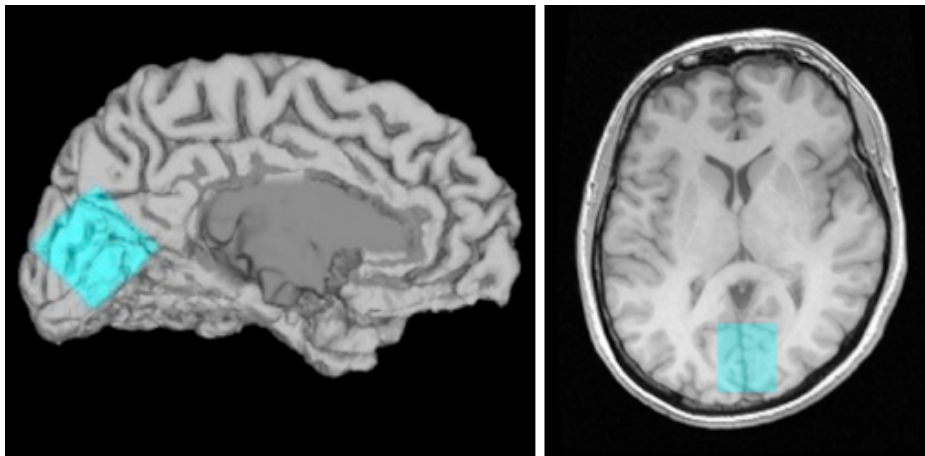


Figure 5.2. Example of the positioning of the MRS voxel in occipital cortex.

MRS data were analysed using the GABA Analysis Toolkit (*Gannet*) (<http://gabamrs.blogspot.co.uk/>). Datasets were zero-filled 8 times, line broadened with a 4Hz exponential function and automatically phased, with minor manual adjustments where necessary. After subtraction of measurements with the editing pulse ‘on’ and ‘off’, Gaussian functions were fitted to the edited difference spectra from 2.75ppm to 3.55ppm using a nonlinear least squares fit. A ratio was calculated between GABA+, which was represented by the integral of the Gaussian peak, and the water integral from a Voigt lineshape in the off spectrum. This ratio was then converted to institutional units to account for the effective visibility of water, differences in $T1$ and $T2$, and editing efficiency. Segmentation of the voxel into grey matter, white matter and CSF was conducted and a measure of tissue fraction obtained using FMRIB’s Automated Segmentation Tool (FAST) (Zhang et al., 2001). The tissue corrected GABA+ values for the two runs of MRS were averaged for each participant.

5.3.7 MEG acquisition and pre-processing

Data were obtained on a CTF 275-channel radial gradiometer system (CTF Systems, VSM MedTech Ltd., Port Coquitlam, Canada), with three channels turned off due to excessive noise. In addition, 29 reference channels were used for the purpose of noise cancellation. The acquisition sampling rate was 1200Hz and data were analysed as

synthetic third-order gradiometers. For coregistration with anatomical MRI images, fiducial markers were placed at fixed distances from the tragi and nose bridge and the location of these markers was monitored continuously throughout the acquisition of the grating task and at the beginning and end of the EO/EC task. A chin rest was used to stabilise the head during the scan. In pre-processing, data were bandpass filtered using a fourth order bi-directional IIR Butterworth filter in the 8-12Hz frequency band. Synthetic aperture magnetometry (SAM) beamforming (Robinson & Vrba, 1999) was used to generate differential images of source power (pseudo-T statistics) between the -14.5 to -0.5 second period before stimulus offset (stimulation) and 0.5 to 14.5 seconds after stimulus offset (baseline). Data were coregistered with high-resolution anatomical MRI scans using the fiducial markers as points of reference. Source localisation was conducted using a multiple local-spheres forward model (Huang, Mosher & Leahy, 1999) on the brain surface, which was obtained using FSL's brain extraction tool (BET) (Smith, 2002).

For the grating task, source peaks in occipital lobes for placement of virtual electrodes were identified from the SAM images. SAM beamformer reconstructions were obtained at these locations using covariance matrices band-pass filtered between 0 and 100Hz. Time frequency analyses using the Hilbert transform were conducted to show frequencies from 1 to 100Hz in 0.5Hz steps. Time-frequency data were represented as a percentage change from the average baseline response (from 4 to 14 seconds) across all trials. In the EO/EC task, a V1 region of interest (ROI) was identified using the SPM anatomy toolbox. On a template brain, a probabilistic V1 mask was created (Amunts et al., 2000) with a cut-off of 50% probability that an individual's V1 would be within that region (Figure 5.3). Each individual's brain was registered to a standard space and the mean alpha desynchronisation (t-score) from within the V1 ROI was obtained.

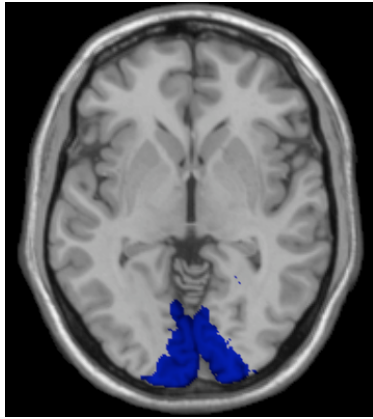


Figure 5.3. V1 ROI mask from a probabilistic map thresholded at 50% probability that the voxel will be within an individual's V1.

5.4 Results

5.4.1 MRS data

Both acquisitions of MRS for one participant and one acquisition for another participant were excluded because too many pairs of measurements were automatically rejected during pre-processing, most likely due to movement. The data reported are therefore 12 participants' GABA values representing the mean of two acquisitions and one value representing a single acquisition. The mean GABA+ concentration in institutional units across participants was 1.49 (SD=0.11). The within-subjects repeatability of GABA+ between acquisitions was good (coefficient of variance (CV) = 4.79%) and was lower than the between subjects variability (CV=7.99%).

5.4.2 MEG data

The aim of the MEG version of the grating task was to measure increases in alpha in the non-stimulated (right) hemisphere. However, the most prominent response for all participants was a strong stimulus-driven oscillation in the left hemisphere at 15Hz and its harmonics, induced by the 7.5Hz stimulus reversal (Figure 5.4A). During presentation of the grating, alpha power increases in non-stimulated cortex were only measurable in five participants (mean change from baseline 14.62% at the peak increase), giving too little data on which to conduct valid statistical analysis. Even after deselecting frequencies reflecting the grating reversal in an effort to remove contamination of the data by these signals, only four participants showed increased alpha in the right hemisphere (mean 18.93%, SD=6.39%). In the left hemisphere,

decreases in alpha power during stimulation were measurable in nine of the 14 participants (mean -17.72%, SD=19.46%) or in eight participants after filtering out frequencies related to the stimulus reversal (mean -16.64%, SD=6.37%), which again was not considered sufficient data on which to conduct analyses. The task was therefore not appropriate for generation of alpha in non-stimulated cortex, since strong stimulus-driven responses caused by contrast reversal of the grating masked other oscillatory rhythms.

On the other hand, the Eyes Open/Eyes Closed task induced clear suppression of the alpha rhythm on opening of the eyes in all participants (mean t score=-8.85; SD=2.34; Figure 5.4B). These data are therefore more reliable, but are not directly related to the BOLD data because they were obtained from a different task.

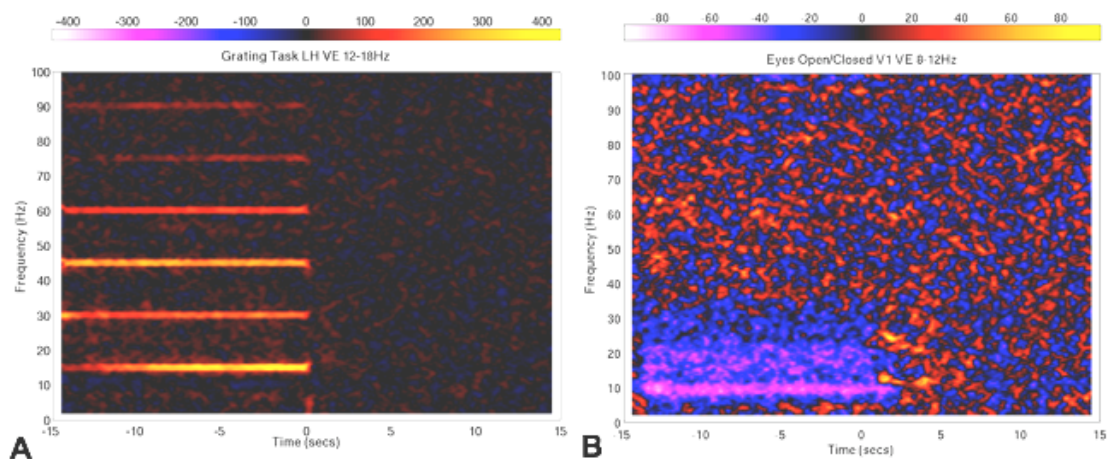


Figure 5.4. Time-frequency spectrograms from a representative participant. A) Response to a grating at the location of the peak response (15Hz) in occipital cortex, showing stimulus-driven oscillations and weak alpha suppression during the stimulus phase (-15-0s). B) Alpha and beta suppression during eyes open (-15-0 seconds) when compared with eyes closed (0-15s) at the peak decrease in alpha in occipital cortex.

5.4.3 BOLD data

BOLD responses to a reversing grating in the lower right visual field were recorded in arbitrary contrast of parameter estimate (COPE) units. In the stimulated (LH dorsal) ROI, the mean BOLD response across participants was 51.37 (SD=60.19), which was significantly greater than zero ($t(13)=3.19$; $p<.05$). Fewer than half of the voxels

(mean 44.39%) were positive ($t(13)=-1.36$; $p=ns$), since the retinotopically defined ROI covered the whole quadrant of V1 but the positive BOLD response was induced by a stimulus of only 4° diameter (Figure 5.5A). In the non-stimulated (RH ventral) ROI, the mean BOLD response was -34.17 ($SD=30.80$), which was significantly smaller than zero ($t(13)=-4.15$; $p<.05$). A mean across participants of 81.2% of the voxels in this region were negative, which was significantly greater than 50% ($t(13)=4.840$; $p<.001$). The non-stimulated ROI therefore indeed contained mostly negative voxels (Figure 5.5B). The variables subsequently used in analysis were therefore the mean response from positive voxels only in the left hemisphere dorsal ROI and the mean response from negative voxels only in the right hemisphere ventral ROI.

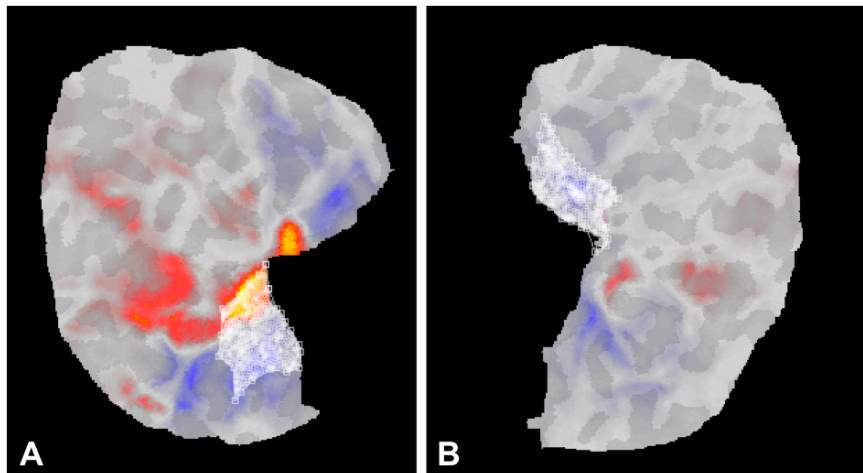


Figure 5.5. BOLD response to a grating in the lower right visual field on the left (A) and right (B) hemisphere flattened occipital cortices for a representative participant. V1 ROIs are shown in white.

5.4.4 Relationships between variables

The aim of this study was to investigate the relationships between GABA, alpha and BOLD in occipital cortex. Since the MEG grating task did not generate alpha oscillations in most participants, these data were not investigated in relation to other variables. The alpha measure was the peak decrease in the Eyes Open minus Eyes Closed condition within the V1 ROI. There were no significant relationships between negative BOLD and alpha ($R=.07$; $p=ns$); negative BOLD and GABA+ ($R=.16$; $p=ns$); or alpha and GABA+ ($R=.47$; $p=ns$). There was also no correlation between positive BOLD and any of the other variables: GABA+ ($R=-.08$; $p=ns$), alpha

suppression ($R=-.10$; $p=ns$), or negative BOLD ($R=-.01$; $p=ns$). Correlations and scatterplots are presented in Appendix 1. Similar results were obtained if the mean alpha desynchronisation in V1 was analysed as opposed to the peak.

Additional alpha and GABA+ data were available for a sample of 15 male participants (mean age=25.3 years, $SD=3.2$), collected by Misses Davis and McNamara as part of a short project within the same research centre. The MRS and EO/EC MEG experimental protocols were the same except that the MRS acquisition in this experiment was longer (552 measurements per voxel with a scan duration of 15 minutes) and only one run was acquired. One participant was excluded due to poor task compliance in the MEG, which meant that alpha suppression could not be measured. The alpha power decrease in the eyes open phase for this dataset was greater than in the original dataset (mean t score= -15.26 , $SD=7.81$), while the GABA+ value was similar (mean=1.50, $SD=0.16$). There was a correlation between GABA+ concentration and alpha suppression in this group of participants ($R=.54$; $p<.05$; 95% CI [.07, .85]; Figure 5.6). Data from this study and the original study were combined, with the average taken for data from two participants who were tested in both studies. The correlation between GABA+ and alpha suppression in the combined dataset was significant ($R=.56$; $p<.05$; 95% CI [.18, .80]; Figure 5.6). Individuals with greater GABA+ concentration therefore showed less alpha suppression than those with less GABA.

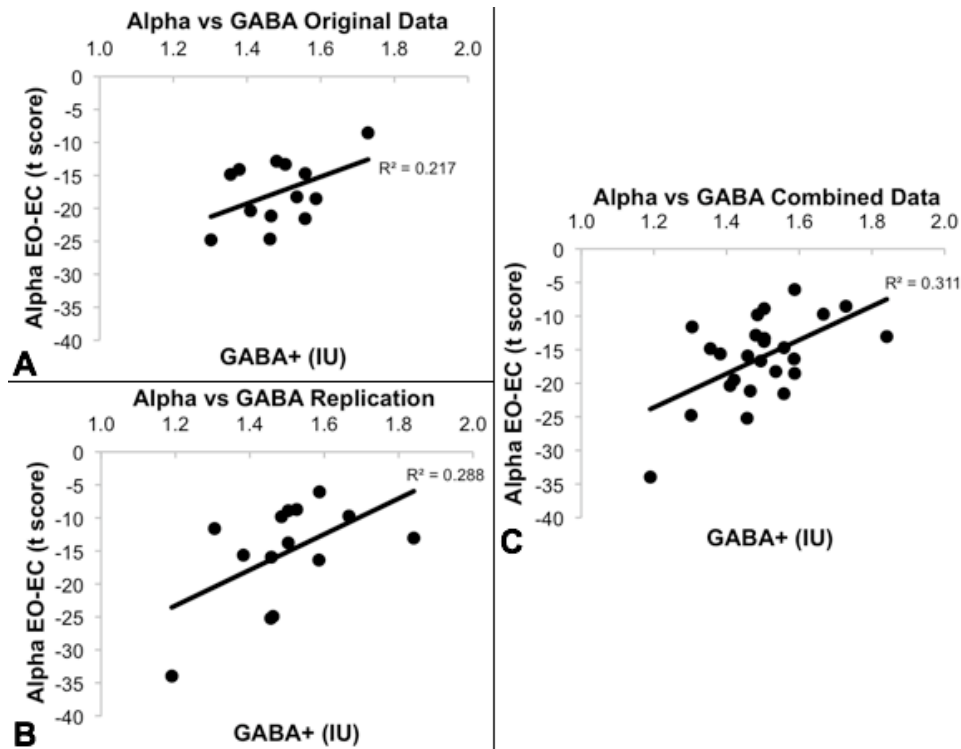


Figure 5.6. Correlations between GABA+ concentration in occipital cortex (institutional units) and peak alpha decreases in V1 during an Eyes Open/Eyes Closed task. Original dataset (A), replication (B) and the two datasets combined (C).

The mean voxelwise correlation between alpha decreases in the EO/EC task and GABA+ concentration across all individuals from the two studies was calculated and plotted on a cortical mesh in mri3dX. This analysis showed an area of high correlation ($R > .5$) in medial occipital cortex (Figure 5.7), suggesting that the mediation of alpha desynchronisation may arise from GABA-ergic inhibition in the occipital lobe.

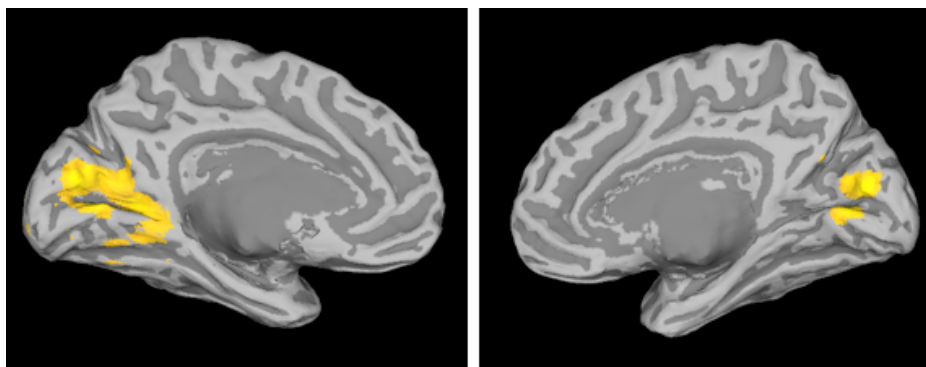


Figure 5.7. Map of voxels with correlations between GABA+ concentration and alpha suppression greater than $R = 0.5$.

5.5 Discussion

In this study, individuals with higher GABA+ concentration in occipital cortex were found to have reduced alpha suppression in V1 during an Eyes Open/Eyes Closed task in comparison to people with less GABA+. A whole brain voxelwise correlation also localised the relationship between GABA+ and alpha suppression to medial anterior occipital areas. There was no significant correlation between GABA+ and negative BOLD in V1 or between negative BOLD and alpha.

The positive correlation between GABA+ and alpha is the opposite direction to that which might intuitively be expected: since GABA is an inhibitory neurotransmitter and alpha oscillations reflect inactive (Pfurtscheller et al., 1996) or suppressed (Jensen & Mazaheri, 2010) cortex, people with more GABA might be expected to show more suppression of inactive cortex and therefore more alpha when the eyes are closed. Perhaps the relationship observed represents a difference in overall cortical reactivity related to GABA+ concentration: high levels of GABA+ may reduce activity in all frequency bands, resulting in a continuously more suppressed state and reducing reactivity to a stimulus. People with greater GABA+ concentration and reduced cortical reactivity would therefore show a smaller increase in alpha on closing the eyes. Separate analysis of individual differences in eyes open and eyes closed phases would allow investigation of this effect. GABA has been said to mediate the transition between resting and active state in the cortex (Qin, Grimm, Duncan, Wiebking, Lyttelton, Hayes et al., 2012) and the current results showing a relationship between GABA+ and alpha may support this theory, but the role of both variables during the transition must be determined in order to further investigate this theory.

Alpha reflects inhibitory interactions on both a local and inter-area scale (Harvey et al., 2012) but the measures of MEG and MRS have poor spatial resolution, therefore cannot distinguish which level of response they are measuring. Use of microscopic measures such as electrocorticography and receptor density mapping would allow investigation of the spatial scale at which GABA influences alpha suppression. Rather than having a discrete source, alpha may be produced in multiple areas of the brain (Başar, Schürmann, Başar-Eroglu & Karakaş, 1997), therefore if GABA-ergic

systems modulate the production or regulation of alpha oscillations, occipital alpha and BOLD may correlate with GABA⁺ in other regions of the brain. This possibility could be investigated by acquiring GABA⁺ from other areas, such as the thalamus.

The inverse correlation expected between GABA concentration and positive BOLD (Muthukumaraswamy et al., 2009; Donahue et al., 2010; Stagg et al., 2011a) was not replicated in this study, and the hypothesised positive correlation between GABA and negative BOLD was also not found. This result may be due to the low numbers of participants tested or to the repeatability of the measures. These issues will be considered in Chapters 6 and 7. There was also no relationship between alpha and BOLD. It had been hypothesised that individuals with more alpha suppression on opening their eyes would also show more negative BOLD in response to a visual stimulus, since both alpha (Foxe et al., 1998) and negative BOLD (Smith et al., 2000) occur in non-stimulated cortex, and because increased alpha surrounds stimulated areas of visual cortex, where negative BOLD can be expected (Harvey et al., 2012). Conversely, an inverse relationship was expected between positive BOLD and alpha, such as has been reported for the temporal relationship between these variables (Goldman et al., 2002; Laufs et al., 2003). One study (Laufs et al., 2003) has claimed that alpha and positive BOLD are not correlated in occipital cortex, though they are related elsewhere in the brain, therefore visual alpha does not represent the neuronal activity that results in a BOLD response. The absence of correlations between BOLD and alpha in the current study is likely to be due to the measurement of these variables using different tasks.

Future studies could aim to investigate the relationship between alpha and negative BOLD using more optimal paradigms. The grating task used to evoke fMRI and MEG responses in this study was ineffective in its aim to generate alpha increases in non-stimulated cortex and decreases in the stimulated hemisphere. If such responses were present, they were masked by signals induced by the contrast reversal of the stimulus. An additional potential issue with the stimulus was the location of the attentional task, since alpha and negative BOLD are involved in suppression of unattended as well as non-stimulated regions (Tootell, Hadjikhani et al., 1998; Smith et al., 2000; Kelly et al., 2006). Presenting the attentional task in the stimulated hemisphere rather than at fixation may therefore improve the chance of detecting

alpha and negative BOLD in the opposite hemisphere. Alternatively, an Eyes Open/Eyes Closed task could be used in the fMRI to maintain the same task as the MEG.

Other potential mediators of the relationships between GABA, alpha and BOLD could be investigated: correlations between alpha and BOLD have been associated with theta and beta oscillations, so other frequencies of neuronal activity may contribute to production of a BOLD response (Laufs, Holt, Elfont, Krams, Paul, Krakow et al., 2006); and structural factors such as the area of V1 may also mediate the relationship between GABA and BOLD (Schwarzkopf et al., 2012). The process of suppression of irrelevant stimuli and of inhibition of areas not required for processing is likely to be a complex interaction between many different variables. Many of these can be measured using different neuroimaging techniques, but the tasks and measurements must be carefully designed in order to make inferences about the true relationships between these variables.

5.6 Conclusion

This study found that individuals with greater GABA+ concentration in occipital cortex showed less alpha suppression in an Eyes Open/Eyes Closed task. This relationship may be attributable to a general reduction in cortical reactivity in participants with high GABA. There was no evidence for a link between GABA+ and negative BOLD, or between negative BOLD and alpha. This finding could suggest that the different measures of inhibition in the brain reflected in each technique are unrelated to each other. Future studies could develop a task that induces both strong alpha and negative BOLD so that the relationship between individual differences in these variables and GABA can be investigated more optimally.

Chapter 6

Methodological Sources of Variability in GABA-Edited Magnetic Resonance Spectroscopy

6.1 Abstract

Recent studies have reported correlations between individual differences in gamma-aminobutyric acid (GABA) concentration and behavioural and neuroimaging responses (Edden et al., 2009; Muthukumaraswamy et al., 2009; Donahue et al., 2010; Stagg et al., 2011a). Studies of individual differences must ensure that variables are reliable across repeated acquisitions in the same participant. This study investigated the influence of acquisition and analysis procedures on the repeatability of GABA measurement using magnetic resonance spectroscopy (MRS) in occipital cortex. Within-subjects repeatability (reflected in the coefficient of variance (CV)) was improved by 4.63% by reversal of the direction of the magnetic field gradients. This effect was explicable on the basis of the chemical shift artefact, whereby different metabolites are acquired from slightly different locations due to their resonant frequencies lying at different positions along the magnetic field gradient. The impact of gradient reversal was to acquire the low frequency component of the spectra from a region further from the skull and scalp and therefore to reduce contamination of the baseline of spectra by lipid signals. It is therefore important to determine the optimal gradient directions for voxels in different regions of the brain so as to minimise the contribution of lipid signals. A further 0.97% improvement in repeatability was produced by manually adjusting the phase of individual spectra to produce optimal absorption spectra. Optimised GABA measurement (with reversed gradients and manual phasing) was reliable (CV=4.54%) and within-session variability in a phantom containing a GABA solution was low (CV=1.9%), indicating that the measurement noise in GABA-edited MRS is small. The majority of test-retest variability in GABA concentration therefore reflects genuine within-subject variability as opposed to measurement noise. However, the between-subjects variability did not sufficiently exceed within-subjects variability to give a meaningful measure of individual differences. Greater numbers of participants and a less

homogenous sample may be required to give a wider range of GABA+ concentrations when investigating relationships with other variables.

6.2 Background

Neuroimaging studies inevitably contain some measurement noise, which can be attributed to factors relating to the participant, the scanner or the testing environment. This noise should be minimised and the repeatability of a measure should be quantified before it is used to test differences between experimental conditions, between groups of participants or between individuals. It is particularly important to determine the test-retest reliability of a measure when studying individual differences, since the absolute value of the measure is the variable of interest, rather than the relative difference between groups or conditions. If very different values are obtained when a participant is tested multiple times, either within a session or across sessions, any individual differences reported by the technique are questionable since they may have arisen from inconsistency in the measurement rather than from genuine differences between participants. Within-subject variability should therefore not exceed between-subject variability.

The reliability of a test (the degree to which repeated observations give a similar result) can be investigated using various statistics. A Pearson's R correlation is often used to test the hypothesised linear relationship between two measures of the same variable, but is in fact inappropriate for assessing reliability as it depends on the range of the values and does not take into account systematic shifts or linear but unequal variability (Bland & Altman, 1986). The coefficient of variation (CV) and intraclass correlation coefficient (ICC) are more appropriate measures of reliability. The CV is the ratio of the standard deviation of a measurement to its mean. Expressed as a percentage, it gives a normalised estimate of within-subject variability of repeated measurements in relation to their mean. The ICC is the ratio of the variability between subjects to the total variability from between subjects and within subjects. The ICC therefore shows the ease with which participants can be discriminated: a high ICC indicates substantial differences between participants and low within subjects variance (Shoukri, Colak, Kaya & Donner, 2008). For a measure to be most

useful, it should show good retest reliability (shown by a low CV) and high discriminability (shown by a high ICC).

Measurement reliability is all the more important when two potentially noisy variables are to be correlated with each other. Several recent studies have described correlations between individual differences in the inhibitory neurotransmitter, gamma-aminobutyric acid (GABA), measured using magnetic resonance spectroscopy (MRS) and measures of neuronal or haemodynamic activity (Muthukumaraswamy et al., 2009; Donahue et al., 2010; Muthukumaraswamy, Evans, Edden, Wise & Singh, 2011). GABA has also been reported to correlate with behaviour (Edden et al., 2009; Boy et al., 2011; Stagg et al., 2011a). MRS has been shown to give reasonably reliable measures of various metabolites (Tedeschi, Bertolino, Campbell, Barnett, Duyn, Jacob et al., 1996; Chard, McLean, Parker, MacManus & Miller, 2002; Gasparovic, Bedrick, Mayer, Yeo, Chen, Damaraju et al., 2011), so may be appropriate for conducting correlations with other variables; however, the preceding two chapters in this thesis have failed to replicate the correlation between GABA and haemodynamic activity. The repeatability of the GABA measurement obtained in these studies was therefore in question.

Previous studies have investigated the reliability of MRS measures of GABA plus macromolecular contributions to the signal (GABA+ (Behar & Rothman, 1994)). Within-subject GABA+ concentration in occipital cortex had a CV of 6.5% across five measurements in one day (Evans et al., 2010), as opposed to a between-subjects variance of 9.1%. Similarly, Bogner and colleagues also reported lower within-subject variability (CV=10-12%) than between-subject variability (CV=13%) in occipital GABA (Bogner et al., 2010). Repeatability of GABA+ in other areas including sensorimotor, anterior cingulate, frontal and dorsolateral prefrontal cortices has also been shown to be acceptable, with within-subjects CVs all less than 13% (Evans et al., 2010; Geramita, van der Veen, Barnett, Savostyanova, Shen, Weinberger et al., 2011). ICCs have also indicated good reproducibility and discriminability of GABA (ICC>0.7) in the lentiform nuclei (LN), left frontal lobe and ACC (Harada et al., 2011). GABA repeatability is therefore within the acceptable range of CVs below 10% (<http://www.westgard.com/lesson34.htm#6>) and ICCs

greater than 0.5 (www.stattools.net/ICC_Exp.php) in most regions of the brain, but some variability remains.

The cause of within-subject variability in the measure of GABA+ and the ways in which it can be minimised were the focus of this study. There are several parameters of the scan sequence and the analysis techniques that may affect the reliability of spectroscopy data. When exposed to a magnetic field, different molecules resonate at different frequencies due to shielding of their nuclei from the magnetic field by electrons (chemical shift). In MRS, the concentration of metabolites is represented by the area under the peaks on the chemical shift axis corresponding to molecules' resonant frequencies. However, the frequency of the MRS signal is also used to encode the position of the voxel. A well-known but little-discussed feature of MRS is the chemical shift artefact, whereby the position of the recorded voxel is shifted for different metabolites. This displacement occurs because radiofrequency (RF) pulses used for slice selection are of finite bandwidth and are positioned by a frequency shift using a magnetic field gradient. These pulses only excite spins with a resonance frequency within that bandwidth, so slice position is shifted in the gradient direction for molecules with different resonance frequencies (Bertholdo et al., 2011). For instance, at 7T, the 1.2 parts per million (ppm) difference between N-acetylaspartate (NAA) and choline (Cho) gives a chemical shift displacement (CSD) of ~9mm (Goelman, Liu, Fleysler, Fleysler, Grossman & Gonen, 2007) and on the 3T GE HDx scanner used in these studies, the difference in position between the water and GABA+ voxels is approximately 3.1mm. The direction in which the gradients are applied can therefore shift the relative position of voxels from which different metabolites are measured in all three dimensions.

Reversing the direction of the gradients may affect the signal obtained, particularly if the tissue compositions of voxels excited by different gradient directions are very different (Howe, Stubbs, Rodrigues & Griffiths, 1993). When acquiring data from a region in close proximity to an area of sinus, skull, scalp or ventricles, changing the gradient direction will shift acquisition of some metabolites towards or away from this area. This is likely to be an issue in the occipital lobe as voxels are inevitably positioned close to the edge of the brain. If the direction of the gradients were such that the low frequency lipid signal was obtained from an area posterior and/or

superior to the GABA+ voxel, in the region of the sagittal sinus and scalp, there would potentially be a high contribution of lipid signals to the spectra. These signals could affect the stability of the baseline adjacent to the GABA+ peak. With gradients in the opposite direction, lipids would be measured in an area anterior and inferior to the GABA+ voxel, in which the tissue composition would be similar and the lipid content would be lower (Figure 6.1). The gradient direction is not generally reported in MRS publications and in fact is not always easy to determine: for the GE HDx scanner in this centre, the orientations are known (x=left/right, y=anterior/posterior, z=superior/inferior); however, the direction of the gradients in these planes is not reported by the scanner. Knowledge of the gradient directions will allow optimal scan parameters to be chosen in order to minimise the contribution of lipids to the spectrum, stabilising the baseline and potentially improving repeatability.

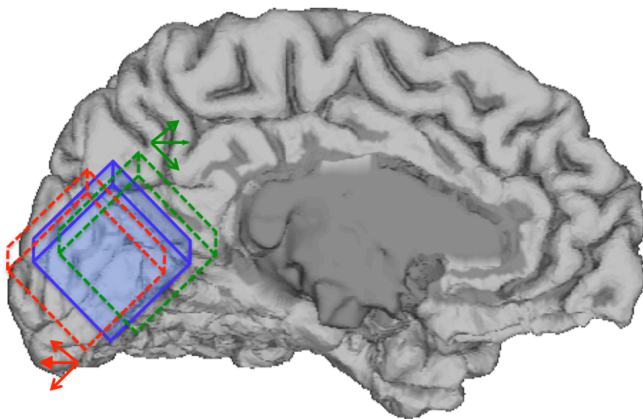


Figure 6.1. An example of the chemical shift artefact with the GABA voxel shown in blue. Reversing the direction of the magnetic field gradients changes the position of other metabolites in relation to this voxel in all three dimensions (red and green voxels).

Another methodological factor that may contribute to repeatability of the GABA measurement is the accuracy of the phasing of the signal (<http://www.cis.rit.edu/htbooks/mri/>). The magnetisation vector produced by a spin gives a cosine wave when plotted over time, with peaks at the duration of rotation. With a single detector, the signal obtained from the Fourier transform of the waveform will not distinguish the direction of rotation. The signal in the orthogonal orientation will be a sine wave, which also does not discriminate the direction of rotation. Combining these two orthogonal signals in the Fourier transform as real

(cosine) and imaginary (sine) components allows the direction of motion to be distinguished and produces a single peak (an absorption spectrum, Figure 6.2A). If the sine and cosine waves were allocated to the orthogonal components, the signal would show a positive then a negative peak (a dispersion spectrum, Figure 6.2B). However, since the detector and the magnetisation vector are rarely on exactly the same axis, the phase of the signal obtained is generally shifted slightly (Figures 6.2C and D). These phase shifts can be corrected by adding or subtracting the appropriate number of degrees to the signal so that the sine and cosine waves begin at a phase of zero.

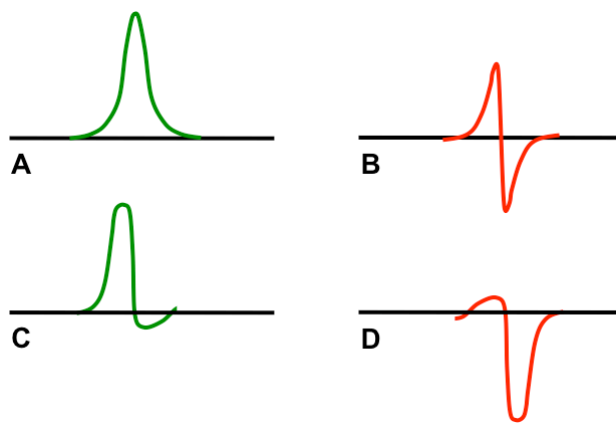


Figure 6.2 A) Real (absorption) and B) imaginary (dispersion) spectral profiles. C and D) The same spectra with a slight phase shift, which can be corrected.

In the GABA analysis toolkit pipeline (*Gannet*; <http://gabamrs.blogspot.co.uk/>) used in this study, data are automatically phased. Occasionally, slight manual adjustments to the phase made by trained operators can further improve the spectra. Correct phasing can make a large difference to the ability to fit a Gaussian model to the acquired data, which may result in improved repeatability between runs. Poorly phased data can show shifts in the baseline or sharp peaks in the spectra, extreme examples of which are shown in Figure 6.3.

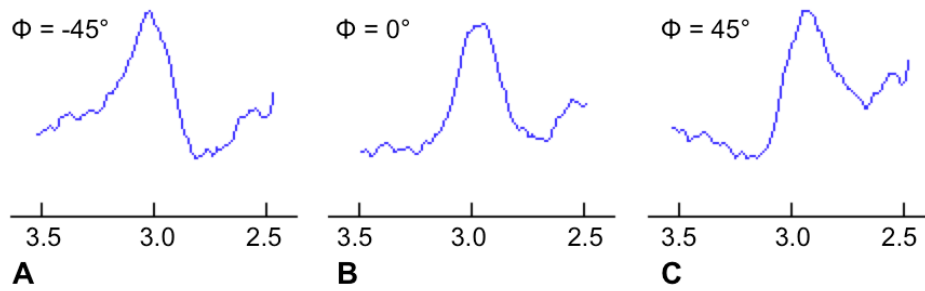


Figure 6.3. The effect of extreme phase differences (Φ) of -45° (A) and 45° (C) on the acquired spectrum (B).

Test-retest repeatability can also be affected by genuine within-subject variability. The most common and potentially the most severe cause of variability between scans is head movement, which causes phase shifts and consequently attenuation of the signal (Thiel, Czisch, Elbel & Hennig, 2002), as well as potentially altering the homogeneity of the B_0 magnetic field (Tyszka & Mamelak, 2002). Physiological factors may also alter the GABA value in the absence of a genuine change in GABA concentration. For instance, during the cardiac cycle, the size of vessels changes, there is movement of CSF and tissue is slightly displaced (Dagli, Ingeholm & Haxby, 1999), causing phase dispersion and signal loss (Felblinger et al., 1998). Variations in blood oxygenation throughout the cardiac cycle may also influence the MRS signal due to the diamagnetic property of oxyhaemoglobin, with greater changes nearer major blood vessels (Dagli et al., 1999). During respiration, movement of the abdominal organs and changes in the volume of air within the chest cavity alter the bulk magnetic susceptibility of the body and the distortion of the principle magnetic field by body tissue (Hu, Le, Parrish & Erhard, 1995). These physiological factors reduce the MRS signal and potentially affect the repeatability of the measurement (Felblinger et al., 1998).

In addition to physiological and methodological sources of variability, within-session differences in GABA are also likely to contain a component of measurement noise, attributable to factors related to the scanner or the scanning environment such as temperature change, magnetic field inhomogeneities, or random (thermal) noise within the voxel. For example, if the scanner has been used for sequences that make heavy use of the imaging gradients, such as echo-planar imaging (EPI), prior to the MRS sequence, the temperature in the gradient coil and magnet structure will be

higher. Changes in temperature can affect magnetic properties of various components in the MR system (e.g. ‘passive shims’ – steel used to correct the magnetic field), causing a change in the magnetic field at the MRS voxel during the session. Since GABA is present in low concentrations (1-1.3 micromol/cm³) in the brain (Rothman et al., 1993), small measurement error may have a large effect on the reported concentration. Measurement noise can be investigated in a phantom containing a solution with a known concentration of GABA, which is not subject to variance induced by human participants such as movement artifacts. If GABA-edited spectroscopy is repeatable in a phantom then any differences at retest *in vivo* can be attributed to genuine within-subject variance rather than to inconsistencies in quantification of the measure.

This study aimed to determine the influence of gradient direction (default or reversed) and phasing technique (automatic or manual) on the repeatability of GABA quantification in occipital cortex using MRS. The consequence of changing these factors was evaluated based on the repeatability (measured by CV and ICC) of the concentrations obtained from two runs in each session and on the difference in the fit error of the GABA peak to the Gaussian modeled peak. It was hypothesised that reversed gradients and manual phase adjustments would increase the within-session repeatability and improve the fit error. The relative contributions of participant and measurement noise were investigated by comparing *in vivo* data with the within-session repeatability of measurements in a phantom with a known concentration of GABA.

6.3 Methods

6.3.1 Participants and procedure

Twelve participants (seven female) of mean age 26 years, 11 months (SD 4 years 10 months) were recruited from students and staff at Cardiff University. All participants were also involved in the study described in Chapter 4. The MRI session lasted 60 minutes in total and consisted of 10 minutes of functional MRI not relevant to this study (the second run of retinotopic mapping for Chapter 4), two short localiser scans for positioning of the MRS voxel, and four runs of spectroscopy, each 10 minutes long.

The GABA phantom was a 10mM solution of GABA in a 500ml plastic bottle (Figure 6.4). The voxel was positioned in the centre of the bottle, avoiding the edges. Two runs of the acquisition were obtained, then the phantom was removed, repositioned and the voxel location re-prescribed. Fifteen pairs of acquisitions were conducted. This procedure simulated investigation of test-retest repeatability in a group of 15 participants, with slightly different positioning of each participant in the scanner. GABA values from the phantom are described as within- and between-session rather than within- and between-subject.



Figure 6.4. GABA phantom containing 10mM solution of GABA.

6.3.2 MRS acquisition and analysis

Data were acquired on a 3.0T GE HDx system (GE Healthcare, Chalfont St Giles, UK) with body coil transmission and an eight-channel receive-only head coil. *In vivo*, fast spin echo sequences were used to acquire seven 2mm sagittal slices through the midline of the brain and one oblique slice aligned along the cerebellar tentorium. These localiser slices were used to position the (3cm)³ spectroscopy voxel with the lower edge along the cerebellar tentorium, the anterior edge aligned with the parieto-occipital sulcus, and the posterior edge avoiding the sagittal sinus as much as possible. The MEGA-PRESS (Mescher et al., 1998) sequence had a TE of 68ms, TR of 1.8s, 332 measurements per voxel and 16ms Gaussian editing pulses applied at 1.9ppm and 7.46ppm in alternate scans. Eight unsuppressed acquisitions were collected at the end of the MEGA-PRESS scan to serve as an internal concentration (and phase) reference. Four runs of the sequence were acquired: two with the gradients in all three orientations in the default direction and two with the gradients in the reversed direction.

A difference spectrum was obtained using *Gannet* software. The edited GABA+ signal at 3ppm and the unsuppressed PRESS water signal were integrated. A measure of GABA+ concentration in institutional units was derived by accounting for the editing efficiency and the T1 and T2 relaxation times of water and GABA. GABA+ peaks were initially phased automatically, then small manual adjustments to the phase were made where necessary and these data were compared. The spectroscopy voxel was segmented into grey matter, white matter and CSF and the fraction of tissue within the voxel was obtained using FMRIB's Automated Segmentation Tool (FAST; (Zhang et al., 2001). GABA+ values were corrected for the tissue fraction in the voxel.

For the phantom sessions, parameters were similar apart from that the voxel was smaller (2cm)³ and only 64 measurements per voxel were acquired. The direction of the magnetic field gradients was always reversed from the default direction. The ratio of GABA, obtained from the integral of the triplet lineshape, to the water integral from a Voigt lineshape was calculated in the off spectrum.

6.4 Results

The effects of the four *in vivo* experimental conditions (default and reversed gradients with automatic or manual phasing) are summarised in Table 6.1. The required adjustments to the phase of spectra, averaged across the two acquisitions and all participants, was greater when gradients were in the default direction, suggesting that automatic phasing was less accurate in identifying the initial point on the GABA+ curve with default gradients. Mean GABA+ fit errors (SDs of the residuals of the Gaussian fit divided by the height of the GABA+ peak) were slightly higher when gradients were in the default direction and when automatic phasing was conducted, with the smallest fit error for reversed gradients and manual phasing. Individual differences in fit error did not correlate with GABA+ concentration with default gradients and automatic or manual phasing, nor with reversed gradients and automatic or manual phasing (R=.33, -.32, .19 and .08, respectively, all p=ns), indicating that there was no systematic effect of the fit of the GABA+ peak on the concentration obtained. The GABA+ concentrations averaged across participants and acquisitions

were similar for all four experimental conditions, as shown in Table 6.1. However, the standard deviations and the distributions in the equality plots in Figure 6.5 indicate that the variance between acquisitions and between participants was greater when the default gradient direction was used, due there being more extreme values in these conditions.

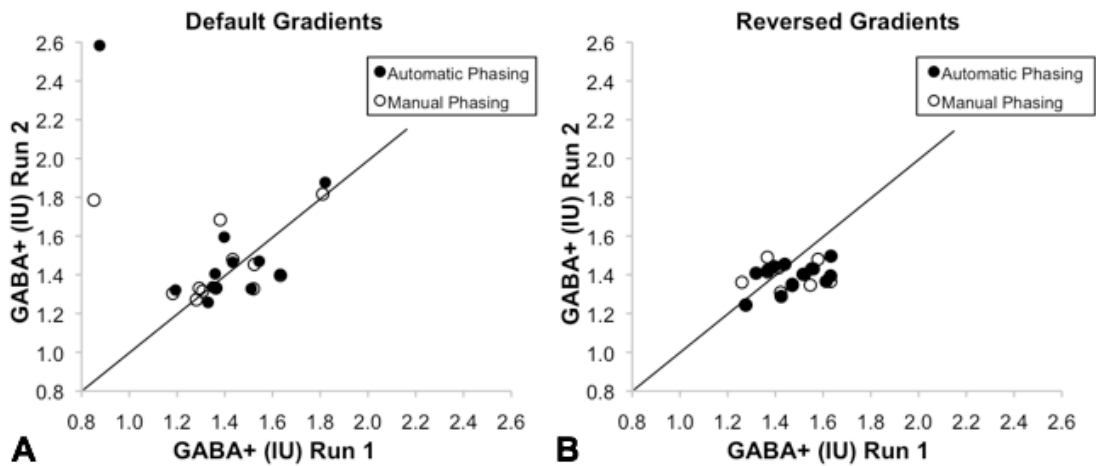


Figure 6.5. Equality plots showing the GABA+ value obtained from two acquisitions using automatically or manually phased spectra and with gradients in the default (A) or opposite (B) direction. Lines of equality are shown, along which all values would lie if both acquisitions gave exactly the same value.

To investigate the repeatability of the GABA+ concentration measurement statistically, within-subjects coefficients of variance (CVs) between the two acquisitions were calculated for each gradient direction and phase method and averaged across all participants. Between subjects CVs were also calculated for each acquisition then averaged over the two acquisitions for each condition. All within-subjects CVs were below 10.14%, indicating good repeatability of the measure across the two acquisitions (Table 6.1). The best within-subject repeatability (CV=4.54%) was in the reversed gradients and manual phasing condition. However, two-way random effects intraclass correlation coefficients (ICCs) with absolute agreement showed poor repeatability of GABA+ measurement for all conditions (all $p > .11$), suggesting that although variability between-subjects was always greater than within-subjects (Table 6.1), this effect was not sufficient to discriminate individuals' data. With automatic phasing and default gradients, the ICC is negative, indicating that the same participants who had higher GABA+ concentrations in one run actually had

lower concentrations in the other run. In the reversed gradient conditions, ICCs were greater, but were not significant. This result may be attributable to the low variability in GABA+ concentration between subjects when reversed gradients were used (Figure 6.5B).

Table 6.1. Effect of phasing technique and gradient direction on mean phase applied (degrees), error in fit to the Gaussian (%), GABA+ concentration (institutional units), between and within subjects CV (%), and ICC (R).

		SD of mean phase	Mean fit error (%)	SD of mean GABA+	Between subjects CV (%)	Within subjects CV (%)	ICC
Automatic phasing	Default gradients	N/A	4.56 (1.21)	1.47 (0.17)	20.38	10.14	-1.20 (p=.89)
	Reversed gradients	N/A	3.84 (0.89)	1.43 (0.08)	6.68	5.51	.45 (p=.11)
Manual phasing	Default gradients	6.80 (8.17)	3.91 (1.00)	1.42 (0.16)	15.38	8.50	.08 (p=.45)
	Reversed gradients	4.20 (8.24)	3.42 (0.25)	1.42 (0.08)	6.69	4.54	.37 (p=.19)

The gradient direction had a greater impact on repeatability than the method of phasing. Within subjects, reversing the gradients improved the CV by 4.63% when automatic phasing was conducted, and by 3.96% with manual phasing. The main impact of reversing the gradients was to reduce the low frequency lipid signals in the spectra, as shown in Figure 6.6. The baseline signal at the lower frequency end of the GABA+ peak was therefore better controlled when the gradients were in the reversed direction, which may explain why automatic phasing was more effective for spectra acquired with reversed gradients. This lipid contamination was caused by the chemical shift artefact, as the volume in which the lipid signal was acquired was shifted more posteriorly in the brain with gradients in the default direction. This directional effect was confirmed *in vivo* in one participant by moving the GABA voxel further back in the brain, which produced a spectrum with a large lipid contribution. *In vitro*, in a phantom containing water below lipid, a voxel placed in the water on the boundary with the lipid contained only water signal. When gradients were in the default direction, decreasing the RF pulse centre frequency moved the

voxel up (into the fat); whereas with reversed gradients, increasing RF frequency moved the voxel up, producing a lipid peak in the spectrum. Manually phasing spectra made only a small improvement in the repeatability of GABA+ measurement compared with automatic phasing. When gradients were in the default direction, manual phasing improved the within subjects CV by 1.64%, while with reversed gradients, it improved the CV by 0.97%.

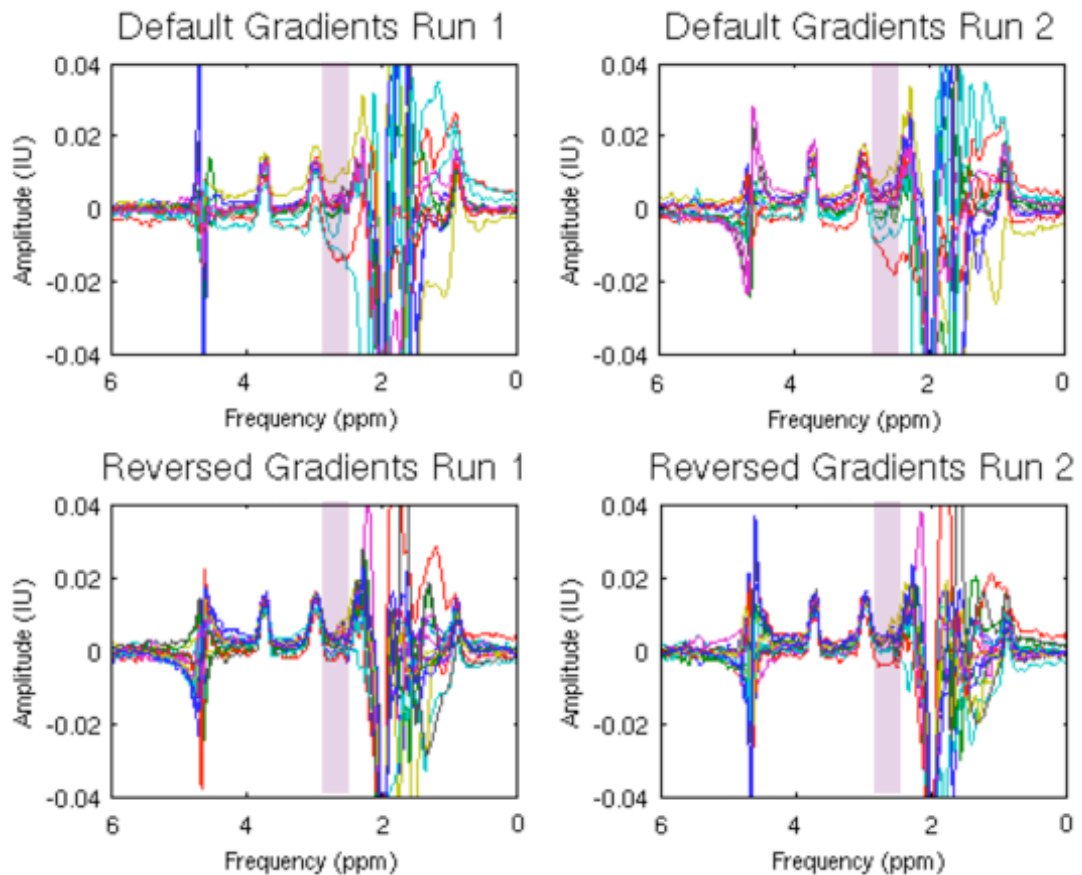


Figure 6.6. Effect of gradient reversal on MRS spectra. Shaded area shows the baseline adjacent to the GABA+ peak in which lipid signals encroach in acquisitions with default gradients. Each line represents one participant's data.

In order to test the contribution of measurement noise to the within-subjects variance in GABA+ concentration, the repeatability of GABA measurement was investigated in a phantom in which GABA concentration was constant and there was no issue of participant movement. In this *in vitro* data, the mean error in the fit of the GABA peak across two acquisitions in 15 sessions was 6.14% (SD=.47), which was greater than the fit error for the comparable condition *in vivo* (3.84%). The mean GABA

concentration (in arbitrary units) was 1.72 (SD=.04), which cannot be compared directly with the *in vivo* data from Experiment 1 since the two experiments involve very different parameters, for example the T1 and T2 of GABA are likely to be different *in vivo* and *in vitro*. The coefficient of variance (CV) indicated very high within-session repeatability of the GABA concentration measurement (CV=1.91%), which was substantially better than the comparable condition in Experiment 1 (5.51%). The between-sessions CV *in vitro* was 2.65% and a two-way random effects intraclass correlation coefficient (ICC) with absolute agreement gave a correlation of .30, which reflects non-significant ($F(14,14)=1.45$; $p=ns$) agreement. As the GABA concentration was constant, both within- and between-session variability were expected to be negligible. The ICC was therefore not expected to be significant as the values from different sessions should not be discriminable from each other.

6.5 Discussion

The optimal parameters for obtaining repeatable GABA+ measurements were to reverse the direction of the magnetic field gradients and to manually phase the spectra. Reversing the direction of the gradients had a much greater effect on the within- and between-subjects variability than the phasing technique. The increase in reliability was reflected in reduced coefficients of variance and improved fit of the spectra to the modeled GABA peak. However, the between-subjects variability did not sufficiently exceed within-subjects variability to show significant repeatability of GABA+ measurement using intraclass correlation coefficients. Within-subjects variability was mostly due to participant-related variability, as opposed to measurement noise.

With the gradients in the default direction for the GE HDx scanner used in this study, there was substantial contamination of the baseline adjacent to the GABA+ peak by lipid signals. This finding suggests that, in this scanner, the default gradients in the y plane project anterior-posterior in the brain, resulting in an increased low frequency lipid contribution to the spectra from a more posterior region that potentially contains more sinus, CSF, skull and scalp. This effect will be greater for some participants than others and will depend strongly on the way in which operators position the occipital MRS voxel: in participants with smaller heads and brains, the relative shift

will be greater so the voxel would potentially contain more lipid signal. Operators who tend to position the voxel closer to the edge of the brain would risk greater contamination of the signal with lipids. The influence of gradient direction on the spectra will also differ in different areas of the brain, depending on the proximity of the voxel to regions with a high lipid content. The results therefore show that it is very important to establish the optimal gradient direction for the particular voxel and scanner in question in order to obtain optimal spectra.

A greater degree of phase correction was required when gradients were in the default direction, but manual phasing resulted in only slight (<2%) improvements in the within-subjects CV over and above the improvement caused by the changing the gradient direction. The degree of phasing required differed for the two acquisitions in each condition, confirming the importance of inspecting and correcting spectra on an individual basis during initial quality control of data. Manual phasing should be conducted by trained individuals, since a spectrum may have contributions from multiple metabolites (for instance GABA as well as macromolecules), and correcting one aspect of the signal may induce artefacts in another. Since manual phasing only results in small improvements to the spectra, requires training to conduct and is only likely to be important in voxels close to areas of different tissue composition such as the occipital lobe, it is recommended in most situations only to automatically phase the data.

When the optimal parameters of reversed gradients and manual phasing were applied, the within-subjects CV in this study showed improved occipital GABA+ repeatability in relation to previous studies (Bogner et al., 2010; Evans et al., 2010). The finding of good repeatability according to the CVs but not the ICCs indicates that improving acquisition and analysis procedures also reduced differences between participants in this sample, making it more difficult to discriminate between individuals' data. While it is more important to ensure that a measure is repeatable within participants, reducing between-subject variance limits the potential to study individual differences in GABA+ concentration. Many more participants may be necessary to obtain a sufficient spread of values in order to conduct meaningful correlations with other variables. The sample tested in this study were of a similar age, therefore a less

homogenous cohort may give greater between subjects variance and therefore a higher ICC.

The within-session repeatability of GABA measurement in a 10mM solution was excellent, indicating there was only a small contribution of unclassified 'noise' to within-session variability. This variability could arise from inconsistencies in the equipment or the scanning environment, such as small magnetic field inhomogeneities or temperature differences. Although the true concentration of GABA present in the phantom was always the same, there was slightly greater variability in the values reported between sessions than within sessions. This finding again suggests that slight differences in voxel position may be an important factor in influencing variability in the measurement.

The results support previous evidence of good repeatability of GABA edited spectroscopy (Bogner et al., 2010; Evans et al., 2010; Geramita et al., 2011; O'Gorman et al., 2011) and extend the literature by showing that within-session variance was very low for phantom data, slightly higher for within-subjects data and slightly higher still between subjects. This is the expected order of variance, because *in vivo*, factors such as participant movement (Thiel et al., 2002; Puts & Edden, 2012) and physiological noise (Felblinger et al., 1998; Evans et al., 2010) can affect the measurement within a session and individual variability should exceed this within-session variability. With optimal scan parameters for reducing variability *in vivo*, around a third of the small amount of within-session variance remaining was attributable to measurement noise from factors unrelated to the participants. The differences between the *in vivo* and *in vitro* data are not simply due to a greater signal to noise ratio (SNR) in the phantom because $SNR = 1/\text{fit error}$ but the fit error was greater in the phantom and consequently the SNR was in fact weaker than *in vivo*. The majority of the *in vivo* variance can therefore be assumed to originate from genuine differences within or between participants.

These differences may be caused by participant movement or physiological factors: throughout the cardiac cycle, the composition of the spectroscopy voxel is altered by changes in vessel size and movement of CSF and tissue (Dagli et al., 1999); while the change in volume of the chest cavity during respiration may alter the bulk magnetic

susceptibility of the body (Hu et al., 1995). Such changes may indirectly affect the repeatability of measurements by weakening the SNR to different extents in different scans or in different people. Future studies could investigate methods for monitoring these variables and correcting for their fluctuations on a continuous basis throughout the spectroscopy acquisition. Variability in GABA concentration between subjects may be influenced artifactually by physiological factors such as differing heart rates across participants. Alternatively, genuine causes of individual differences in GABA concentration may include structural features of the cortex, such as its volume or thickness, the number of inhibitory interneurons, or the density of GABA receptors in the cortex.

6.6 Conclusion

This study showed that the repeatability of measurement of GABA+ concentration with MRS was improved by reversing the direction of the magnetic field gradients, which stabilised the baseline by reducing contributions of lipid signals to the spectra. Small manual adjustments to the phase of the spectra where required also slightly improved repeatability. Test-retest repeatability of GABA measurement was very high in a phantom. GABA-edited spectroscopy therefore has the potential to be very repeatable within subjects and to show genuine variability within and between subjects. However, the limited range of GABA values between subjects in this cohort made it difficult to discriminate individuals' data. This issue may explain the difficulty in this thesis in replicating previous findings of correlations between individual differences in metabolite concentrations and other behavioural or neuroimaging factors (Muthukumaraswamy et al., 2009; Donahue et al., 2010; Boy et al., 2011; Stagg et al., 2011a). A larger and less homogenous sample may be necessary in order to detect a sufficient range of between-subjects differences to conduct correlations between variables.

Chapter 7

Simulating the Influence of Measurement Noise on the Relationship Between GABA and BOLD in Visual Cortex

7.1 Abstract

Individuals with a greater concentration of the inhibitory neurotransmitter, gamma-aminobutyric acid (GABA) in their occipital cortex have been reported to show smaller blood oxygen level-dependent (BOLD) fMRI responses to visual stimuli (Muthukumaraswamy et al., 2009; Donahue et al., 2010); however, this relationship was not replicated in previous experiments in this thesis (Chapters 4 and 5). The difficulty in replicating these results may have been due to measurement noise, as this decreases the strength of correlations. The current study therefore investigated the relationship between BOLD and GABA through simulated correlations between distributions based on real data, to which noise was added from known test-retest repeatability values for the measures. As expected, increasing the intrinsic correlation and the sample size increased correlation strength. Measurement noise had a negative impact on the strength of the relationship at low sample sizes. Negative BOLD responses were less reliable than positive BOLD, so showed weaker correlations with GABA. When the simulated relationship between positive BOLD and GABA was as strong as published studies have reported ($R < -0.6$), a sample size of 12 was sufficient to detect a correlation of this strength 50% of the time. However, when estimates of the relationship between positive BOLD and GABA from published studies and from this thesis were combined, the predicted intrinsic correlation was only $R = -0.25$ and the probability of detecting a relationship of this strength was low, whether noise was present in the data (12%) or not (13%). A better estimate of the intrinsic correlation is required, but studies of the relationship between BOLD and GABA should take into account the expected intrinsic correlation between the variables and the amount of noise present in the variables when selecting the sample size.

7.2 Background and Rationale

Neuroimaging techniques allow investigation of differences between participants in the structure and function of the brain. These data can then be related to individual differences in many other variables such as cognition, behaviour, genetics and neurophysiology, in order to elucidate potential links between these factors. Similarly, the relationship between neuroimaging measures of different functions can be investigated, such as between neurotransmitter concentrations measured with magnetic resonance spectroscopy (MRS) and the brain's haemodynamic response to a stimulus, measured with functional magnetic resonance imaging (fMRI). These two factors have been reported to be inversely correlated in visual cortex: individuals with a greater concentration of the inhibitory neurotransmitter, gamma-aminobutyric acid (GABA) have shown a smaller increase in the fMRI blood oxygen level-dependent (BOLD) response to a visual stimulus (Muthukumaraswamy et al., 2009). Decreases in the BOLD response observed in non-stimulated regions of cortex may represent inhibition of areas not required for processing the stimulus and these negative BOLD responses may therefore also correlate with the concentration of inhibitory neurotransmitters. Supporting this theory, negative BOLD in the anterior cingulate cortex induced by an emotion processing task has been shown to positively correlate with GABA concentration in the same region (Northoff et al., 2007).

The relationship between GABA and positive BOLD in visual cortex has been replicated by the original group (Muthukumaraswamy, Evans et al., 2012) and in another centre (Donahue et al., 2010), providing support for a link between GABA concentration and cortical reactivity. Similarly, pharmacologically increasing GABA concentration also results in decreased positive BOLD in rat somatosensory cortex (Chen et al., 2005) and human visual cortex (Licata et al., 2011). However, in this thesis, three experiments have failed to replicate this finding or to show a correlation between GABA and negative BOLD in visual cortex. The inconsistency between experimental results may be caused by noise in the measurements, by low statistical power due to insufficient numbers of participants, or to type I error in previous reports of correlations. With neuroimaging techniques such as fMRI and MRS, repeated measurements of variables are unlikely to produce exactly the same result when the same participant is tested on multiple occasions. It is important that studies investigating relationships between individual differences in variables take into

account the within-subject repeatability of the measures (McGonigle, Howseman, Athwal, Friston, Frackowiak & Holmes, 2000); otherwise, variability could be reported as genuine differences between participants when in fact, if the same participants were tested again, the measures obtained and the relationships between them would be different. If two measures are not repeatable within subjects, the correlation between them consequently will not be robust.

In fMRI and MRS, within-subject variability may be caused by factors related to the participant such as differences in alertness, task strategy, movement and physiological state due to drugs such caffeine, alcohol and nicotine, or hormone levels in women at different stages of the menstrual cycle (Epperson, O'Malley, Czarkowski, Gueorguieva, Jatlow, Sanacora et al., 2005a). Alternatively it could reflect factors related to hardware, such as differences in the homogeneity of the magnetic field in the MRI scanner caused by fluctuations in temperature affecting magnetic components in the scanner. These sources of variability should be minimised in order to obtain a representative measure of the factor of interest. It is common in fMRI studies to conduct multiple acquisitions of the same task within a session and to average across these in order to obtain a better estimate of the measure of interest (McGonigle et al., 2000). The same procedure is sometimes used in MRS where repeated acquisitions from a session are averaged. The repeatability of fMRI and MRS can therefore be estimated within the session and this information can be used to give weight to conclusions about the strength of the relationship between the means of the measures.

Several studies have been conducted into the within- and between-subjects repeatability of fMRI (McGonigle et al., 2000; Loubinoux et al., 2001; Peelen & Downing, 2005), generally suggesting that within subject variability is acceptable, particularly within the same session (Rombouts et al., 1997; Rombouts & Barkhof, 1998; Loubinoux et al., 2001; Peelen & Downing, 2005; Menz, Neumann, Müller & Zysset, 2006), although poor within-subject repeatability has also been described (Zandbelt, Gladwin, Raemaekers, van Buuren, Neggers, Kahn et al., 2008). Reasonable within-subject repeatability of MRS measures of GABA concentration has also been reported (Bogner et al., 2010; Evans et al., 2010; Geramita et al., 2011; O'Gorman et al., 2011). The repeatability of BOLD and GABA therefore seems to be

acceptable but the impact of any within-subject variability on the *correlation* between these two factors has not been empirically investigated.

Correlations between two completely noise-free measures will be perfectly repeatable if the same sample of participants is retested; whereas correlations between variables containing noise will be slightly different each time they are sampled. If two measures are sufficiently repeatable, the correlation between them measured from a sample (r) will be close to the true population correlation (ρ). Noisy measures will on average give weaker correlations than this intrinsic relationship because the noise increases the standard deviation of the distributions of the variables, increasing the variance around the line of best fit and reducing the correlation strength. However, spuriously high correlations can occur by chance with small numbers of subjects. In any correlation, factors influencing the probability of obtaining a strong relationship and contributing to the replicability of effects are the sample size, the threshold chosen for significance and the size of the intrinsic correlation in the population. The threshold for significance is typically set at an alpha of 5%. Sample sizes in neuroimaging studies are often small, so the power to detect effects is reduced. A typical power calculation uses these variables to predict the probability of detecting a difference or correlation between two variables.

In fMRI, simulations have shown that approximately 24 participants are required to give sufficient power to detect differences between experimental conditions (Desmond & Glover, 2002). The power to detect between-subjects effects, such as in studies of individual differences is lower than the power for within-subjects effects, such as in experimental manipulations; for instance, with a sample size of 20, the intrinsic correlation must be as high as $\rho=0.6$ in order to have an 80% chance of detecting a correlation, yet brain-behaviour relationships are unlikely to be stronger than $\rho=0.5$ (Yarkoni, 2009). Simulations have not previously been conducted investigating correlations of two neuroimaging variables with each other. The issue of low statistical power is also likely to be conflated if the measurements are noisy, with poor repeatability.

In this study, data on the repeatability of the measures were available, allowing estimation of the influence of the additional factor of measurement noise on the

relationship between GABA and positive and negative BOLD. The current study therefore investigated the influence of sample size, intrinsic correlation and measurement noise on the correlation between GABA and positive and negative BOLD in visual cortex. The intrinsic correlation is generally not known, but can be estimated from samples tested. Measurement noise was quantified by calculating the percentage difference between pairs of acquisitions of GABA and BOLD from experimental studies of repeatability in Chapters 4 and 5. Data with distributions and noise levels equivalent to these data were entered into simulations of an experimental design in which the mean responses from two acquisitions of two measures were correlated with each other. Based on known contributions to statistical power, it was expected that the correlation obtained through simulations would increase with the number of participants and the intrinsic correlation, and decrease with the addition of noise to the distributions. Based on correlations obtained in previous studies, an estimate was made of the intrinsic correlation between GABA and BOLD. The aim of this study was to use this estimate and measured information about noise to make predictions about the sample sizes required and the probability of detecting correlations of this strength.

7.3 Methods

7.3.1 Participants and stimuli

Experimental data for informing simulation parameters were obtained from three studies: Experiments 1 and 2 were the first and second experiments in Chapter 4, Experiment 3 was the data from Chapter 5. In Experiment 1, there were 15 participants (eight female) of mean age 26 years 11 months (SD 4 years 8 months), one of whom was excluded due to poor fixation when mapping his visual field. In Experiment 2, there were 14 male participants (mean 30 years 1 month, SD 5 years 8 months). Experiment 3 involved 14 male participants (mean 31.2 years, SD 4.8 years) but two were excluded due to poor quality MRS data. Three participants took part in both Experiments 1 and 3, while the second experiment was an entirely independent sample. BOLD responses were evoked by maximum contrast achromatic stimuli. In Experiment 1, these were $4 \times 4^\circ$ 1cpd squarewave gratings presented in the lower right visual field. In Experiment 2, the stimulus was a 5° radius chequerboard presented at fixation. The stimulus in Experiment 3 was a 4° diameter circle

containing a sinusoidal grating presented in the lower right visual field. All stimuli were presented in 15-second boxcar paradigms with simple button press response tasks to encourage participants to maintain attention.

7.3.2 MRI acquisition and analysis

All data were acquired on a 3.0T GE HDx system (GE Healthcare, Chalfont St Giles, UK), with a body coil for transmission and an eight-channel receive-only head coil. Gradient-echo echoplanar imaging (EPI) sequences took 22 slices through occipital cortex using a 64x64 matrix. In Experiment 1, voxels were 4x4x3mm with a repetition time (TR) of 1.5s, while in Experiments 2 and 3, voxels were 3mm isotropic and the TR was 3.0s. Echo time (TE) was 35ms, and the flip angle was 90°. High-resolution anatomical images (1mm isotropic) were acquired with a 3D Fast Spoiled Gradient-Echo (FSPGR) sequence (TR/TE/inversion time = 7.8/3.0/450ms; flip angle = 20°). Whole brain EPI images with equivalent slice thickness and field of view to the fMRI sequences were also obtained for registering the visual task data to the structural scans.

The fMRI data were analysed using the FMRIB software library (FSL; www.fmrib.ox.ac.uk/fsl) with preprocessing parameters of motion correction using MCFLIRT (Jenkinson et al., 2002); non-brain removal with BET (Smith, 2002); high-pass temporal filtering and gamma convolution of the HRF. Spatial smoothing was applied using a Gaussian kernel of 5mm full-width-half-maximum (FWHM) for Experiments 1 and 3, and 1mm FWHM for Experiment 2. In Experiments 1 and 3, occipital cortices were flattened using Freesurfer (Fischl et al., 1999) and primary visual cortex (V1) regions of interest (ROIs) in the stimulated and opposite quadrants of the visual field were identified from retinotopic mapping data. In Experiment 2, V1 was delineated based on cortical folds in the anatomical scan and separated into 10 regions of equal length along the calcarine sulcus (Hinds et al., 2008). BOLD responses in the ROIs were measured using mri3dX (<https://cubic.psych.cf.ac.uk/Documentation/mri3dX/>).

BOLD responses measured were the unthresholded contrast of parameter estimate (COPE) values, which are in arbitrary units. The responses recorded from Experiments 1 and 3 were the mean COPE value from the positive voxels in the

stimulated quadrant of V1 and from the negative voxels in the opposite quadrant. In Experiment 2, the responses were the mean COPE value from all voxels in the most positive (the second most posterior) and the most negative (the third most anterior) of the 10 regions of V1. The repeatability of positive and negative BOLD was represented as the percentage difference between the two acquisitions in Experiments 2 and 3, and the mean percentage difference between all possible combinations of the five blocks in Experiment 1. Data could not be combined across experiments because different stimuli were used, which induced different BOLD amplitudes.

7.3.3 MRS acquisition and analysis

GABA acquisition and analysis procedures were the same for all three experiments. A 3x3x3cm voxel was positioned at an angle that ensured that the lower edge of the voxel was aligned with the bottom of the occipital lobe across the two hemispheres, the anterior edge was roughly aligned with the parieto-occipital sulcus and the posterior edge remained as much inside the cortex as possible. Two acquisitions were obtained for each participant, each with 332 measurements per voxel, with a TE of 68ms, TR of 1.8s and a 16ms Gaussian editing pulse applied at 1.9ppm in alternate scans. The GABA Analysis Toolkit (*Gannet*) (<http://gabamrs.blogspot.co.uk/>) was used to apply a high-pass water filter and to produce a MEGA-PRESS difference spectrum. Automatic phasing of the GABA peaks was conducted, with small manual adjustments made where necessary. The concentration of GABA was converted to institutional units by accounting for the editing efficiency and the T1 and T2 relaxation times of water and GABA. The voxel was segmented into grey matter, white matter and CSF using FMRIB's Automated Segmentation Tool (Zhang et al., 2001), giving the fraction of tissue in the voxel. GABA concentrations were corrected for this tissue fraction. The percentage difference was calculated between the GABA concentrations obtained from the two acquisitions in each participant and the average of these values was taken across all participants to give a metric of the noise in the measure.

7.3.4 Values used in the simulations

The BOLD and GABA data obtained from the three experiments described above are shown in Table 7.1. These data were used as the basis for creation of distributions for simulations of experiments in the current study. Since the GABA peak measured with

MRS is also likely to contain contributions from macromolecules, it is reported as GABA+ and is measured in institutional units (IU). Means and standard deviations (SD) across the two acquisitions and all participants are reported. The SD of the noise was calculated from the percentage difference between acquisitions across all participants and was then converted back to experimental units by multiplying by 1% of the mean. The SD of the noise for positive and negative BOLD was calculated in the same way as for GABA, from the percentage difference between the COPE values from the two runs in Experiments 2 and 3 and between all possible combinations of the five runs in Experiment 3. The percentage differences between runs indicate that GABA was the most repeatable variable, followed by positive BOLD. Negative BOLD showed poor repeatability.

Table 7.1. Data used for creation of distributions in the simulated experiments: mean and SD of GABA, positive and negative BOLD, and SD of the noise (SD of the percentage difference between runs, converted to experimental units). Also shows the noise converted to experimental units.

Experiment	Variable	Variable Mean	Variable SD	Difference between runs (%)	Noise SD	Noise SD (% of mean)
1	GABA	1.42	0.09	7.38	0.06	4.23
	Positive BOLD	136.92	61.78	25.54	33.92	24.77
	Negative BOLD	-32.54	32.02	95.24	18.67	57.38
2	GABA	1.45	0.11	6.41	0.05	3.45
	Positive BOLD	301.64	116.58	17.17	59.17	19.62
	Negative BOLD	-37.20	32.89	164.91	73.45	197.45
3	GABA	1.47	0.11	6.77	0.08	5.44
	Positive BOLD	183.54	64.20	12.05	26.40	14.38
	Negative BOLD	-102.24	48.33	43.95	46.32	45.31

7.3.5 Simulation parameters and procedure

Initially, a normally distributed simulated random GABA variable with the mean and standard deviation from the acquired GABA data in Experiment 1 was created in Matlab (The Mathworks, Inc). Another normally distributed random variable with the desired intrinsic correlation with this GABA variable was then generated and scaled to the mean and standard deviation of the acquired positive BOLD data from

Experiment 1. These simulated GABA and BOLD distributions represented the ‘intrinsic’ data between which the underlying correlation was known. In simulations, new GABA and BOLD distributions could then be created, each with noise added with a standard deviation equivalent to half of the calculated noise SD in order to simulate samples of measured data. The means of these noisy GABA and BOLD distributions were then calculated and represent the ‘sample’ data.

Datasets were simulated for sample sizes of three to fifty participants and intrinsic correlations between 0 and 1 were evaluated in steps of 0.025, giving 41 steps in total. For each sample size and intrinsic correlation, 10,000 iterations of the correlation between the sample (noisy) BOLD and GABA data for each variable were conducted. The mean correlation across iterations was plotted as temperature on a heat map, with the intrinsic correlation and the number of participants on the x- and y-axes, respectively. In addition, heat maps were created on the same axes with temperature representing the probability of obtaining a correlation exceeding the Pearson’s R value required for significance ($p < .05$). These simulated experiments were repeated for the relationship between GABA and negative BOLD, and for data based on the other two experiments. In order to confirm that the data showed the profiles expected for a standard power calculation and to determine whether adding noise to data affected the outcome of the simulations, data were also simulated from Experiment 3 without any noise added to the variables.

7.4 Results

7.4.1 Confirmation of expected outcomes

As expected, increasing the simulated intrinsic population correlation coefficient (ρ) between GABA+ and positive or negative BOLD resulted in increases in the mean measured sample correlation (r) from 10,000 iterations of the experiment (Figure 7.1A), and consequently increased the mean probability of returning a significant correlation (Figure 7.1B). With large numbers of participants, the simulated correlation is equal to the intrinsic correlation since the noise added is centred on the intrinsic correlation. Figure 7.1A therefore acts as a ‘sanity check’ indicating that the simulations give an accurate estimate of the relationship at high sample sizes. However, with very low numbers of participants, correlations are not robust, therefore

the mean sample correlation was lower than the intrinsic correlation (Figure 7.1A) and the range of acquired correlation coefficients was wide. For example, with the intrinsic correlation $\rho=.53$, required for significance ($p<.05$) with the sample size used in Experiments 1 and 2 ($N=14$), the difference between the 10th and 90th percentiles of the 10,000 obtained r values was 1.67 when only three participants were tested, but only 0.27 when fifty participants were tested. Above approximately 10 participants, correlations were stable with a tighter range, and were closer to ρ .

In Figure 7.1B, the probability of obtaining a significant correlation is negatively skewed on the x-axis because r cannot be greater than 1, therefore at high values of the intrinsic correlation, the sample correlation will also be close to 1 (<http://onlinestatbook.com>). The negative skew on the y-axis occurs because increasing the number of participants increases the power of an experiment to detect the true relationship (e.g. http://www.power-analysis.com/sample_size.htm), though this effect levels off with high numbers of participants. These probability plots would show similar profiles if different thresholds for significance were used, but the size of the area with high temperature would change.

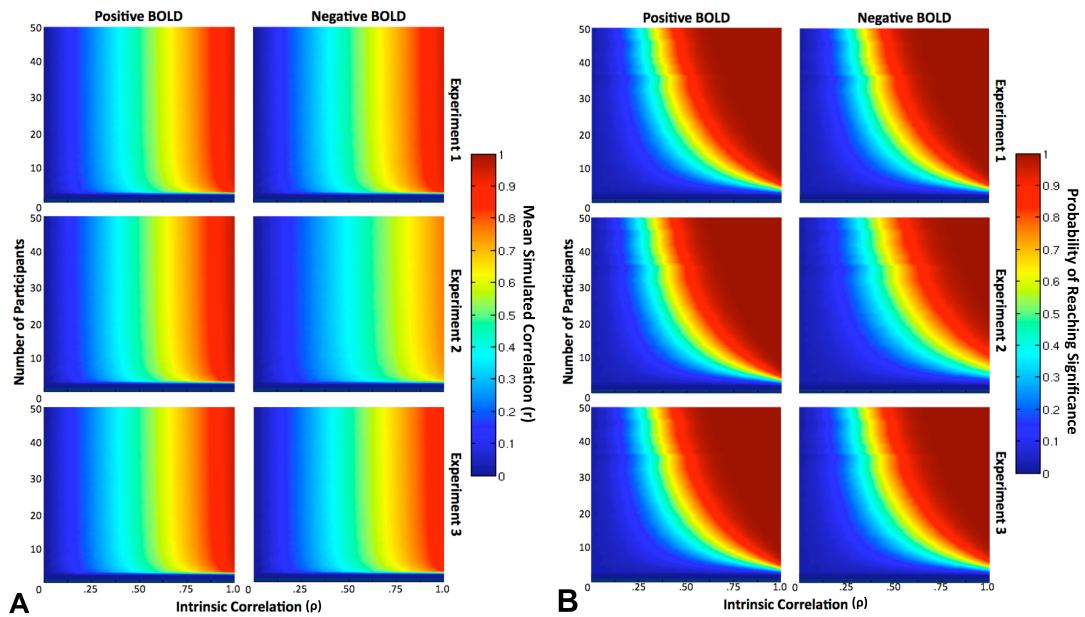


Figure 7.1A) Mean sample correlation between GABA and positive and negative BOLD from 10,000 iterations of the experiment at intrinsic correlations between 0 and 1 for between 3 and 50 participants. The results of data based on three experimentally measured distributions are shown. B) The mean probability of obtaining a significant correlation ($p < .05$) between GABA and BOLD for intrinsic correlations of 0-1 with 3-50 participants.

Increasing sample size generally increases the power to detect a correlation, but there is an interaction whereby if the intrinsic correlation is high, the number of participants required to detect it a given proportion of the time can be lower. For example, with $\rho = 0.6$, 12 participants were required to obtain a significant correlation at least 50% of the time when the repeatability of measures was equivalent to GABA+ and positive BOLD in Experiment 3 (13 participants for negative BOLD). However, with $\rho = 0.3$, 46 participants were required to obtain a significant correlation 50% of the time for positive BOLD and over 50 participants were required for negative BOLD (Figure 7.2A). The intrinsic correlation between variables must therefore be high in order for a sample size as small as those often used in imaging experiments to consistently detect a significant effect.

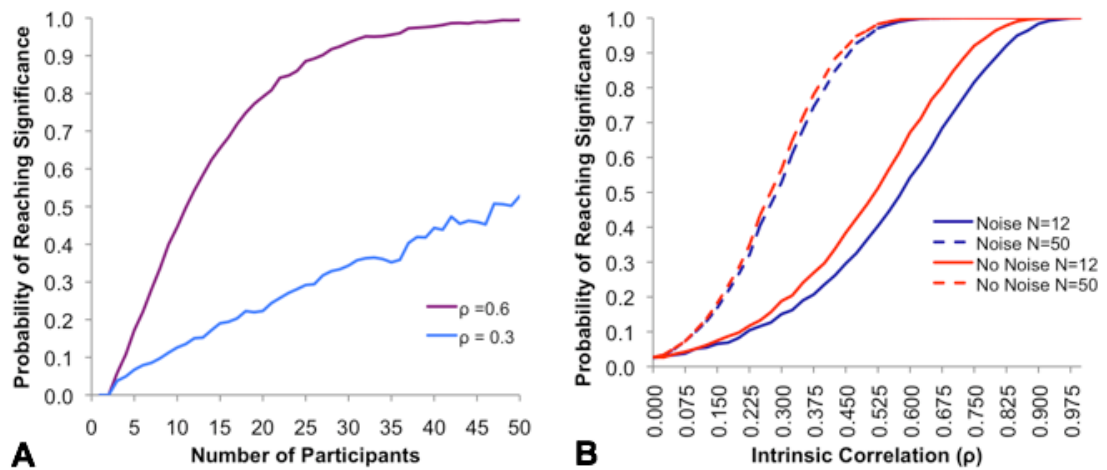


Figure 7.2A) The effect of the number of participants and the intrinsic correlation on the probability of obtaining a significant correlation between GABA+ and positive BOLD given the noise present in Experiment 3. B) The probability of obtaining a significant correlation given sample sizes of 12 or 50 and in the presence or absence of noise (measured from Experiment 3).

In order to test the influence of measurement noise on the correlation between GABA+ and BOLD, the distributions from Experiment 3 were simulated with and without the addition of noise. As expected, without noise, the mean sample correlation from 10,000 iterations of the experiment was equivalent to the intrinsic correlation, indicating that repeated measurements of the relationship would give the same result. With the addition of noise in the distributions that reflected differences between repeated acquisitions of the same measure, the mean sample correlations between GABA+ and BOLD were lower than the intrinsic correlations, particularly with small sample sizes. For example, with the intrinsic correlation required for significance in a sample of 12 participants, as used in Experiment 3 ($\rho=0.58$), the sample correlation obtained between the means of GABA+ and BOLD data with noise added was $r=0.56$ for positive BOLD and $r=0.53$ for negative BOLD. The effect of adding noise to the distributions was greater with smaller numbers of participants, as shown in Figure 7.2B.

The effect of noise attributable to known within-session variability on the correlation between BOLD and GABA+ differed between positive and negative BOLD and across the three experiments, as can be seen in the heat maps in Figure 7.1. The

difference between positive and negative BOLD in the probability of obtaining a significant correlation with GABA+ with a sample size of 14 (as used in Experiments 1 and 2) is also shown in Figure 7.3. Positive BOLD showed very similar probabilities of obtaining a strong correlation across the three experiments, whereas negative BOLD was more variable. The difference between positive and negative BOLD was most prominent in Experiment 2. As shown in Table 7.1, Experiment 2 gave the poorest negative BOLD repeatability and consequently, the SD of the noise added to this experiment was very large, particularly in relation to the low mean negative BOLD. These results indicate that the addition of measurement noise reduced correlations between BOLD and GABA+. Since positive BOLD tended to be more repeatable than negative BOLD, it gave slightly higher correlations with GABA+ and higher probabilities of obtaining a significant effect for all experiments.

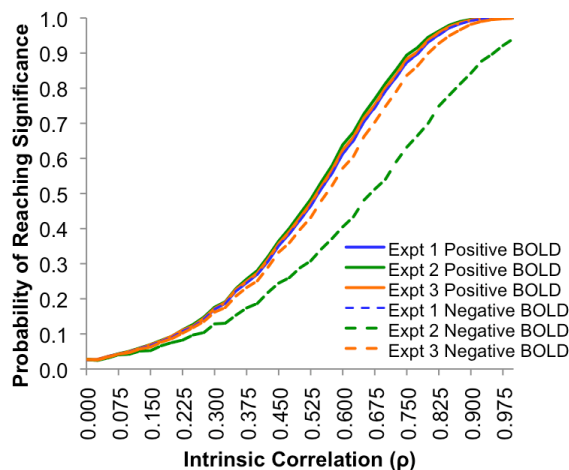


Figure 7.3. The probability of obtaining a significant correlation between GABA and positive or negative BOLD given 14 participants, intrinsic correlations between 0 and 1 and noise as measured from three different experiments.

7.4.2 Quantitative implications for studies of GABA+ and BOLD.

The average correlation between GABA+ and positive BOLD from data obtained in earlier chapters of this thesis and in previous studies (Table 7.2) is $R = -.25$. This is not an ideal means of combining data, as the studies did not all use the same paradigms; the published studies reported percentage signal change whereas this thesis investigated COPE values; and the different studies gave very varied reports of the correlation (between $R = -0.70$ and $R = 0.43$). However, it gives an estimate of the

intrinsic correlation that can be used to obtain information from the simulations about the number of participants required to detect a meaningful correlation a given proportion of the time it is tested.

Table 7.2. Summary of the sample sizes and correlations between BOLD and GABA+ in the three experiments on which the current simulations were based (Experiments 1-3) and in previous published studies.

Study	Sample size	Positive BOLD vs GABA (R)	Negative BOLD vs GABA (R)
Experiment 1 (Chapter 3, Expt 1)	14	.43	-.58
Experiment 2 (Chapter 3, Expt 2)	14	.15	.12
Experiment 3 (Chapter 4)	12	-.08	.16
Muthukumaraswamy et al. (2009)	12	-.64	N/A
Donahue et al (2010)	12	-.70	N/A
Muthukumaraswamy et al. (2012)	15	-.64	N/A

If $\rho = -.25$, in measures containing no additional session-to-session noise, the probability of detecting a correlation of this strength with 14 participants (a common number for neuroimaging experiments) would be 13%; while with the noise present in GABA+ and positive BOLD in Experiment 3, the chance of reporting a correlation of $r = \pm .25$ would be only 12%. Over 50 participants would be needed to obtain a correlation of this strength over 50% of the time, either with noise or without. An intrinsic correlation of 0.6 is necessary to show a significant relationship with a sample size of 12 and the noise present in positive BOLD from Experiment 3.

7.5 Discussion

The current findings build on common knowledge about the importance of the number of participants and the intrinsic correlation between variables on the statistical power to detect correlations (Desmond & Glover, 2002) by incorporating information about measurement noise from estimates of within-subject repeatability of the measures. Simulations were used to quantify the effect that variability between repeated acquisitions of GABA+, positive and negative BOLD has in reducing the

correlations between these variables. This effect was prominent at low sample sizes such as those typically used in neuroimaging experiments.

The difficulty in replicating previous findings of a correlation between positive BOLD and GABA⁺ (Muthukumaraswamy et al., 2009; Donahue et al., 2010; Muthukumaraswamy, Evans et al., 2012) in previous chapters of this thesis may therefore have been partly due to noise in the measures. However, the influence of the intrinsic correlation and the sample size had a much greater effect on correlation strength than the addition of noise. With a typical sample size and noise level, the intrinsic correlation had to be as high as $\rho=0.6$ in order to be reliably detected. Although correlations between GABA⁺ and BOLD of this strength have previously reported (Muthukumaraswamy et al., 2009; Donahue et al., 2010; Muthukumaraswamy, Evans et al., 2012), such a strong relationship may not be physiologically valid as the mechanisms through which GABA may influence the BOLD response are not currently clear. GABA-ergic interneurons have been shown to interact with microvasculature and to influence dilation and constriction of vessels (Vaucher, Tong, Cholet, Lantin & Hamel, 2000; Cauli, Tong, Rancillac, Serluca, Lambalez, Rossier et al., 2004; Hamel, 2006), but the influence of this interaction on the variables contributing to a BOLD response (blood flow, blood volume and oxygen consumption) have not yet been specifically investigated. The influence of GABA⁺ concentration on BOLD may be more likely to be through an intermediate step of alteration of levels of neuronal activity. GABA⁺ measured with MRS and BOLD may therefore be too far removed in terms of the physiological processes that they represent to show such strong correlations.

An estimate of the intrinsic correlation between GABA⁺ and positive BOLD based on these published studies and experiments in previous chapters of this thesis suggested that the relationship was $\rho=-.25$. The sample size required to detect a correlation of this strength was over 50, which is far greater than the number typically tested in neuroimaging experiments, given the time requirements and expense of such studies. If this intrinsic correlation coefficient is accurate, the strong relationship between GABA⁺ and BOLD reported in previous studies may have been due to chance. However, the estimate of the intrinsic correlation was obtained simply by averaging correlation coefficients from several previous studies. This method is not ideal as

there were methodological differences between studies in factors such as the stimulus used to induce a BOLD response, the number of acquisitions of each measurement, the demographic of participants and potentially the MRS voxel positioning. The correlation values averaged were also from two clusters: one with high negative R values and the other with slightly positive values. More data are therefore required to give a better estimate of the true correlation between GABA+ measured using MRS and positive BOLD.

Positive BOLD was found to be more repeatable than negative BOLD both within and between experiments, so gave more reliable correlations with GABA. The poorest negative BOLD repeatability and hence the lowest correlations with GABA were obtained for Experiment 2. In this experiment, a chequerboard stimulus was used, whereas in Experiments 1 and 2, the stimulus was a small grating. Chequerboards have previously been shown to give less repeatable BOLD responses than simpler stimuli (Miki et al., 2001); however the current study does not fully replicate this finding since the positive BOLD in Experiment 2 was in fact more repeatable than one of the experiments using a grating stimulus. The stimulus size or position may have been more important: the stimulus in Experiment 2 was larger than in the other experiments and was presented at the fovea as opposed to the parafoveal region, which meant that negative BOLD was measured from a peripheral ring as opposed to an area in the opposite quadrant of visual cortex. Since the central stimulus induced a very strong positive BOLD response, small shifts in attention or fixation may have had a greater effect on negative BOLD repeatability than with a stimulus inducing less positive BOLD. The poorer repeatability of negative BOLD is also present in Experiments 1 and 3, though is not as clear as in Experiment 2.

The results therefore suggest that in addition to the known predictors of correlation strength of the sample size and the intrinsic correlation, the relationship between BOLD and GABA+ is also dependent on the stimulus and the measurement noise. The findings have an impact on studies aiming to investigate correlations between individual differences in neuroimaging measures, since at low intrinsic correlations and with noisy measures, the number of participants required to detect an effect close to the true correlation is greater than the number typically recruited for neuroimaging studies. It is therefore important to have an estimate of the expected strength of the

correlation between two variables and the potential measurement noise in order to determine the sample size required. Development of standardised acquisition protocols across multiple studies or research centres may allow data to be combined in order to give much larger sample sizes, from which more reliable estimates of correlations between individual variability can be made.

7.6 Conclusions

Simulations of the relationship between GABA+ and positive and negative BOLD have shown that measurement noise can reduce correlations, particularly at sample sizes as low as those commonly used in neuroimaging studies. With such small numbers of participants and in the presence of noise, the intrinsic correlation required to reliably detect an effect may be greater than the physiologically plausible relationship. The numbers of participants required to detect a correlation of the estimated strength between GABA+ and BOLD was substantially greater than the number typically tested in neuroimaging studies.

Chapter 8

Structural and Neurochemical Parameters Driving Individual Variability in Gamma Frequency

8.1 Abstract

Neuronal oscillations in the gamma (~30-100Hz) frequency range are thought to play an active role in stimulus processing in the brain (Singer, 1999). The frequency of these oscillations can vary widely between participants (Muthukumaraswamy et al., 2010), but the reason for this individual variability is not fully understood. Previous studies have reported correlations between gamma frequency and age (Gaetz, Roberts, Singh & Muthukumaraswamy, 2012), gamma-aminobutyric acid (GABA+) concentration (Muthukumaraswamy et al., 2009) and primary visual cortex (V1) area (Schwarzkopf et al., 2012) and thickness (Muthukumaraswamy et al., 2010). This study therefore used regression analyses to investigate the contribution of these variables to prediction of individual variability in peak gamma frequency in V1. Age was found to explain 13% of the variance and once this was accounted for, no other variables contributed significantly to prediction of gamma frequency. In a replication dataset with a wider age range, 27% of the variance was explained by age. It was speculated that strengthening of synaptic connections or reductions in contrast sensitivity with age might reduce the excitation/inhibition ratio, resulting in reductions in gamma frequency. The source of the large amount of remaining variance in gamma frequency is not clear, but may be due to neurophysiological factors such as the number of GABA receptors, the number of GABA-ergic interneurons or the action of other neurotransmitters.

8.2 Background

Neuronal oscillatory signals are generated by the synchronous activity of large numbers of neurons and different frequencies of oscillation may have different roles in neuronal processing in the brain. Gamma frequency (~30-100Hz) oscillations have been associated with various different functions, including basic sensory processing (Friedman-Hill et al., 2000; Donner & Siegel, 2011), movement generation (Cheyne

et al., 2008), orientation discrimination (Edden et al., 2009), visual attention (Fries et al., 2001) and serial processing of short-term memories (Lisman & Idiart, 1995). The presence of gamma oscillations also predicts the temporal coordination of neuronal activity in spatially distinct areas of the cortex (Gray & Singer, 1989; Maldonado et al., 2000), so gamma oscillations may play a role in synchronising activity between different areas of the brain.

The mechanisms behind the production of gamma oscillations and the modulation of their frequency have been investigated both in vivo and through modelling of neurophysiological pathways. Gamma band neuronal activity may originate in "chattering cells": pyramidal cells in superficial cortical layers, which have been said to fire repetitively at 20-70Hz in response to depolarising currents (Gray & McCormick, 1996). The synchronisation of this firing can be caused by the action of inhibitory or excitatory neurotransmitters, but is predominantly due to inhibition through gamma-aminobutyric acid-A ($GABA_A$) receptors (Bartos, Vida & Jonas, 2007). The generation of gamma oscillations is therefore likely to be due to networks of $GABA_A$ interneurons modulating activity in pyramidal cells to give synchronous activity in the gamma frequency (Wang & Buzsáki, 1996). This activity produces rhythmic modulation of the membrane potential of pyramidal cells (Buzsaki & Chrobak, 1995) and this signal can be measured using magnetoencephalography (MEG). The frequency of oscillations may depend on the strength of excitation and on the balance between inhibitory and excitatory interactions between pyramidal cells and interneurons (Traub, Whittington, Colling, Buzsáki & Jefferys, 1996; Brunel & Wang, 2003). Features of the stimulus can also modulate the frequency of the gamma band response: in visual cortex, higher frequency oscillations have been reported for moving (Friedman-Hill et al., 2000) high contrast stimuli (Ray & Maunsell, 2010), as opposed to static, lower contrast stimuli.

Gamma oscillation frequency has also been shown to differ across participants, but to be stable within a participant over time (Muthukumaraswamy et al., 2010). The cause of individual differences in gamma frequency is not yet entirely clear. Since GABA-ergic inhibition is important in the generation of gamma, individual differences in the concentration of the neurotransmitter GABA (plus macromolecules ($GABA^+$)) have been investigated in relation to gamma oscillations. $GABA^+$ concentration measured

using magnetic resonance spectroscopy (MRS) was found to be positively correlated with gamma frequency but not amplitude in visual (Muthukumaraswamy et al., 2009) and motor (Gaetz et al., 2011) cortices. This relationship was said to reflect the increased inhibition in participants with more GABA⁺ reducing the excitation/inhibition ratio within the network of pyramidal neurons and interneurons.

It is possible that this relationship between gamma frequency and GABA⁺ concentration is mediated by a third factor, which causes individual variability in both measures. For instance, the frequency of gamma oscillations in visual cortex has also shown a positive correlation with retinotopically defined V1 and V2 surface area (Schwarzkoepf et al., 2012). This finding was explained in terms of neurophysiological homogeneity, in that in a large V1, a smaller area of the visual field is represented by the same area of cortex as in a smaller V1, therefore homogeneity of factors such as stimulus preferences and receptor density is higher. In more homogenous areas, neurons oscillate at similar frequencies and conduction delays between neurons are shorter, therefore gamma oscillations are higher frequency. If the area of V1 is indeed predictive of gamma frequency, since there are more GABA_A receptors in V1 than in other areas of cortex (Zilles & Amunts, 2009), the correlation between gamma frequency and GABA⁺ concentration may be confounded by the area of V1 (Schwarzkoepf et al., 2012).

GABA-ergic neurons and receptors are relatively evenly distributed in the horizontal plane in the cortex (Albus & Whale, 1994) but are more dense in certain layers of the cortex (layers II-III, IVA, IVC and VI (Hendry, Fuchs & Jones, 1990; Hendry & Huntsman, 1994; Munoz, DeFelipe & Jones, 2001)). If GABA-ergic neurons are involved in influencing the frequency of gamma oscillations, the thickness of V1 might therefore also be expected correlate with gamma frequency, because individuals with a thicker cortex may have more GABA⁺ in a given volume. A positive correlation between gamma frequency and cortical thickness has been reported in one previous study (Muthukumaraswamy et al., 2010), but not in other studies (Edden et al., 2009; Muthukumaraswamy et al., 2009; Schwarzkoepf et al., 2012). A mediating factor in this relationship is likely to be the participants' age, as cortical thickness declines with age (Magnotta & Andreasen, 1999) and participant age has shown an inverse relationship with gamma frequency in some

(Muthukumaraswamy et al., 2010; Gaetz et al., 2011; Gaetz et al., 2012) but not all (Muthukumaraswamy et al., 2009; Schwarzkopf et al., 2012) studies. This inconsistency may be related to the small age ranges generally tested in the latter studies.

Various factors have therefore been linked to gamma frequency, but many of these variables are also mutually correlated with each other. This shared variance may cause incorrect inferences about relationships between variables to be made, whereby correlations are attributed to a covariate rather than to the true correlate, or several variables are said to independently predict gamma frequency when in fact their predictive power is shared. The small sample sizes often used in neuroimaging studies also limit the probability of detecting the true relationship, given the noise present in neuroimaging measures (see Chapter 7 for more detail). The current analysis brings together data from several studies to obtain a larger sample and uses a hierarchical regression model in order to investigate potential predictors of gamma frequency, accounting for measures that covary. Based on previous correlative data, it was hypothesised that GABA+ (Muthukumaraswamy et al., 2009) and V1 area (Schwarzkopf et al., 2012) would predict gamma frequency.

8.3 Methods

8.3.1 Participants

Data were collated from four sets of studies: Study 1 consists of MRS data described in Chapters 4 and 5 of this thesis; Study 2 is unpublished data collected by Misses McNamara and Davis as part of an 11 week project in this centre; data from Study 3 have been published previously (Muthukumaraswamy et al., 2010); Study 4 is in press (Perry, Hamandi, Brindley, Muthukumaraswamy & Singh, 2012). After exclusion of data from participants who were tested in more than one study, there were 90 participants (74 male). Each study recorded some or all of the variables of interest: gamma frequency, GABA+ concentration, V1 area, V1 thickness and age.

8.3.2 MEG acquisition and analysis

Stimuli in all studies were 4° square patches containing vertical, stationary, maximum-contrast, 3 cycles per degree (cpd) square wave gratings. They were

presented with the top right corner 0.5° below and to the left of fixation, other than in Study 4 in which the corner of the square touched fixation. The timings for presentation of the stimuli are shown in Table 8.1. In all studies, a simple button-press response was required from participants.

All MEG data were obtained on a 275-channel CTF MEG system, with two channels switched off due to excessive sensor noise. An additional 29 reference channels were recorded for noise cancellation purposes, and the primary sensors were analysed as synthetic third-order gradiometers (Vrba & Robinson, 2001). Data were sampled at 1200 Hz. MEG data were coregistered with individuals' anatomical MRI scans using fiducial markers placed at fixed, identifiable locations from anatomical landmarks (nasion and pre-auricular), which were verified using high-resolution digital photographs. Trials containing artefacts were discarded offline during manual inspection of the data.

Data were bandpass filtered using a fourth-order bi-directional IIR Butterworth filter at the image frequencies chosen in each study (displayed in Table 8.1). The synthetic aperture magnetometry (SAM) beamformer algorithm (Robinson & Vrba, 1999) was used to calculate pseudo-T statistics from the contrast between source power in the stimulus and baseline phases (Robinson & Vrba, 1999; Vrba & Robinson, 2001; Hillebrand et al., 2005) for all trials in each study (timings shown in Table 8.1). A multiple local-spheres forward model (Huang et al., 1999) was derived for source localisation by fitting spheres to the brain surface extracted using FSL's Brain Extraction Tool (Smith, 2002). Estimates of the three-dimensional distribution of source power were derived for the whole head at 4mm isotropic voxel resolution for each participant.

Peak locations of gamma band activity in visual cortex were identified for each participant. At these locations, a virtual sensor analysis was conducted whereby the SAM beamformer weights were obtained from covariance matrices bandpass filtered between the frequency bands specified in Table 8.1. Data were then multiplied by the weights in order to produce a time-series of activity at that location for each trial and a time-frequency analysis was performed using the Hilbert transform with the bandwidth and steps specified in Table 8.1. The signal was calculated as the

percentage change in power relative to the average power at that frequency in the baseline period. The peak frequency within the gamma range was then identified for each participant. Data were quality controlled by excluding participants who did not show a clear gamma peak.

Table 8.1. Parameters for MEG acquisition and analysis across the four studies. The number of participants included (N) and additional participants tested but later excluded (excl) are shown.

Study	N (excl)	Task timing (on/off)	Stimulus/ baseline timings	SAM image frequencies (Hz)	Virtual sensor covariance frequencies (Hz)
1	N/A	N/A	N/A	N/A	N/A
2	15 (3)	2s / 2s	0.3-0.9 / -0.6-0	40-60, 30-70	30-70
3	24 (2)	1.5-2s / 2s	0-1.5 / -1.5-0	0-20, 20-40, 40- 60, 60-80, 0-100	0-100
4	7 (1)	1-1.5s / 2.5s	0-1s / -1-0s	30-70	30-70

8.3.3 MRS acquisition and analysis

Data were acquired on a 3.0T GE HDx system (GE Healthcare, Chalfont St Giles, UK), with a body coil for transmission and an eight-channel receive-only head coil. Voxels of 3x3x3cm were positioned in occipital cortex across the two hemispheres, with the lower edge aligned with the bottom of the occipital lobe, the anterior edge roughly aligned with the parieto-occipital sulcus and the posterior edge as much within the cortex as possible. The TE was 68ms, TR was 1.8s and Gaussian editing pulses were applied on alternate scans at 1.9ppm and 7.46ppm. Additional parameters that varied across different studies are shown in Table 8.2.

Table 8.2. MRS parameters that differed across experiments. Again, the number of participants in addition to those reported who were tested but subsequently excluded are shown in parentheses.

Study	N (excl)	Acquisitions per voxel	Editing pulse duration (ms)	Number of acquisitions
1	34 (1)	332	16	2
2	23	512	16	1
3	16	512	20	2
4	N/A	N/A	N/A	N/A

All data were analysed using the GABA Analysis Toolkit (*Gannet*) (<http://gabamrs.blogspot.co.uk/>). A high-pass water filter was applied to produce a MEGA-PRESS difference spectrum. Automatic phasing of the GABA peaks was conducted, with small manual adjustments made where necessary. The ratio of GABA to creatine was calculated and the concentration of GABA/Cr was converted to institutional units by accounting for the editing efficiency and the T1 and T2 relaxation times of the two molecules. Creatine was chosen as the reference molecule as it has been shown to be more repeatable than using water as the reference, or not using internal referencing (Bogner et al., 2010). GABA/Cr also does not require correction for the fraction of tissue in the voxel since both molecules are measured from the same location, whereas the water voxel is slightly shifted in comparison to the GABA voxel. Since there are likely to be macromolecular contributions to the GABA signal in MRS, the variable measured is described as GABA+. For studies in which two acquisitions were taken, the mean GABA+ concentration was calculated.

8.3.4 V1 structure acquisition and analysis

V1 area and thickness data were obtained from high-resolution anatomical images (1mm isotropic), acquired with a 3D Fast Spoiled Gradient-Echo (FSPGR) sequence (TR/TE/inversion time = 7.8/3.0/450ms; flip angle = 20°). V1 was delineated in each individual's brain based on the location and angle of cortical folds (Hinds et al., 2008). Area and thickness values were recorded for the right hemisphere (RH), as this was the hemisphere stimulated in the MEG task.

8.3.5 Regression analysis

Data from the four studies were pooled to give measures of the five variables: gamma oscillation frequency, GABA+ concentration, age, and V1 area and thickness within the stimulated (right) hemisphere. Because some of the predictor variables (V1 thickness and age) are expected to correlate with each other and therefore to share variance, they cannot all be entered into a multiple regression simultaneously. A hierarchical regression with gamma frequency as the outcome measure was therefore conducted. Age was entered at the initial stage because demographic variables are typically entered first as covariates over which the researcher has no control (e.g. www.upa.pdx.edu/IOA/newsom/da2/ho_model.pdf). V1 thickness was entered at the second stage as a potential covariate previously reported to be related to age (Magnotta & Andreasen, 1999) and gamma frequency (Muthukumaraswamy et al., 2010). GABA+ and V1 area were entered at the final stage to determine whether they contributed significantly to prediction of gamma frequency once age and V1 thickness were controlled for. This order of addition separates variables known to share variance and therefore investigates their influence independently of each other. Variables were excluded on a pairwise basis, as values were not available for every measure for every participant.

8.4 Results

Descriptive statistics for the five variables measured are shown in Table 8.3. All distributions were normal, there were no extreme outliers and there was low collinearity between variables (variance inflation factors (VIF) all <1.07). The relationships between variables were all linear. The number of participants exceeded the minimum of five times the number of predictor variables. For the pair of variables with the smallest number of participants (GABA+ and gamma frequency), data were available for 31 participants, which does not reach the optimal ratio of 10 participants to every predictor variable.

Table 8.3. Mean, standard deviation (SD) and number of participants (N) for variables measured.

	Mean	SD	N
Gamma frequency (Hz)	52.89	5.65	45
Age (years)	29.00	5.54	90
RH V1 thickness (mm)	1.85	0.14	88
GABA+ concentration (IU)	1.45	0.15	73
RH V1 area (cm ²)	24.10	3.65	88

Bivariate correlations indicated that gamma frequency correlated with age, V1 thickness and GABA+ concentration (Table 8.4 and Figure 8.1). There was also covariance between the predictor variables of V1 thickness and age. The non-significant correlations are plotted in Appendix 2.

Table 8.4. Correlations between variables entered into the regression equation.

		Gamma frequency	Age	RH V1 thickness	GABA+	RH V1 area
Gamma frequency	R	1.00				
	N	46				
	p					
Age	R	-.40*	1.00			
	N	46	90			
	p	.003				
RH V1 thickness	R	.32*	-.27*	1.00		
	N	46	88	88		
	p	.017	.006			
GABA+	R	.32*	-.09	.08	1.00	
	N	32	73	71	73	
	p	.036	.217	.249		
RH V1 area	R	.13	-.04	-.12	.09	1.00
	N	46	88	88	71	88
	p	.203	.357	.139	.219	

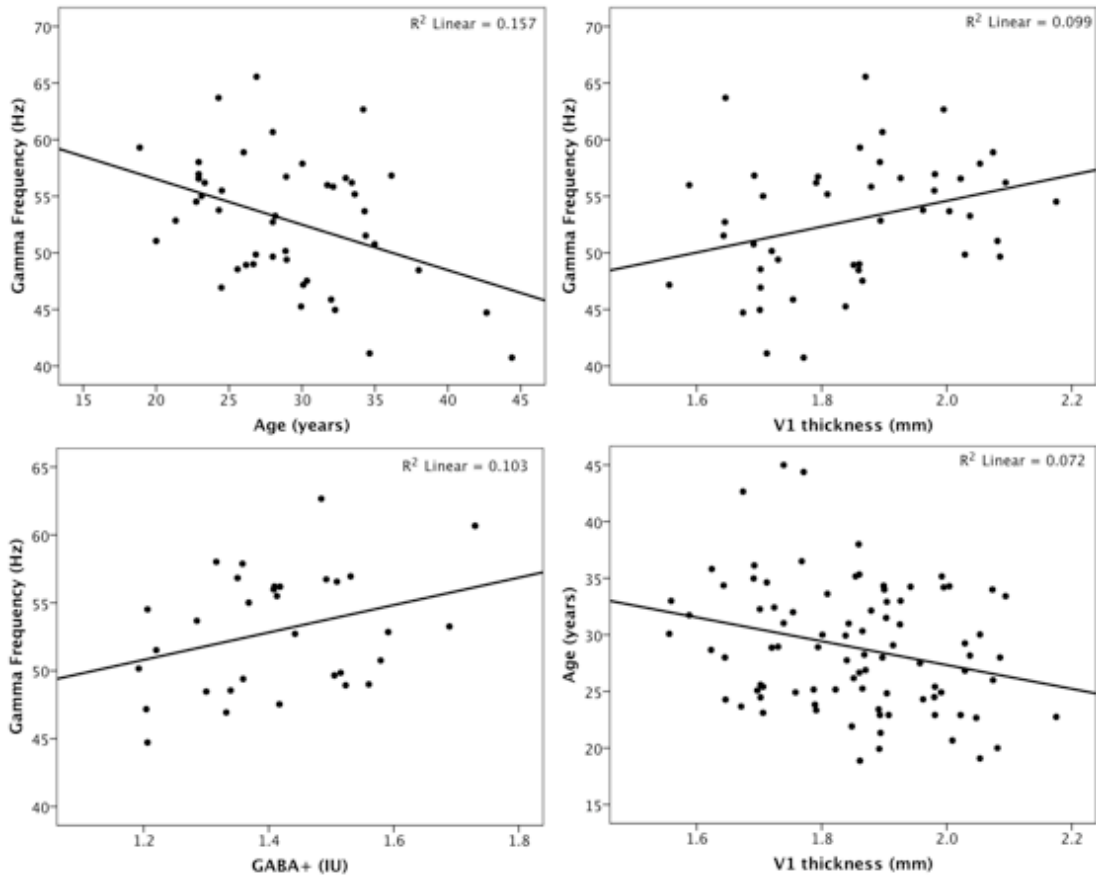


Figure 8.1. Correlations between variables of interest in this study that showed significant relationships.

Since the GABA+ value obtained is a ratio between the area under the GABA curve and the area under the creatine curve in the spectrogram, the specificity of the current relationships to GABA as opposed to creatine was investigated in a subset of participants in whom GABA data referenced to water were also available. The correlation between gamma frequency and GABA+/Cr ($R=.18$) was similar to that between gamma frequency and GABA+/H₂O ($R=.17$), whereas the correlation between gamma frequency and Cr/H₂O was much lower ($R=.00$). This finding confirms that the relationship described is indeed due to variance in GABA as opposed to in the reference molecule, creatine.

At the first stage of the hierarchical regression, age accounted for 13% of the variance in gamma frequency ($R^2_{adj}=.13$; $F(1,30)=5.60$; $p<.05$), with a standardised beta coefficient (β) of $-.40$, which was significant ($t(30)=-2.37$; $p<.05$). The addition of V1 thickness only accounted for a further non-significant 2% of the variance in gamma

frequency ($\beta=.18$; $t(29)=1.31$; $p=.20$), indicating the significance of the second model ($R^2_{adj}=.15$; $F(2,29)=3.71$; $p<.05$) was still due to the predictive power of age. At the final stage of the regression, the addition of GABA+ concentration and V1 area added 4% to the explanation of the variance in gamma frequency ($R^2_{adj}=.19$; $F(4,27)=2.78$; $p<.05$), but neither GABA+ ($\beta=.25$; $t(27)=1.61$; $p=.12$) nor right hemisphere V1 area ($\beta=.15$; $t(26)=.70$; $p=.49$) contributed significantly to the model. These results indicate that of the variables measured, age was the only significant predictor of gamma frequency and once age was accounted for, addition of other factors did not explain significant amounts of the remaining variance. This finding had an impact on the correlation between gamma frequency and GABA+, since when age was partialled out, the relationship drops from $R=.32$ ($p<.05$) to $R=.28$ ($p=.12$; Figure 8.2). Similarly, the relationship between gamma frequency and V1 thickness drops from $R=.32$ ($p<.05$) to $R=.22$ ($p=.15$).

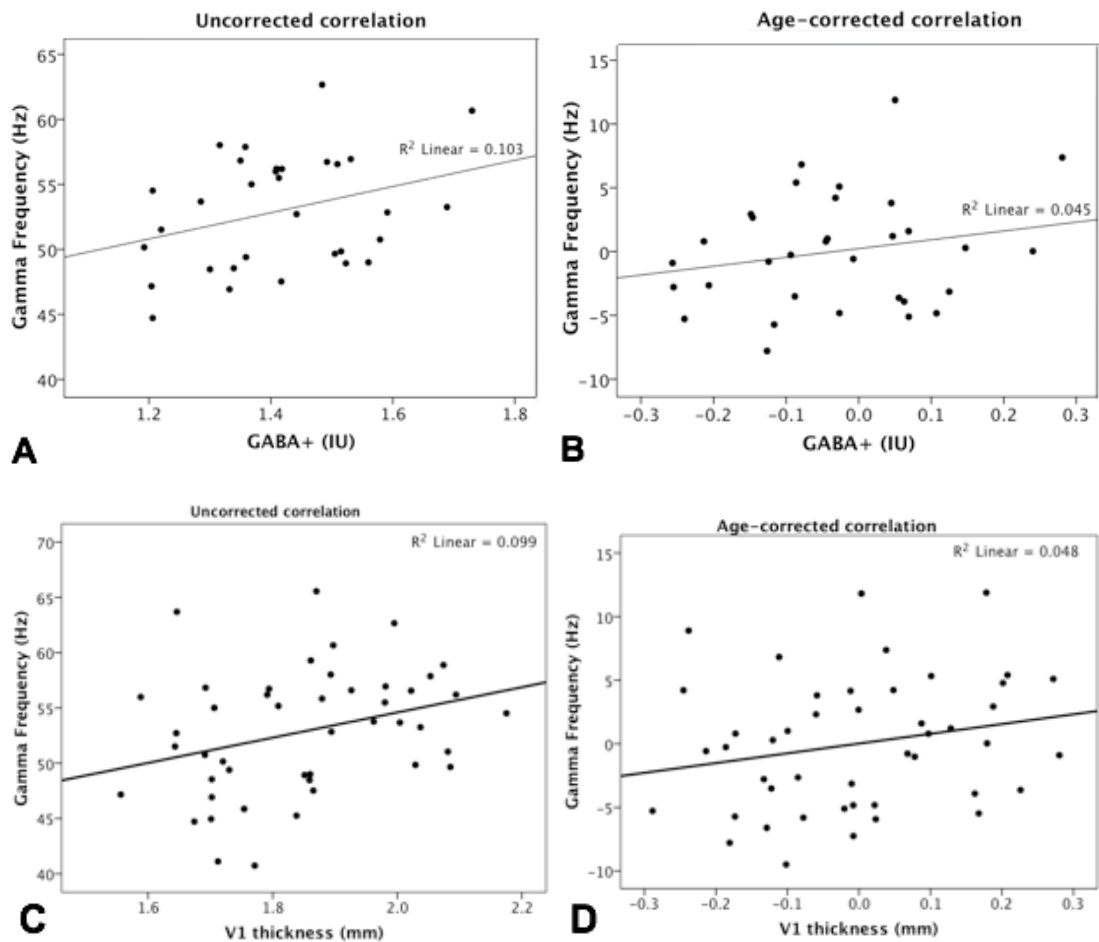


Figure 8.2. Correlations between gamma frequency and GABA+ and V1 thickness before (A&C) and after (B&D) correcting for participants' age.

A limitation of the analysis described above is that the order of entry of variables into the hierarchical regression is specified *a priori*, which although accounting for covariance between predictors, biases the results of the regression. An alternative method of analysis that still takes into account the covariance of age and V1 thickness is to conduct two simultaneous multiple regressions, excluding age in one and V1 thickness in the other. When this approach was taken, a regression model containing GABA+, V1 thickness and V1 area predicted a non-significant 12% of the variance ($R^2_{\text{adj}}=.12$; $F(3,31)=67.54$; $p=\text{ns}$). There were trends towards significance of V1 thickness ($\beta=.31$; $t(31)=1.80$; $p=.08$) and GABA+ ($\beta=.28$; $t(31)=1.67$; $p=.11$), while V1 area did not predict gamma frequency ($\beta=.14$; $t(31)=.79$; $p=.44$). A model including age, GABA+ concentration and V1 area predicted 17% of the variance in gamma frequency ($R^2_{\text{adj}}=.17$; $F(3,31)=3.05$; $p=.045$), which was just significant. Age contributed significantly to the model ($\beta=-.37$; $t(31)=-2.23$; $p<.05$), while GABA+ showed a trend towards significance ($\beta=.28$; $t(31)=1.69$; $p=.10$) but V1 area ($\beta=.09$; $t(31)=.52$; $p=.61$) did not.

Since the age range in the data entered into the regression was small (range=18-45 years, mean=29.0, SD=5.5), the potential for age to predict gamma frequency may have been limited. In order to further investigate the predictive power of age, a linear regression was conducted on a dataset with a larger age range. This study was a combination of data in press (Shaw, Brealy, Richardson, Edden, Evans, Singh et al.) and additional data in preparation for publication collected by the same researchers with the same procedures but in a different cohort. There were 32 participants, of mean age 28.5 years (SD=10.4 years, range=18.9-57.9 years). The stimuli used to evoke visual gamma oscillations in this study were circular sine wave gratings centred 2.2° below and to the left of fixation. These gratings were presented for between 0.8 and 1.3 seconds, with a 1.5 second baseline. Data from 0-0.8 seconds were taken for the stimulus phase and from -0.8-0 seconds for the baseline. Preprocessing and analysis procedures were the same as in the studies previously described. Gamma frequency (mean=50.04Hz, SD=6.75Hz) was normally distributed across participants, but age was positively skewed.

A linear regression of age on gamma frequency accounted for 27% of the variance in gamma oscillation frequency ($R^2_{\text{adj}}=.27$; $F(1,30)=12.39$; $p<.05$). Age was a strong predictor of gamma frequency ($\beta=-.54$; $t(30)=21.44$; $p<.001$). Combining these data with the previous dataset showed that the model explained 19% of the variance in gamma frequency ($R^2_{\text{adj}}=.19$; $F(1,76)=19.54$; $p<.001$) and the predictive power of age was strongly significant ($t(30)=27.19$; $p<.001$). The results support those from the original dataset, indicating that age is a significant predictor of gamma frequency. The proportions of variance accounted for in this dataset were greater, which is likely to be due to the wider age range studied.

8.5 Discussion

A hierarchical regression, correcting first for age, demonstrates that individual differences in the frequency of visual gamma oscillations are predicted by the participant's age, and that once age is taken into account, no further predictive power is added by the thickness or area of V1 or the concentration of GABA+ in the participant's occipital lobe. It may therefore be important to account for age when conducting correlations involving individual differences in gamma frequency. However, age itself cannot directly influence gamma frequency; there must be a mediating variable affecting both of these factors.

The relationship between gamma frequency and age has been reported to be non-linear, beginning to decrease in adulthood (Gaetz et al., 2011). It is therefore likely to reflect a feature of cortical maturation that occurs after neuronal growth and development has stabilised. During adulthood, there is little change in the number of neurons in visual cortex (Leuba & Kraftsik, 1994) or the number of synapses in the brain (Bruer, 1999); therefore the decrease in gamma frequency with age is not likely to be related to a loss of neurons or synaptic connections. The strength of synaptic connections with age may be more relevant: synapses between pyramidal cells are strengthened by experience (Cheetham, Barnes, Albieri, Knott & Finnerty, 2012), which may mean that less excitation is required to produce the same response, or that a stronger response is induced by the same excitatory signal. If gamma frequency represents the balance between excitation and inhibition, stronger synaptic connections requiring reduced excitation would decrease gamma frequency. Another

potential mediator of the relationship between age and gamma frequency is contrast sensitivity. Gamma frequency has been shown to increase with contrast due to increased excitability in the cortex (Ray & Maunsell, 2010). Since contrast sensitivity to medium and high spatial frequencies decreases with age (Ross, Clarke & Bron, 1985), the visual stimulus may induce less excitation in the cortex in older participants, which subsequently reduces gamma frequency.

The current results suggest that previously reported correlations between gamma frequency and GABA+ (Muthukumaraswamy et al., 2009) or V1 area (Schwarzkopf et al., 2012) may have been mediated by age, or another factor that changes with age. Although the correlations between age and gamma frequency did not reach significance in these studies, this may have been due to the small numbers of participants (12 and 16, respectively) and relatively narrow age ranges tested. Age may still have affected correlations with gamma frequency, since the age range in the main data in the current study was also small but age still predicted gamma frequency, perhaps due to the greater power from having more participants. Although the number of participants in the main dataset was relatively small for a hierarchical regression (minimum pairwise comparison $N=31$), the sample size exceeded the minimum requirement of five samples per predictor variable and the results were replicated in an independent dataset. A greater amount of variance in gamma frequency (27%) was accounted for in the replication sample than the original dataset (13%). Age was skewed in the replication so caution should be taken in interpreting this result; however, it is logical that the proportion of variance in gamma frequency attributable to age is greater with the wider age range tested in the replication.

A potential issue with the current analysis is that age is a known value whereas the other predictor variables in this regression contain some measurement error. Some of the variability accounted for by age may therefore simply be due to the estimate of the age being more accurate. GABA+ concentration showed a slight trend towards predicting gamma frequency ($p \sim .10$); however, it inevitably contains more measurement error than age. It is possible that if the measure of GABA+ concentration contained less noise, it would be a more effective predictor of gamma frequency. The data in this study were strongly quality controlled: gamma data were rejected if they did not show a clear peak; and GABA data were validated by showing

that the relationship with gamma frequency was specifically attributable to individual differences in GABA and not in the reference molecule. However, measurement of these variables cannot be as accurate as age.

The relationship between gamma frequency and V1 area (Schwarzkoepf et al., 2012) was not replicated in this study even before controlling for age, which may be due to different methods of delineating V1. In the current study, V1 was identified anatomically, based on the curvature of the gyri around the calcarine sulcus (Hinds et al., 2008); whereas Schwarzkoepf and colleagues (2012) used retinotopic mapping. The boundaries of V1 may be clearer in some participants than others when retinotopic mapping is used, due to different levels of task compliance across participants. Similarly, the curvature of the gyri may be sharper in some participants than others, allowing clearer definition of the boundaries of V1. These methods may therefore not provide the same rank order of participants in terms of the size of V1, which may explain the different relationships with gamma frequency. Retinotopic mapping also stimulates only the more central area of the visual field, generally to approximately 15° into the periphery, due to the limitations on the size of the stimulus that can be projected in the MRI scanner. Variability in the size of V1 identified from structural or functional methods could produce the different relationships with gamma frequency described.

Even after accounting for age, GABA⁺ concentration and V1 area and thickness, a large amount (>80% in the original dataset) of the variance in gamma frequency remained unexplained; therefore other factors must contribute to this individual variability. As described above, contrast sensitivity and synaptic strengthening may contribute to modulation of gamma oscillation frequency. Structural measures such as the number of GABA-ergic interneurons or pyramidal cells, the distance between synapses or the density of GABA_A receptors may also affect the ease with which activity can be synchronised and therefore predict gamma frequency. Neurophysiological techniques could be used to investigate these variables. Other neurotransmitters such as glutamate and glutamine may also have a role in modulating gamma frequency, and MRS could be used to investigate the influence of their concentration. The size and homogeneity of the cortex has also been proposed to influence gamma frequency (Schwarzkoepf et al., 2012): in smaller visual cortices, a

greater area of visual space is covered by the same area of cortex; therefore homogeneity, synchronicity and consequently gamma oscillation frequency in that area is lower. The current study did not investigate cortical homogeneity, but did show that cortical area was not a strong predictor of gamma frequency. Gamma oscillations may be initiated in a different region of the brain to where they are measured, which may explain why the area, thickness and GABA+ concentration in visual cortex did not predict gamma frequency. Evidence for this theory is equivocal: gamma is present in long-range oscillatory networks (Uhlhaas et al., 2009); however, it has been reported that gamma oscillations are generated locally (White, Banks, Pearce & Kopell, 2000), whereas theta (White et al., 2000) and alpha (De Munck et al., 2007) oscillations can originate in other regions.

There are many other demographic factors that could be added to a regression with the aim of explaining some of the variance in gamma frequency, but the covariance of these factors must be considered, as few would make an independent contribution to the model. For instance, gender may appear to contribute to prediction of gamma but may in fact be mediated by gender differences in GABA+ concentration (O'Gorman et al., 2011) and cortical thinning (Magnotta & Andreasen, 1999). It is therefore important that models tested do not contain many covarying predictor variables.

To experimentally test the influence of GABA concentration on gamma frequency, GABA could be modulated within the same participants using pharmacological methods. Elevated levels of GABA induced by blockade of the GABA membrane transporter, GAT1 using tiagabine have been shown to correlate with increased gamma synchrony measured using EEG (Hilton, Hosking & Betts, 2004). This effect was not replicated with MEG, although tiagabine did increase beta oscillation amplitude (Muthukumaraswamy, Myers, Wilson, Nutt, Lingford-Hughes, Singh et al., 2012). An alternative method of investigating individual variability in gamma frequency could be to study its outcome in terms of behavioural performance on relevant tasks and to make inferences about the cause of individual differences based on these functional outcomes. Gamma oscillations are likely to be more than just a consequence of the extent of cortical stimulation, as their frequency is related to behavioural performance in stimuli that induce the same level of stimulation (Edden et al., 2009). Gamma oscillations occur during many processes in the brain, including

sensory processing (Friedman-Hill et al., 2000), movement (Cheyne et al., 2008) and higher-order functions such as memory (Lisman & Idiart, 1995). Investigation of how differences in gamma oscillation frequency across participants and age groups affect neuronal and consequently behavioural functioning may give additional information about the role of individual differences in gamma frequency and the neurophysiological source of this variability.

8.6 Conclusion

The main predictor of individual variability in visual gamma frequency was participants' age, which accounted for 13% of the variance in a sample with a small age range and 27% in a sample with a greater age range. The area and thickness of V1 and the concentration of GABA in individuals' occipital cortex did not independently contribute to the prediction of gamma frequency. Decreases in gamma frequency with age may be due to increased synaptic strength or decreased contrast sensitivity altering the excitation/inhibition balance. It is important for future studies to continue to investigate the large amount of variance in gamma frequency still unexplained and to take into account age and potential mediating variables in studies of gamma frequency oscillations.

Chapter 9

General Discussion

9.1 Summary of findings

This thesis investigated increases and decreases in functional neuroimaging measures of visual processing in relation to the anatomy and physiology of visual cortex. Negative BOLD fMRI responses were found to show different tuning profiles to features of a visual stimulus than positive BOLD, suggesting that the two responses are at least partially independent. The direction of magnetic field gradients was found to be an important factor in achieving high repeatability of MRS measures. Individuals with a greater concentration of GABA⁺ in their occipital cortex showed a smaller difference in alpha band oscillations between resting and active states than individuals with less GABA⁺, which may indicate that they have generally reduced levels of cortical reactivity. Neither positive nor negative BOLD showed the anticipated correlation with individual differences in GABA⁺ concentration, which was likely to be due to the low power of correlational studies of neuroimaging measures. The major determinant of the peak gamma oscillation frequency in response to a visual stimulus was age.

9.2 Interpretation of findings, context and future directions

9.2.1 Negative BOLD

The role of non-stimulated visual cortex in processing a stimulus presented in the adjacent topographical area was investigated through the negative BOLD response to stimulus contrast and spatial frequency. Negative BOLD in the periphery in response to a central stimulus increased with contrast in a similar but lower amplitude profile to positive BOLD, replicating previous findings (Shmuel et al., 2002). In the periphery, negative BOLD was greatest for low spatial frequencies, reflecting the optimal behavioural (Wright & Johnston, 1983) and neurophysiological (De Valois et al., 1982) responses. This finding does not replicate a previous study showing similar spatial frequency tuning profiles for positive and negative BOLD in cat visual cortex (Harel et al., 2002); however Harel and colleagues measured negative BOLD in extrastriate areas, rather than in adjacent areas of V1. Cats show the same preferences

for lower frequencies in more peripheral regions of V1 as humans (Movshon et al., 1978), therefore restricting analyses to striate cortex in cats would be expected to show similar negative BOLD profiles as in humans.

Since the negative BOLD response profile was not always the same as positive BOLD and the amplitude of the two responses were never correlated, negative BOLD is unlikely to be solely caused by blood steal from stimulated areas. Rather, although not actively contributing to stimulus processing itself, negative BOLD is likely to represent changes in haemodynamic activity that result from stimulus-specific suppression of neuronal activity reducing the demand for oxygen in the non-stimulated area (Shmuel et al., 2006; Boorman et al., 2010). Alternatively, negative BOLD may reflect a change in interneuron activity that acts to reduce the vascular response (Vaucher et al., 2000). The role of reductions in neuronal or vascular activity may be to suppress irrelevant areas of the visual scene and to consequently improve perception of the stimulated areas.

It would be interesting to investigate the contribution of different components of the BOLD signal (blood flow, blood volume and the rate of oxygen consumption) to negative BOLD, as a change in oxygen consumption would give stronger evidence for a change in neuronal activity than changes in perfusion. Calibrated BOLD could be used to investigate the coupling between cerebral blood flow and the rate of oxygen consumption (Blockley, Griffeth, Simon & Buxton, 2012). An issue with using this technique with negative BOLD is that it relies on an estimate of the maximum possible *increase* in BOLD signal in a particular voxel, obtained using a respiratory manipulation; whereas estimating the cerebral metabolic rate of oxygen consumption (CMRO₂) in areas of negative BOLD would require quantification of the maximum possible *decrease* in BOLD. An alternative calibrated BOLD design to investigate negative BOLD has been employed by Pasley and colleagues (2007), who found that the change in CMRO₂ between stimulation and a negative baseline condition induced by the presence of a sustained stimulus was greater than the change in CMRO₂ between stimulation and a resting baseline, indicating that negative BOLD reflected reductions in neuronal activity. Studies of calibrated BOLD could therefore give useful information as to the contribution of neuronal activity to stimulus specific negative BOLD responses.

Perhaps the most interesting finding relating to negative BOLD was its dependence on underlying neuronal preferences for particular stimulus features in the cortex, because this indicates that information about stimulus features is somehow transferred to non-stimulated cortex. The mechanism by which this information could be transferred is not entirely clear. It could be a bottom-up process, whereby information about the stimulus location and features are transferred from earlier in the visual pathway, such as from the lateral geniculate nucleus to areas of V1 in addition to the receptive field corresponding to the stimulated area. Perhaps a more likely mechanism is that information is transferred either through horizontal connections within the visual cortex to areas outside the stimulated receptive fields, or by top-down feedback from higher visual areas to non-stimulated V1. The findings of strong attentional influences on negative BOLD (Heinemann et al., 2009) support the theory that it may represent top-down processes. It has also been reported that attention has a greater impact on negative BOLD in higher visual areas than in V1 (Tootell, Hadjikhani et al., 1998), which again suggests that it may be generated at later levels of processing and be fed back to V1. The lack of negative BOLD in the cortical representation of the centre of the visual field in this and previous studies (Wade & Rowland, 2010) implies that negative BOLD is not an automatic consequence of a stimulus in adjacent cortex, but that it is under top-down control as it is never relevant to inhibit the foveal area of vision. Unfortunately the temporal sequence of positive and negative BOLD activity cannot be investigated using fMRI because the temporal resolution is not good enough to distinguish between feedforward and feedback processes as these happen in the order of tens of milliseconds (Lamme & Roelfsema, 2000).

Consideration of the amplitude of both the positive and negative BOLD responses to a visual stimulus gives more information than the positive BOLD response alone when identifying the spatial location of a stimulus (Bressler et al., 2007). It would be interesting to determine whether the same is true for other stimulus features such as spatial frequency. The optimal positive BOLD response at the centre seems to be between 1 and 3cpd and is lower further from the fovea, based on the current results and on previous findings (Henriksson et al., 2008). This thesis has also shown that negative BOLD is only mildly tuned to spatial frequency; therefore, the combination of both measures may provide a better estimate of visual processing than negative

BOLD alone. Pattern matching techniques have shown that the response in non-stimulated quadrants of the visual field can be used to discriminate between different visual scenes (Smith & Muckli, 2010). Negative BOLD therefore gives useful information about stimulus properties, which can add to that provided by positive BOLD. Since negative BOLD can be detected in many fMRI studies, particularly those of sensory perception, without requiring any additional acquisitions, it would be of benefit for more studies to measure and report negative BOLD.

9.2.2 Multiple measures of inhibition

In this thesis, it was hypothesised that there would be relationships between various measures of inhibition in the brain: the concentration of the inhibitory neurotransmitter, GABA+; the amplitude of a neuronal marker of inhibition, alpha oscillations; and the reduction in haemodynamic activity represented by negative BOLD. To first consider the relationship between GABA+ and negative BOLD: no correlation was found between these variables, which may suggest that GABA+ and BOLD represent processes that are too far removed from each other to show a strong relationship, as they may be linked by an intermediate step of a change in neuronal activity. GABA-ergic interneurons can interact with microvasculature in the brain and dilate or constrict vessels (Vaucher et al., 2000; Cauli et al., 2004; Hamel, 2006), but this process has not yet been linked to changes in the BOLD response. Negative BOLD was also a weak response and was not generally repeatable, which further decreases the power to detect correlations between variables.

Another potential limiting factor in the relationship between GABA+ and BOLD is that MRS measures the overall concentration of GABA in a voxel without distinguishing between intracellular and extracellular GABA. These two types of GABA have different influences on neuronal activity (Farrant & Nusser, 2005) and one may be more relevant than the other in terms of influencing neuronal activity and BOLD responses. The MRS measure of the total concentration of GABA+ may be less relevant in explaining the BOLD response than more specific measures such as the activity in GABA-ergic interneurons and the cycling rate of GABA-ergic transmission at the synapse. Even if there were only a small amount of GABA in a particular area, if it was passed on at the synapse, broken down and regenerated rapidly, greater changes in the BOLD response could be induced than if a higher

concentration of GABA⁺ was present but was not involved in synaptic inhibition or was slower to act. The MRS measure of GABA concentration also includes a potential contribution of macromolecules, which could reduce the correlation between GABA⁺ and BOLD. A recent study has shown that adjustment of the editing pulse can more effectively suppress these signals (Edden, Puts & Barker, 2012), so this technique should be used in future studies to obtain a more pure measure of GABA in edited MRS.

It would be interesting for future studies to use techniques that specifically measure GABA actively involved in neurotransmission. For example, GABA cycling could be studied using ¹³C labeling to follow the movement of the neurotransmitter through metabolic pathways (Otsuki, Kanamatsu, Tsukada, Goto, Okamoto & Watanabe, 2005). Individual differences in this measure of GABA could then be correlated with the amplitude of negative BOLD. Alternatively, MRS could be used to measure functional changes in GABA⁺ concentration in order to give a better measure of GABA⁺ specifically involved in neurotransmission than the measure of resting GABA⁺ generally taken. At present, MRS is most commonly used to report the baseline level of metabolites measured over a long period of time (several minutes); however, increases in glutamate concentration have been reported in response to pain stimulation (Gussew, Rzanny, Erdtel, Scholle, Kaiser, Mentzel et al., 2010). Measurement of these functional changes in metabolites with MRS currently has a temporal resolution of several seconds, but in the future, it may be possible to measure more transient changes in GABA⁺ concentration using MRS and this measure could be conducted simultaneously with fMRI to determine temporal correlations between GABA⁺ and negative BOLD.

Another functional measure of neuronal inhibition (alpha suppression) was obtained in this thesis, but the correlation between alpha and negative BOLD could not be effectively investigated as the task used to generate alpha drove an oscillatory response in the MEG, which masked the stimulus-induced oscillations. It is likely that a neuronal marker of negative BOLD could be identifiable using MEG if a suitable task were designed. Reductions in the MEG evoked response have been reported in a similar spatial profile to that expected for negative BOLD: event-related magnetic fields in response to distractor stimuli were suppressed for stimuli adjacent

to a target, but increased with distance from the target (Hopf, Boehler, Luck, Tsotsos, Heinze & Schoenfeld, 2006). An induced equivalent of negative BOLD may also be expected as BOLD is generally more strongly related to oscillatory activity than evoked responses (Logothetis et al., 2001). Supporting this theory, increased alpha has previously been detected using electrocorticography in areas surrounding a visual stimulus where negative BOLD would be expected (Harvey et al., 2012). Given the appropriate task, either evoked, induced or both types of neuronal activity may therefore be measurable in areas also displaying negative BOLD. An improvement to the experimental design used in this thesis would be to position the attentional task in the same location as the visual stimulus, since both negative BOLD (Smith et al., 2000; Heinemann et al., 2009) and alpha oscillations (Foxe et al., 1998; Kelly et al., 2006; Thut et al., 2006) are induced in non-attended areas. Such a task would allow investigation of whether alpha oscillations contribute to generation of negative BOLD.

Alpha oscillations in resting cortex were expected to be of greater amplitude in participants with greater GABA⁺ concentration, as GABA⁺ reflects increased inhibitory neurotransmission and alpha is present in inhibited areas of cortex. However, the opposite relationship was in fact observed. This finding may suggest that individuals with greater GABA⁺ concentration have generally reduced neuronal reactivity: the difference in alpha power with the eyes open as opposed to closed is smaller in individuals with more GABA⁺. In addition to the amplitude of alpha measured in this thesis, it would be interesting to investigate individual differences in the peak frequency of alpha in relation to GABA⁺ concentration. The frequency of beta and gamma oscillations has been shown to relate to GABA⁺ (Muthukumaraswamy et al., 2009; Gaetz et al., 2011) and the same mechanism driving individual differences in gamma frequency may apply to differences in alpha: GABA-ergic inhibition may reduce the excitation/inhibition ratio, making the cycle of activation and suppression of neuronal firing shorter, and consequently increasing the oscillatory frequency in individuals with more GABA⁺.

Individual differences in various neuroimaging measures of inhibition in the brain were considered in relation to each other in this thesis; however, these measures would also be expected to have an impact on behaviour in terms of individuals'

perceptions. Individual differences in GABA+ concentration have previously been shown to predict behaviour, with associations made with impulsivity (Boy et al., 2011), orientation discrimination (Edden et al., 2009), tactile discrimination (Puts et al., 2011), motor learning (Stagg et al., 2011a) and eye movements (Sumner et al., 2010). GABA+ concentration is therefore likely to be related to other measures of visual perception. It would also be interesting to develop tasks to investigate the behavioural consequences of negative BOLD and alpha. In somatosensory cortex, tactile discrimination thresholds have been shown to be increased by the presence of negative BOLD in the stimulated area (Kastrup et al., 2008) and are also related to GABA+ concentration (Puts et al., 2011), suggesting a link between GABA+, negative BOLD and behaviour. A potential visual correlate of this experiment would be to conduct a cueing paradigm in which a central arrow directs attention to one hemisphere, inducing alpha and negative BOLD in opposite hemisphere. The extent of these responses could be correlated with individual differences in behavioural responses to a stimulus presented in the attended or unattended hemisphere. The hypothesis would be that individuals with greater negative BOLD or alpha and therefore increased inhibition would be expected to show slower reaction times or poorer discrimination of visual features of a stimulus presented in the unattended (potentially inhibited) hemisphere. Such combinations of different imaging techniques and behavioural measures will be important to enhance our understanding of how the many stages of stimulus processing contribute to perception.

To summarise the relationships between measures of inhibition obtained in this thesis: negative BOLD may be better predicted by measures of GABA-ergic interneuron activity and GABA molecule cycling than by GABA+ concentration; individual differences in negative BOLD did not relate to GABA+ concentration and were not directly comparable with alpha oscillations; and alpha reactivity was reduced in individuals with a greater GABA+ concentration in comparison to those with less GABA+. A task could be developed to allow investigation of both alpha oscillations and negative BOLD in the same paradigm and the peak alpha frequency could also be investigated in relation to negative BOLD. The impact of these different measures of inhibition on behaviour should be determined.

9.2.3 Relationships between measures of excitation

The most unexpected finding in this thesis was the absence of a correlation between individual differences in GABA+ concentration and positive BOLD. This relationship has been previously reported in more than one study using similar acquisition techniques (Muthukumaraswamy et al., 2009; Donahue et al., 2010; Muthukumaraswamy, Evans et al., 2012) but was not replicated in three experiments in this thesis (Chapters 4 and 5). It was proposed that one potential reason for the lack of replication of this relationship was the individual measures were not sufficiently repeatable themselves and therefore would be unlikely to reproduce the same correlation on repeated testing. However, the test-retest reliability of GABA+ and BOLD were both found to be acceptable, with GABA+ measurement showing better repeatability than BOLD. The between-subjects variability in GABA+ concentration was also very low, resulting in a small range of GABA+ values, which consequently greatly reduces the potential for correlations with other variables. The between-subjects variability was in fact not sufficiently greater than the within-subjects variability to allow discrimination of repeated measurements of an individual participants' GABA+ data from measures obtained from other participants. Care must therefore be taken when interpreting results of relationships between individual differences in GABA+ concentration and other variables. The sample size tested must be large enough to give a wide range of GABA+ values for correlations. A further recommendation for MRS studies is to obtain two acquisitions in order to ensure that within-subjects variance is smaller than between-subjects because if not, conclusions about individual differences in a variable cannot be made.

Simulations of the relationship between GABA+ and BOLD in this thesis aimed to build on prior knowledge of issues of statistical power in correlations (Faul et al., 2007) and in fMRI studies (Desmond & Glover, 2002). Correlations between the mean of two acquisitions of both variables were simulated, given the specific amounts of measurement noise known to be present in each. At sample sizes equivalent to those generally used in neuroimaging studies, measurement noise in MRS and fMRI data had a substantial effect on the probability of detecting the true correlation between the variables. Correlations between individual differences in functional imaging measures and behaviour are underpowered and are unlikely to show intrinsic correlations of greater than $R=0.5$ (Yarkoni, 2009). The relationship between

individual differences in different neuroimaging measures is unlikely to be any stronger than these brain-behaviour relationships, so these studies also suffer from lack of power. It is therefore important to report confidence intervals or effect sizes for these correlations. More importantly, the sample size should be maximised, potentially by developing standardised protocols to be used by different researchers within and between research centres.

Testing differences between conditions provides greater statistical power than conducting correlations, so splitting the sample into groups of individuals with low, medium and high neurotransmitter concentrations may be a more effective experimental paradigm for investigating the effects of MRS measures on other neuroimaging variables and on behaviour (Falkenberg, Westerhausen, Specht & Hugdahl, 2012). Alternatively, pharmacological manipulation can be used to test the impact of different concentrations of neurotransmitters on other factors within the same participants. For instance, in rat somatosensory cortex, the positive BOLD response is reduced when GABA concentration is elevated due to pharmacological inhibition of GABA transaminase, which breaks down GABA (Chen et al., 2005). Similarly, visual BOLD in humans is reduced by application of a GABA agonist (Licata et al., 2011). In terms of neuronal measures, the power of beta oscillations in motor cortex is increased by blocking GABA uptake using tiagabine (Muthukumaraswamy, Myers et al., 2012). Experimental manipulation of GABA either through pharmacological intervention or through designation of group membership therefore has a measurable impact on functional neuroimaging measures. Testing differences in these ways provides more power for investigation of the impact of GABA on other variables than studies of individual differences in baseline GABA+ concentration measured with MRS.

There may be variables that mediate the relationship between various neuroimaging measures, which should be taken into consideration when making conclusions about relationships between variables. Previous studies (Muthukumaraswamy et al., 2009; Gaetz et al., 2011) have described a correlation between gamma oscillation frequency and GABA+ concentration; however, in this thesis, once age was taken into account, GABA+ was no longer a significant predictor of gamma frequency. There was a slight trend towards significance ($p=.1$) in the predictive power of GABA+ and it is

possible that age is a better predictor because it can be more accurately estimated: with a more robust measure of GABA concentration (perhaps by reducing the contribution of macromolecules to the measure of GABA), the predictive power of GABA on gamma frequency might be greater. In the same regression analysis, the area and thickness of V1 also did not predict individual differences in gamma frequency; therefore, a previous finding of a relationship between gamma frequency and V1 area (Schwarzkopf et al., 2012) was not replicated. This result suggests that studies investigating gamma frequency should control for age. There are many other potential neurological, genetic and demographic variables that may predict oscillatory frequency (Van Pelt, Boomsma & Fries, 2012) and one of the challenges for the neuroscience community is to ensure that findings are attributed to the correct source and to develop our understanding of the stages involved in producing the outcome that is measured.

9.2.4 MRS methods and repeatability

The direction of the magnetic field gradients was found to be an important factor contributing to the repeatability of GABA-edited MRS in this thesis. The region from which different metabolites in a spectrum are acquired is slightly different due to the chemical shift artefact. This effect occurs because the bandwidth of slice-selective radiofrequency pulses is limited and spins are only excited by pulses at the resonant frequency of the molecule; therefore slice position for molecules with different resonance frequencies is shifted along the gradient used to position the radiofrequency pulse. When acquiring a voxel from the occipital lobe, if the gradients were in the default direction, the lipid signal was obtained from an area posterior to the GABA voxel, which contained sinus, skull and scalp, therefore the baseline of the spectrum was contaminated by lipid signals, resulting in a poorer fit of the Gaussian model to the GABA+ peak and poorer repeatability of the measure. Manually adjusting the phase of individual spectra made only a small improvement in addition to this effect. It is therefore important that future MRS studies determine the optimal direction of gradients for the particular voxel location of interest to prevent acquisition of lipid signals from regions of substantially different tissue composition to the GABA+ voxel. The within- and between-session repeatability of GABA-edited MRS was very high when the gradients were reversed and when a phantom containing a GABA solution was tested, indicating that MRS is a reliable technique.

9.3 Summary of the impact of the current research

The work described in the early chapters of this thesis suggests that negative BOLD may be a useful source of information in fMRI studies of visual processing, giving additional signal to that provided by positive BOLD. Since negative BOLD in response to a centrally-presented stimulus is modulated by features of the stimulus, the signal could be used in conjunction with the positive BOLD signal to fully characterise an individual's haemodynamic response to the stimulus.

The studies presented in this thesis also found that there are several limitations to the investigation of the relationships between individual differences in structural, neurophysiological, neuronal and haemodynamic variables potentially contributing to processing of a visual stimulus. Correlations between two imaging measures are typically underpowered due to low sample sizes increasing sensitivity to outliers and measurement noise. Limited between-subjects variability also reduces the power of correlations. As a result of these limitations, care must be taken when conducting and interpreting studies of individual differences because spurious significant relationships can occur by chance. Tests of group differences or manipulations of experimental conditions may be preferable methods for ensuring adequate statistical power in studies relating different neuroimaging measures. For comparison of individual differences, the anticipated strength of the relationship between the two variables should be hypothesised in advance based on known physiological mechanisms linking the variables, so that the minimum sample size can be determined.

Many variables can be measured using neuroimaging, therefore when investigating correlations between or predictions of variables, it is important to understand the role of each in stimulus processing and to consider potential covariates. Additional factors may be relevant in generation of an individual's visual percept, such as the concentration of other neurotransmitters, the number or firing rate of interneurons, receptor density and other demographic variables.

In general, this thesis suggests that greater consideration of the functional activity in non-stimulated cortex should be taken when characterising a response to a stimulus. Overall, individual differences in various measures of the structure and function of visual cortex did not show convincingly strong relationships with each other. In investigations of relationships between individual differences in neuroimaging measures, greater acknowledgment should be made of issues of statistical power and care should be taken to ensure optimal methods are used to increase the likelihood of measuring the true relationships.

References

- Adjamian, P. & Hadjipapas, A. (2008). Induced Gamma activity in primary visual cortex is related to luminance and not color contrast: An MEG study. *Journal of Vision*, 8, 1-7.
- Aguirre, G., Zarahn, E. & D'esposito, M. (1998). The variability of human, BOLD hemodynamic responses. *Neuroimage*, 8, 360-369.
- Albus, K. & Whale, P. (1994). The Topography of Tangential Inhibitory Connections in the Postnatally Developing and Mature Striate Cortex of the Cat. *European Journal of Neuroscience*, 6, 779-792.
- Allison, J. D., Meador, K. J., Loring, D. W., Figueroa, R. E. & Wright, J. C. (2000). Functional MRI cerebral activation and deactivation during finger movement. *Neurology*, 54, 135-142.
- Amunts, K., Malikovic, A., Mohlberg, H., Schormann, T. & Zilles, K. (2000). Brodmann's areas 17 and 18 brought into stereotaxic space-where and how variable? *NeuroImage*, 11, 66-84.
- Andrews, T. J., Halpern, S. D. & Purves, D. (1997). Correlated size variations in human visual cortex, lateral geniculate nucleus, and optic tract. *The Journal of Neuroscience*, 17, 2859-2868.
- Baillet, S., Mosher, J. C. & Leahy, R. M. (2001). Electromagnetic Brain Mapping. *IEEE Signal processing magazine*, 18, 14-30.
- Bandettini, P. A., Wong, E. C., Hinks, R. S., Tikofsky, R. S. & Hyde, J. S. (1992). Time course EPI of human brain function during task activation. *Magnetic Resonance in Medicine*, 25, 390-397.
- Banks, M. I., White, J. A. & Pearce, R. A. (2000). Interactions between distinct GABA(A) circuits in hippocampus. *Neuron*, 25, 449-457.
- Barker, P. & Lin, D. (2006). In vivo proton MR spectroscopy of the human brain. *Progress in Nuclear Magnetic Resonance Spectroscopy*, 49, 99-128.
- Barnes, G. R., Hillebrand, A., Fawcett, I. P. & Singh, K. D. (2004). Realistic spatial sampling for MEG beamformer images. *Human brain mapping*, 23, 120-127.
- Bartos, M., Vida, I. & Jonas, P. (2007). Synaptic mechanisms of synchronized gamma oscillations in inhibitory interneuron networks. *Nature Reviews: Neuroscience*, 8, 45-56.
- Başar, E., Schürmann, M., Başar-Eroglu, C. & Karakaş, S. (1997). Alpha oscillations in brain functioning: An integrative theory. *International Journal of Psychophysiology*, 26, 5-29.
- Behar, K. & Rothman, D. (1994). Analysis of macromolecule resonances in ¹H NMR spectra of human brain. *Magnetic Resonance in Medicine*, 32, 294-302.
- Belliveau, J. W., Kennedy, D. N., McKinstry, R. C., Buchbinder, B. R., Weisskoff, R. M., Cohen, M. S. et al. (1991). Functional mapping of the human visual cortex by magnetic resonance imaging. *Science*, 254, 716-719.
- Berger, H. (1929). Über das elektrenkephalogramm des menschen. *Archives für Psychiatrie*, 87, 527-570.
- Bernstein, E. M. & Quick, M. W. (1999). Regulation of gamma-aminobutyric acid (GABA) transporters by extracellular GABA. *The Journal of Biological Chemistry*, 274, 889-895.
- Bertholdo, D., Watcharakorn, A. & Castillo, M. (2011). Brain Proton Magnetic Resonance Spectroscopy *American Journal of Neuroradiology*.

- Bland, J. M. & Altman, D. (1986). Statistical methods for assessing agreement between two methods of clinical measurement. *The Lancet*, *8*, 307-310.
- Bloch, F., Hansen, W. & Packard, M. (1946). Nuclear Induction. *Physical review*, *738*, 1939.
- Blockley, N. P., Griffeth, V. E. M., Simon, A. B. & Buxton, R. B. (2012). A review of calibrated blood oxygenation level-dependent (BOLD) methods for the measurement of task-induced changes in brain oxygen metabolism. *NMR in Biomedicine*.
- Bogner, W., Gruber, S., Doelken, M., Stadlbauer, A., Ganslandt, O., Boettcher, U. et al. (2010). In vivo quantification of intracerebral GABA by single-voxel (1)H-MRS-How reproducible are the results? *European Journal of Radiology*, *73*, 526-531.
- Boorman, L., Kennerley, A. J., Johnston, D., Jones, M., Zheng, Y., Redgrave, P. et al. (2010). Negative blood oxygen level dependence in the rat: a model for investigating the role of suppression in neurovascular coupling. *The Journal of neuroscience : the official journal of the Society for Neuroscience*, *30*, 4285-4294.
- Boy, F., Evans, C. J., Edden, R. a. E., Lawrence, A. D., Singh, K. D., Husain, M. et al. (2011). Dorsolateral prefrontal γ -aminobutyric acid in men predicts individual differences in rash impulsivity. *Biological Psychiatry*, *70*, 866-872.
- Boynton, G. M., Demb, J. B., Glover, G. H. & Heeger, D. J. (1999). Neuronal basis of contrast discrimination. *Vision Research*, *39*, 257-269.
- Boynton, G. M., Engel, S. A., Glover, G. H. & Heeger, D. J. (1996). Linear systems analysis of functional magnetic resonance imaging in human V1. *The Journal of Neuroscience*, *16*, 4207-4221.
- Bressler, D., Spotswood, N. & Whitney, D. (2007). Negative BOLD fMRI response in the visual cortex carries precise stimulus-specific information. *PloS One*, *2*, e410.
- Brookes, M., Hale, J., Zumer, J. & Stevenson, C. (2011). Measuring functional connectivity using MEG: Methodology and comparison with fcMRI. *NeuroImage*, *56*, 1082-1104.
- Brookes, M. & Woolrich, M. (2011). Investigating the electrophysiological basis of resting state networks using magnetoencephalography. *Proceedings of the National Academy of Sciences*.
- Brookes, M. J., Gibson, A. M., Hall, S. D., Furlong, P. L., Barnes, G. R., Hillebrand, A. et al. (2005). GLM-beamformer method demonstrates stationary field, alpha ERD and gamma ERS co-localisation with fMRI BOLD response in visual cortex. *NeuroImage*, *26*, 302-308.
- Bruer, J. (1999). Neural connections: Some you use, some you lose. *Phi Delta Kappan*, *81*, 264-277.
- Brunel, N. & Wang, X.-J. (2003). What determines the frequency of fast network oscillations with irregular neural discharges? I. Synaptic dynamics and excitation-inhibition balance. *Journal of Neurophysiology*, *90*, 415-430.
- Buxton, R., Wong, E. & Frank, L. (2005). Dynamics of blood flow and oxygenation changes during brain activation: The balloon model. *Magnetic Resonance in Medicine*, *855-864*.
- Buzsaki, G. & Chrobak, J. J. (1995). Temporal structure in spatially organized neuronal ensembles: A role for interneuronal networks. *Current Opinion in Neurobiology*, *5*, 504-510.

- Buzsaki, G., Kaila, K. & Raichle, M. (2007). Inhibition and brain work. *Neuron*, 56, 771-783.
- Buzsaki, G. & Wang, X.-J. (2012). Mechanisms of gamma oscillations. *Annual Review of Neuroscience*, 35, 203-225.
- Campbell, F. & Robson, J. (1968). Application of Fourier analysis to the visibility of gratings. *The Journal of Physiology*, 197, 551-566.
- Cauli, B., Tong, X.-K., Rancillac, A., Serluca, N., Lambolez, B., Rossier, J. et al. (2004). Cortical GABA interneurons in neurovascular coupling: relays for subcortical vasoactive pathways. *The Journal of Neuroscience*, 24, 8940-8949.
- Chard, D., McLean, M., Parker, G., MacManus, D. & Miller, D. (2002). Reproducibility of in vivo metabolite quantification with proton magnetic resonance spectroscopic imaging. *Journal of Magnetic Resonance Imaging*, 15, 219-225.
- Cheetham, C. E. J., Barnes, S. J., Albieri, G., Knott, G. W. & Finnerty, G. T. (2012). Pansynaptic enlargement at adult cortical connections strengthened by experience. *Cerebral Cortex*, 1-11.
- Chen, Z., Silva, A. C., Yang, J. & Shen, J. (2005). Elevated endogenous GABA level correlates with decreased fMRI signals in the rat brain during acute inhibition of GABA transaminase. *Journal of Neuroscience Research*, 79, 383-391.
- Cheyne, D., Bells, S., Ferrari, P., Gaetz, W. & Bostan, A. C. (2008). Self-paced movements induce high-frequency gamma oscillations in primary motor cortex. *NeuroImage*, 42, 332-342.
- Cohen, D. (1968). Magnetoencephalography: Evidence of magnetic fields produced by alpha-rhythm currents. *Science*, 18-20.
- Cohen, D. (1972). Magnetoencephalography: Detection of the brain's electrical activity with a superconducting magnetometer. *Science*, 175, 664.
- Cornwell, B. R., Johnson, L. L., Holroyd, T., Carver, F. W. & Grillon, C. (2008). Human hippocampal and parahippocampal theta during goal-directed spatial navigation predicts performance on a virtual Morris water maze. *The Journal of Neuroscience*, 28, 5983-5990.
- Crunelli, V. & Hughes, S. (2009). The slow (<1Hz) rhythm of non-REM sleep: A dialogue between three cardinal oscillators. *Nature Neuroscience*, 13, 9-17.
- Dagli, M. S., Ingeholm, J. E. & Haxby, J. V. (1999). Localization of cardiac-induced signal change in fMRI. *NeuroImage*, 9, 407-415.
- Daniel, P. & Whitteridge, D. (1961). The representation of the visual field on the cerebral cortex in monkeys. *The Journal of Physiology*, 203-221.
- De Graaf, R., A. (2007). *In Vivo NMR Spectroscopy: Principles and Techniques, 2nd Edition*. Chichester, UK: John Wiley & Sons.
- De Munck, J. C., Gonçalves, S. I., Huijboom, L., Kuijter, J. P. A., Pouwels, P. J. W., Heethaar, R. M. et al. (2007). The hemodynamic response of the alpha rhythm: An EEG/fMRI study. *NeuroImage*, 35, 1142-1151.
- De Valois, K. K., Morgan, H. & Snodderly, D. M. (1974). Psychophysical studies of monkey Vision-III. Spatial luminance contrast sensitivity tests of macaque and human observers. *Vision Research*, 14(1), 75-81.
- De Valois, R. L., Albrecht, D. G. & Thorell, L. G. (1982). Spatial frequency selectivity of cells in macaque visual cortex. *Vision Research*, 22, 545-559.
- Desmond, J. E. & Glover, G. H. (2002). Estimating sample size in functional MRI (fMRI) neuroimaging studies: statistical power analyses. *Journal of Neuroscience Methods*, 118, 115-128.

- Devor, A., Tian, P., Nishimura, N., Teng, I. C., Hillman, E. M. C., Narayanan, S. N. et al. (2007). Suppressed neuronal activity and concurrent arteriolar vasoconstriction may explain negative blood oxygenation level-dependent signal. *The Journal of Neuroscience*, *27*, 4452-4459.
- DeYoe, E. A., Carman, G. J., Bandettini, P., Glickman, S., Wieser, J., Cox, R. et al. (1996). Mapping striate and extrastriate visual areas in human cerebral cortex. *Proceedings of the National Academy of Sciences*, *93*, 2382-2386.
- Donahue, M. J., Near, J., Blicher, J. U. & Jezzard, P. (2010). Baseline GABA concentration and fMRI response. *NeuroImage*, *53*(2), 392-398.
- Donner, T. H. & Siegel, M. (2011). A framework for local cortical oscillation patterns. *Trends in Cognitive Sciences*, *15*, 191-199.
- Doppelmayr, M., Klimesch, W., Pachinger, T. & Ripper, B. (1998). Individual differences in brain dynamics: important implications for the calculation of event-related band power. *Biological cybernetics*, *79*, 49-57.
- Edden, R. A. E., Muthukumaraswamy, S. D., Freeman, T. C. A. & Singh, K. D. (2009). Orientation discrimination performance is predicted by GABA concentration and gamma oscillation frequency in human primary visual cortex. *The Journal of Neuroscience*, *29*, 15721-15726.
- Edden, R. A. E., Puts, N. a. J. & Barker, P. B. (2012). Macromolecule-suppressed GABA-edited magnetic resonance spectroscopy at 3T. *Magnetic Resonance in Medicine*, *68*, 657-661.
- Engel, S. A., Glover, G. H. & Wandell, B. A. (1997). Retinotopic organization in human visual cortex and the spatial precision of functional MRI. *Cerebral Cortex*, *7*, 181-192.
- Epperson, C., Haga, K., Mason, G., Sellers, E., Gueorguieva, R., Zhang, W. et al. (2002). Cortical Y-Aminobutyric Acid Levels Across the Menstrual Cycle in Healthy Women and Those With Premenstrual Dysphoric Disorder. *Archives of General Psychiatry*, *59*, 851-858.
- Epperson, C. N., O'Malley, S., Czarkowski, K. a., Gueorguieva, R., Jatlow, P., Sanacora, G. et al. (2005a). Sex, GABA, and nicotine: The impact of smoking on cortical GABA levels across the menstrual cycle as measured with proton magnetic resonance spectroscopy. *Biological Psychiatry*, *57*, 44-48.
- Epperson, C. N., O'Malley, S., Czarkowski, K. a., Gueorguieva, R., Jatlow, P., Sanacora, G. et al. (2005b). Sex, GABA, and nicotine: the impact of smoking on cortical GABA levels across the menstrual cycle as measured with proton magnetic resonance spectroscopy. *Biological psychiatry*, *57*, 44-48.
- Evans, C. J., McGonigle, D. J. & Edden, R. A. E. (2010). Diurnal stability of gamma-aminobutyric acid concentration in visual and sensorimotor cortex. *Journal of Magnetic Resonance Imaging*, *31*, 204-249.
- Eysel, U. T., Shevelev, I. A., Lazareva, N. A. & Sharaev, G. A. (1998). Orientation tuning and receptive field structure in cat striate neurons during local blockade of intracortical inhibition. *Neuroscience*, *84*, 25-36.
- Falkenberg, L. E., Westerhausen, R., Specht, K. & Hugdahl, K. (2012). Resting-state glutamate level in the anterior cingulate predicts blood-oxygen level-dependent response to cognitive control. *Proceedings of the National Academy of Sciences of the United States of America*, *109*, 5069-5073.
- Farrant, M. & Nusser, Z. (2005). Variations on an inhibitory theme: phasic and tonic activation of GABA(A) receptors. *Nature reviews. Neuroscience*, *6*, 215-229.

- Faul, F., Erdfelder, E., Lang, A.-G. & Buchner, A. (2007). G*Power 3: A flexible statistical power analysis program for the social, behavioral, and biomedical sciences. *Behavior Research Methods*, *39*, 175-191.
- Felblinger, J., Kreis, R. & Boesch, C. (1998). Effects of physiologic motion of the human brain upon quantitative 1H-MRS: Analysis and correction by retro-gating. *NMR in Biomedicine*, *11*, 107-114.
- Fischl, B., Sereno, M. I. & Dale, A. M. (1999). Cortical surface-based analysis. II: Inflation, flattening, and a surface-based coordinate system. *NeuroImage*, *9*, 195-207.
- Fox, P. T. & Raichle, M. E. (1986). Focal physiological uncoupling of cerebral blood flow and oxidative metabolism during somatosensory stimulation in human subjects. *Proceedings of the National Academy of Sciences*, *83*, 1140-1144.
- Foxe, J. J., Simpson, G. V. & Ahlfors, S. P. (1998). Parieto-occipital ~10Hz activity reflects anticipatory state of visual attention mechanisms. *Neuroreport*, *9*, 3929-3933.
- Friedman-Hill, S., Maldonado, P. E. & Gray, C. M. (2000). Dynamics of striate cortical activity in the alert macaque: I. Incidence and stimulus-dependence of gamma-band neuronal oscillations. *Cerebral Cortex*, *10*, 1105-1116.
- Fries, P., Reynolds, J. H., Rorie, A. E. & Desimone, R. (2001). Modulation of Oscillatory Neuronal Synchronization by Selective Visual Attention. *Science*, *291*, 1560-1563.
- Fu, K. M., Foxe, J. J., Murray, M. M., Higgins, B. A., Javitt, D. C. & Schroeder, C. E. (2001). Attention-dependent suppression of distracter visual input can be cross-modally cued as indexed by anticipatory parieto-occipital alpha-band oscillations. *Cognitive Brain Research*, *12*, 145-152.
- Gaetz, W., Edgar, J. C., Wang, D. J. & Roberts, T. P. L. (2011). Relating MEG measured motor cortical oscillations to resting γ -aminobutyric acid (GABA) concentration. *NeuroImage*, *55*(2), 616-621.
- Gaetz, W., Roberts, T. P. L., Singh, K. D. & Muthukumaraswamy, S. D. (2012). Functional and structural correlates of the aging brain: Relating visual cortex (V1) gamma band responses to age-related structural change. *Human Brain Mapping*, *33*, 2035-2046.
- Gasparovic, C., Bedrick, E. J., Mayer, A. R., Yeo, R. A., Chen, H., Damaraju, E. et al. (2011). Test-retest reliability and reproducibility of short-echo-time spectroscopic imaging of human brain at 3T. *Magnetic Resonance in Medicine*, *66*, 324-332.
- Geramita, M., van der Veen, J. W., Barnett, A. S., Savostyanova, A. A., Shen, J., Weinberger, D. R. et al. (2011). Reproducibility of prefrontal γ -aminobutyric acid measurements with J-edited spectroscopy. *NMR in Biomedicine*, *24*, 1089-1098.
- Goelman, G., Liu, S., Fleysher, R., Fleysher, L., Grossman, R. I. & Gonen, O. (2007). Chemical-shift artifact reduction in Hadamard-encoded MR spectroscopic imaging at high (3T and 7T) magnetic fields. *Magnetic Resonance in Medicine*, *58*, 167-173.
- Goldman, R. I., Stern, J. M., Engel, J. & Cohen, M. S. (2002). Simultaneous EEG and fMRI of the alpha rhythm. *Neuroreport*, *13*, 2487-2492.
- Gonçalves, S. I., de Munck, J. C., Pouwels, P. J. W., Schoonhoven, R., Kuijter, J. P. A., Maurits, N. M. et al. (2006). Correlating the alpha rhythm to BOLD using simultaneous EEG/fMRI: inter-subject variability. *NeuroImage*, *30*, 203-213.

- Gonzalez-Burgos, G. & Lewis, D. A. (2008). GABA neurons and the mechanisms of network oscillations: implications for understanding cortical dysfunction in schizophrenia. *Schizophrenia Bulletin*, *34*, 944-961.
- Gray, C. & McCormick, D. (1996). Chattering Cells: Superficial pyramidal neurons contributing to the generation of synchronous oscillations in the visual cortex. *Science*, *274*, 109-113.
- Gray, C. M. & Singer, W. (1989). Stimulus-specific neuronal oscillations in orientation columns of cat visual cortex. *Proceedings of the National Academy of Sciences of the United States of America*, *86*, 1698-1702.
- Grill-Spector, K. & Malach, R. (2004). The human visual cortex. *Annual Review of Neuroscience*, *27*, 649-677.
- Gu, H., Chen, X. & Yang, Y. (2012). Baseline GABA concentration predicts functional connectivity strength. On *Organisation of Human Brain Mapping*.
- Gujar, S., Maheshwari, S., Bjorkman-Burtscher, I. & Sundgren, P. (2005). Magnetic resonance spectroscopy. *Journal of Neuro-Ophthalmology*, *25*, 217-226.
- Gupta, M., Jansen, E. E. W., Senephansiri, H., Jakobs, C., Snead, O. C., Grompe, M. et al. (2004). Liver-directed adenoviral gene transfer in murine succinate semialdehyde dehydrogenase deficiency. *Molecular Therapy*, *9*, 527-539.
- Gussev, A., Rzanny, R., Erdtel, M., Scholle, H. C., Kaiser, W. A., Mentzel, H. J. et al. (2010). Time-resolved functional 1H MR spectroscopic detection of glutamate concentration changes in the brain during acute heat pain stimulation. *NeuroImage*, *49*, 1895-1902.
- Hall, S. D., Stanford, I. M., Yamawaki, N., McAllister, C. J., Rönqvist, K. C., Woodhall, G. L. et al. (2011). The role of GABAergic modulation in motor function related neuronal network activity. *NeuroImage*, *56*, 1506-1510.
- Hämäläinen, M. & Hari, R. (2002). Magnetoencephalographic characterization of dynamic brain activation: Basic principles and methods of data collection and source analysis. *Brain Mapping: The Methods*, 227-253.
- Hämäläinen, M., Hari, R., Ilmoniemi, R., Knuutila, J. & Lounasmaa, O. (1993). Magnetoencephalography - theory, instrumentation, and applications to noninvasive studies of the working human brain. *Reviews of Modern Physics*, *65*, 413-506.
- Hamel, E. (2006). Perivascular nerves and the regulation of cerebrovascular tone. *Journal of Applied Physiology*, *100*, 1059-1064.
- Handwerker, D. A., Ollinger, J. M. & Esposito, M. D. (2004). Variation of BOLD hemodynamic responses across subjects and brain regions and their effects on statistical analyses. *im*, 1639-1651.
- Hanslmayr, S., Klimesch, W., Sauseng, P., Gruber, W., Doppelmayr, M., Freunberger, R. et al. (2005). Visual discrimination performance is related to decreased alpha amplitude but increased phase locking. *Neuroscience Letters*, *375*, 64-68.
- Harada, M., Kubo, H., Nose, A., Nishitani, H. & Matsuda, T. (2011). Measurement of variation in the human cerebral GABA level by in vivo MEGA-editing proton MR spectroscopy using a clinical 3 T instrument and its dependence on brain region and the female menstrual cycle. *Human Brain Mapping*, *32*, 828-833.
- Harel, N., Lee, S.-P., Nagaoka, T., Kim, D.-S. & Kim, S.-G. (2002). Origin of negative blood oxygenation level-dependent fMRI signals. *Journal of Cerebral Blood Flow and Metabolism*, *22*, 908-917.
- Harvey, B. M., Vansteensel, M. J., Ferrier, C. H., Petridou, N., Zuiderbaan, W., Aarnoutse, E. J. et al. (2012). Frequency specific spatial interactions in human

- electrocorticography: V1 alpha oscillations reflect surround suppression. *NeuroImage*, 1-9.
- Heeger, D. J., Huk, A. C., Geisler, W. S. & Albrecht, D. G. (2000). Spikes versus BOLD: what does neuroimaging tell us about neuronal activity? *Nature Neuroscience*, 3, 631-633.
- Heinemann, L., Kleinschmidt, A. & Müller, N. G. (2009). Exploring BOLD changes during spatial attention in non-stimulated visual cortex. *PloS one*, 4, e5560.
- Hendry, S. & Carder, R. K. (1992). Organization and plasticity of GABA neurons and receptors in monkey visual cortex. *Progress in Brain Research*, 90, 477-502.
- Hendry, S., Fuchs, J. & Jones, E. (1990). Distribution and plasticity of immunocytochemically localized GABA receptors in adult monkey visual cortex. *The Journal of Neuroscience*, 10, 2439-2450.
- Hendry, S. & Huntsman, M. (1994). GABA receptor subunit immunoreactivity in primate visual cortex: Distribution in Macaques and humans and regulation by visual input in adulthood. *The Journal of Neuroscience*, 14, 2382-2401.
- Henriksson, L., Nurminen, L., Hyvarinen, A. & Vanni, S. (2008). Spatial frequency tuning in human retinotopic visual areas. *Journal of Vision*, 8, 5.
- Henson, R. (2005). A mini-review of fMRI studies of human medial temporal lobe activity associated with recognition memory. *The Quarterly Journal of Experimental Psychology. B, Comparative and Physiological Psychology*, 58, 340-360.
- Hillebrand, a. & Barnes, G. R. (2002). A quantitative assessment of the sensitivity of whole-head MEG to activity in the adult human cortex. *NeuroImage*, 16, 638-650.
- Hillebrand, A., Singh, K. D., Holliday, I. E., Furlong, P. L. & Barnes, G. R. (2005). A new approach to neuroimaging with magnetoencephalography. *Human Brain Mapping*, 25, 199-211.
- Hilton, E. R., Hosking, S. & Betts, T. (2004). The effect of antiepileptic drugs on visual performance. *Seizure*, 1311, 113-128.
- Hinds, O. P., Rajendran, N., Polimeni, J. R., Augustinack, J. C., Wiggins, G., Wald, L. L. et al. (2008). Accurate prediction of V1 location from cortical folds in a surface coordinate system. *NeuroImage*, 39, 1585-1599.
- Hopf, J. M., Boehler, C. N., Luck, S. J., Tsotsos, J. K., Heinze, H.-J. & Schoenfeld, M. A. (2006). Direct neurophysiological evidence for spatial suppression surrounding the focus of attention in vision. *Proceedings of the National Academy of Sciences*, 103, 1053-1058.
- Howe, F. A., Stubbs, M., Rodrigues, L. M. & Griffiths, J. R. (1993). An assessment of artefacts in localized and non-localized ³¹P MRS studies of phosphate metabolites and pH in rat tumours. *NMR in Biomedicine*, 6, 43-52.
- Hu, X., Le, T. H., Parrish, T. & Erhard, P. (1995). Retrospective estimation and correction of physiological fluctuation in functional MRI. *Magnetic Resonance in Medicine*, 34, 201-212.
- Huang, M. X., Mosher, J. C. & Leahy, R. M. (1999). A sensor-weighted overlapping-sphere head model and exhaustive head model comparison for MEG. *Physics in Medicine and Biology*, 44, 423-440.
- Huang, W., Plyka, I., Li, H., Einstein, E., Volkow, N. & Springer, C. (1996). Magnetic resonance imaging (MRI) detection of the murine brain response to light: temporal differentiation and negative functional MRI changes. *Proceedings of the National Academy of Sciences of the United States of America*, 93, 6037-6042.

- Hubel, D. (1995). Chapter 4: The primary visual cortex *Eye, brain and vision* (pp. 1-30): Henry Holt and Company.
- Hubel, D. & Wiesel, T. (1963). Shape and arrangement of columns in cat's striate cortex. *The Journal of Physiology*, *165*, 559-568.
- Hubel, D. H. & Wiesel, T. N. (1974). Uniformity of monkey striate cortex: A parallel relationship between field size, scatter, and magnification factor. *The Journal of Comparative Neurology*, *158*, 295-305.
- Jamar, J. H., Kwakman, L. F. & Koenderink, J. J. (1984). The sensitivity of the peripheral visual system to amplitude-modulation and frequency-modulation of sine-wave patterns. *Vision Research*, *24*, 243-249.
- Jenkinson, M., Bannister, P., Brady, M. & Smith, S. (2002). Improved optimization for the robust and accurate linear registration and motion correction of brain images. *NeuroImage*, *17*, 825-841.
- Jensen, O. & Mazaheri, A. (2010). Shaping functional architecture by oscillatory alpha activity: gating by inhibition. *Frontiers in Human Neuroscience*, *4*, 1-8.
- Jinno, S., Klausberger, T., Marton, L. F., Dalezios, Y., Roberts, J. D. B., Fuentealba, P. et al. (2007). Neuronal diversity in GABAergic long-range projections from the hippocampus. *The Journal of Neuroscience*, *27*, 8790-8804.
- Kastner, S., De Weerd, P., Desimone, R. & Ungerleider, L. G. (1998). Mechanisms of directed attention in the human extrastriate cortex as revealed by functional MRI. *Science*, *282*, 108-111.
- Kastrup, A., Baudewig, J., Schnaudigel, S., Huonker, R., Becker, L., Sohns, J. M. et al. (2008). Behavioral correlates of negative BOLD signal changes in the primary somatosensory cortex. *NeuroImage*, *41*, 1364-1371.
- Ke, Y., Cohen, B. M., Bang, J. Y., Yang, M. & Renshaw, P. F. (2000). Assessment of GABA concentration in human brain using two-dimensional proton magnetic resonance spectroscopy. *Psychiatry Research*, *100*, 169-178.
- Kelly, S. P., Lalor, E. C., Reilly, R. B. & Foxe, J. J. (2006). Increases in alpha oscillatory power reflect an active retinotopic mechanism for distracter suppression during sustained visuospatial attention. *Journal of Neurophysiology*, *95*, 3844-3851.
- Klimesch, W. (1996). Memory processes, brain oscillations and EEG synchronization. *International Journal of Psychophysiology*, *24*, 61-100.
- Kuffler, S. W. & Edwards, C. (1958). Mechanism of gamma aminobutyric acid (GABA) action and its relation to synaptic inhibition. *Journal of Neurophysiology*, *21*, 589-610.
- Kulikowski, J., Abadi, R. & King-Smith, P. (1973). Orientational selectivity of grating and line detectors in human vision. *Vision Research*, *13*, 1479-1486.
- Kwong, K. K., Belliveau, J. W., Chesler, D. A., Goldberg, I. E., Weisskoff, R. M., Poncelet, B. P. et al. (1992). Dynamic magnetic resonance imaging of human brain activity during primary sensory stimulation. *Proceedings of the National Academy of Sciences*, *89*, 5675-5679.
- Lamme, V. A. F. & Roelfsema, P. R. (2000). The distinct modes of vision offered by feedforward and recurrent processing. *Trends in Neurosciences*, *23*, 571-579.
- Laufs, H., Holt, J. L., Elfont, R., Krams, M., Paul, J. S., Krakow, K. et al. (2006). Where the BOLD signal goes when alpha EEG leaves. *NeuroImage*, *31*, 1408-1418.
- Laufs, H., Kleinschmidt, A., Beyerle, A., Eger, E., Salek-Haddadi, A., Preibisch, C. et al. (2003). EEG-correlated fMRI of human alpha activity. *NeuroImage*, *19*, 1463-1476.

- Lauterbur, P. (1973). Image formation by induced local interactions: Examples employing nuclear magnetic resonance. *Nature*, *242*, 190-191.
- Leuba, G. & Kraftsik, R. (1994). Changes in volume, surface estimate, three-dimensional shape and total number of neurons of the human primary visual cortex from midgestation until old age. *Anatomy and Embryology*, *190*, 354-356.
- Licata, S. C., Lowen, S. B., Trksak, G. H., Maclean, R. R. & Lukas, S. E. (2011). Zolpidem reduces the blood oxygen level-dependent signal during visual system stimulation. *Progress in Neuro-Psychopharmacology & Biological Psychiatry*, *35*, 1645-1652.
- Lisman, J. & Idiart, M. (1995). Storage of 7 ± 2 short-term memories in oscillatory subcycles. *Science*, *267*, 1512-1515.
- Liu, Y., Shen, H., Zhou, Z. & Hu, D. (2011). Sustained negative BOLD response in human fMRI finger tapping task. *PloS one*, *6*, e23839.
- Logothetis, N. K. (2002). The neural basis of the blood-oxygen-level-dependent functional magnetic resonance imaging signal. *Philosophical transactions of the Royal Society of London. Series B, Biological sciences*, *357*, 1003-1037.
- Logothetis, N. K., Pauls, J., Augath, M., Trinath, T. & Oeltermann, A. (2001). Neurophysiological investigation of the basis of the fMRI signal. *Nature*, *412*, 150-157.
- Lopes da Silva, F. H. (1991). Neural mechanisms underlying brain waves: from neural membranes to networks. *Electroencephalography and Clinical Neurophysiology*, *79*, 81-93.
- Loubinoux, I., Carel, C., Alary, F., Boulanouar, K., Viillard, G., Manelfe, C. et al. (2001). Within-session and between-session reproducibility of cerebral sensorimotor activation: A test-retest effect evidenced with functional magnetic resonance imaging. *Journal of Cerebral Blood Flow and Metabolism*, *21*, 592-607.
- Macdonald, S. W. S., Nyberg, L. & Backman, L. (2006). Intra-individual variability in behavior: Links to brain structure, neurotransmission and neuronal activity. *Trends in Neurosciences*, *29*, 474-480.
- Magnotta, V. & Andreasen, N. (1999). Quantitative in vivo measurement of gyrification in the human brain: changes associated with aging. *Cerebral Cortex*, *9*, 151-160.
- Maldonado, P., Friedman-Hill, S. & Gray, C. (2000). Dynamics of striate cortical activity in the alert macaque: II. Fast time scale synchronization. *Cerebral Cortex*, *10*, 1117-1131.
- Mannion, D. J., McDonald, J. S. & Clifford, C. W. G. (2010). Orientation anisotropies in human visual cortex. *Journal of Neurophysiology*, *103*, 3465-3471.
- Mansfield, P. (1973). NMR 'diffraction' in solids? *Journal of Physics C: Solid state*, *6*, 422-426.
- Martin, D. L. & Rimvall, K. (1993). Regulation of gamma-aminobutyric acid synthesis in the brain. *Journal of Neurochemistry*, *60*, 395-407.
- McGonigle, D. J., Howseman, a. M., Athwal, B. S., Friston, K. J., Frackowiak, R. S. & Holmes, a. P. (2000). Variability in fMRI: an examination of intersession differences. *NeuroImage*, *11*, 708-734.
- Meier, J. D., Aflalo, T. N., Kastner, S. & Graziano, M. S. A. (2008). Complex organization of human primary motor cortex: A high-resolution fMRI study. *Journal of Neurophysiology*, *100*, 1800-1812.

- Menz, M. M., Neumann, J., Müller, K. & Zysset, S. (2006). Variability of the BOLD response over time: an examination of within-session differences. *NeuroImage*, *32*, 1185-1194.
- Mescher, M., Merkle, H., Kirsch, J., Garwood, M. & Gruetter, R. (1998). Simultaneous in vivo spectral editing and water suppression. *NMR in Biomedicine*, *11*, 266-272.
- Miki, A., Liu, G. T., Englander, S. a., Raz, J., van Erp, T. G., Modestino, E. J. et al. (2001). Reproducibility of visual activation during checkerboard stimulation in functional magnetic resonance imaging at 4 Tesla. *Japanese Journal of Ophthalmology*, *45*, 151-155.
- Miki, A., Raz, J., van Erp, T. G., Liu, C. S., Haselgrove, J. C. & Liu, G. T. (2000). Reproducibility of visual activation in functional MR imaging and effects of postprocessing. *American Journal of Neuroradiology*, *21*, 910-915.
- Moratal, D., Vallés-Luch, A., Martí-Bonmatí, L. & Brummer, M. (2008). k-Space tutorial: An MRI educational tool for a better understanding of k-space. *Biomedical Imaging and Intervention Journal*, *4*, e15.
- Movshon, J., Thompson, I. & Tolhurst, D. (1978). Spatial and temporal contrast sensitivity of neurones in areas 17 and 18 of the cat's visual cortex. *The Journal of Physiology*, *283*, 101-120.
- Mukamel, R., Gelbard, H., Arieli, A., Hasson, U., Fried, I. & Malach, R. (2005). Coupling between neuronal firing, field potentials, and fMRI in human auditory cortex. *Science*, *309*, 951-954.
- Mullen, K. & Dumoulin, S. (2007). Selectivity of human retinotopic visual cortex to S-cone-opponent, L/M-cone-opponent and achromatic stimulation. *European Journal of Neuroscience*, *25*, 491-502.
- Munneke, J., Heslenfeld, D. J. & Theeuwes, J. (2008). Directing attention to a location in space results in retinotopic activation in primary visual cortex. *Brain Research*, *1222*, 184-191.
- Munoz, A., DeFelipe, J. & Jones, E. G. (2001). Patterns of GABA(B)R1a,b receptor gene expression in monkey and human visual cortex. *Cerebral Cortex*, *11*, 104-113.
- Murthy, V. & Fetz, E. (1992). Coherent 25-to 35-Hz oscillations in the sensorimotor cortex of awake behaving monkeys. *Proceedings of the National Academy of Sciences of the United States of America*, *89*, 5670-5674.
- Muthukumaraswamy, S. D., Edden, A., Jones, D., Swettenham, J. & Singh, K. (2009). Resting GABA concentration predicts peak gamma frequency and fMRI amplitude in response to visual stimulation in humans. *Proceedings of the National Academy of Sciences*, *106*, 2-7.
- Muthukumaraswamy, S. D., Evans, C. J., Edden, R. A. E., Wise, R. G. & Singh, K. D. (2011). Individual variability in the shape and amplitude of the BOLD-HRF correlates with endogenous GABAergic inhibition. *Human Brain Mapping*, *33*(2), 455-465.
- Muthukumaraswamy, S. D., Evans, C. J., Edden, R. A. E., Wise, R. G. & Singh, K. D. (2012). Individual variability in the shape and amplitude of the BOLD-HRF correlates with endogenous GABAergic inhibition. *Human Brain Mapping*, *33*, 455-465.
- Muthukumaraswamy, S. D., Myers, J. F. M., Wilson, S. J., Nutt, D. J., Lingford-Hughes, A., Singh, K. D. et al. (2012). The effects of elevated endogenous GABA levels on movement-related network oscillations. *NeuroImage*, *66C*, 36-41.

- Muthukumaraswamy, S. D. & Singh, K. D. (2008). Spatiotemporal frequency tuning of BOLD and gamma band MEG responses compared in primary visual cortex. *NeuroImage*, *40*, 1552-1560.
- Muthukumaraswamy, S. D. & Singh, K. D. (2009). Functional decoupling of BOLD and gamma-band amplitudes in human primary visual cortex. *Human Brain Mapping*, *30*, 2000-2007.
- Muthukumaraswamy, S. D., Singh, K. D., Swettenham, J. B. & Jones, D. K. (2010). Visual gamma oscillations and evoked responses: Variability, repeatability and structural MRI correlates. *NeuroImage*, *49*, 3349-3357.
- Neuper, C. & Pfurtscheller, G. (2001). Event-related dynamics of cortical rhythms: frequency-specific features and functional correlates. *International Journal of Psychophysiology*, *43*, 41-58.
- Niessing, J., Ebisch, B. & Schmidt, K. (2005). Hemodynamic signals correlate tightly with synchronized gamma oscillations. *Science*, *309*, 948-951.
- Nikulin, V. V. & Brismar, T. (2004). Long-range temporal correlations in alpha and beta oscillations: Effect of arousal level and test-retest reliability. *Clinical Neurophysiology*, *115*, 1896-1908.
- Northoff, G., Walter, M., Schulte, R. F., Beck, J., Dydak, U., Henning, A. et al. (2007). GABA concentrations in the human anterior cingulate cortex predict negative BOLD responses in fMRI. *Nature Neuroscience*, *10*, 1515-1517.
- O'Gorman, R. L., Michels, L., Edden, R. A., Murdoch, J. B. & Martin, E. (2011). In vivo detection of GABA and glutamate with MEGA-PRESS: reproducibility and gender effects. *Journal of Magnetic Resonance Imaging*, *33*, 1262-1267.
- Ogawa, S., Lee, T. M., Kay, A. R. & Tank, D. W. (1990). Brain magnetic resonance imaging with contrast dependent on blood oxygenation. *Proceedings of the National Academy of Sciences*, *87*, 9868-9872.
- Ogawa, S., Tank, D., Menon, R., Ellermann, J., Kim, S.-G., Merkle, H. et al. (1992). Intrinsic signal changes accompanying sensory stimulation: Functional brain mapping with magnetic resonance imaging. *Proceedings of the National Academy of Sciences, USA*, *89*, 5951-5955.
- Olman, C. & Yacoub, E. (2011). High-field fMRI for human applications: An overview of spatial resolution and signal specificity. *The Open Neuroimaging Journal*, *5*, 74-89.
- Otsuki, T., Kanamatsu, T., Tsukada, Y., Goto, Y., Okamoto, K. & Watanabe, H. (2005). Carbon 13-labeled magnetic resonance spectroscopy observation of cerebral glucose metabolism. *Archives of Neurology*, *62*, 485-487.
- Pasley, B., Inglis, B. & Freeman, R. (2007). Analysis of oxygen metabolism implies a neural origin for the negative BOLD response in human visual cortex. *Neuroimage*, *36*, 269-276.
- Peelen, M. V. & Downing, P. E. (2005). Within-subject reproducibility of category-specific visual activation with functional MRI. *Human Brain Mapping*, *25*, 402-408.
- Perry, G., Hamandi, K., Brindley, L. M., Muthukumaraswamy, S. D. & Singh, K. D. (2012). The properties of induced gamma oscillations in human visual cortex show individual variability in their dependence on stimulus size. *NeuroImage*, *In Press*.
- Pfurtscheller, G., Stancák, A. & Neuper, C. (1996). Event-related synchronization (ERS) in the alpha band - an electrophysiological correlate of cortical idling: A review. *International Journal of Psychophysiology*, *24*, 39-46.

- Purcell, E. & Torrey, H. (1946). Resonance absorption by nuclear magnetic moments in a solid. *Physical Review*, *69*, 37-38.
- Puts, N. A. J. & Edden, R. A. E. (2012). In vivo magnetic resonance spectroscopy of GABA: A methodological review. *Progress in Nuclear Magnetic Resonance Spectroscopy*, *60*, 29-41.
- Puts, N. A. J., Edden, R. A. E., Evans, C. J., McGlone, F. & McGonigle, D. J. (2011). Regionally Specific Human GABA Concentration Correlates with Tactile Discrimination Thresholds. *The Journal of Neuroscience*, *31*, 16556-16560.
- Qin, P., Grimm, S., Duncan, N., Wiebking, C., Lyttelton, O., Hayes, D. et al. (2012). *GABA-A receptors and the transition from resting-state to stimulus induced activity*. Paper presented at the Organisation of Human Brain Mapping.
- Raichle, M. (1998). Behind the scenes of functional brain imaging: A historical and physiological perspective. *Proceedings of the National Academy of Sciences*, *95*, 765-772.
- Ray, S. & Maunsell, J. H. R. (2010). Differences in gamma frequencies across visual cortex restrict their possible use in computation. *Neuron*, *67*, 885-896.
- Ritter, P., Moosmann, M. & Villringer, A. (2009). Rolandic alpha and beta EEG rhythms' strengths are inversely related to fMRI-BOLD signal in primary somatosensory and motor cortex. *Human Brain Mapping*, *30*, 1168-1187.
- Robinson, S. E. & Vrba, J. (1999). *Functional neuroimaging by synthetic aperture magnetometry (SAM)*. Paper presented at the Recent Advances in Biomagnetism, Sendai, Japan.
- Rombouts, S. & Barkhof, F. (1998). Within-subject reproducibility of visual activation patterns with functional magnetic resonance imaging using multislice echo planar imaging. *Magnetic Resonance Imaging*, *16*, 105-113.
- Rombouts, S. a., Barkhof, F., Hoogenraad, F. G., Sprenger, M., Valk, J. & Scheltens, P. (1997). Test-retest analysis with functional MR of the activated area in the human visual cortex. *American Journal of Neuroradiology*, *18*, 1317-1322.
- Ross, J. E., Clarke, D. D. & Bron, A. J. (1985). Effect of age on contrast sensitivity function: unocular and binocular findings. *The British journal of Ophthalmology*, *69*, 51-56.
- Rothman, D. L., Petroff, O. A., Behar, K. L. & Mattson, R. H. (1993). Localized ¹H NMR measurements of gamma-aminobutyric acid in human brain in vivo. *Proceedings of the National Academy of Sciences*, *90*, 5662-5666.
- Sabate, M., Llanos, C., Enriquez, E., Gonzalez, B. & Rodriguez, M. (2011). Fast modulation of alpha activity during visual processing and motor control. *Neuroscience*, *189*, 236-249.
- Schwarzkopf, D. S., Robertson, D. J., Song, C., Barnes, G. R. & Rees, G. (2012). The frequency of visually induced γ -band oscillations depends on the size of early human visual cortex. *The Journal of Neuroscience*, *32*, 1507-1512.
- Sereno, M. I., Dale, A. M., Reppas, J. B., Kwong, K. K., Belliveau, J. W., Brady, T. J. et al. (1995). Borders of multiple visual areas in humans revealed by functional magnetic resonance imaging. *Science*, *268*, 889-893.
- Sestieri, C., Sylvester, C. M., Jack, a. I., D'Avossa, G., Shulman, G. L. & Corbetta, M. (2008). Independence of anticipatory signals for spatial attention from number of nontarget stimuli in the visual field. *Journal of Neurophysiology*, *100*, 829-838.
- Shaw, A., Brealy, J., Richardson, H., Edden, R. A. E., Evans, C. J. E., Singh, K. D. et al. Normal gamma oscillations but reduced M100 in remitted depression: A combined MEG-MRS study. *Biological Psychiatry*.

- Shmuel, A., Augath, M., Oeltermann, A. & Logothetis, N. K. (2006). Negative functional MRI response correlates with decreases in neuronal activity in monkey visual area V1. *Nature Neuroscience*, *9*, 569-577.
- Shmuel, A., Yacoub, E., Pfeuffer, J., Van De Moortele, P. F., Adriany, G., Hu, X. et al. (2002). Sustained negative BOLD, blood flow and oxygen consumption response and its coupling to the positive response in the human brain. *Neuron*, *36*, 1195-1210.
- Shoukri, M. M., Colak, D., Kaya, N. & Donner, A. (2008). Comparison of two dependent within subject coefficients of variation to evaluate the reproducibility of measurement devices. *BMC Medical Research Methodology*, *8*, 1-11.
- Silverman, M. S., Grosz, D. H., De Valois, R. L. & Elfar, S. D. (1989). Spatial-frequency organization in primate striate cortex. *Proceedings of the National Academy of Sciences*, *86*, 711-715.
- Singer, W. (1999). Neuronal synchrony: A versatile code for the definition of relations? *Neuron*, *24*, 49-65.
- Singh, K. D. (2006). Magnetoencephalography. In C. Senior, T. Russell & M. S. Gazzaniga (Eds.), *Methods in Mind* (pp. 291-326). Cambridge, MA: Massachusetts Institute of Technology.
- Singh, K. D. (2012). Which “neural activity” do you mean? fMRI, MEG, oscillations and neurotransmitters. *NeuroImage*, 1-10.
- Singh, K. D., Barnes, G. R., Hillebrand, A., Forde, E. M. E. & Williams, A. L. (2002). Task-related changes in cortical synchronization are spatially coincident with the hemodynamic response. *NeuroImage*, *16*, 103-114.
- Singh, K. D., Smith, A. T. & Greenlee, M. W. (2000). Spatiotemporal frequency and direction sensitivities of human visual areas measured using fMRI. *NeuroImage*, *12*, 550-564.
- Slotnick, S. D., Schwarzbach, J. & Yantis, S. (2003). Attentional inhibition of visual processing in human striate and extrastriate cortex. *NeuroImage*, *19*, 1602-1611.
- Smit, D. J. A., Boomsma, D. I., Schnack, H. G., Hulshoff Pol, H. E. & de Geus, E. J. C. (2012). Individual differences in EEG spectral power reflect genetic variance in gray and white matter volumes. *Twin Research and Human Genetics*, *15*, 384-392.
- Smith, A. T., Singh, K. D. & Greenlee, M. W. (2000). Attentional suppression of activity in the human visual cortex. *Neuroreport*, *11*, 271-277.
- Smith, A. T., Singh, K. D., Williams, A. L. & Greenlee, M. W. (2001). Estimating receptive field size from fMRI data in human striate and extrastriate visual cortex. *Cerebral Cortex*, *11*, 1182-1190.
- Smith, A. T., Williams, A. L. & Singh, K. D. (2004). Negative BOLD in the visual cortex: evidence against blood stealing. *Human Brain Mapping*, *21*, 213-220.
- Smith, F. W. & Muckli, L. (2010). Nonstimulated early visual areas carry information about surrounding context. *Proceedings of the National Academy of Sciences of the United States of America*, *107*, 20099-20103.
- Smith, M. J., Keel, J. C., Greenberg, B. D., Adams, L. F., Schmidt, P. J., Rubinow, D. A. et al. (1999). Menstrual cycle effects on cortical excitability. *Neurology*, *53*, 2069-2072.
- Smith, S. M. (2002). Fast robust automated brain extraction. *Human Brain Mapping*, *17*, 143-155.

- Snyder, A. C. & Foxe, J. J. (2010). Anticipatory attentional suppression of visual features indexed by oscillatory alpha-band power increases: a high-density electrical mapping study. *The Journal of Neuroscience*, *30*, 4024-4032.
- Somers, D. C., Dale, a. M., Seiffert, a. E. & Tootell, R. B. (1999). Functional MRI reveals spatially specific attentional modulation in human primary visual cortex. *Proceedings of the National Academy of Sciences of the United States of America*, *96*, 1663-1668.
- Somersalo, E. (2007). The inverse problem of magnetoencephalography: Source localization and the shape of a ball. *SIAM News*, *40*, 1-2.
- Stagg, C. J., Bachtiar, V. & Johansen-Berg, H. (2011a). The role of GABA in human motor learning. *Current Biology*, *21*, 480-484.
- Stagg, C. J., Bachtiar, V. & Johansen-Berg, H. (2011b). What are we measuring with GABA magnetic resonance spectroscopy? *Communicative & Integrative Biology*, *4*, 573-575.
- Stefanovic, B., Warnking, J. M. & Pike, G. B. (2004). Hemodynamic and metabolic responses to neuronal inhibition. *NeuroImage*, *22*, 771-778.
- Stensaas, S., Eddington, D. & Dobbelle, W. (1974). The topography and variability of the primary visual cortex in man. *Journal of Neurosurgery*, *40*, 747-755.
- Stevenson, C. M., Wang, F., Brookes, M. J., Zumer, J. M., Francis, S. T. & Morris, P. G. (2012). Paired pulse depression in the somatosensory cortex: associations between MEG and BOLD fMRI. *NeuroImage*, *59*, 2722-2732.
- Sumner, P., Edden, R. A. E., Bompas, A., Evans, C. J. & Singh, K. D. (2010). More GABA, less distraction: a neurochemical predictor of motor decision speed. *Nature Neuroscience*, *13*, 825-827.
- Tedeschi, G., Bertolino, A., Campbell, G., Barnett, A. S., Duyn, J. H., Jacob, P. K. et al. (1996). Reproducibility of proton MR spectroscopic imaging findings. *American Journal of Neuroradiology*, *17*, 1871-1879.
- Tesche, C. D. & Karhu, J. (2000). Theta oscillations index human hippocampal activation during a working memory task. *Proceedings of the National Academy of Sciences*, *97*, 919-924.
- Thiel, T., Czisch, M., Elbel, G. K. & Hennig, J. (2002). Phase coherent averaging in magnetic resonance spectroscopy using interleaved navigator scans: compensation of motion artifacts and magnetic field instabilities. *Magnetic Resonance in Medicine*, *47*, 1077-1082.
- Thompson-Schill, S., Braver, T. & Jonides, J. (2002). Individual differences. *Cognitive, Affective and Behavioural Neuroscience*, *5*, 115-116.
- Thut, G., Nietzel, A., Brandt, S. A. & Pascual-Leone, A. (2006). Alpha-band electroencephalographic activity over occipital cortex indexes visuospatial attention bias and predicts visual target detection. *The Journal of Neuroscience*, *26*, 9494-9502.
- Tootell, R. B., Mendola, J. D., Hadjikhani, N. K., Liu, A. K. & Dale, A. M. (1998). The representation of the ipsilateral visual field in human cerebral cortex. *Proceedings of the National Academy of Sciences*, *95*, 818-824.
- Tootell, R. B., Silverman, M. S. & De Valois, R. L. (1981). Spatial frequency columns in primary visual cortex. *Science*, *214*, 813-815.
- Tootell, R. B., Silverman, M. S., Hamilton, S. L., Switkes, E. & De Valois, R. L. (1988). Functional anatomy of macaque striate cortex. V. Spatial frequency. *The Journal of Neuroscience*, *8*, 1610-1624.

- Tootell, R. B. H., Hadjikhani, N., Hall, E. K., Marrett, S., Vanduffel, W., Vaughan, J. T. et al. (1998). The retinotopy of visual spatial attention. *Neuron*, *21*, 1409-1422.
- Traub, R. D., Whittington, M. A., Colling, S. B., Buzsáki, G. & Jefferys, J. G. (1996). Analysis of gamma rhythms in the rat hippocampus in vitro and in vivo. *The Journal of Physiology*, *493*, 471-484.
- Tuladhar, A. M., Ter Huurne, N., Schoffelen, J.-M., Maris, E., Oostenveld, R. & Jensen, O. (2007). Parieto-occipital sources account for the increase in alpha activity with working memory load. *Human Brain Mapping*, *28*, 785-792.
- Tyszka, J. M. & Mamelak, A. N. (2002). Quantification of B0 homogeneity variation with head pitch by registered three-dimensional field mapping. *Journal of Magnetic Resonance*, *159*, 213-218.
- Uhlhaas, P., Pipa, G. & Lima, B. (2009). Neural synchrony in cortical networks: History, concept and current status. *Frontiers in Integrative Neuroscience*, *3*, 1-19.
- Van Dijk, H., Schoffelen, J.-M., Oostenveld, R. & Jensen, O. (2008). Prestimulus oscillatory activity in the alpha band predicts visual discrimination ability. *The Journal of Neuroscience*, *28*, 1816-1823.
- Van Horn, J., Grafton, S. & Miller, M. (2008). Individual Variability in Brain Activity: A Nuisance or an Opportunity? *Brain Imaging and Behavior*, *2*, 327-334.
- Van Pelt, S., Boomsma, D. I. & Fries, P. (2012). Magnetoencephalography in twins reveals a strong genetic determination of the peak frequency of visually induced γ -band synchronization. *The Journal of Neuroscience*, *32*, 3388-3392.
- Vanni, S., Revonsuo, A. & Hari, R. (1997). Modulation of the parieto-occipital alpha rhythm during object detection. *The Journal of Neuroscience*, *17*, 7141-7147.
- Vaucher, E., Tong, X. K., Cholet, N., Lantin, S. & Hamel, E. (2000). GABA neurons provide a rich input to microvessels but not nitric oxide neurons in the rat cerebral cortex: a means for direct regulation of local cerebral blood flow. *The Journal of comparative neurology*, *421*, 161-171.
- Vazquez, A. L., Masamoto, K., Fukuda, M. & Kim, S.-g. (2010). Cerebral oxygen delivery and consumption during evoked neural activity. *Frontiers in Neuroenergetics*, *2*, 1-12.
- Vrba, J. & Robinson, S. E. (2001). Signal processing in magnetoencephalography. *Methods*, *25*, 249-271.
- Wade, A. R. & Rowland, J. (2010). Early suppressive mechanisms and the negative blood oxygenation level-dependent response in human visual cortex. *The Journal of Neuroscience*, *30*, 5008-5019.
- Wang, X. J. & Buzsáki, G. (1996). Gamma oscillation by synaptic inhibition in a hippocampal interneuronal network model. *The Journal of Neuroscience*, *16*, 6402-6413.
- White, J. A., Banks, M. I., Pearce, R. A. & Kopell, N. J. (2000). Networks of interneurons with fast and slow γ -aminobutyric acid type A (GABAA) kinetics provide substrate for mixed gamma-theta rhythm. *Proceedings of the National Academy of Sciences*, *97*, 8128-8133.
- Winterer, G., Carver, F. W., Musso, F., Mattay, V., Weinberger, D. R. & Coppola, R. (2007). Complex relationship between BOLD signal and synchronization/desynchronization of human brain MEG oscillations. *Human Brain Mapping*, *28*, 805-816.

- Worden, M. S., Foxe, J. J., Wang, N. & Simpson, G. V. (2000). Anticipatory biasing of visuospatial attention indexed by retinotopically specific alpha-band electroencephalography increases over occipital cortex. *The Journal of Neuroscience*, *20*, 1-6.
- Wright, M. J. & Johnston, A. (1983). Spatiotemporal contrast sensitivity and visual field locus. *Vision Research*, *23*, 983-989.
- Wu, L., Eichele, T. & Calhoun, V. D. (2010). Reactivity of hemodynamic responses and functional connectivity to different states of alpha synchrony: a concurrent EEG-fMRI study. *NeuroImage*, *52*, 1252-1260.
- Xu, X., Anderson, T. J. & Casagrande, V. A. (2007). How Do Functional Maps in Primary Visual Cortex Vary With Eccentricity? *The Journal of Comparative Neurology*, *501*, 741-755.
- Yamawaki, N., Stanford, I. M., Hall, S. D. & Woodhall, G. L. (2008). Pharmacologically induced and stimulus evoked rhythmic neuronal oscillatory activity in the primary motor cortex in vitro. *Neuroscience*, *151*, 386-395.
- Yarkoni, T. (2009). Big correlations in little studies: Inflated fMRI correlations reflect low statistical power - Commentary on Vul et al. (2009). *Perspectives on Psychological Science*, *4*, 294-298.
- Young, A. & Chu, D. (1990). Distribution of GABAA, and GABAB, receptors in mammalian brain: Potential targets for drug development. *Drug Development Research*, *167*, 161-167.
- Zaehle, T., Fründ, I. & Schadow, J. (2009). Inter- and intra-individual covariations of hemodynamic and oscillatory gamma responses in the human cortex. *Frontiers in Human Neuroscience*, *3*, 1-12.
- Zandbelt, B. B., Gladwin, T. E., Raemaekers, M., van Buuren, M., Neggers, S. F., Kahn, R. S. et al. (2008). Within-subject variation in BOLD-fMRI signal changes across repeated measurements: quantification and implications for sample size. *NeuroImage*, *42*, 196-206.
- Zhang, Y., Brady, M. & Smith, S. (2001). Segmentation of brain MR images through a hidden Markov random field model and the expectation-maximization algorithm. *IEEE Transactions on Medical Imaging*, *20*, 45-57.
- Zhang, Y., Perez Velazquez, J. L., Tian, G. F., Wu, C. P., Skinner, F. K., Carlen, P. L. et al. (1998). Slow oscillations (≤ 1 Hz) mediated by GABAergic interneuronal networks in rat hippocampus. *The Journal of Neuroscience*, *18*, 9256-9268.
- Zilles, K. & Amunts, K. (2009). Receptor mapping: architecture of the human cerebral cortex. *Current Opinion in Neurology*, *22*, 331-339.
- Zilles, K., Palomero-Gallagher, N. & Schleicher, A. (2004). Transmitter receptors and functional anatomy of the cerebral cortex. *Journal of anatomy*, *205*, 417-432.
- Zumer, J., Brookes, M., Stevenson, C. & Francis, S. (2010). Relating BOLD fMRI and neural oscillations through convolution and optimal linear weighting. *Neuroimage*, *49*, 1479-1489.

Appendices

Appendix 1.

Correlations between variables measured in Chapter 5

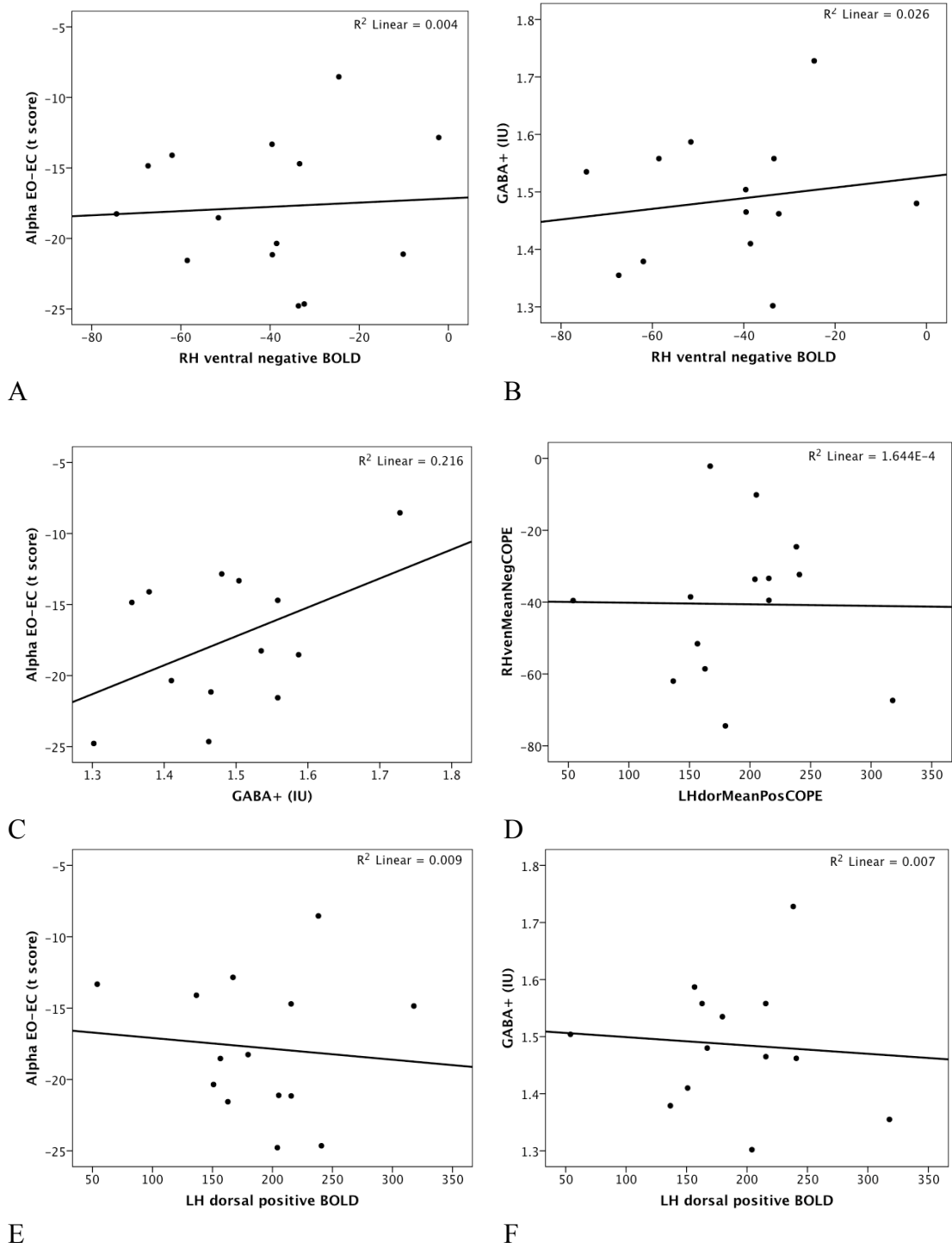


Figure 1 A-F) Scatterplots showing relationships between variables measured in Chapter 5.

Appendix 2.

Correlations between variables measured in Chapter 8.

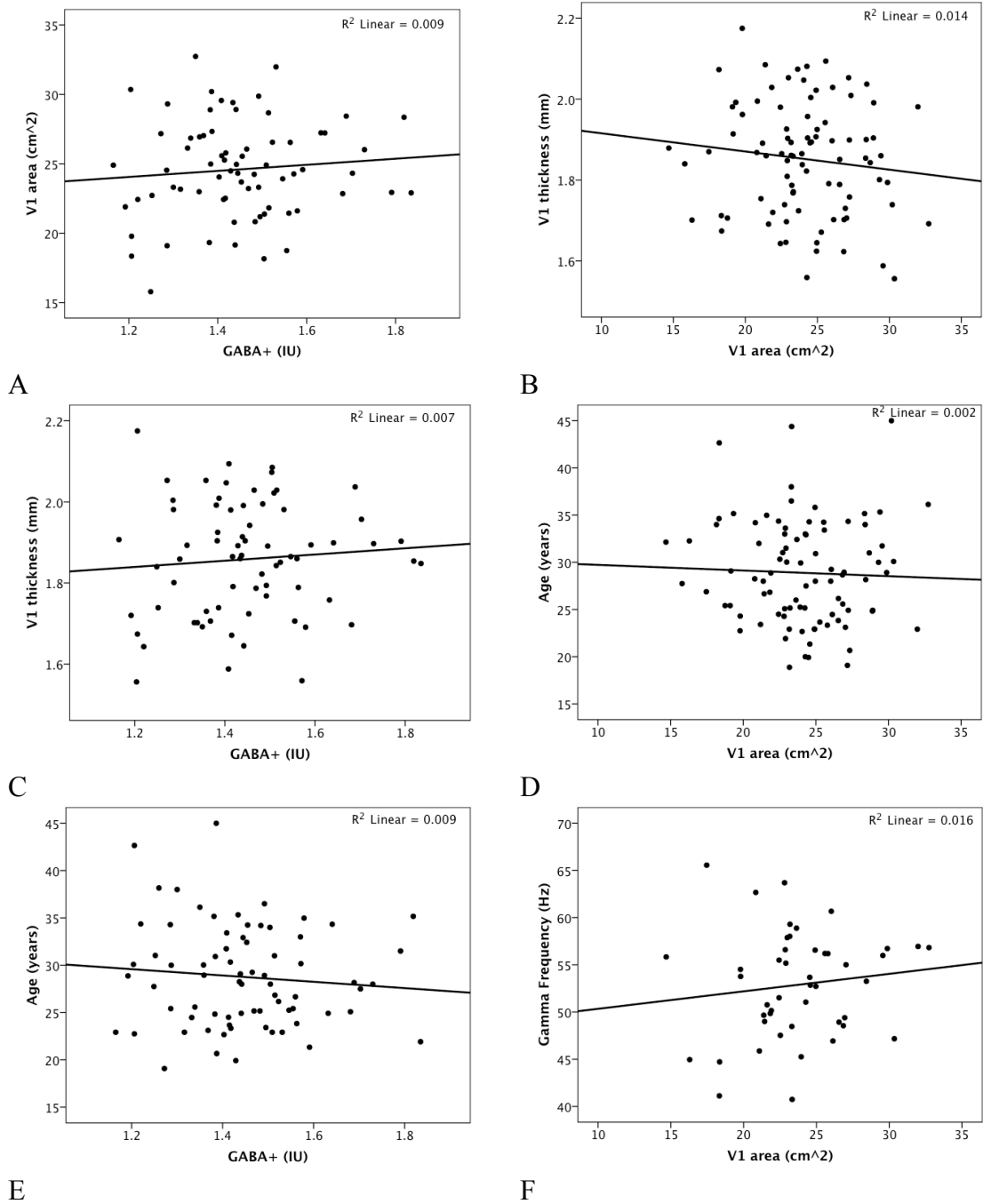


Figure 1. Correlations between variables of interest in Chapter 8. All correlations plotted in this figure were non-significant.